The Analysis of Inquiry in Students' Conversations in the Biochemistry Laboratory.

The Elucidation of Proton-Coupled Electron-Transfer Reaction Mechanism in Manganese Superoxide Dismutase through Structural Analysis of Mutants.

A dissertation presented in partial fulfilment of the

requirements for the degree of

Doctor of Philosophy

in

Chemistry

at Massey University, Manawatū,

New Zealand

Jatnika Hermawan

2023

ABSTRACT

Superoxide dismutases (SODs) have very significant biological importance, protecting organisms against reactive oxygen species such as superoxide. They are also known as the fastest enzyme with the largest k_{cat}/K_m of any known enzyme. To perform super-fast enzymatic function, SOD must shuttle proton-coupled electrons in an efficient systematic way. However, since its discovery in 1968, the mechanistic nature of SOD catalytic function remains vague. Wide-ranging approaches have attempted to uncover the catalytic mechanism of the manganese-containing SOD, MnSOD, but there were experimental limitations that obstructed the investigations. Here, the structural analyses of two dimer interface mutants of MnSOD, S126D and S126W, explored possible changes in water structure near the active site providing new information to examine the hypothesis of the Glu170 bridge as a key player in the proton shuttle in the outer-sphere mechanism.

To gain insight into the mechanism of the proton-coupled electron-transfer (PCET) reaction mechanism, the technique of single-crystal X-ray crystallography was used to observe the three-dimensional structure of *Escherichia coli* MnSOD mutants, analytical ultracentrifugation was used to observe quaternary association in solution, and protein stability was assessed by differential scanning calorimetry. The key residue Ser126 at the conserved but asymmetric dimer interface of the MnSOD was mutated with the initial intent to generate a monomeric species. Ser126 is not essential for activity and is not part of the active site, whereas Glu170 forms part of the dimer interface where Glu170 from one subunit forms part of the active site of the second subunit of the dimer. The loss of activity occurring in a monomeric MnSOD may indicate an alternative catalytic mechanism of the MnSOD enzyme.

The substitution of Ser126 to Asp, intended to produce a monomeric species by charge repulsion, surprisingly produced a dimer at pH>7.5 with little change in structure at the Mn active site, but there was a 94 % reduction in catalytic activity. Partial loss of activity in *Ec*-MnSOD-S126D may be due to electrostatic effects of the negative charge ~7 Å from metal centre perturbing the Mn^{III}/Mn^{II} redox couple.

The substitution of Ser126 to Trp, intended to produce a monomeric species by steric bulk, enforces mostly monomeric *Ec*-MnSOD S126W in solution form, coupled with a 99.9 % reduction in catalytic activity. Here one mutation to a conserved dimer interface led to altered tertiary structure and a completely different dodecameric domain-swapped quaternary association in the crystalline state and complete loss of activity in *Ec*-MnSOD-S126W in the solution state. In the course of evolution, higher and less often lower degrees of oligomerisation have arisen. Evolving complexity does not require multiple mutations.

As part of the scholarship requirements, this dissertation contains a pedagogical component. Student conversations in a guided inquiry third-year biochemistry laboratory were recorded and analysed to discover the extent of higher-order critical thinking that might occur. Although students initially struggled to move beyond core first-year laboratory skills, they were at all times strongly engaged in the project-style experiment, which ran over three five- to eight-hour sessions. Some progress in the level of inquiry was captured from their conversations from the first to the third laboratory session. A simple diagram and table were developed to help guide teachers in a guided inquiry-based learning in higher education.

Preface

Before you lies the doctoral dissertation "(1) The Analysis of Inquiry in Students' Conversations in the Biochemistry Laboratory; (2) The Elucidation of Proton-Coupled Electron-Transfer Reaction Mechanism in Manganese Superoxide Dismutase through Structural Analysis of Mutants." It has been written to fulfill the graduation requirements of the doctoral of philosophy program at the Massey University, New Zealand.

This thesis is in three parts. Chapter 1 is a pedagogical component, required by conditions on the Indonesian Government Scholarship, where student conversations in an inquiry-based laboratory were recorded and analysed for evidence of critical thinking. Chapters 2-6 focus of mutations to the dimer interface of manganese superoxide dismutase with the goal of clarifying the role of an absolutely conserved glutamate in the diffusion-limited proton-coupled electron transfer reactions. An Appendix documents early studies on mutants of bovine β-lactoglobulin, learning techniques of molecular biology and protein expression, purification and characterisation.

I have presented aspects of the research at:

Melbourne, Australia. 9 July 2015 at the Higher Education Research and Development Society of Australasia 2015, entitled: *The analysis of inquiry in students' conversations in the biochemistry laboratory.*

Lorne, Australia. 9 February 2015 at the 40th Lorne Conference on Protein Structure and Function 2015, entitled: *Towards elucidation of the proton-coupled electron transfer reaction mechanism in manganese superoxide dismutase through disruption of the dimer interface*.

Hanmer Springs, New Zealand. 1 July 2014 at the New Zealand Structural Biology Conference 2014, 30 Jun-2 Jul 2014. *Towards elucidation of proton-coupled electron-transfer reaction mechanism in manganese superoxide dismutase through disruption of the dimer interface*.

Malang, Indonesia. 14 February 2015 at the 1st International Conference of Environmental Pollution on Human Health 2015. *The mystery of reaction mechanism of manganese superoxide dismutase. Does the disruption of the dimer interface strategy work?*

Acknowledgement

Financial Acknowledgements

Financial support for my PhD was provided by a scholarship from the Ministry of Education, Culture, Research, and Technology, Republic of Indonesia and the generosity of Prof Geoff Jameson through his project.

Financial support for my PhD research on structural biology was provided by a grant from the Marsden Fund.

Financial support for my PhD research on education and participating in the conference in Higher Education in Melbourne (Australia, 2015) were provided by a grant from the Massey University Research Fund.

Financial support for my participation in three conferences of Biochemistry in Hanmer Springs (New Zealand, 2013), Lorne (Australia, 2014), and Malang (Indonesia, 2014), were provided by grants from the Institute of Fundamental Sciences Postgraduate Travel Fund, Massey University.

Financial support for the X-xay beamline travel to Australian Synchrotron in Clayton (Australia, 2014) were provided by grants from the New Zealand Synchrotron Group Ltd funded in part by Massey University.

I also received Bailey Bequest Bursary scholarship in 2018.

I would like to acknowledge and give my warmest thanks to Prof. Geoff Jameson, Mr. Sumarna Surapranata PhD, Assoc. Prof. Gill Norris, and Dr. Zoe Jordens for their recommendations to those scholarships and grants.

Personal Acknowledgements

I am very proud to have been engaged in researching and writing this dissertation because the reaction mechanism of MnSOD had remained a mystery for decades. There is a bright spot that might be the sign, and sometimes the path comes unexpectedly. This way is tortuous and uphill, and I won't give up chasing the destiny. No result betrays the effort.

This dissertation and the research behind it would not have been possible without the exceptional support of my main supervisor, Prof. Geoffrey B. Jameson (BSc(Hons), PhD, FNZIC, FRSNZ). His enthusiasm, expertise, and exacting attention to detail have been an inspiration and kept my work on track from my first encounter with the PyMol and WinCoot to the final draft of this dissertation. The challenges you have given to me maximised my learning opportunities, for which I am very grateful. You have sincerely supported me in all aspects, so that I finally could achieve this point.

I am also very proud to have received invaluable guidance throughout my PhD program from my co-supervisors, Assoc. Prof. Gillian E. Norris PhD for her motivation, ideas, and opportunities to work in her biochemistry lab, and Dr. Zoe Jordens for her support to seek funding for educational research and the inspiration to be both scientist and educational practitioner and expert in the same time.

And I am very grateful for the great support, sacrifices, and loves from my parents and my wife Rina, my children Harits, Tsabita, and Maryam, also the last two, Afiya and Yusuf who were born during my PhD. They complete my happiness and challenges at the same time to make me strong. Gratitude to my siblings Dini and Rizal, and my parents in law.

I also would like to thank Trevor Loo who became my mentor at the Lab, I really learnt a lot from him. I would like to thank all the participants (anonymous) in my educational study. I am so grateful to Prof. Renwick Dobson and Dr. Sarah Kessans for providing me with the opportunity in using AUC facilities at the University of Canterbury. I would also like to thank to Massey staff, especially Ann Truter, Peter Lewis, and Penny Abercrombie. I would like also to thank Jacqueline Koenders and Assoc. Prof. Catherine Whitby for your support regarding my study. My thanks also to the great Lab-X superteam members: Fareeda, Jan, Kelvin, Rafea, Stuart, Jennifer, Marc, and Jack, who have helped in the Lab and shared success and 'tears' in Friday meetings.

Special thanks to my best friends Br. Putra Asga Elevri, Neneng Heryati, as well as my cousin Teddy and Nila, who have incredibly supported me to complete my PhD. Special gratitudes for the Fergusons: Yuni, Yulfia, Neneng, Kodrad, and Rijal, the first gens: Prof. Bambang Kusumo, Nina, Yuliandri, Sandi, Fachrul, Bayu, Ifa, Erika, Yudi, Wira, Aulya, Erwin, Achmad, Bachtiar, Bhawat, Saiful, Reagan, and Cleave, and everyone in MMS, MMA, and my Palmy vibes.

I would like to express special thanks to those who encouraged me with incredible supports from leaders to colleagues in the Ministry of Education, Culture, Research, and Technology: Mr. Sumarna Surapranata PhD, Dr. Poppy D. Puspitawati, Mr Iwan Syahrir PhD, Dr. Praptono, Dr Rachmadi, Prof. Abdorrakhman Gintings PhD, Mr A. Hendra Sudjana, Mr. Mamat, Dr Nita Isaeni, Mrs. Esti Widyastuti, Mrs. Ana Budi K, Rohmi, Amar, and colleagues in Ditjen GTK, MoECRT.

Finally, I would like to thank Allah The Almighty, for letting me through all the difficulties, and to everyone who has supported me directly and indirectly in Indonesia and New Zealand.

"Indeed, in the creation of the heavens and the earth and the alternation of the day and night there are signs for people of reason" (Ali Imran : 190)

"Read! And your Lord is the Most Generous,
who taught by the pen, taught humanity what they knew not." (Al Alaq 3-5)

Table of Contents

List of Figures

List of Tables

Chapter 1 Inquiry-Based Learning

1.1 Introduction

Recently, educators and education researchers are calling for change. They argue that the twenty-first-century skills, such as **critical thinking**, problem solving, collaboration, motivation, persistence and communication can, and should, be taught and adopted through well-designed courses, beside the deep knowledge of a discipline and mastery of the scientific method ("The scientist of the future," 2015).

Inquiry-based education is believed to be effective in promoting communication and critical thinking skills, which are essential in the modern world (Chen, 2021; Magnussen, Ishida, & Itano, 2000; Thaiposri, Wannapiroon, & Sciences, 2015; Zain, 2018). Many reports highlight that inquiry-based learning (IBL) was found to be more effective than traditional cookbook experiments in promoting student engagement in learning in the laboratory (Acar Sesen & Tarhan, 2013; Wheeler, Clark, & Grisham, 2017). There are three types of student engagement: cognitive engagement, where students are engaged with the process and progressions of their learning; behavioural engagement, where students show they are ready and willing to learn; and emotional engagement, where students feel secure in their relationships with their teachers, classmates and the school (Furrer & Skinner, 2003; Voelkl, 1997). Implicitly, the New Zealand government highlighted the importance of using inquiry in their school curriculum policy:

'Students learn most effectively when they understand what they are learning, why they are learning it, and how they will be able to use their new learning. Effective teachers stimulate the curiosity of their students, require them to search for relevant information and ideas, and challenge them to use or apply what they discover in new contexts or in new ways. They look for opportunities to involve students directly in decisions relating to their own learning. This encourages them to see what they are doing as relevant and to take greater ownership of their own learning.' ("The New Zealand Curriculum," 2015).

Moreover, the American Chemical Society guidelines explicitly invite educators to use guided inquiry and collaborative learning since it is considered to be more effective than verification

experiments (Larive & Polik, 2008). In these guidelines, the advantages of using "inquiry-driven and open-ended investigations" were also identified for chemistry laboratory classes.

Although inquiry-based learning and collaboration have been shown to enhance learning in laboratory classes, little is known about how this is achieved. There are many ways to identify how students use communication skills and critical thinking skills in their learning. In laboratory class, students' communication and critical thinking skills can be captured from students' conversation. In students' conversation, critical thinking skills is reflected by their curiosity, by how and to what extent the students are posing questions. Students' conversations provide authentic evidence about their interest and their engagement in learning. However, little research has been conducted on how and to what extent students actually inquire. This study aimed to investigate the nature of student inquiry in an undergraduate biochemistry laboratory class at a New Zealand university through analysis of their conversations during laboratory classes.

1.2 Literature Review

1.2.1 What is inquiry?

Scientific inquiry itself is defined as activities in which students develop knowledge and understanding of scientific ideas, as well as an understanding of how scientists study the natural world. Inquiry is also believed to be a way of thought, a general process by which humans seek information or understanding.

Allen, Barker, and Ramsden (1986) compared the cookbook nature of verification experiments with the guided inquiry laboratory. They found that cookbook experiment can potentially inhibit intellectual stimulation as students were only asked to follow a prescribed procedure to produce a known answer as right and wrong. Allen et al. (1986) also found that even if the students thought the inquiry experiments were more difficult and frustrating than the standard verification experiments, the students ranked guided inquiry highly in terms of interest, development of analytical thinking ability, and problem solving.

1.2.2 The goals and the roles of inquiry

Pavelich and Abraham (1977) postulated three goals of inquiry-based learning: (1) to acquaint students with fundamental lab techniques and procedures; (2) to enhance students' thinking ability towards more abstract tasks; (3) to provide students with experiences of aspects of scientific inquiry: data interpretation, hypothesis formation and testing.

In inquiry, students are engaged to think about larger purposes of the investigation. It helps students to see the connection between their science ideas and experiences. Collins (1986) postulated that the inquiry, as a tool of cognitive apprenticeship, plays two distinct roles: (1) to enable students to implement their knowledge as strategies in different contexts and (2) to teach students questioning skills enabling them to learn and solve novel problems on their own.

Based on the paragraph above, students' critical thinking seem to be an important characteristic of inquiry, which has a strong interrelationship with the students' questioning skills. These skills, in particular questioning skills, can be enhanced through the teachers' involvement.

1.2.3 Teacher roles in inquiry-based learning

Vygotsky first introduced zone of proximal development, often abbreviated as ZPD, as the zone limit of learning possible by a student given the proper learning condition (Vygotsky, 2011). He believed that a student follows the teacher's example and gradually develops the ability to do certain tasks without help (Figure 1.1). This concept is relevant with the scaffolding concept where the students' learning can be guided by a teacher through giving the hardest task with scaffolding (Wood, Bruner, & Ross, 1976), that is through a series of steps which leads the student to the greatest learning gains within the ZPD. In inquiry-based learning, to guide students into a successful inquiry in a specific discipline, the teacher often gives positive interactions and poses focused questions in a specific knowledge that is required in the discipline.

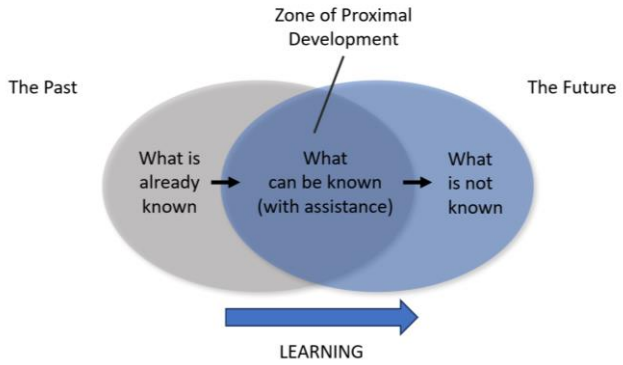

Figure 1.1. Vygotsky's zone of proximal development (ZPD)

Moreover, collaboration among students and teachers is increasingly seen as an important part in learning science. Collaboration among students and teachers, in many forms such as collaborative support (tutorial), peer-models, or small group, is used as a tool to provide an opportunity for explicit feedback and discussion of scientific concepts and reflection that promotes metacognition and self-regulation (Davis, 2003). Pajares (1996) suggested that peer tutors who are judged to be of similar ability can increase self-efficacy. In IBL, peer-tutoring can be done by sharing roles between students in a small group to accomplish an inquiry collaboratively.

1.2.4 IBL in higher education

There are shifts toward more inquiry-based classes occurring worldwide. In a survey conducted over a decade, the number of colleges using inquiry-based laboratory increased from 10% to 70% (Sundberg & Armstrong, 1993). However, most undergraduate laboratory activities can still be categorised as cookbook in nature (Buck, Bretz, & Towns, 2008), which is perhaps due to lack of definition in understanding IBL (Brown, Abell, Demir, & Schmidt, 2006). Moreover, in their study that involved faculty members who held an authentic and open inquiry, Brown et al. (2006) found that inquiry-based learning was seen as time-consuming, unstructured, student-directed, and was believed to be more appropriate for upper-level

science majors. Therefore, Buck et al. (2008) followed up the poor understanding of IBL by designing a quantitative rubric to characterize the level of inquiry in the undergraduate laboratory (Table 1.1). The rubric describes levels of students' independence on doing laboratory practices. At the top level, the authentic inquiry describes the highest level of inquiry where the students are highly engaged in constructing knowledge autonomously where the problem/question is for the student to design (Table 1.1, far right column). Posing questions by students is very challenging and reflects how interested the students are in learning and how deeply the students are engaged. Little research has been conducted on how students pose questions in an inquiry-based laboratory and to what extent the questions are posed by students.

Table 1.1. A rubric to characterise inquiry in the undergraduate laboratory

Far right: Characteristic	Level 0: Confirmation	Level ½: Structured	Level 1: Guided	Level 2: Open	Level 3: Authentic
Problem/Question	Provided	Provided	Provided	Provided	Not provided
Theory/Background	Provided	Provided	Provided	Provided	Not provided
Procedures/Design	Provided	Provided	Provided	Not provided	Not provided
Results analysis	Provided	Provided	Not provided	Not provided	Not provided
Results communication	Provided	Not provided	Not provided	Not provided	Not provided
Conclusions	Provided	Not provided	Not provided	Not provided	Not provided
More structure <----------->Less structure					

(Buck et al., 2008).

Although a protocol to help teachers to evaluate their classroom practice has been developed (Table 1.2), this protocol does not explain how teachers can analyse students' questions and help develop students' questioning to enhance their learning (Marshall, Smart, & Horton, 2010). Understanding on how the students are questioning is essential, not only for the teacher to improve their teaching skills, but also for the students to improve their learning.

Table 1.2. Descriptive rubric for discourse indicator (Marshall et al., 2010).

Indicator measured from discourse factors	Pre-inquiry	Developing inquiry	Proficient inquiry	Exemplary inquiry
1. Questioning level	Questioning rarely challenged students above the remembering level.	Questioning rarely challenged students above the understanding level.	Questioning challenged students up to application or analysis level.	Questioning challenged students at various levels, including at the analysis level or higher; level was varied to scaffold learning.
2. Complexity of questions	Questioning focused on one correct answer; typically short answer responses.	Questions focused mostly on one correct answer; some open response opportunities.	Questions challenged students to explain, reason, and/or justify.	Questions required students to explain, reason, and/or justify. Students were expected to critique others' responses.
3. Questioning ecology	Teacher lectured or engaged students in oral questioning that did not lead to discussion.	Teacher occasionally attempted to engage students in discussions or investigations but was not successful.	Teacher successfully engaged students in open-ended questions, discussions, and/or investigations.	Teacher consistently and effectively engaged students in open-ended questions, discussions, investigations, and/or reflections.
4. Communication pattern	Communication was controlled and directed by teacher and followed a didactic pattern.	Communication was typically controlled and directed by teacher with occasional input from other students; mostly didactic pattern.	Communication was often conversational with some student questions guiding the discussion.	Communication was consistently conversational with student questions often guiding the discussion.

1.2.5 Learning model and learning styles

Kolb (1984) experiential learning model is one of the most well-known models of learning in higher education (Figure 1.2). Kolb (1984) expanded on Dewey (1933) ideas and promoted a four-stage cycle that included active experimentation, reflective observation, actual experience, and abstract conception (Healey, Kneale, Bradbeer, Styles, & Area, 2005). Although learners can join the cycle at any stage, the stages must be completed in order. Kolb argued that the key to developing new understanding was reflective observation.

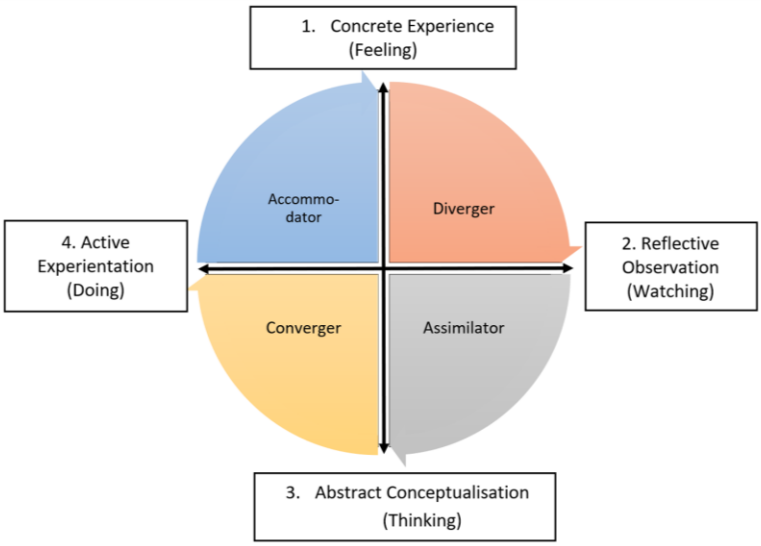

Figure 1.2. The experiential learning model and associated learning styles (Healey et al., 2005).

Concrete experience aims to create a concrete experience through doing. It means that it is not enough to watch other people do or read, instead we must do it ourselves to learn. Reflective observation means taking a step back from the act of doing to look at the bigger picture and review what we have just experienced. Tools to help us achieve reflective observation include giving our observations or being asked questions. Abstract conceptualisation means that we make sense of what we have just experienced by integrating the new information into what we already know. The final stage, active experimentation, happens when we consider how we will put what we have learned into practice.

The Kolb's learning styles are explained based on two dimensions. First, the east-west line is whether we prefer active experimentation so that means doing or whether we prefer reflective observations so watching. Secondly, the north-south access, is whether we prefer abstract conceptualisation basically thinking or concrete experience so feeling the experience.

Regarding the four learning styles, first we have ***diverger***. Diverger can see things from different perspectives. They prefer to watch rather than do. They prefer to collect information

and then solve the problem by using their imagination. Secondly, ***assimilator***. They will be more interested in the logic of a theory than actually its practical application. Assimilator enjoys ideas and theories, but is less interested in the people side of things.

Thirdly is ***converger***. Convergers enjoy ideas and theories, and they also enjoy using their knowledge to solve practical problems. Converger prefer to actually solve problems. They do enjoy the doing aspect but are not concerned with inter-personal issues. The last teaching style is ***accommodator***. They are hands-on learner, learning through doing, using their intuition and gut instinct to figure things out.

1.2.6 Bloom's Taxonomy

Bloom's taxonomy is a hierarchical structure that identifies thinking skills from low to high level. Bloom's Taxonomy was first published in 1956 by an educational psychologist, Benjamin Bloom (Bloom & Krathwohl, 2020). Then in 2001 it was revised by Krathwohl and experts from a group of cognitive psychologists, curriculum theorists and instructional researchers, and testing and assessment specialists (Anderson & Krathwohl, 2001). The results of this revision are what we know as the Revised Bloom's Taxonomy. Revisions are made only in the cognitive domain using verbs.

Bloom's taxonomy is divided into three domains: cognitive, affective and psychomotor. These three domains are important in learning. However, the cognitive domain as explained above is more widely used. Here, in the revised version of Bloom's Taxonomy, types of knowledge are divided into four domains:

- Facts: information that shows phenomena in learning
- Conceptual: includes categories, structures, and theories
- Procedures: how to use specific techniques and methods, and when to use them
- Metacognitive: decision strategies, self-knowledge, and "thinking about thinking"

Of the four types of knowledge, they are then divided into six levels of learning (Figure 1.3). In this revision of Bloom's taxonomy, each level shows more active verbs to describe what students must do. This level of knowledge is described in the form of a pyramid, which the basic level is described as broader than the level above it. This suggests that more people

persist at these lower levels of knowledge. Bloom's taxonomy revision verbs are described as follows:

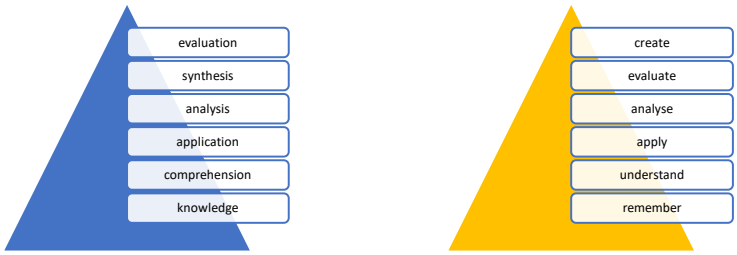

Bloom’s taxonomy Revised Bloom’s taxonomy

Figure 1.3. Comparison of Bloom's taxonomy and its revision in the cognitive domain

Bloom's taxonomy revision verbs are described as follows:

Remember: the most basic of learning (although it can involve complex information). At this level, students may know key terminology for a particular subject, relevant facts and figures, systems or theories that others have developed.

Understand: people know more about what the information actually means.

Apply: at this level, knowledge is used in new ways and applied to solve more complex problems.

Analyse: involves breaking information into pieces to examine them individually and to see how the information relates to each other.

Evaluate: people make judgments about what they have discovered so far. This level allows them to make recommendations or suggest innovative ideas.

Create: at this final level, people can rearrange the information they have and then combine it with the information they have obtained and then create something new.

1.2.7 Objectives

The purpose of this study was to investigate the extent to which the students are actually inquiring in biochemistry laboratories. It was proposed to do this through analysing the student groups' conversations and addressing the following questions:

1. How much of the student conversation is inquiry?
2. What is the nature of the questions asked by students and how do they respond to these?
3. What implications do the findings have for tertiary science educational practice?
4. How could lecturers further encourage inquiry?

1.3 Methods

1.3.1 Context

The institution in which a final-year biochemistry course unit investigated was located at Massey University, Palmerston North, New Zealand. This course, 122.322 (Protein Structure and Function), was chosen as the laboratory was intended to form a coherent inquiry-led investigation. The course in total consisted of 24 lectures and 6 laboratory sessions. The researcher focused on three lab sessions that constituted an integrated experiment on a single topic about protein purification of lactate dehydrogenase (LDH). To enrol in this course students needed to have passed 122.232 (Protein Biochemistry).

In this experiment students assessed the relative effectiveness of two different purification procedures for the enzyme LDH from an extract of chicken breast muscle. Briefly, the first step in the purification of LDH from this extract used ammonium sulfate precipitation to separate the enzyme from some of the other proteins present. At this stage the preparation was divided into portions that were purified by three methods - ion exchange chromatography, affinity elution from an ion exchange adsorbent, and dye ligand chromatography with each group of students assessing the relative effectiveness of two of these procedures. In all of these procedures the purity of the enzyme was assessed at each stage by measuring its specific activity and by examining the proteins present using gel electrophoresis.

The prerequisite course, Protein Biochemistry (122.232), had previously introduced protein and enzyme kinetics assays, which meant that some of the techniques were relatively familiar to the students. In addition, the lectures and laboratories at this time were designed to be

complementary. To provide students with the opportunity to simulate protein purification discussed in lectures prior to the actual experiment, a virtual (computer-based) laboratory on protein purification was also introduced and held before the experimental laboratory classes.

Topics and skills covered in this laboratory included:

- Solution preparations and dilutions
- SDS PAGE
- Three chromatographic techniques for protein purification
- Enzyme activity assay
- Recording data and managing lab work (this was often confounded by lack of understanding or misinterpretation and by technical problems on experiments)
- Analysing data
- Critical thinking (including determining what constitutes evidence and debate)

From the teachers' perspective, this laboratory focussed on:

- Teacher guided inquiry
- Answers with understanding
- Concepts
- Student-staff interactions

1.3.2 Participants

The participants were students enrolled in, and the staff delivering, the paper 122.322 (Protein Structure and Function) at Massey University, Palmerston North in 2013. A total of 12 students were enrolled in this course. Only one student came from a migrant background and there were no international students. For the LDH laboratory exercise, the students were grouped into threes, making four groups in total. The students were given the opportunity to choose their group themselves. Students worked in three same-sex groups and one mixed-sex group, which did not change during the three laboratory sessions.

The study involved three staff delivering the 122.322 laboratory classes. Two were academic staff (senior lecturers) in biochemistry and structural biology. The third member of staff was a teaching technician, who attended all the laboratory sessions. As the academic staff shared

the supervision role, there were at least two members of staff in each session. During laboratory work, the staff were responsible for supervising the work of all four groups of students.

1.3.3 Data gathering

Recording of Group Conversation

The conversations within each group of three students in 122.322 (Protein Structure and Function) in three laboratory sessions were recorded as unobtrusively as possible using digital voice recorders in weeks 2, 3, and 4 of the first semester in 2013. All of the students and staff agreed to participate voluntarily in this research (100% response rate). During laboratory classes, one voice-recorder was placed between each group of three students (four groups) and a total of 84 h of voice-recording was made. Participants were assured of confidentiality of the recordings as part of the ethical approval process obtained from Massey University Human Ethics Committee (MUHEC) and written consent was obtained from participating students and staff. A transcriber with confidentiality agreement was also hired professionally. These recordings were the main data source.

The conversation recordings predominantly came from students talking. This was much harder to transcribe than when supervisors were talking, as students tended to speak softly with their peers and there was considerable background noise from other groups talking and equipment sounds. While the students were doing laboratory work, the staff walked around to guide and supervise the students in their groups. Therefore, the staff voices popped up intermittently during the recordings.

Questionnaire

After the completion of the lab work, student and staff were invited to complete a written questionnaire. The views of individual students and staff were sought on various aspects of the course, including what they found most interesting and challenging (See appendix for questionnaires). Two thirds of student questionnaires were completed from each students'

group, and all the staff returned their completed questionnaire. So, we have eight student questionnaires and 3 staff questionnaires collected, which have been analysed.

1.3.4 Analysis

The recordings were transcribed and the transcripts were analysed with the aid of NVivo qualitative analysis software. In the first stage of the analysis, key themes were identified. This method enables researchers to conceptualise their data by discovering and naming themes/categories that emerged as repeatedly salient in the data. Each of the categories that emerged from the laboratory conversation was given a name. The analysis initially focused on questions that students asked during conversations when they were working in groups. A second and more intensive analysis followed, seeking to systematically substantiate and refine themes initially identified. The final stage of analysis concerned the manner of student's conversation. As this was a long conversation comprised of multiple topics over multiple sessions between multiple people involving students and staff, the analysis was also done by looking at who initiated and who responded to a question in a particular conversation and asking why the question was initiated and responded to in this way.

Questionnaire responses were analysed for themes and research findings compared with those from the groups' conversation in the laboratory.

1.4 Results and Findings

1.4.1 Preliminary study

A self-reflection as a student perspective when sitting in an undergraduate biochemistry laboratory prior to research in inquiry-based learning

Investigating the students' conversations from voice recordings alone without any class observation is more challenging compared to analysing the conversations from video recordings: we need to understand the content and the context of the topics of what the students are talking about in the laboratory class.

This study took place in the Biochemistry laboratory, an experiment in the course 123.322 Protein Structure and Function, more specifically about protein purification, which is also one of my research foci in my PhD study. However, this still did not provide enough context. In order to understand the content and the context of what the students were talking about from the voice recording, I needed to experience the environment to learn the culture as a student and the context in protein purification. Having a background knowledge of being a student in the class before conducting the research became necessary. This was reached by doing a reflective journal as a student, which was conducted one year before data collection began. What I have here is a journal that reflects on how I am reacting to the situation as a student and an understanding of the student tradition. In order to do a self-reflection in the laboratory classes, it was important for me to focus only on my own learning as a student and to avoid undertaking observation and evaluation due to ethical constraints on this project. It was also important to avoid correcting student mistakes directly, but to behave as a student group peer by helping them to think and to find out the answer by themselves by questioning.

The situation of academic activities prior to the laboratory work

The experiment that I investigated is entitled 'Purification of Lactate Dehydrogenase (LDH)'. The experiment was carried out consecutively in three weeks in week two, three, and four of the course (See Table 1.3) Prior to this laboratory, there were three lectures and one virtual lab which I attended. The first lecture discussed advanced protein biochemistry: amino acid, polypeptide, chemical and physical interactions, and protein folding. The second and third lectures talked about chromatography for protein purification: types, characteristics, and applications. A virtual lab was delivered on Wednesday in week 1. In the computer lab, I learnt how to purify protein virtually by combining some alternative techniques in order to get the most effective purification strategy to obtain a pure protein. The software also provided information about techniques in addition to chromatography, such as salt precipitation, and it provided visualisation of the SDS PAGE of my results, as well as the amount of protein recovered in each step. Therefore, we could simulate the process of finding the most effective protein purification strategy in a simple and interesting manner.

Table 1.3. The timetable of the laboratory work in protein purification of LDH.

Week	Day	Lecture/Laboratory
1	Monday	Lecture 1
	Wednesday	Virtual Lab
	Friday	Lecture 2
2	Monday	Lecture 3
	Wednesday	Lab 1: Protein Purification LDH
3	Wednesday	Lab 2: Protein Purification LDH
4	Wednesday	Lab 3: Protein Purification LDH

The students' activities when doing inquiry-based biochemistry laboratory on purification of LDH

The laboratory: purification of lactate dehydrogenase (LDH) was believed to be a semi-guided inquiry-based experience where the students were asked to purify LDH protein enzyme with a multi-step purification process but ending by two different chromatography columns they had chosen.

In this experiment the LDH was extracted from chicken breast muscle. The breast chicken was stirred with the extraction buffer and centrifuged to get the supernatant liquid which contained the LDH. The first step of the purification was separating the LDH by ammonium sulfate precipitation. The preparation was divided into two portions that were subsequently purified separately by two of three different columns: ion exchange chromatography, affinity elution from an ion exchange adsorbent, and dye ligand chromatography. To assess the relative effectiveness of these procedures, the specific activities of the enzyme from these two procedures were compared. The challenge of this experiment was that the SDS PAGE, which used to visualise the purity of protein, was only performed once at the end of the labs. Therefore, the students needed to track the presence of the protein by monitoring the specific activity in each stage by assessing two variables: the activity of the LDH, and protein yield.

What I learnt from the biochemistry aspect

In a group, the three students were asked to accomplish the experiment in three consecutive three-hour periods by sharing the tasks between the students. For example, on Day 1, the first

task included sample preparation, centrifugation, and carrying out ammonium sulfate fractionation of LDH, and dialysing ammonium sulfate fractions. The second task included preparation of two protein standard lines, diluting protein samples and standards, and measuring the absorbance of protein samples. The third task included practising the assay of LDH and carrying out assays on fractions from all steps. Sharing the roles did not mean that students do not need to know and understand the other roles, but it did mean that collaborative practices helped the group to accomplish multiple tasks in a very limited time. Practically, we helped each other when one task needed another person to complete. This sharing of roles was also applied in Day 2, but the roles were changed to make sure that we had different experiences in every single day. In Day 2, the second and third tasks of Day 1 were met again, plus a new task was introduced, which was running two of the three listed chromatographic procedures to further purify the LDH dialysis fraction. In the Day 3, there were fewer tasks than on the other days. The protein from all fractions in every single purification stage was concentrated and analysed by denaturing SDS gel electrophoresis. Finally all the results were tabulated and compared with the results from other groups using the different chromatographic procedure.

During the experiment, several problems were encountered by my group. The first was the justification to make two linear standard lines of the BSA protein at two different concentration ranges at two wavelengths. Regarding the enzyme assays, we initially struggled to obtain the slope corresponding to the initial rate. The problems commonly caused by lack of well-managed laboratory practices, such as labelling, calculations, and lack of experience and self-confidence in using standard experimental tools such as pipetting and diluting. The other problem was taking notes, collecting data into our laboratory books, but at the same time we needed to accomplish the laboratory work in a limited time. Using the kinetics software to analyse assay data was also challenging as this was a relatively new skill.

I found that there was a gap in interpreting the chromatograms. Indeed, this part was absolutely important to answer the big question of the inquiry about the most effective chromatographic procedure for LDH purification. For example, to understand that the *y* axis constitutes absorbance at 280 nm, which corresponds to the protein yield in each fraction (*x* function). The highest peak does not necessarily correspond to the fraction that contains the LDH. The presence of LDH needed to be tracked by LDH assays. Furthermore, the purest

fraction could be checked by the highest value of specific activity as the ratio of the activity value divided by the protein yield.

The most critical and curious part I learnt in Day 3 was the calculation of the results and tabulating these into the table that had been provided in lab manual. This table summarised all the results and the experimental process of purification of LDH, as well as helping us to answer the big question of which chromatographic procedure for obtaining pure LDH was the more effective.

What I learnt from the educational aspect

The arrangement of the three lectures and a virtual laboratory prior to experiment in purification of LDH was very helpful for me to prepare the basic concepts and fundamentals of protein technology. Even though the concept of protein purification had not been introduced in Lecture 1, the teacher gave an introduction about what was going to happen in the laboratory in the weeks after, the principles and technical aspects of protein purification and students were also given the opportunity to do simulations of protein purification using the virtual lab software.

Overall, this experiment was very challenging and I was afraid if my group would not have pure protein in the end. Most students should be very excited to know the results, especially to see the SDS gel. It was never known if the protein purified truly contained the LDH until it was shown exactly in the SDS PAGE since the molecular weight of the LDH was known, as the SDS PAGE results were available only the day after Day 3 in the laboratory. In other words, the only evidence we had in Day 3 to justify which purification strategy was the more effective was based on the value of specific activity, which all came from the LDH assays, which in turn required comprehensive interpretation, accuracy, dexterity, and hands-on skills. In this part, I will not describe in detail the education aspect except on the students' conversations analysis at the part of research. As mentioned in the first section, this part was intended to help the investigator to understand the context of what the students were talking about and discussing during the lab, either between their peers or with the teacher.

1.4.2 Data scope

The conversations within groups of third-year students investigating protein biochemistry during three laboratory sessions were recorded. A total of 12 students participated in this study and they were distributed into four self-selected groups. The conversations from each of the three student groups were analysed. Three of the four groups' conversations were chosen based on the richness of data containing the most conversations to be transcribed as considering the limitation of the research funding. After the laboratory sessions finished, the students as well as the staff answered an open-ended questionnaire to be used as secondary data (the main data are student conversations). Findings from the questionnaire help to confirm whether the student can following the general ideas of the lab or not, also the student and the staff confirmed at which part of the laboratory work they were more interested and challenged. Overall, what they explained is consistent with what was recorded, in terms of the frequency of the themes emerged in their talks. From the recordings, there was a total of 9 documents of conversations transcribed, each consisting of 150-200 pages. Here, NVivo was used to help analyse the conversations for categories associated with inquiry, emerging from the data (e.g. questionnaire, lab manual), or derived from the literature.

1.4.3 How much inquiry is there in students' conversations?

Based on Buck et al. (2008), which designed to characterise the level of inquiry in the undergraduate laboratory, the LDH labs observed in this research have characteristics of the inquiry-based laboratory at the Level 2 since the problem/question and the theory/background are provided. However, the procedure, the results' analysis, the results' communication and the conclusions are not specified.

As the research was purposed to investigate the extent to which the students are actually inquiring in biochemistry laboratories by analysing the students' group conversations, the Marshall descriptive rubric (Marshall et al., 2010) is more applicable. Based on the discourse indicator in the Marshall descriptive rubric, the inquiry-based learning of the LDH is at the top level, an exemplary inquiry level. The evidence of the students' conversations shows that questioning challenged students at various levels, including at the analysis level or higher, and the level was varied to scaffold learning. From the recording when the teachers were giving the introduction in the opening lab, as well as from the lab manual, the questions required

students to explain, reason and/or justify with evidence their results. As the students from a group were asked to share their results to the other groups, the students were allowed to give feedback to the results or to critique others' responses during the labs. Captured from the conversation timeline during the labs and from the conversations' transcript, the teachers consistently and effectively engaged students in open-ended questions, discussions, investigations and reflections (see Fig. 1.3 to 1.5 for the time lines). Communication was consistently conversational with student questions often guiding the discussion.

The rubric shows that the measure of IBL's success in the ecological aspect of asking in IBL can be seen from the extent to which the teacher tries to involve students in discussions and investigations by looking at two indicators. The first indicator was the intensity of the teacher's role in guiding students in groups. The second indicator was the extent that the students were involved in discussion, investigation and reflection. In this study, the level of inquiry and the two indicators mentioned are suggested by evidence as follows:

1. *Discourse timeline.* This graph shows traces of when each individual was involved in a conversation by leaving a trail of spots on each timeframe on the x-axis. The results showed how the teacher was actively and consistently involved in guiding each group, and how students carried out intense inquiry in conversations with other students in one group, and sometimes they also had discussions with other groups. (See Fig. 1.3 to 1.5).

2. *Word-cloud*. This graphical representation visualises words' frequency that gives greater prominence to words that appear more frequently in a source text. Each word is counted and visualised with the font size representing the frequency with which the word appears, with analysis criteria that can be set in the software. The words that often appeared from each group are relevant to the keywords in the inquiry questions in Table 1.5.

1.4.4 Discourse timeline

The discourse timelines for the three groups are shown in Figures 1.4 to 1.6 below. They show a high level of conversation among the students, frequent engagement with the teachers and limited engagement with the other groups.

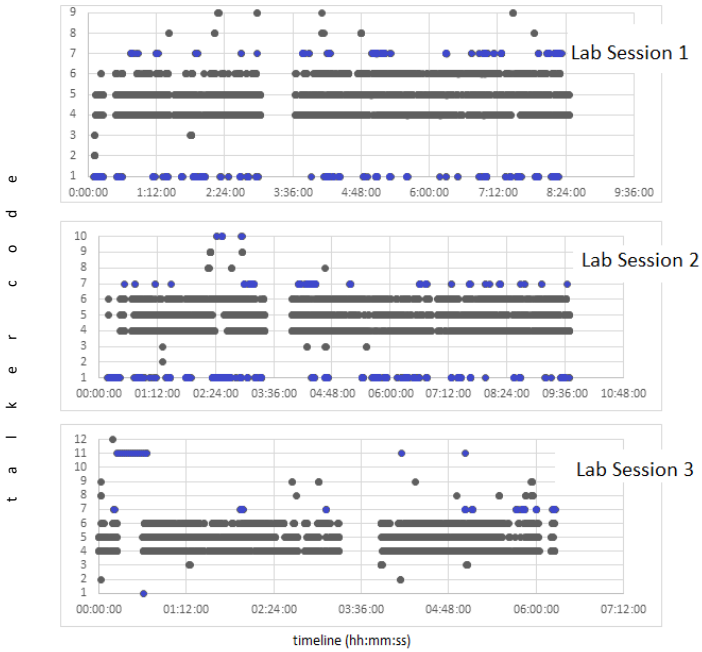

Figure 1.4. Discourse time-line for Group 1.

There are 3 students (black) in group 1: numbered 4, 5, and 6. There are 4 students (black) from other group involved in the recording, numbered 2, 3, 8, and 9. There are four teachers/staff (blue) voices recorded: numbered 1 (present in days 1 and 2), numbered 11 (present at day 3), numbered 7 (present at every day 1 to 3), and numbered 10 (at day 2).

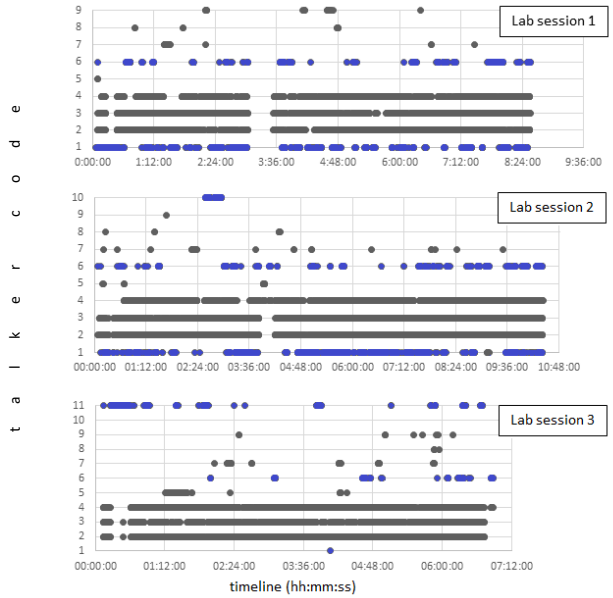

Figure 1.5. Discourse timeline for Group 2.

There are 3 students (black) in group 2 : numbered 2, 3 and 4. There are 4 students from other group (black) involved in the recording, numbered 5, 7, 8 and 9. There are four teachers/staff (blue) voices recorded: numbered 1 (present in days 1 and 2), numbered 11 (present at day 3), numbered 7 (present at every day 1 to 3), and numbered 10 (at day 2).

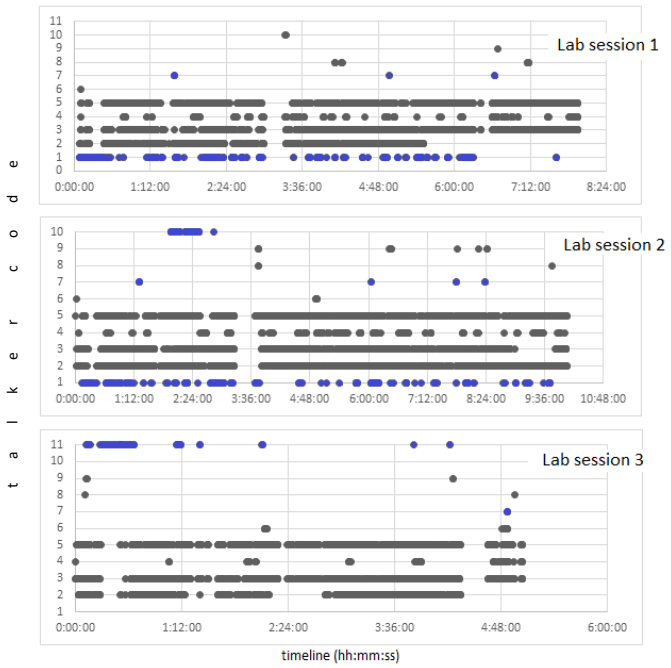

Figure 1.6. Discourse time line for Group 3.

There are 3 students (black) in group 3: number 2, 3 and 5. There are 4 students (black) from other group involved in the recording, numbered 5, 7, 8 and 9. There are four teachers/staff (blue) voices recorded: numbered 1 (present in days 1 and 2), numbered 11 (present at day 3), numbered 7 (present at every day 1 to 3), and numbered 10 (at day 2).

1.4.5 Word-cloud

The word-clouds for three weeks over the three groups conversations are shown in Figure 1.7 below. Word-Clouds visualise words' frequency in students' conversations. They reveal a clear focus on how to prepare solutions with words such as dilution and concentration. At day two, they reveal a clear focus on activity and dilute. At day three, T they reveal a clear focus on concentration, protein, and gel. These figures support the more detailed analysis described later.

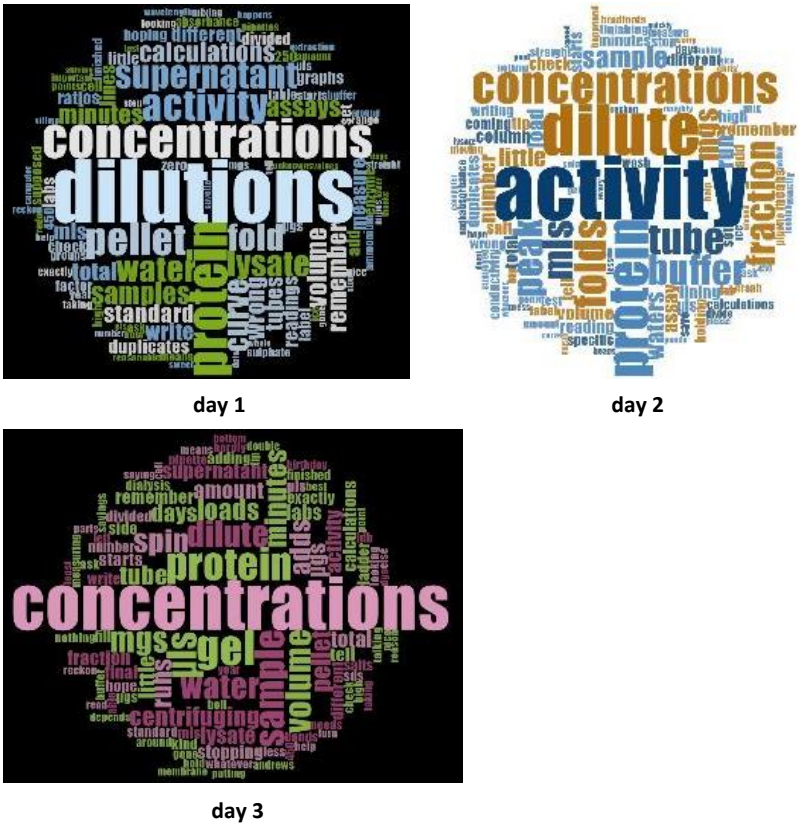

day 1 **day 2**

day 3

Figure 1.7. The progress is based on the word cloud from day 1 to day 3.

Day 1 (top), Day 2 (middle), and Day 3 (bottom). Greater prominence is given by font size to words that appear more frequently in the over three lab sessions.

The conversation transcript and the word cloud advise that in the beginning, the students involved in trivial improvements due to struggling with calculation, diluting tasks, and misslabelling. The word frequency of *activity* increased in day 2 indicating that the students became more focused on achieving the goal, and meaning that the level of students' inquiry is developed (Table 1.4). They learn a new instrument, AKTA, and they have to collect tubes or fractions containing the desired protein. Here they have to focus on the activity. The number of mentions of *specific activity* words is ~10 times higher than that of the day 1. At

day 3, students ran SDS-PAGE and related discussion. They adjusted the protein concentration of each stage of purification step to give proportional band for better visualisation of the gel based on protein purity.

Table 1.4. The top 30 most talked-about words in the lab conversations.

Day 1			Day 2			Day 3		
Word	Count	Weighted Percentage (%)	Word	Count	Weighted Percentage (%)	Word	Count	Weighted Percentage (%)
dilutions	570	0.66	activity	772	0.60	concentrations	553	0.71
concentrations	356	0.41	dilute	611	0.47	gel	342	0.44
protein	355	0.41	protein	490	0.38	protein	312	0.40
pellet	283	0.33	concentrations	447	0.35	sample	281	0.36
activity	279	0.32	folds	394	0.30	µls	280	0.36
supernatant	239	0.28	tube	378	0.29	volume	243	0.31
fold	235	0.27	mls	362	0.28	dilute	242	0.31
water	223	0.26	buffer	360	0.28	water	239	0.31
lysate	219	0.25	peak	357	0.28	mgs	234	0.30
curve	209	0.24	fraction	352	0.27	spin	215	0.28
samples	182	0.21	mgs	272	0.21	minutes	198	0.26
calculations	170	0.20	sample	254	0.20	adds	185	0.24
volume	170	0.20	little	223	0.17	loads	185	0.24
assays	166	0.19	waters	216	0.17	runs	173	0.22
remember	163	0.19	run	211	0.16	tube	172	0.22
minutes	161	0.19	load	195	0.15	pellet	168	0.22
standard	156	0.18	number	191	0.15	centrifuging	167	0.22
Total	153	0.18	assay	180	0.14	days	152	0.20
tubes	148	0.17	volume	166	0.13	µgs	146	0.19
Write	146	0.17	column	157	0.12	amount	139	0.18
mLs	138	0.16	lining	152	0.12	little	138	0.18
lines	126	0.15	remember	152	0.12	lysate	137	0.18
measure	124	0.14	total	151	0.12	total	135	0.17
different	122	0.14	reading	150	0.12	supernatant	127	0.16
readings	121	0.14	starts	149	0.12	activity	124	0.16
duplicates	113	0.13	tip	148	0.11	labs	121	0.16
ratios	107	0.12	check	147	0.11	fraction	113	0.15
labs	104	0.12	salt	145	0.11	starts	105	0.14
add	103	0.12	duplicates	144	0.11	tell	105	0.14
graphs	99	0.11	tell	142	0.11	remember	103	0.13

1.4.6 Analysis of teachers' talks and questions

Transcript of teachers' introduction talk

These were given at the beginning of the labs in front of the lab class.

Lab session 1

"OK, so has everybody looked at the lab manual? Yes. You've all read your lab? I am sure that you have. So basically, we are carrying on from last year but we are not going to tell you all the things that you need to do, like how to do your protein concentrations and how to do your assays. We will give you some guidance for your assays but your protein concentrations remember that you have to organise these. …

What I am going to do is I am going to give you your lab talk after we've commenced because the first is taking the chicken tissue and stirring it for 20 minutes in buffer and you've got to do that with a glass rod and sit there doing it so essentially we will do it, um, I will talk to you while you are doing it. Ok, so, the first thing is, you got to take about 20 g of tissue, it doesn't matter, it doesn't, don't worry about weighing it out exactly, as long as you know the weight, it can be plus or minus 5. Ok. I am happy with that, possibly even better on the higher side because you'll have more enzyme, but it can be plus or minus 5. You will have to join a group.

So, these groups of 3 are now the groups, that you are going to be in for the whole lactate dehydrogenase lab, and you can't change ok so everybody's got to stay together. The main reason for this is that you are going to have a little competition to see who can get the best yield. So you are going to take your experiment right through to the end. And I like doing this, and take, and instead of combining things, take each individual extraction and keep it within your group. So at the end you are going to tally up what you would have got if you had used the method all the way through. Now remember that we are going to swap the chromatography, we are going to do 2 types of chromatography and because you are going to put on a known amount, you can relate that back to your starting material.

Does everyone get what I mean? So, you're not going to purify your whole amount of protein so you've got to work back if you did purify the whole amount you would have got more enzyme. OK. So if you take 10% of your, of the protein, that you extract and you purify that through, that means you would have got, and if you divide that by 0.1 you get the full amount. Ok. So what I want you to do, is to go and, the most important thing I am going to say here is you have to keep everything cold. You must keep all your samples on ice even the samples that you're going to keep all the way through. And you are going to start taking samples from when you get your clarified cell lysate which will be after the segregation step. So I want you to go and weigh out approximately 20 g of tissue, approximately. And then I want you to bring your ice bucket, there's your extraction buffer, I want you to put it in a beaker, put in your extraction buffer, all bring your ice buckets and come up the front and we will go through what's important in the lab. So, one person from each group go and weigh out.

So the others of you remember that you are going to have to do lots of protein assays to measure, to do a standard curve so I would be labeling tubes while you wait if I were you. So start labeling your tubes for your standard curve.

Ok so this is a lab which goes over 3 days and there are things that….

It requires a lot of thought from you guys because we can't guarantee that it will go the way that it is written ok so you need to use your common sense and remember that we talked about this in lectures. One of the reasons, one of the things that you need to fill in the table, because it will tell you if your have gone wrong in any assay…

Essentially, there are 2 things you've got to do today. You are going to a crude fractionation, so that's a just a rough extraction of the enzyme, and you are going to do some assays.

And the 2 assays you are going to do are (1) protein concentration, now you are going to use the Coomassie blue dye, which is, and do a range of assays based on that. we are measuring at 2 different wavelengths so you will see that you are doing 450 nm and 590 nm. Now remember with Coomassie, is the plastic can get start to get stained. So don't let them get too stained but start at the most dilute and work you way up and if you have to wash with ethanol…

Ok so the next thing are (2) the activity assays. So there are 2 specs on each station, the one without the computer is for the protein concentration the one with the computer is for the assay LDH and we will just remind you how to use those before you start the experiment…

Biggest mistakes in this lab is that people forget what dilutions they are so you must keep a record. Even if you photocopy this and get several sheets or have a piece of paper, whatever, make yourself a table like this. Write down on the tubes what the dilution is, so if your dilution in the eppendorf, write its 1/10, 1/100, 1/1000 whatever because believe me it is really easy to forget. Try and use buffer to dilute for the assay, for the protein concentrations use water…

Then you write in here the dilution factor and work out your concentration. The most important thing is this one, which is total protein. So this is your concentrated concentration times the volume."

Lab session 2

"So today we are going to take the, our 80% pellet and -NAME STAFF- has dialysed that, he's dialysed it against the loading buffer that you are loading onto your column. And we've already programmed those for you, … So you need to do your first, everyone is going to do their ion-exchange, which is, there are 3 methods in your book. Everybody will do the ion exchange, I want you guys here to do the blue affinity, the blue column. And I want you 2 groups to do the affinity elution. Ok. So you'll do, you'll each do 2 but then you've got to swap the results with the other group. OK, to get, um, or so you can report on other groups….

Ok, so once you have got your sample ready, what you're going to do then is you're going to, um, you're going to put, start your chromatography and hopefully we will get the chromatography started and, um, we have automatic fractioning. These are the AKTA, they're AKTA prime basics. This is the little column that you will be using, here. And, um, you are going to load your sample from the pump. So this is where we are going to load from, this is our loading, um, um, pump. And the most important thing about these is that you get rid of all the liquid. …

Um, so, the first thing to do is to get your sample ready, to check, so you've got an, again you're going to, all your fractions that come off, so remember they are gonna come off as peaks, coz this has a, um in here we've got a little 280 detector, so it's actually reading the absorbance at 280 as the flow comes of the column and through, um, and is eluted. The waste goes into here and there are 3 different, um, lines here. Fractions are collected in here, and you are going to use, um, 5 mL. Ok…

So what you will get is you will get a series of peaks coming off, something like this. The first thing you do is you just take the apex of the peak and you check for activity. Ok. Once you know that this peak here is your active one, say, then you want to test all the fractions around it because you want to see where the start is and where the end is.

When you do your protein, you might find for example that this is your 280, and your activity is something like this. So your activity's on the tail of that. And you are going to pool based on activity. So you have to pool, and you have to work out specific activity, so you can see that this here will have a much lower specific activity than this point here. So you want to pool your specific activity, so you've got to test each fraction."

Lab session 3

"Ok day 3 of the LDH lab. Moment of truth. You get to see how good your protein concentration measurements are when we look at your gels. So, today's an analysis of the practical so, as you've undergone a fractionation and purification on day 1 and 2. You have been collecting samples from different stages, you've been measuring the activity, you've been measuring the total protein concentration, remember you're not just measuring the concentration of LDH, its all the protein present in that sample at the time. And if your purification has been successful, then you should see your specific activity, which is the ratio of your activity to your total protein, increasing. Because hopefully you're keeping the activity, or as much as you possibly can and that total protein is decreasing as you purify away everything that isn't LDH. So specific activity is one really good measure for that. It doesn't tell you the identity of course. But sometimes you get a bit of an idea from molecular weight. So, that/s what

we are going to do today, so it should be reasonably straightforward, you've all run SDS PAGE gels before. …"

Questions written at the lab manual.

From your LDH assays and the volumes measured, calculate the total activities and yields (%) of LDH at each stage of the purification on Days 1 and 2. Calculate the specific activities (μmoles / minute / mg of protein) of LDH in the tissue extract and calculate the purification and total yield for the whole process. Tabulate your results.

To help you follow your results fill out the table overleaf. The table template should be available to download from Stream. Remember that the total activity at any step cannot be greater than that of the step before it. Likewise you cannot make protein. If you find your results do not make sense, you may have to repeat some measurements.

Provide a photograph of the bands revealed by staining the gel after electrophoresis of the samples you saved at various stages of the purifications and comment on what was disclosed in relation to the data you obtained on days 1 and 2. Determine the Mw of LDH by calculation of a relative mobility standard curve.

Discuss your results in terms of the gel analyses and the specific activities measured. Discuss the different methods used, their effectiveness, in terms of yield and purity.

1.4.7 The nature of students' questioning

How questioning is generated

The characteristics of students' conversations in a group in a science laboratory with IBL are unique. Here, the students' conversations were essentially non-stop from the start to the end of the laboratory session. The conversations in the lab were predominantly between students, informal, relaxed and natural. The conversations also captured that the staff often encouraged the students to actively participate in their group. The staff walked around from one group to another group, observed the students, posed a question if the student was doing the lab work erroneously, and monitored students' progress until the end.

There are 1680 pages of transcripts analysed by using NVivo version 10. Key themes (nodes) identified in the first step have various topics as below with one example of conversation for each theme (node). Key themes that were not analysed, as not directly relevant to the experiment being conducted.

Key themes that were analysed included critical thinking and applying theory into practice: Without prompting, a group of students discussed how the centrifuge works including factors of radius, speed, gravitation, time length, to the separation of proteins and membrane which have different molecular weight. This discussion shows how strongly the students' prior learning lead the inquiry-based learning success.

Enzyme assay and calculations. There are very many conversations between students related to the enzyme assay and associated calculations. Without knowing in which fraction the enzyme of interest belonged, the students realised that they had to do the activity assays carefully and to do the calculation for its specific activity, including determining protein concentrations. Otherwise, they will lose the desired protein, LDH enzyme.

Dilution. From the conversations, I found, surprisingly, that the students had difficulties making dilutions, and, unfortunately, mistakes were made repeatedly. Some students confused the principle of dilution, but some students understood. The students who understood, mentioned the formula. Sometimes, however, they still made mistakes, and used the formula in a complicated way. Sometimes they mixed different units of concentrations or volumes in calculations. However, students learn from their mistakes. In Group 1 transcripts, word 'mistake' were only found many times in lab session 1 only, mentioned by both students and staff.

Lab management. It was also found in conversation that mislabelling of the sample tubes was a common mistake among the students. Some students simply numbered their samples and then forgot what protein was associated with a particular sample number, especially when doing dilution for protein assays. Staff shared tips that there were more practical ways, such as labelling a dilution factor and purification step.

"Biggest mistakes in this lab is that people forget what dilutions they made. So you must keep a record… Write down on the tubes what the dilution is, so if your dilution in the eppendorf, write its 1 in 10, 1 in 100, 1in 1000 whatever because believe me it is really easy to forget."

Following and understanding a procedure. Unlike traditional laboratory, in inquiry-based learning the procedure information was limited and protocol was not mentioned in detail. In the conversations, the students discussed how to use Spins and Vivaspin centrifugal microconcentrators to desalt protein sample for SDS PAGE analysis and how to do it efficiently (faster). Again, the problems with dilutions also applied here.

Connect science with daily life. For example, there was a conversation between students in one group explaining to his peer, used the analogy of desalting high protein concentration samples using a microcentrifuge with washing towels using washing machine. The process requires more time as those retain more water.

Chromatography. In one conversation, a team got a chromatography fraction with a nice peak, not only based on its absorbance at 280 nm, but with the evidence of its specific activity. Then they collected that fraction and added it to another fraction that has also similar specific activity value. Immediately the teacher came and suggested to stop the machine. Then a student asked why they had to stop while the absorbance remains so high. The teacher reminds that the sample also contains NADH which absorbs at 340 nm. The student then had to decide whether the purification ends or not based on the chromatogram reading.

Problem solving. When the reading of spectrophotometer was inconsistent, a student suggested to his peer to use other cuvete as a substances might still left in it. Otherwise, he suggested washing the cuvette properly with ethanol and re-auto zero the spectrometer.

Publication or scientific communication. Sequencing samples for SDS PAGE analysis a common sense but this is essential to produce a high quality of publication as a scientist. The lane sequence would make sense if the student having a good understanding of the purification step process to communicate or publish their lab experiment results in an easy way. The challenge was that 10 lanes available per group.

Leadership. In the conversation it is revealed that there is always a student in a group who has better leadership than others. He/she naturally dares to take risks and distribute tasks to the team to meet the targets or time. In average, they had better lab skills, but it does not mean

that he/she is better in everything. Sometimes the other student has better data analysis and interpretation skills.

Data interpretation. The conversation between two students below is a good example of how skills in analyzing and interpreting data become important to achieve the main goal in inquiry-based learning. These data become evidence and the basis for deciding which protein fractions to collect. These students

S1 Look! How far those 2 are off!
S3 In a good way or a bad way?
S1 Bad way.
S1 Alright, um, we'd have to get it up to like 2, so that would be, it would be like 3 concentrations, so. We probably don't want to, how many of these do we want to do. Um. What's the call guys do we want to do 16? It's got like about 0.4 mgs/mL. We'll have to concentrate it like 4 times.
S2 But the activity?
S1 The activity's just not.
S2 Yeah!
S2 Compared to the others
S1 But I might like to see what's in there.
S2 You want to see what's in there?
S1 I mean, hey, there's a lot of protein, which is good!
S2 There's a,
S2 There might be a lot of protein, but it's not the one we're looking for.
S1 Yeah but it will be, weeeee, look at all the bands!
S2 Yeah, but we don't want to look at the bands, we want to look at our one.
S3 We want to look at our protein
S1 Fine, skipping number 16.

It is important for the teacher to make sure that the students know what they are doing and why they are doing things. When something wrong happened, the teacher helped to evaluate the mistake. "*They helped me understand what was going on in the experiment, or if something went wrong. E.g. on the first day, a major step went wrong and had to be fixed. When I got confused, -TEACHER'S NAME- was able to guide me in the right direction"* (Student's questionnaire).

Formatted: Not Highlight

For example, in lab session 2 a teacher approached to a group when the student should be on doing purification and comparing two chromatography results. The teacher digging information by posing questions to make sure that the students are on the right track to

achieve the learning objective. The student was almost lost when he/she thought the second chromatography was the next stage instead of to be compared with the first one.

T	You guys are alright? So you know what you're doing with the affinity elution, you don't have to do anything, just do the same as you did before. But you just have to change buffers
S1	Oh, OK!
T	So you should be getting the next one started. What are you waiting for? You should be on it.
S1	Um, protein concentration.
T	But you don't have to do it, because you are doing now another, you're doing another, chromatography. You're doing it again with affinity elution.
S1	Are we pooling our fractions?
T	No, you are just taking the new stuff.
S1	That's what I mean
T	You are doing the same thing again with your original
S1	Why?
T	because you are doing 2 different things and comparing them
S2	told you
S1	oh. I thought we were getting that and putting it through. alright

Lack of understanding or misinterpretation. When each group shared their work with fellow students, there were still some students who only partially focused on the work they were doing at that time. On his assignment, for example, he can measure LDH activity correctly. However, to select a sample, the reference should be the specific activity, namely after dividing it by the amount of protein. So for cases like this, I noticed how the teacher reminded them repeatedly to focus on global goals in order to ensure they could achieve the target. Cases like this occur with students who lack of understanding which results in misinterpretation.

Critical thinking. In the conversation I is revealed that there were some students who were critical and did not easily believe the results obtained by peer in their group, until they made sure, what their friends were doing was supported by correct understanding and right information. Actually, it is good to do this at the beginning, so that peer assistance and cross-checking occurs, especially at the tasks that were done repeatedly. So that the results of the work have a high standard, and there is not a big gap of students' understanding.

Technical problem on experiments. There were so many technical problems that arose during the experiment that were actually not principle, but students were trapped into these topics of discussion and these occurred repeatedly, such as dilution. But it does not mean they like this topic. The questionnaire results shows that the majority (5/8) of student respondents admitted that the lab session 2 was more enjoyable for them than other days, and 4/7 of the students admitted that the lab session 1 was the most challenging. In lab session 2, we know that the students were introduced to how they were using chromatography column (AKTA) for the first time. The topic of chromatography was related to the material given in lectures, so this becomes actual and more interesting. I recommend that the concept of dilution might need to be reinforced before they enter the lab, so that they would enjoy more of what they are doing on dilution and protein assays.

"Backed up with lectures that overlapped the Labs so well, provided the theory and background needed to make sense of the rest."

"Explanation from an expert in understanding how the equipment work help the student to connect the theory with practical."

"Learning about them is one thing, but transferring that knowledge to a device in front of you is different. Therefore I asked the demonstrators what was happening at each step and I quickly understood it all." (Student's Questionnaires).

Questioning Process to achieve higher level of inquiry

The obstacles to achieve higher level of inquiry occurred, first when the student is not ready with sufficient preparation and, secondly, when the student does not have sufficient basic understanding or basic skill. In fact, when carrying out a long series of experiments in IBL, students wish that they understand everything they are doing and they know what is actually happening with the tools they are using on their samples. From this curiosity, conversation initiatives emerge which are often preceded by questions. Some students had also prepared questions that came up when they were doing preparations the day before from what they read in the lab manual.

"Having questions in the lab book to provoke learning more about protein purification."
"Asking to making sure what they are doing, are they on the right track so I didn't waste time."

(Student's Questionnaires).

We see in the discourse timeline why conversations and discussions are so intense while students are carrying out experiments in small groups? We found that when questions suddenly arise during the experiment, they often ask their teachers and friends instead of looking for answers from other sources, such as the internet or textbooks. The third alternative, they also choose to ask students in other groups, and sometimes they open their lecture notes.

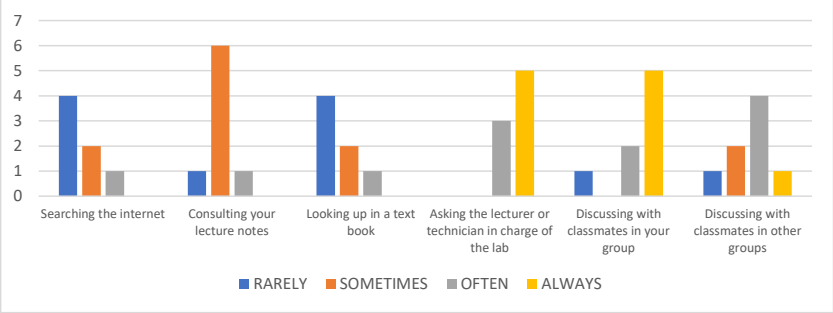

Figure 1.8. The way how to find the answer if student has a question in student perception.

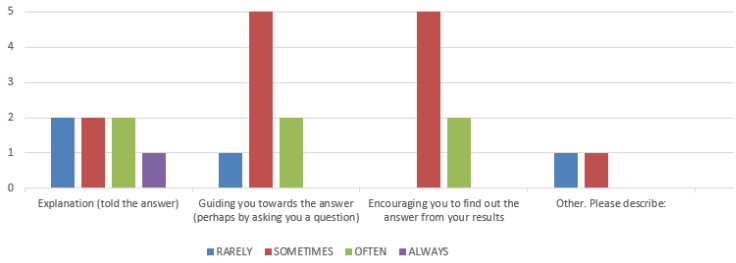

Figure 1.9. The way how the staff helped the student to answer a question in student perception.

*Other: Making light of mistakes, causing a closer look (rarely);

Making trial and error with a little sport (sometimes).

So how do teachers respond to students' questions? According to students' perceptions as shown in Figure 1.9, teachers sometimes/often answer in a way to guide the students towards the answer and perhaps by asking the students a question back. The students also admitted that the teachers sometimes/often respond the students'question by encouraging them to find out the answer from the students' result.

The recordings revealed that the conversations were often initiated by a particular question, as illustrated in Figure 1.10. In many instances, a question also provoked further questions. The question was followed by responses, and the conversations mostly extended a particular topic. Closure of a question was generally not very clear other than in teacher-student conversations. When this conversation was initiated by a question, the closure occurred when all of the questions had been answered. The conversations between the students and the teacher in the laboratory are less formal, more relaxed, and natural than the conversations between the students and the teachers in the lectures.

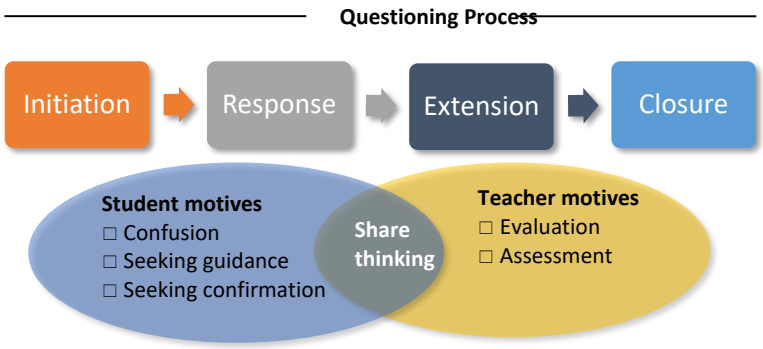

Figure 1.10. The process of questioning generated from students' laboratory conversations and their motivations.

What are the motives for these questions and at what level are the students questioning?

The findings indicated that the questions were generated by a variety of motives. The motives behind the questions in science laboratory conversations were classified into at least five categories. They are, from the students' perspective, confusion, seeking guidance, seeking confirmation and sharing thinking, and, from the teachers' perspective, guiding, evaluation, or assessment (See Figure 1.10).

The findings revealed that the majority of conversations concerned 'what' questions, which required definitive answers. These 'what' questions are categorised at the low level of learning in the revised taxonomy of Bloom (Krathwohl, 2002), which places remembering at the lowest level. The moderate level is 'how' questions which require an exploratory answer about understanding or applying a procedure. In the conversations, the number of these 'how' questions was also considerable, but very few conversations asked 'why'. A 'why' question is at the highest questioning level and requires an explanatory answer by analysis and evaluation. To what extent inquiry is actually going on in inquiry-based learning could be reflected in how often students or teachers are posing 'why' questions in their conversations when doing laboratory work. These 'why' questions may guide students to develop scientific analysis and interpretation skills like a scientist (See Figure 1.11).

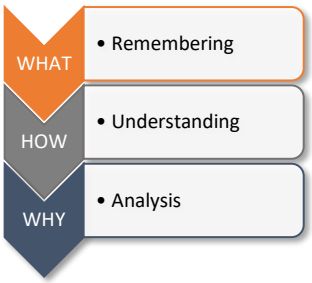

Figure 1.11. The level of questioning in students' laboratory conversations. The higher the level of questioning posed, the longer the conversation is extended.

The 'why' question required critical thinking skills. To answer the 'why' question often required comprehensive answers. It was also found that if the conversation involved a 'why' question, the conversations tend to be prolonged conversation. In some cases, the

conversations were extended until the question was answered or until the problem was resolved. The following conversation demonstrated that a student (S1) was curious when he found the absorbance reading was unexpectedly getting lower during measurement. He observed and found that the protein was denatured. His questioning was closed after he discussed and found himself when the blank reading was not valid instead of changing the cuvette. The questions in the following conversation were driven by confusion and seeking confirmation rather than seeking guidance. Finally, his questioning was able to guide himself to find the answers.

S1: It's starting lower. Why is that?
S2: What number you got?
S1: 0.596, its about 40 units off where it normally starts. Its wobbly, I'm gonna change it. Something weird going on there. I've rinsed it so much though, it shouldn't, there shouldn't be any. There might be some sort of substance on there, I might have to. Sh*t there could be a protein caked on there bro, on the side of the … (not finished)
S2: Use a different cuvette!
S1: I am just going to test it with water to see if it zeros.
S2: Yep.
S1: Yeah, it's not quite. So I'll, um, I'll swap it out, re-auto zero it, wash it with ethanol.

The next conversation, reproduced below, demonstrated a 'how' question that was driven by the motive of seeking guidance. In many instances, the 'how' question was often related to the understanding level, the procedures, or how a device/instrument works.

S1: So how do we rinse them out, do we just pour water in and pour it out?
S2: Yeah!
S3: I think it is pour in, spin, pour out.
S2: It doesn't say spin, it says if these interfere with analysis, they can be removed by rinsing full volume of buffer solution, or deionised water through the concentrator
S3: Ok!

Furthermore, the study found that students more often focused on the data rather than what the data meant. But, somehow the students were seeking confirmation just to make sure that what they were doing was correct. The conversation below occurred when two students in group were seeking confirmation on using a spectrometer for protein concentration.

S1: Do you blank it with water or the buffer?
S2: Do I have to blank at the new wavelength?
T : Water is fine.
S2: Do I have to blank it at the new wavelength?
T : Yes.
T : Ok, so now take the measurement of your liquid. That's right, and then put it in a beaker!

1.4.8 Social interaction and emotional response in inquiry-based laboratory

Three patterns of social interaction were observed within students'conversations in the laboratory, depending on who initiated the conversation: first, student and student(s); secondly, students and teacher; thirdly, teacher and student (see Figure 1.12).

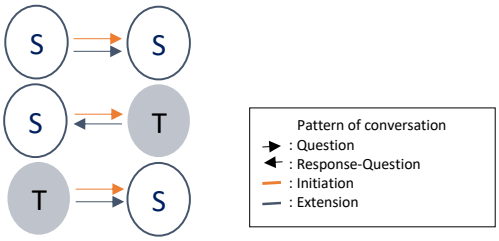

Figure 1.12. The patterns of social interaction within students' conversations in the laboratory.

For the first pattern and for some of the second pattern of social interaction, most of the topics discussed or asked by the students were relevant to the laboratory class and included procedures, equipment, theoretical concepts, laboratory skills, calculations and management with little social chat. However, theoretical concepts, expected to elicit higher order thinking (for example, analysing, synthesising or evaluating), were discussed infrequently by students, but quite often were asked by the teacher to the students, for example... It can help students to think 'why', but student ownership of basic skills for a particular concept is also necessary to engage themselves in these higher-level conversations. The challenged question works when it is at proper level of difficulty. Otherwise, the students will get frustrated if it is too difficult.

S1: I'm doing something wrong with this.
S2: What's happened S1...?
S1: The um, spectrophotometer, the spectrophotometer is dying. It's dying.
S3: What's wrong with it?
..... then the teacher approached...
S3: Ah, yes it has stopped! Why is this remaining so high?
T: Because you have NADH in it.
S3: That's absorbing at 280.
T: Remember that absorbs at 340 so you will get some absorbance from it.
S3: Ok, so the peak pretty much ends here.
T: So you have to test it.

S3: Yep.
T: You will be surprised how far it goes.

In many instances in this inquiry-based learning, such emotional responses were seen in conversations such as the above. Involving emotion in learning, like excited, frustrated, can help student to memorise the learning episodes of a multistage sequential experiment. However, students' acknowledgement of scientific fascination did not always reflect their understanding. Thus, the teacher's guidance is critical to follow up their emotional responses. The emotional expressions below are also examples of frustation captured in students' conversations when they were struggling with (ostensibly simple) diluting tasks.

"I'm stuck. What do you do after that?"
"How much I can dilute. It's a confusing concept."
"Yeah dude, it has to drop all the way. Ohhh. Its going to make assaying so much harder."

1.4.9 How much inquiry is actually going on?

Did students do critical thinking in lab conversations?

The finding shows that questioning and critical thinking are essential in inquiry-based learning. But questioning and critical thinking are dependent on observational skills, and the observational skills are a tool the gather evidence to answer a research question.

This study revealed that some students tended to answer questions briefly without explanation. There was little evidence of the students forming logical arguments from the experimental evidence and communicating these within the lab. Students may have done this in the written laboratory reports independently, but these reports were not studied in this project. Students rarely connected the knowledge that they had learnt or received from the lecture to this biochemistry laboratory.

For example, in the conversation below, the students really did not get the big ideas of why they should assay all peaks in the chromatogram, and how to do their protein concentrations, calculate the specific activity of the sample and to interpret which peak represented the pure fraction, in order to conclude which column chromatographic method was the better of the two methods tested.

T: You know how you've got a big peak and a little peak. Have you assayed that little peak?
S1: That first big peak...
T: And then you've got a little peak after it haven't you?
S2: Oh, in the first chromatogram.
S1: Yeah.
T: No, in the second chromatogram, you've got a big peak and then a little peak.
S1: Oh,
S3: See there's a big peak and there's a little peak.
S2: Oh, yeah, we haven't assayed it yet.
S2: Alright.

What caused students to struggle on posing a 'why' question and developing a logical argument?

Students struggled to move beyond basic tasks with which by their third year they should have been familiar. The conversation below shows that student was struggling with basic dilution skills in Day 3.

S1: How do you do the calculations to figure out, to figure out how much protein is going to be in each of these?
S2: Ok, so we have taken half a mL of each. So its going to be half of that.
S1: What, no, sorry, I'm thinking we need a final concentration of 1 mg per mL. Will the all give us that?
S2: They will all give us, we want 2 so we can do 50/50 with SDS buffer.
S1: Oh yeah, got that one, that's alright, um yes that's fine.

In Day 1, there are more conversation that show that the students are struggling in diluting skills as well (see statements below). These findings have been reported to the academic staff and have been followed up. In the same laboratory in the following year, the feedback was able to reduce 2 of 8 hours for completion of the lab at Day 1.

"I'm stuck. What do you do after that?"
"How much I can dilute. It's a confusing concept."
"Yeah dude, it has to drop all the way. Ohhh. Its going to make assaying so much harder."

Those are some frustated expressions in students' conversations when they were struggling with diluting skills. But this struggle did not mean they gave up, but kept learning. Finally, after 6 h of struggling and practising on doing similar things, the students found the easiest way to do dilutions.

S2: It's not hard doing this.

S3: It's not hard.
S1: It's super easy, it shouldn't take too long because it's only 2 values. Like if, let me ease your pain. I think the 1 in 10 and the 1 in 10 are too high in concentration, they're not going to work with ours, so just do the 1 in 1000.

The conversation below shows that the teacher approached a group which was struggling on calculating protein concentrations. The way how the teacher guided the students was by posing several sequential questions to evaluate what they have done, to mention the lab details, and to show the evidence. The teacher seemed to expect the students to state their actual problem and to work out the solution to the problem. This conversation also revealed motivation and provided an alternate solution to the students. These 'how' questions required the explanation about the procedure, technique, and some detailed information, which reflected an understanding of what they were doing.

T: Right, what are we doing?
S3: We are being stuck.
T: So, if you're wrong, you just have to repeat them. You can either do it now, or you can do it next lab session.
S2: We would have to be very very sure.
T: So I would do just, you can get an estimate. How long does it say you have to wait for them, 5 minutes, coomassie. So I would just do something, where do you think you're wrong?
S3: Our pellet is out.
T: So do your pellet again. And where did you read that off the high curve or the low curve?
S2: Low.
T: Ok, so, and where did come, in the middle?
S2: It, no, no down around this end.
T: So you've diluted it too much and it could be that it, so why don't you just do, another … (etc)

Crucial step on guiding students to achieve the final goal of the inquiry-based learning

After students go through a series of learning processes from the stage of carrying out active experiments, through concrete experiences of facing several failures and success in practices, analyzing, interpreting observed data, the next phase which is very crucial for students to pass is whether they are able to reflect a series of experiments they have carried out, to the point where they can answer the biggest question then finally draw conclusions from the experiments strengthened by valid and authentic evidence, and at the end the students need to communicating the results in written or verbal form with abstract scientific arguments. At this crucial point, the teacher is present to determine whether students can reach a higher

level of inquiry by exploring key questions. The following conversation shows how a staff guided the students to pass a crutial moment just before the last session of the laboratory finished.

T: How did your table end up looking like?
S1: Table?
S2: What table
S1: It's on excel now, but it looked good didn't it guys.
T: And how was your recovery off your columns? Was that good? You put so much activity on the column and so much came off.
S3: Haven't compared.
T: OK, yes.
S1: That just went way over my head, and I was like what?
T: You do understand the whole idea. You know how much activity you put on the column.
S1: Yeah. And then you see how much you have coming off.
T: So presumably you should have the same amount come off.
S1: Yeah.
T: Either in that first peak because it didn't bind, or in that second peak where it was nice and clean and pure.
S1: Right.
S1: We will.
T: One of the things we used to asked, and I presume we still do, is, which technique is the best technique, for purifying this? Is it?
S2: The second one.
T: Is it, is it the salt elution, is it the affinity elution or is it the dye binder?
S1: Yeah you did ask that.
T: They did ask that, sure.
S1: I want to say that it was our first one, it worked really well or did we get a better separation off the second one?
S2: Ah, we, right, this, the specific activity was much better off the second one.
S1: Right.
T: Sure.
S1: So we had all sorts of different peaks in that area.
T: The specific activity suggests that it is the best method.
S1: It's better, yeah.
T: It may not be the easiest. It may not be the most economic. Sure. But hey, enjoy the afternoon its still sunny out side.

1.5 Discussion

An authentic evidence is needed to know how much of the student conversation is inquiry. The authenticity of natural environment in the conversation recording is captured from the students' conversations. Notwithstanding the microphone was present at the bench during lab sessions, all students considered it did not affect the conversation content. Thus, the

conversations occurred naturally without any pretence. This is supported by the following quotes from the students' questionnaire:

"I forgot about them after a minutes"

"At the beginning it felt a bit weird but after 5 minutes I forgot it was there and it did not change anything."

From the recording of students' conversations in an Inquiry-based learning in the laboratory, we found that the students made long but discontinuous conversations and the topics were relevant to the laboratory class with little social chat. They made conversation with their peers while doing experiments without significant disruption to the experimental work. These conversations were revealed through a recording where the sounds of experimental tools were simultaneously heard with students' conversations. There were some expressions that indicated feelings of frustration and excitement. It is suggested that the tasks were sufficiently challenging in terms of difficulty and complexity of laboratory skills and theoretical content. Confronting students with this particular state of perplexity prompted the students to seek questions and evidence to resolve the discrepancy or problem. Questions were posed to the other students more often than to the teachers. The expression of excitement was clearly captured when students solved the problem by themselves. Students were strongly motivated by complex personally relevant questions. Bransford, Brown, and Cocking (2000) also suggested that tasks must be challenging but at the proper level of difficulty to remain motivating.

Inquiry-based learning seems driven by two question categories. The first is a question that constructs students' knowledge when they complete the IBL (See Table 1.5). This type of question becomes the spirit of each stage that students must complete. Secondly, personal questions that arise suddenly during the student learning process which are influenced by the student's previous level of knowledge and the problems exposed in each group.

In the context of the LDH laboratory, the first category questions were collected and grouped from 3 sources: the Lab manual, teachers' introduction talk, and student's conversation. The questions are listed in the Table 1.5. These questions are classified to help students achieving goals at every stage of the LDH laboratory from basic level to the top level. The questions' table is also helping the teacher to maximise student success differentially based on their

particular level of inquiry. Ideally in the IBL, the students are encouraged to construct their knowledge by confronting them with questions from themselves or from the teacher. The students are then supported to investigate the questions during the inquiry-based laboratory.

The second category of questions, which arise spontaneously, was identified from the students' conversations, and they were classified by the level of difficultly. The questions were predominantly the 'what' question, rather than the 'how' or 'why'. The type of question could represent how much inquiry is going on indirectly. This type of question from a student or a staff member most likely triggers students to answer with a particular level of thinking. Some 'what' questions at the level of remembering can be answered directly by other students.

The characteristics of 'why' questions are higher than 'what' questions. They are more likely require analysis and interpretation. The 'why' question mostly generated longer conversation. Students or teachers posing 'why' questions more likely occurred when they want to know what was going on in the experiment or the reason why the student doing something, or if something went wrong to give a suggestion politely.

Generally speaking, in teaching practice, a teacher responds to the students' errors in different ways, such as telling the students directly if they are wrong then demonstrating the proper way, or directly guiding them to repeat the work. The other approach, which is mostly occurred in the conversations and more politely, is by initiates a conversation including 'why' questions to let the students find the error by themselves. The questions may allow the student look up the more information either from notes, lab manual, or lab book, which then guides the students to do a trial with simple inquiry.

Here, guided inquiry-based learning with multi-task laboratories (three consecutive laboratory sessions within three weeks) and the lab not being so detailed enabled students to have experiences like a professional scientist working in a team. Students are encouraged to prepare for their experiments with proper laboratory skills and to master the theoretical background prior to the laboratory work. "*Backed up with lectures that overlapped the Labs so well, provided the theory and background needed to make sense of the rest*," a student said in a questionnaire.

The ability to work in a team has also become one of the keys to success in the laboratory. This IBL with student groups elevated persistence and social-communication skills through

intensive scientifically related conversations, as well as building up a critical-thinking through scientifically related questions.

Narayan (2010) highlighted hypothesis-related discourse as a feature of IBL. In a multi-task laboratory, students need to focus not only on a partial research question in each laboratory session, but also to focus on the ultimate research question as a big picture. This point is very important and is to be reinforced by the staff. As the students have abundant data within three weeks, they need to review and to reflect on the data they have and what they mean as results. Students' pre-laboratory preparation is a must, as this helps students to manage their time to complete their tasks efficiently.

In the third-year level of undergraduate studies, the laboratory is designed to reach several teaching goals, including a scientific concept and learning outcome. In an inquiry-based laboratory, especially in the third year of undergraduate teaching, experiments can span a longer time than at lower levels. The students are introduced to use more sophisticated laboratory equipment with supervision. The more inquiry the teaching has, the better the learning for the students in the laboratory. The students will be more confident to do the tasks more independently, which are essential characters to have when they soon graduate and go into the work-place.

"I enjoyed the labs not being so detailed that we were just following a recipe, it was nice to have accomplished something ourselves, and felt like we did a lot of it on our own knowledge. I also liked working in a group and having people to discuss the experiment with , but yet still have a lot of work to do ourselves."

"I know how to assay! It was a great lab for teaching us how to work with little help, so therefore a lot of trial and error. I find after doing this lab my other labs for other papers seem extremely easy and are more just like following a recipe. This lab got me more confident with a lot of equipment and I feel like I gained a lot of skills."

"We were in the lab for such a long time (i.e. 5 hours 1 week). I wasn't interested in going home and finding out more. I found what we were doing interesting, but did not have the time to find out more."

(Student's questionnaire).

In the other words, in order to foster student learning in IBL, the teachers should consider the decision on how they respond to the student question by considering at which experimental stage they are doing their inquiry and which style the students are adopting. Students can pose a question at any stage of the cycle, then the answer should promote the student understanding to the following sequences. By these means, regardless of the stage of the students, students can examine the overall inquiry as a whole, not partially. This is particularly relevant in a multi-session lab teaching, where the students may struggle with the many concepts and procedures they encounter.

The data sources suggested that the inquiry question which leads the lab achieving the goal are listed at the Table 1.5. There are levels of questions: remembering (1^{o}), understanding (2^{o}), and analysis (3^{o}). The levels of questions refer to the descriptive rubric for discourse indicator (Marshall et al., 2010) which is relevant with the context of this inquiry-based laboratory. The combination of these question will be defined in other section. In the rubric, those four levels of questions constitute the pre-inquiry, developing inquiry, proficient inquiry, and exemplary inquiry.

Table 1.5. Gradual critical questions of the LDH experiment.

Remembering (1^{o})	Understanding (2^{o})	Analysis (3^{o})
		Based on the SDS PAGE results, what is the molecular weight of the LDH enzyme?
Does your sample contain LDH protein? What is the LDH activity of the sample?	Which protein sample/part/fraction(s) contain active LDH to collect?	Among the techniques used, what is the most effective way among the three chromatography methods?
What is the protein concentration of the sample?	What is the total protein concentration and the protein yield (%) of desired protein at each purification step?	
	What is the specific activity at each purification step?	Why is one chromatographic method is better than the other two to purify LDH?
How much volumes of samples containing active LDH that you have collected?		

The questions that arose from the students' and teachers' talks enable students to achieve the goals of the LDH labs from the very beginning to the end of the laboratory. So, the level 1^{o} question (remembering) are the basic questions that prevail for all protein samples at each step. This level requires **level of remembering** of the formula of diluting, protein concentration, and the technique and method that we used. In the end of this level, the students have to sort and combine *which sample or fraction or part are containing LDH* based on enzyme activities and concentration as raw data.

Level 2^{o} questions aims to produce processed data based on the question level 1^{o} output through a series of calculations of specific activity and LDH protein yield of each step of purification. This prevails for all protein contains LDH at each stage of purification. This level requires a deep **level of understanding** of how the AKTA machine works, the ability how to observe the curve and chromatogram and to reflect *which sample or fraction or part are containing purer LDH* based on enzyme specific activities and its concentration as **processed data**.

Questions at level 3^{o} requires the ability to **analyse** and to **interpret** the data that have been processed to produce an abstract concept, **result, and finding**. In this 3^{o} question level, the students have to answer the key question and to solve the problem using their logic. The students can define their results and declare their findings of the inquiry. In this case, the students will be able to show a single protein band which is LDH and to estimate the LDH size by comparison of its migration distance with that of a standard of known molecular weight. Secondly, the students, based on their comparison of the calculation results of the specific activities of the three methods, are able to conclude which chromatography technique is the most effective way to purify LDH. The questions of level 1^{o} and 2^{o}, and 3^{o} are gradual, the student will have successfully answered the questions at level 3^{o} only when they successfully answer questions at level 1^{o} and 2^{o}.

The ability to generate inquiry report both **written report** and **presentation** requires the students' competency at the synthesis level. The level of synthesis requires a comprehensive students' ability including remembering, understanding, and analysis to evaluate the overall laboratory results and findings, and if lucky, to create a new model, new concept, or new theory, as our contribution to science and society.

The experience on doing scientific inquiry process benefits students to do inquiry-based laboratory more often with more easily and more confidently. Still, with their synthesis ability, students will be able to enter a new cycle of the scientific inquiry process, started by creating hypothesis and followed by applying their new knowledge that they have built on.

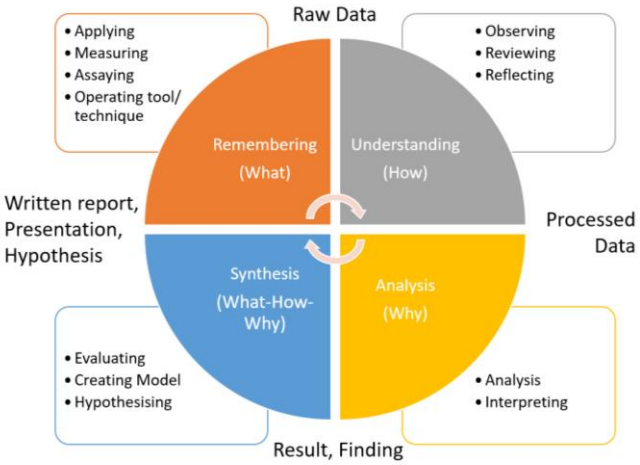

Figure 1.13. A process of scientific inquiry and its products, in higher education science laboratory.

Based on the paragraphs above, here we proposed a learning cycle of inquiry-based laboratory with the attribute of questioning level and hands on/minds on (act-think) activity and the product of each level for higher education (Fig. 1.13). The diagram is used to generate open questions with gradual level of question like the Table 1.5 above. Furthermore, the diagram is used to determine at which level the students are doing inquiry in an easy way. This becomes the baseline where the teacher can improve students' achievement at possible highest level, or within the zone of proximal development (ZPD) by 'scaffolding'. The diagram (Figure 1.13) is more applicable than the experiential learning model (Figure 1.2) as here the teachers do not classify the students' learning style; rather they encourage the students to achieve a higher level of inquiry, especially for third-year undergraduate students.

“Students at all grade levels and in every domain of science should have the opportunity to use scientific inquiry and develop the ability to think and act in ways associated with inquiry, including asking questions, planning and conducting investigations, using appropriate tools and techniques to gather data, thinking critically and logically about relationships between evidence and explanations, constructing and analysing alternative explanations, and communicating scientific arguments" (National Research Council, 1996, p. 105).

How important a students’ prior knowledge in inquiry-based learning?

When doing inquiry-based learning, students find something interesting or perplexing which leads to scientific questions and also to reflections on what the students already know about the questions. The students may need to understand some concepts and vocabulary first from the lectures or learning materials to begin the IBL, although the investigations can also be designed and performed without knowing all terminologies and definitions used. The context for developing operational definitions and science concepts can be provided in the process of observations, data collection, and analysis involved in an investigation which later on is called "vocabulary." In a student-centred group, the students can master the concepts and ideas that they did not understand on their own with the help of a more experienced peer by building conversation which is relevant to the Vygotsky’s concept of the zone of proximal development (ZPD) (Schwebel, 1979).

The findings from this study can be organised into a chart (see Figure 1.14) which is constructed to summarise the aspects involved in an inquiry-based learning for continuous development of students’ inquiry and questioning skills. On the left and top sides of the chart, a process represents how questioning is generated in the lab conversation and identifies the motives of questioning. The level of questioning in the centre is used for our self-reflection on applying inquiry-based learning. Finally, the bottom left of the chart is designed to help ourselves to improve scientific communication among student-teacher social interaction by practising questioning with higher level.

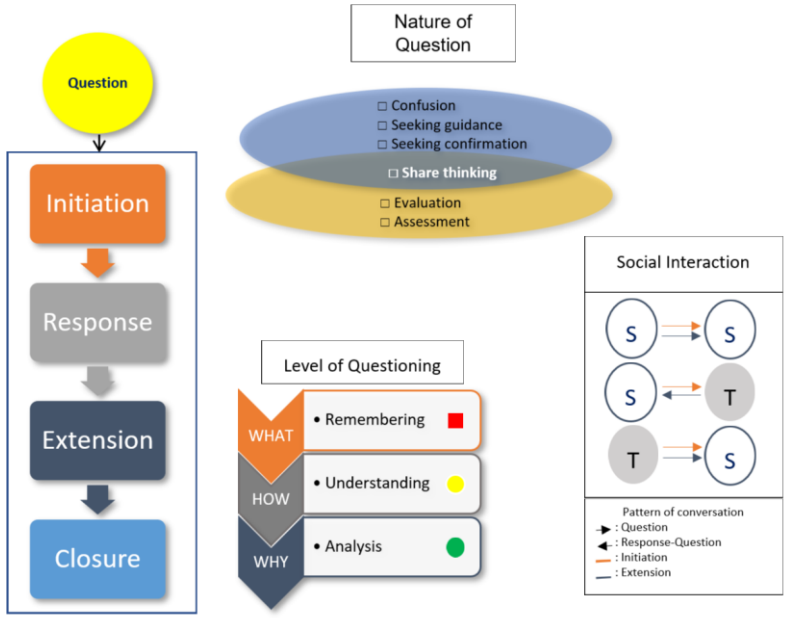

Figure 1.14. The process of questioning obtained from students' conversations forming a platform for inquiry-based learning.

Extension of any inquiry is determined by who initiates inquiry, the nature and level of questioning, and how is the inquiry maintained. S: Student; T: Teacher.

1.6 Conclusions

- There are more conversations involving questioning in inquiry-based learning.
- Conversation occurs as a part of social-interaction among students and teachers, furthering collaboration which leads to learning. Conversation occurs by motive, topic, and interest.
- Questioning is posed when there are problems, uncertainty, challenges, and confusion. A question requires a response, feedback, from peers or teacher. Feedback is given from the teacher to guide students to an understanding. Questions has levels: remembering, understanding, and analysis.
- Inquiry often involves emotions: excited or frustrated because of challenges and difficulties. Challenges and difficulties at the proper level will remain motivating. Otherwise, the teaching would become bored, or make the students frustrated. This is where the role of the teacher becomes essential in IBL success or fail. Therefore, in the discourse time-line, it shows how the teacher interacts very intensely in guiding students to accomplish the task themselves and for the students to feel that they did a lot of it on their own knowledge. Thus, when the students have a question, the teachers tend to answer student questions in a way encouraging them to find out the answers from their results, and secondly the teacher guides the students towards the answer perhaps by asking them a question, not by being told the answer.
- In inquiry-based laboratory, students enjoy the lab not being so detailed. Students' curiosity encourages intensive conversation, consists of discussion (questions-answers) which focused on learning. Students enjoy the lab if they understand what was going on, how does it work, and know why something went wrong.
- Not only does an inquiry-based laboratory improve communication skill, students also learn to work collaboratively. The students are motivated when they work together with hardworking people. They learn how to trust the team and to be responsible as part of a teamwork.
- The conversation transcript and the word cloud indicate that in the beginning, the students were involved in trivial improvements due to struggling with calculations, dilution tasks, and misslabelling of samples. The word frequency of *activity* and *specific*-

activity increased in day 2, indicating that that the students became more focused on achieving the goal, and meaning the level of students' inquiry had increased.

- The students were excited to learn how to use a new machine (e.g. AKTA chromatography) in the lab. This is because the lab was backed up with lecture that overlapped the lab so well, including using virtual lab regarding protein purification.
- The students sometimes became trapped in a routine task. Teachers often encouraged students to take a step back from the routine task to look at the bigger picture and to review what the students have just performed to purify the desired protein. These efforts elevated students' level of inquiry to a higher level.
- The descriptive rubric for discourse indicator (Marshall et al., 2010) is relevant with the context of this inquiry-based laboratory. Here, there are levels of questions: remembering, understanding, analysis, and the combination of these. In the rubric, the level of question are attributes of the pre-inquiry, developing inquiry, proficient inquiry, and exemplary inquiry.
- In this study, it is proposed that a learning cycle of inquiry-based laboratory with the attribute of questioning level and hands on/minds on (act-think) activity and the product of each level. The diagrams (Figures 1.13 and 1.14) are developed based on research findings that emerged from students' conversation and are applicable to higher education.
- The diagrams can be used to generate open questions at various gradual levels of question. Furthermore, the diagrams can be used to determine in an easy way at which level the students are doing inquiry. This becomes the baseline where the teacher can improve students' achievement at possible highest level, or within the zone of proximal development (ZPD) by 'scaffolding'.

Recommendations

- Before doing inquiry-based lab, the students need to be competent in the basic laboratory skills, so the students do not get stuck in a routine task which could shift students' focus to non-learning goals.
- When the tasks are distributed to the students in a small group, teachers have to make sure that each student does not lose opportunities to learn about particular tasks that

they have not actually done. So, they are being able to watch each step, especially to a new task/method/instrument they have not ever performed/used. For example, as one student noted, “One person would be doing the chromatography whilst I was doing assays, so I did not get time to watch the whole chromatography process from the start. This is more of a self-management problem from my end though.”

- It is important for science undergraduate students at the final year to be exposed to inquiry-based learning to experience working like a real scientist in order to improve their 4C 21st century skills: Critical thinking, Communication, Creative thinking, and Collaboration.
- The analysis of inquiry in students’ conversations in the laboratory underlined the important teacher roles in guiding students during the learning process in the lab. On this basis, future research should examine the inquiry in students’ written reports, group presentations, and comments to other groups in discussion sessions, to complement the current findings.

References

Acar, S. B., & Tarhan, L. J. (2013). Inquiry-based laboratory activities in electrochemistry: High school students' achievements and attitudes. *Research in Science Education, 43*, 413-435.

Allen, J., Barker, L., & Ramsden, J. (1986). Guided inquiry laboratory. *Journal of Chemical Education, 63*(6), 533.

Anderson, L. W., & Krathwohl, D. R. (2001). *A taxonomy for learning, teaching, and assessing: A revision of Bloom's taxonomy of educational objectives: complete edition.* Addison Wesley Longman, Inc.

Bloom, B. S., & Krathwohl, D. R. (2020). *Taxonomy of educational objectives: The classification of educational goals. Book 1, Cognitive domain.* longman.

Bransford, J. D., Brown, A. L., & Cocking, R. R. (2000). How people learn. In: Washington, DC: National Academy Press.

Brown, P. L., Abell, S. K., Demir, A., & Schmidt, F. J. (2006). College Science teachers views of classroom inquiry. *Science Education, 90*(5), 784.

Buck, L. B., Bretz, S. L., & Towns, M. H. (2008). Characterizing the level of inquiry in the undergraduate laboratory. *Journal of College Science Teaching, 38*(1), 52-58.

Chen, R. H. (2021). Fostering students' workplace communicative competence and collaborative mindset through an inquiry-based learning design. *Education Sciences, 11*(1), 17.

Collins, A. (1986). *Different goals of inquiry teaching*: BBN Laboratories Incorporated.

Davis, H. A. (2003). Conceptualizing the Role and Influence of Student-Teacher Relationships on Children's Social and Cognitive Development. *Educational Psychologist, 38*(4), 207-234.

Dewey, J. (1933). *How We Think: A restatement of the relation of reflective thinking to the educative process.* : Boston: D.C. Heath.

The New Zealand Curriculum. (2015). Ministry of Education. https://nzcurriculum.tki.org.nz/content/download/1108/11989/file/The-New-Zealand-Curriculum.pdf

Furrer, C., & Skinner, E. (2003). Sense of relatedness as a factor in children's academic engagement and performance. *Journal of educational psychology, 95*(1), 148.

Healey, M., Kneale, P., Bradbeer, J., & with other members of the INLT Learning Styles and Concepts Group. (2005). Learning styles among geography undergraduates: an international comparison. *Area, 37*(1), 30-42.

Kolb, D. A. (1984). *Experiential Learning: Experience as the source of learning and development*: Englewood Cliffs, NJ: Prentice-Hall.

Krathwohl, D. R. (2002). A revision of Bloom's taxonomy: An overview. *Theory into practice, 41*(4), 212-218.

Larive, C. K., & Polik, W. F. (2008). New ACS guidelines approved by CPT. *Journal of Chemical Education, 85*(4), 484.

Magnussen, L., Ishida, D., & Itano, J. (2000). The impact of the use of inquiry-based learning as a teaching methodology on the development of critical thinking. *Journal of Nursing Education, 39*(8), 360-364.

Marshall, J. C., Smart, J., & Horton, R. M. (2010). The design and validation of EQUIP: An instrument to assess inquiry-based instruction. *International Journal of Science and Mathematics Education, 8*(2), 299-321.

Pajares, F. (1996). Self-Efficacy Beliefs in Academic Settings. *Review of Educational Research, 66*(4), 543-578.

Pavelich, M. J., & Abraham, M. R. (1977). Guided Inquiry Laboratories for General Chemistry Students. *Journal of College Science Teaching, 7*(1), 23-26.

Schwebel, M. (1979). Review of Mind in society: The development of higher psychological processes. *American Journal of Orthopsychiatry, 49*(3), 530–536.

Sundberg, M. D., & Armstrong, J. E. (1993). *The status of laboratory instruction for introductory biology in US universities. 55*(3), 144-146.

Thaiposri, P., Wannapiroon, P. J. P.-S., & Sciences, B. (2015). Enhancing students' critical thinking skills through teaching and learning by inquiry-based learning activities using social network and cloud computing. *Procedia-Social and Behavioral Sciences, 174*, 2137-2144.

Voelkl, K. E. (1997). Identification with school. *American Journal of Education, 105*(3), 294-318.

Vygotsky, L. S. (1978). Interaction between learning and development. In Gauvain & Cole (Eds.) *Reading on the Development of Children.* (pp. 34-40). New York: Scientific American Books.

Wheeler, L. B., Clark, C. P., & Grisham, C. M. (2017). Transforming a traditional laboratory to an inquiry-based course: Importance of training TAs when redesigning a curriculum. *Journal of Chemical Education, 94*(8), 1019-1026.

Wood, D., Bruner, J. S., & Ross, G. (1976). The role of tutoring in problem solving. *Journal of Child Psychology and Psychiatry, 17*(2), 89-100.

Zain, A. R. (2018). *Effectiveness of guided inquiry based on blended learning in physics instruction to improve critical thinking skills of the senior high school student.* In *Journal of Physics: Conference Series*, *1097*(012015), 2-7.

Chapter 2 Introduction to MnSOD

In this chapter structure and properties of the superoxide ion ($O_2^{\bullet -}$) and the superoxide dismutase enzymes (SODs) that destroy superoxide are reviewed. Attention is then focussed on the iron and manganese family (FeSOD and MnSOD) and the role that conserved residues in the active site play in the mechanism of dismutation. The generally accepted mechanism is critically reviewed and the research planned to test an alternative mechanism is outlined.

2.1 Superoxide, superoxide dismutases and disease

Superoxide, $O_2^{\bullet -}$, is a small reactive anion which is formed in all living organisms that are exposed to molecular oxygen. Superoxide is often discussed together with hydrogen peroxide (H_2O_2) and the peroxyl radical ($OH^{\bullet}$). They are classified as reactive oxygen species (ROS). Superoxide is highly soluble in water. Superoxide predominates in its protonated form, hydroperoxyl $HO_2^{\bullet}$, at physiological pH. Narayana, Suryanarayana, and Kevan (1982) reported that, in solution, superoxide is surrounded by four tightly hydrogen-bonded water molecules (See Figure 2.1).

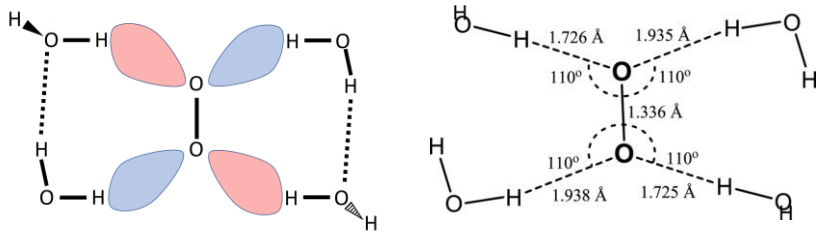

Figure 2.1. The solvation structure of superoxide in H_2O model with a π^* orbital containing a pair of electrons.

To optimise hydrogen bonding, the O-H bond of each water is approximately oriented toward this orbital. Superoxide forms a coplanar shape to the nearest O-H bonds, while the other O-H bond alternates approximately perpendicular to this plane as shown. The model is adapted from Narayana et al. (1982) and Janik and Tripathi (2013). Note: the other π^* orbital is orthogonal to that illustrated and contains just one electron.

Hydrogen peroxide is thermodynamically unstable and decomposes to form water and oxygen. Hydrogen peroxide is toxic to cells. Its reactivity can lead to oxidation of DNA, membrane lipids, and proteins. Compared to superoxide, hydrogen peroxide has different characteristic O-O distances that correlate with the order of the O-O bond, 1.5 for superoxide and 1 for hydrogen peroxide (Table 2.1).

Superoxide as well as other reactive oxygen species (ROS), in moderate levels, are also important for the control of cell signalling and gene expression. In the immune system, many eukaryotic host cells produce superoxide to defend themselves against invading microorganisms with coordinated expression of MnSOD (Visner, Dougall, Wilson, Burr, & Nick, 1990).

Table 2.1. The O-O distances and oxidation states of oxygen and its derivatives.

Compound	Name	O-O distance (Å)	Oxidation state of oxygen [O-O bond order]
O_2	Dioxygen	1.21	0 [2]
$O_2^{\bullet-}$	Superoxide	1.28	-1/2 [1.5]
H_2O_2	Hydrogen peroxide	1.46	-1 [1.0]
H_2O	Water	N/A	-2 [N/A]

Superoxide dismutase is apparently inherited from an ancient past when oxygenic photosynthesis arose. In phagocytes, superoxide is generated in large quantities by NADPH oxidase to provide oxygen-dependent killing mechanism of invading pathogens. The NADPH oxidase family is known to reside in the outer cellular membrane and functions to produce extracellular superoxide (Bedard, Lardy, & Krause, 2007). Mutations in the gene coding for the NADPH oxidase lead to an immunodeficiency syndrome. The syndrome is characterised by extreme susceptibility to infection, particularly by catalase-positive organisms (Thomas, 2018). The toxicity of superoxide was first discovered by Touati and co-workers (Carlioz & Touati, 1986). They found that *Escherichia coli* engineered with no SOD genes was incompetent to grow aerobically on minimal glucose medium.

Superoxide is also deleterious when produced as a byproduct of mitochondrial respiration and by xanthine oxidase (Muller, Lustgarten, Jang, Richardson, & Van Remmen, 2007). Imbalances in the electron transport chain produce increased superoxide and hydrogen peroxide (Shigenaga, Hagen, & Ames, 1994). During oxidative phosphorylation, electrons are transferred from electron donor to electron acceptor and ultimately onto dioxygen. Here, superoxide and hydrogen peroxide are produced from miss-firing of oxidative phosphorylation and pose a threat to cells when they lead to propagation of free radicals, especially the hydroxyl radical $OH^{\bullet}$. Thus, cell damage and disease are related to the production of superoxide. Obligate anaerobes cannot tolerate oxygen and exposure to dioxygen leads to cell damage caused by superoxide and hydrogen peroxide. Therefore, anaerobes need to utilise metabolic schemes built around enzymes that do not require oxygen (Imlay, 2002).

2.2 Superoxide dismutases: their roles and importance

The reactive oxygen species mediate cellular damage that is associated with many human pathologies, including cancer, cardiovascular disease, ischemic reperfusion injury, aging and neurodegenerative disease (Stadtman & Berlett, 1998). Many different kinds of tumours express low levels of MnSOD. Overexpression of human mitochondrial MnSOD suppresses tumorigenicity (Zhao et al., 2001; Zhong, Oberley, Oberley, & St Clair, 1997). Much evidence supports that MnSOD is a tumour suppressor, which is leading to new therapies for the treatment of cancer (Oberley, 2005). So how do we explain biochemically that cells exposed to superoxide and other ROS such as hydrogen peroxide are associated with high risks of human pathologies?

Excess harmful radical-anion superoxide in the cell is dismutated rapidly by nature's fastest enzymes, superoxide dismutases. Superoxide dismutases (SODs) are ubiquitous antioxidant metalloenzymes (McCord & Fridovich, 1988) that have important roles in biological protection systems against oxidative destruction. They catalyse the disproportionation of the superoxide anion-radical, a reactive oxygen species (ROS) that propagates free radical chain reactions, to hydrogen peroxide and oxygen through a two-step, one-electron redox cycle (Fridovich, 1997). In the case of the manganese superoxide dismutases (MnSODs), the reactions are:

$$O_2^{\bullet-} + H^+ + Ez(Mn^{3+}) \rightarrow O_2 + EzH^+(Mn^{2+}) \quad (1)$$

$$O_2^{\bullet-} + EzH^+(Mn^{2+}) + H^+ \rightarrow H_2O_2 + Ez(Mn^{3+}) \quad (2)$$

(Miller, Padmakumar, Sorkin, Karapetian, & Vance, 2003)

yielding an overall reaction

$$2O_2^{\bullet-} + 2H^+ \rightarrow O_2 + H_2O_2 \quad (3)$$

where Ez indicates the enzyme, including all the metal-ion ligands. This radical-scavenging performance protects the cell from oxidative structural damage produced by toxic oxygen metabolites of aerobic respiration.

It is a dichotomy that SOD is considered as protective agent, as SOD itself produces H_2O_2, another reactive oxygen species. Interestingly, to deal with hydrogen peroxide, MnSOD has intrinsic peroxidase activity (Ansenberger-Fricano et al., 2013) that is possessed when the enzyme is overexpressed, although peroxidase activity is relatively low compared to those of other peroxidases and catalases. The mechanism was proposed from a preliminary study with the hypothesis that MnSOD promotes better health at an optimal level of MnSOD with bifunctional activities: superoxide dismutation and hydrogen peroxide detoxification (Figure 2.2). Thus, MnSOD has been labelled as 'sink and source' (Sedlak & Musatov, 2017).

Fortunately, in eukaryotes H_2O_2 is disproportionated by glutathione peroxidase-1 (GPX1) which is partitioned between cytosol and mitochondria. Manganese superoxide dismutase and glutathione peroxidase-1 contribute to the rise and fall of mitochondrial reactive oxygen species, which can drive oncogenesis. GPX1 can act as a gatekeeper restraining the oncogenic power of mitochondrial H_2O_2 generated by superoxide dismutase (Ekoue, He, Diamond, & Bonini, 2017). H_2O_2 can also be scavenged by monofunctional heme peroxidases, bifunctional catalase-peroxidases and by mono-functional catalases, usually located in peroxisomes, in a different mechanism. The overall reactions are given in reaction (4).

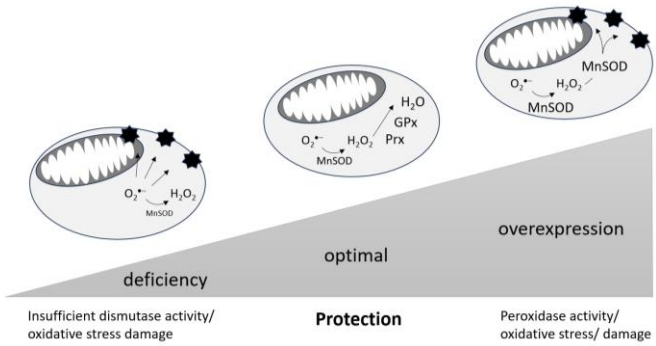

Figure 2.2. Schematic representation of bifunctional defence of MnSOD against $O_2^{\bullet-}$ and H_2O_2 at various level of superoxide (adapted from Ansenberger-Fricano et al. (2013)).

The hypothesis proposed that either under- or overexpression of MnSOD in mitochondria results in oxidative stress and damage (represented by black stars), but optimal levels of MnSOD promote health. The white curve shape represent mitochondria in a cell.

$$\text{Catalase: } 2H_2O_2 \rightarrow O_2 + 2H_2O \quad (4a)$$

$$\text{Peroxidase: } H_2O_2 + R \rightarrow H_2O + \text{“RO”} \quad (4b)$$

$$\text{e.g. } H_2O_2 + Cl^- \rightarrow H_2O + ClO^-$$

FeSOD, which is found in plants, bacteria and archaea but not in humans, interestingly has a parallel peroxidative mechanism to catalyse the disproportionation of hydrogen peroxide as described in reactions 6 and 7 (Abreu & Cabelli, 2010). The reduction of Fe^{3+}SOD by H_2O_2 (reaction 6) is faster than the corresponding reaction with Fe^{2+}SOD (reaction 7), which creates an Fe-bound hydroxyl radical that then, in the absence of sacrificial reductants, can oxidise nearby amino-acids.

$$2O_2^{\bullet-} + 2H^+ \xrightarrow{\text{FeSOD}} O_2 + H_2O_2 \quad (5)$$

$$Fe^{3+}SOD + H_2O_2 \rightarrow Fe^{2+}SOD + HO_2 + H^+ \quad (6)$$

$$Fe^{2+}SOD + H_2O_2 (+2H^+) \rightarrow Fe^{3+}SOD\cdots OH + OH^- \quad (7)$$

An increase in the production of reactive oxygen species (ROS) and changes in the expression of antioxidant enzymes are signs of cancer cells. A novel approach to potential chemotherapy

has recently emerged and can be a future therapeutic target in cancer by using pro-oxidant approaches. The approach performs by controlling catalase expression targeted to the redox status of cancer cells (Glorieux & Calderon, 2017). Studies on knockout and transgenic mice reveal inconsistent and controversial results. However, the evidence is still limited and unclear that the oxidative damage has correlation with the alteration of the mitochondrial antioxidant mechanism. Therefore, further investigations are required to give a detailed mechanism (Sedlak & Musatov, 2017).

In eukaryotes, electron-transfer enzymes are the first objects facing oxidative damage by hydrogen peroxide attacks. Thus, electron-transfer enzymes have their own way of protecting themselves against hydrogen peroxide. Some of these enzymes have the ability to decompose hydrogen peroxide, such as complex IV (cytochrome c oxidase CcO), cytochrome c, and complex III (ubiquinol-cytochrome c oxidoreductase) (Sedlak & Musatov, 2017).

2.3 Types of SODs: distinct evolutionary classes of SODs

Generally speaking, SODs are categorised into four different classes depending on their active metal cofactor. They are Cu-ZnSOD, FeSOD, MnSOD, and NiSOD (McCord & Fridovich, 1969; Yost & Fridovich, 1976) (see Figure 2.3). Each class of SOD requires for function the specific metal ion cofactor (Parker et al., 1987). Cu-ZnSOD is the only dinuclear SOD, whereas the three other classes are mononuclear SODs. The Cu-ZnSOD and NiSOD family are structurally unrelated, but FeSOD and MnSODs share both substantial amino-acid sequence and three-dimensional structural homology (McCord, 1976; Parker et al., 1987). Thus, the Fe-and MnSODs are usually grouped in the same family.

Table 2.2. Distribution, location and quaternary structure of SODs.

SOD class	Archaea	Eukarya	Bacteria
MnSOD	Cytosol (tetramer)	Mitochondrial matrix (tetramer), cytosol*(dimer) peroxisomes (tetramer)	Cytosol (dimer or tetramer)
FeSOD	Cytosol (tetramer)	Cytosol, glycosomes, mitochondria** (tetramer)	Cytosol (dimer or tetramer)
CuZnSOD	Genes identified in Methanobacteria***	Cytosol (dimer), mitochondrial IMS, nucleus (dimer) chloroplasts, peroxisomes (dimer), extracellular space≠ (tetramer)	Periplasm (monomer or dimer)
NiSOD	None	Cytosol (unknown)	Cytosol (hexamer)

*Cytosolic MnSOD is found in *Candida albicans* and many crustaceans, which also express a mitochondrial MnSOD. **FeSOD is found in protist *Tetrahymena pyriformis*. ***The genes of CuZnSOD have been identified in two Methanobacteria: *Methanosarcina acetivorans* and *Methanocella arvoryzae*. #Extracellular CuZnSOD is found in mammals and many plants.

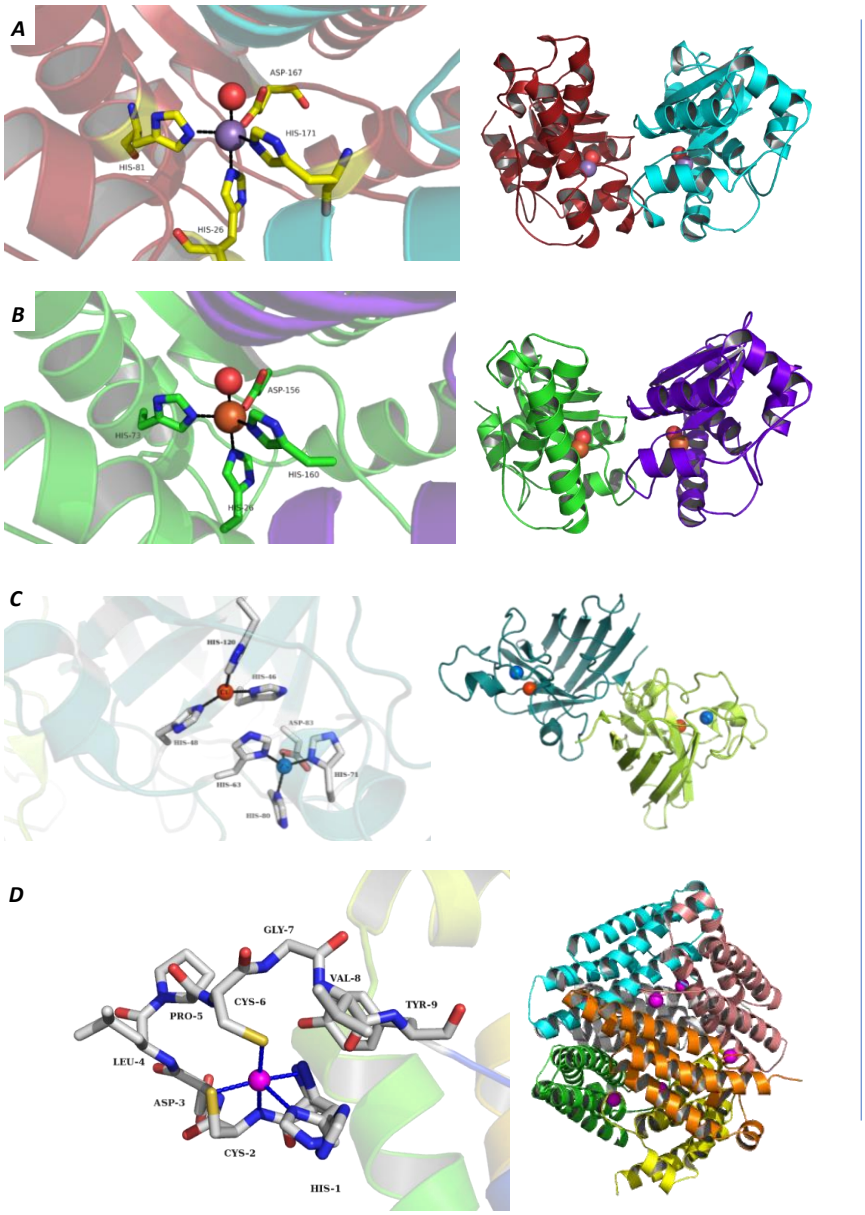

Figure 2.3. Comparison of the active sites (left) and the quaternary structure (right) of SODs.

(A) *E. coli* MnSOD (PDB: 1VEW), (B) *E. coli* FeSOD (PDB: 1ISA), (C) human CuZnSOD (PDB: 1PUO), and (D) *Streptomyces coelicolor* NiSOD (PDB: 1T6U). Diagrams created with PyMOL.

In terms of the origins of SODs, they have distinctive evolutionary relationships. For example, Cu-ZnSOD is not only found in eukaryotes (also referred to as SOD1 and SOD3 in humans) but also in some prokaryotes and archaea. However, NiSOD, the most recently discovered SOD, occurs only in several bacterial species. Moreover, a phylogenetic analysis found evidence that MnSOD, also known as the human SOD2, occurs in all major domains of life of eukaryotes and the cytoplasm of many bacteria (Smith & Doolittle, 1992). On the other hand, FeSOD can be found in the plastids of plants, primitive eukaryotes, archaea and bacteria. MnSOD and FeSOD, which share the same tertiary and dimer quaternary structures as well as active-site ligands to the metal centre (See Figure 2.4), have evolved from the same ancestral gene. However, they have diverged significantly from one another so that in many but not all cases the two metal ions, Mn and Fe, cannot functionally replace each other in the Mn/FeSODs. See active sites in Figure 2.3A and B.

Based on crystal structures tracing from the Protein Data Bank (rcsb.org, accessed on 3 December 2019), there have been 372 structures of SODs collected by X-ray crystallography. Taxonomically, they consist of 238 eukaryotes, 120 bacteria, 13 archaea and 1 virus. Of the total number of structures, they are dominated by the crystal structures of human (136), followed by the cow (*Taurus boss*) (23), *Escherichia coli* (20), *Saccharomyces cerevisiae* (19), *Photobacterium leiognathi* (9), *Candida albicans* (9), *Caenorhabditis elegans* (7) and other species in limited numbers. Based on the metal center, the Cu-ZnSOD family has the most entries (185), followed by the Mn/Fe SOD family (137) and NiSOD (12).

There is only one wild-type human MnSOD (no human FeSOD) and it is observed in a homo-tetrameric form. Currently, there are 27 crystal structures of human MnSOD identified. Of these, 25 structures were identified in homo-tetrameric form and two as modified homo-dimers. There are 11 crystal structures of wildtype and mutants of *E. coli* MnSOD (abbreviated *Ec*-MnSOD); all are homo-dimers. All MnSODs and FeSODs share a common dimer structure, referred to as the canonical dimer.

Beside some obvious differences, there are also some general similarities of these four metalloenzyme types. Firstly, the disproportionation reaction of superoxide takes place through alternate one-electron reduction and oxidation of their catalytic metal ions. Secondly, and this is the most prominent feature of SODs, the catalysis occurs at a rate close to the

diffusion limit. Thirdly, although the protein architectures of the four SOD classes are distinct, they all provide electrostatic guidance to the radical superoxide anion substrate and adjust the redox potential of the metal ions to a range appropriate for superoxide disproportionation. Lastly, the mechanism of disproportion requires the availability of a suitable proton source and enzymatic activity may be controlled through product (H_2O_2) inhibition.

2.4 The Fe/MnSOD family

The cytoplasmic FeSODs and MnSODs in bacteria have defensive functions in protecting the cell from superoxide. However, there are indications that in pathogenic bacteria they may have extra roles in infecting and colonising their host. Structurally, Fe/MnSODs share a high-degree of sequence and three-dimensional structural homology (McCord, 1976).

In addition, FeSOD and MnSOD have also a similarity in the mechanism in which the metal-ion oxidation state alternates between II and III. However, FeSOD and MnSOD are generally strict in recognising their metal ion. Thus, in spite of the high degree of structural similarity, either FeSOD or MnSOD requires a specific metal ion for activity (Parker et al., 1987). The structural basis of this high specificity of the enzymes remains elusive (Edwards, Whittaker, Whittaker, Jameson, & Baker, 1998). Nevertheless, a number of cambialistic enzymes have been reported that are mildly active with either Mn or Fe (Asensio et al., 2011; Lancaster, LoBrutto, Selvaraj, & Blankenship, 2004; Tabares, Bittel, Carrillo, Bortolotti, & Cortez, 2003).

A structure-based alignment of the FeSOD and MnSOD from *E. coli* is shown in Figure 2.4.

Alignment statistics

Score	Expect	Method	Identities	Positives	Gaps
159 bits(401)	3e-54	Compositional matrix adjust.	88/206(43%)	118/206(57%)	17/206(8%)

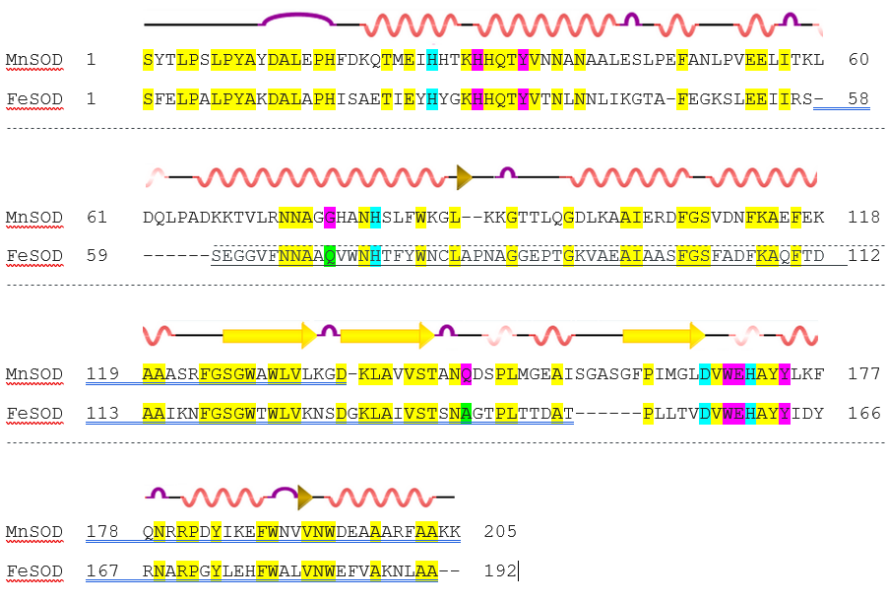

Figure 2.4. Structure-based alignment of MnSOD and FeSOD of *E. coli*.

The yellow shade highlights identical residues, and the cyan shade highlights the position of protein ligands in the active site. Residues in contact with active-site residues are highlighted in magenta and the Gln69 in *Ec*-FeSOD that plays the role of Gln146 in *Ec*-MnSOD (and the complementary residue Ala141) are highlighted in green. The result was analysed by BLASTP. Pink coils denote α-helices; yellow arrows denote β-strands; and purple lines denote coils.

The active-site structures of all MnSOD and FeSOD are absolutely conserved (Figure 2.5). The metal ion is coordinated by three histidines (for the *Ec*-MnSOD, His26, His81 and His171) and an aspartate (Asp167). An hydroxide ion (or water) from the solvent is also coordinated to the

metal. The active sites of the resting enzymes in both redox states (oxidised and reduced) exhibit an absolutely conserved trigonal-bipyramidal coordination in which an Asp and two His ligands are equatorial, and a His and a solvent-derived ligand are axial. Moreover, with two exceptions, residues in contact with the metal ligands are also identical. One exception is that the Gln equivalent to Gln146 of *Ec*-MnSOD, which interacts with the water-derived ligand, is Gln69 in *Ec*-FeSOD. The other exception is that His replaces the Gln equivalent to Gln146 of *Ec*-MnSOD in several cambialistic Fe/MnSODs.

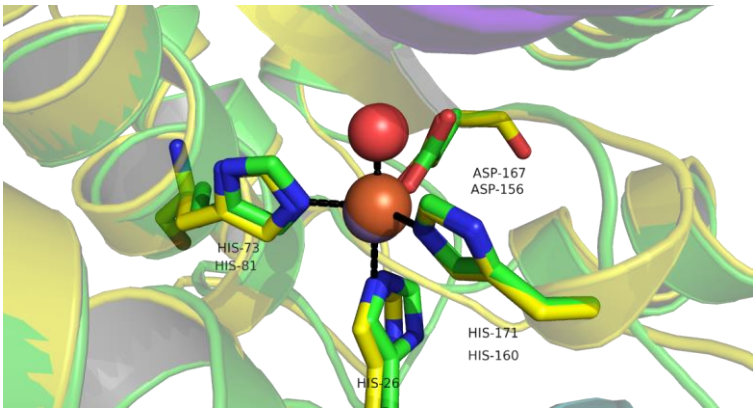

Figure 2.5. Superposition of wt MnSOD and wt FeSOD from *E. coli*.

The manganese and iron ions are represented by light purple and light brown, respectively, while the α-carbon backbones (cartoon) and side chains of *Ec*-MnSOD and *Ec*-FeSOD are in yellow and green, respectively. The side chains of protein ligands of *Ec*-MnSOD (His26, His81, His171, and Asp 167) and *Ec*-FeSOD (His26, His73, His160, and Asp156) share similarities in orientation and distances to the center metal. PDB entries, respectively: 1VEW and 1ISA.

In terms of structural studies of MnSOD and FeSOD, high-resolution crystal structures are now accessible from Protein Data Bank (PDB). *Ec*-MnSOD structures of the catalytically active Y174F mutant have been determined at 0.90 Å, the highest resolution among SODs. The others are from *Deinococcus radiodurans,* and *Aspergillus fumigatus*. FeSOD structures have been determined from more organisms, including *E. coli*, *Vigna unguiculata*, *Aliivibrio salmonicida*, *and Thermosynechococcus elongatus*.

The MnSOD and FeSOD are isolated as dimers. In addition to shared tertiary structure, the interface between monomers is highly conserved. Many other Fe/MnSOD enzymes further associate into tetramers, such as the MnSOD from eukaryotic mitochondria, preserving the canonical dimer interface. The tetramers preserve nearly exact two-fold symmetry within the dimeric elements. Among Fe- and MnSODs, high sequence identity and shared dimeric structure are evidence that the MnSOD and FeSOD are family-related.

2.5 Structural similarity of human and *E. coli* MnSOD

MnSOD is found in both eukaryotes and prokaryotes. Human-MnSOD and *E. coli* MnSOD both have a subunit size of ~22 kDa and share substantial sequence identity of 43% when compared on a pairwise basis (see Figure 2.6). Three-dimensional structures of both wild-type *E. coli* MnSOD (1VEW) and human MnSOD (1N0J) are accessible in Protein Data Bank. A superposition of the structures of the MnSODs from *E. coli* and human is shown in Figure 2.7.

Alignment statistics

Score	Expect	Method	Identities	Positives	Gaps
173 bits(439)	7e-60	Compositional matrix adjust.	90/209(43%)	123/209(58%)	18/209(8%)

```
Ec-MnSOD   2    YTLPSLPYAYDALEPHFDKQTMEIHHTKHHQTYVNNANAALESLPEFANLPVEELITKLD   61
H-MnSOD    2    HSLPDLPYDYGALEPHINAQIMQLHHSKHHAAYVNNLNVTEEKYQEA--LAKGDVTAQIA   59

Ec-MnSOD  62    QLPADKKTVLRNNAGGHANHSLFWKGLKK--GTTLQGDLKAAIERDFGSVDNFKAEFEKA   119
H-MnSOD   60    LQPA-----LKFNGGGHINHSIFWTNLSPNGGGEPKGELLEAIKRDFGSFDKFKEKLTAA   114

Ec-MnSOD 120    AASRFGSGWAWLVLKGDK--LAVVSTANQDSPLMGEAISGASGF-PIMGLDVWEHAYYLK   176
H-MnSOD  115    SVGVQGSGWGWLGFNKERGHLQIAACPNQDP------LQGTTGLIPLLGIDVWEHAYYLQ   168

Ec-MnSOD 177    FQNRRPDYIKEFWNVVNWDEAAARFAAKK  205
H-MnSOD  169    YKNVRPDYLKAIWNVINWENVTERYMACK  197
```

Figure 2.6. Structure-based alignment of MnSOD from two organisms, *E. coli* and human.

The yellow shade highlights identical residues, the cyan shade highlights the position of protein ligands in the active site, and the magenta shade highlights key residues in hydrogen-bonding contact with or in close proximity to the active-site ligands. The alignment was made with BLASTP.

Human MnSOD is a mitochondrial enzyme, a homotetramer constructed as a dimer of dimers with dimeric and tetrameric interfaces (Borgstahl et al., 1992). *Ec*-MnSOD is a cytosolic enzyme and structurally is a compact homodimer in solution. Each subunit of *Ec*-MnSOD and human MnSOD is structurally divided into a two-domain structure comprising an all α-helical N-terminal domain and an α/β C-terminal domain. In the *E. coli* MnSOD structure, the N-terminal helices (A1 and A2, see Figure 2.7) are much shorter than those in human where they form a helical hairpin. On the other hand for the *E. coli* structure, there is an extended loop and a short helix (coloured purple-blue in Figure 2.7).

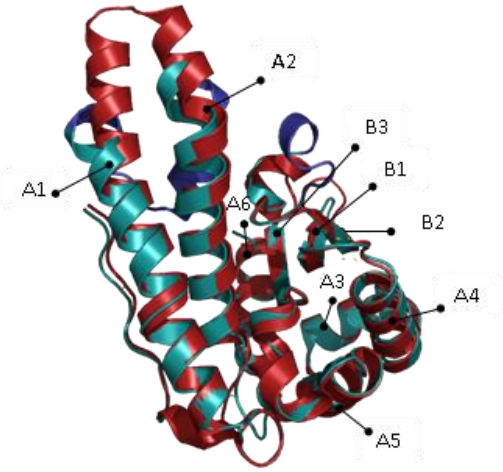

Figure 2.7. Superposition of the structures of the monomer subunits from the homotetrameric human MnSOD (1VEW, cyan) and homodimeric *Ec*-MnSOD (1N0J, red).

Helices are labelled A1-A6 and β-strands B1-B3. *Ec*-MnSOD has 7 more residues than human MnSOD. Significant conformational differences (dark blue-purple) and an evolutionary extension of *Ec*-MnSOD compared to human MnSOD spans Ser44 to Pro64. This conformational difference is also accompanied by the differences in the length of the *Ec*-MnSOD chain until it overlaps the next in helix A2. The structure is visualised using Pymol.

The active-site region and the dimer interface are structurally conserved with small variations between *Ec*-MnSOD and human MnSOD. Two of the metal ligands come from the N-terminal domain and two from the C-terminal domain, comprising three His (His26, His81, His171 in *E. coli* MnSOD, and His26, His74, His163 in human MnSOD) and one Asp (Asp167 *E. coli* MnSOD

and Asp159 in human MnSOD). All four protein ligands at the active sites have essentially identical metal-bound distances and angles to form a trigonal-bipyramidal geometry, including a water-derived hydroxo axial ligand. The active-site residues of human MnSOD and *Ec*-MnSOD are closely superimposable in the vicinity of the manganese ion (see Figure 2.8).

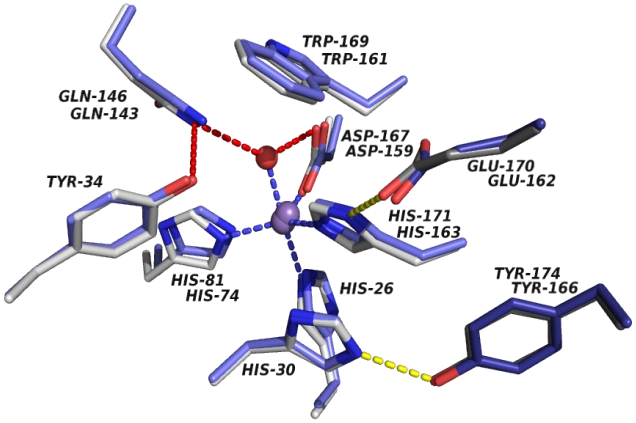

Figure 2.8. Residues at the inner and outer spheres of *Ec*-MnSOD and human MnSOD are absolutely conserved.

The *Ec*-MnSOD (PDB: 1VEW) and human MnSOD (PDB: 1N0J) are represented by light grey and purple, respectively; residue labelling places the *Ec*-MnSOD label above that for human MnSOD, where they differ. Covalent bonds (between metal and protein ligands), hydrogen-bond networks and hydrogen bonds that span the dimeric interface of *Ec*-MnSOD and human MnSOD are represented by blue, red and yellow dashes, respectively. For *Ec*-MnSOD (human MnSOD), Glu170 (Glu162) and Tyr174 (Tyr166) from one subunit hydrogen bond across the canonical dimer interface to His171 (His163) and His30 (His30) of the other subunit For human MnSOD, a water-mediated hydrogen-bond network linking the -OH of Tyr34 to His30 and Tyr166 is not shown.

Table 2.3. Comparison of the lengths of hydrogen and covalent bonds in the active site of *Ec*-MnSOD and human MnSOD.

***Ec*-MnSOD (1VEW)[a]**					**Human wt MnSOD (1N0J)**		
	Chain A	Chain B	Chain C	Chain D	Chain A	Chain B	
Covalent bonds (Å)							Covalent bonds (Å)
Mn-$N^{\varepsilon 2}$(H26)	2.15	2.09	2.19	2.12	2.10	2.09	Mn-$N^{\varepsilon 2}$(H26)
Mn-$N^{\varepsilon 2}$(H81)	2.22	2.21	2.20	2.21	2.08	2.11	Mn-$N^{\varepsilon 2}$(H74)
Mn-$O^{\delta 2}$(D167)	2.01	2.03	2.02	2.01	1.94	1.94	Mn-$O^{\delta 2}$(D159)
Mn-$N^{\varepsilon 2}$(H171)	2.16	2.17	2.15	2.18	2.09	2.09	Mn-$N^{\varepsilon 2}$(H163)
Mn-O(OH)	2.16	2.18	2.28	2.20	2.02	2.01	Mn-O(OH)
Hydrogen bonds (Å)							Hydrogen bonds (Å)
$N^{\varepsilon 2}$(Q146)-O(OH)	2.92	3.01	2.82	2.86	2.94	2.96	$N^{\varepsilon 2}$(Q143)-O(OH)
$N^{\varepsilon 2}$(Q146)-OH(Y34)	3.00	3.04	2.95	2.97	2.88	2.98	$N^{\varepsilon 2}$(Q143)-OH(Y34)
$N^{\delta 1}$(H171)-$O^{\varepsilon 2}$ (E170*)	2.79	2.78	2.85	2.78	2.88	2.99	$N^{\delta 1}$(H163)-$O^{\varepsilon 2}$ (E162*)

[a] Chains A and B form one dimer for *Ec*-MnSOD and chains C and D the other dimer.

[b] For human MnSOD, a crystallographic two-fold axis forms the tetrameric association.

Extending from the active site is a hydrogen-bonded network involving the side chains of Glu146 and Tyr34 in *Ec*-MnSOD. These residues are conserved in human MnSOD (as Glu143 and Tyr34) and the network is extended to His30 *via* a water relay. The side chain of Trp169 (*Ec*-MnSOD) or Trp161 (human MnSOD) is also strictly conserved in its position. This side chain forms one hydrophobic side of the active-site cavity of the MnSOD with the Nε of its indole ring less than 6 Å to Mn metal and indole carbon atoms making close contacts of ~3.1-3.2 Å with the hydroxo ligand.

Another residue strictly conserved across all Mn and FeSODs is Glu170 in *E. coli* MnSOD (Glu162 in human MnSOD). This residue is part of the absolutely conserved DXW**E**HXXY sequence motif, which includes metal ligands Asp167 and His171 in *E. coli* MnSOD (Asp159 and His 163 in human MnSOD). Glu170 (*E. coli* MnSOD) and Glu162 (human MnSOD) span a

dimeric interface and hydrogen bond with manganese ligand His171 (*E. coli* MnSOD) or His163 (human MnSOD) of the adjacent subunit.

The other residue strictly conserved in the dimer interface is Tyr174 (in *E. coli* MnSOD) or Tyr166 (in human MnSOD). The side chain of His30 forms a hydrogen bond across the dimer interface with the Tyr174 (*E. coli* MnSOD) or Tyr166 (human MnSOD) from the adjacent subunit. In the homo-tetramer human MnSOD, Tyr166 participates in a hydrogen-bonded network that extends to the active site.

The structural similarity of *E. coli* MnSOD and human MnSOD is worth highlighting in this introduction since the structure of human MnSOD has been extensively studied in human MnSOD and it will be frequently discussed. Because they have many similarities, it is worthwhile to take advantage of the findings from those studies as a benchmark for further analysis of the mechanism of superoxide dismutation.

2.6 Studies on the mechanism of proton-coupled electron-transfer of MnSODs

There are at least two reasons why the mechanism of the proton-coupled electron transfer reaction of MnSOD is still mysterious despite the discovery of MnSOD half a century ago by McCord and Fridovich (1969). Firstly, it has been difficult to determine the location of hydrogen atoms from a typical protein crystal structure, since a hydrogen atom has only one electron and sits very close to its C/N/O atom, bond length ~0.9 Å in X-ray structures. Secondly, it has been difficult to investigate how superoxide interacts with the catalytic site owing to the short half-life and high reactivity of superoxide in solution.

The mechanism of disproportionation of superoxide to hydrogen peroxide and dioxygen involves alternating reduction and oxidation of the catalytic metal ion. Here, two protons together with two superoxide anions are supplied to generate the products, molecular oxygen and hydrogen peroxide. Electron transfer to $O_2^{\bullet-}$ is actually unfavourable because $O_2^{\bullet-}$ is already negatively charged, while in the LUMO state, an antibonding orbital, protonation is most likely to be a pre- or co-requisite for reduction of $O_2^{\bullet-}$. The second proton may aid in product dissociation by displacing the nascent product from the metal ion in an inner-sphere

mechanism (Bull & Fee, 1985). MnSOD takes up one proton upon reduction (Miller et al., 2003) throughout the pH range of activity (Eq. 1). The redox-coupled proton is then released upon metal-ion oxidation (Eq. 2) and becomes available locally as substrate $O_2^{\bullet-}$ becomes reduced. Thus, reduction of substrate can be thought of as proton-coupled electron-transfer (PCET) (Roth, Yoder, Won, & Mayer, 2001).

To study the mechanism of the proton-coupled electron transfer, structural biologists have made extensive analysis of structure and enzyme activity using mutational analysis. Essentially, the structure-based mutational analysis of *E. coli* and human MnSOD revealed that any mutagenesis of residues in the hydrogen bond network or around the outer-sphere area affected the activity or the stability, or both the activity and the stability of the enzyme, notwithstanding the mutations causing only minimal structural changes to the active site.

There are several methods to characterise the superoxide dismutase activity. The first is the SOD activity assay, which was first introduced by McCord and Fridovich (1969). At the first stage (Eq. 8), superoxide is generated through the oxidation of xanthine in the presence of dioxygen, a reaction catalysed by xanthine oxidase. Subsequently, the superoxide reduces cytochrome-c (Eq. 9). The rate of cytochrome-c reduction is measured at 550 nm spectrophotometrically. At the final stage, MnSOD inhibits cytochrome-c reduction by catalysing superoxide dismutation (Eq. 10; see Chapter 3 Methodology). This widely used method has been chosen to assay the superoxide dismutase activity for *E. coli* MnSOD and other SODs.

$$\text{Xanthine} + O_2 + H_2O \xrightarrow{\text{XOD}} \text{Uric acid} + O_2^{\bullet-} + H^+ \quad (8)$$

$$\text{Cytochrome-}c(Fe^{3+}) + O_2^{\bullet-} \longrightarrow \text{Cytochrome-}c(Fe^{2+}) + O_2 \quad (9)$$

$$O_2^{\bullet-} + 2\,H^+ \xrightarrow{\text{SOD}} O_2 + H_2O_2 \quad (10)$$

The second method to measure superoxide dismutase activity is to produce superoxide ions by pulse radiolysis, a method that has been used to study human MnSOD. This method can be used to determine directly the rate constants for catalysis. The mechanism involves not only cycling between oxidised (Mn^{+3}) and reduced (Mn^{+2}) metal, reactions 11 and 12, but also involves additional processes as simple first-order disappearance of $O_2^{\bullet-}$ is not observed at

sufficiently high ratios of $[O_2^{\bullet-}]$:[MnSOD]. There is a burst phase and a zero-order step, which leads to a mechanism where MnSOD, in its reduced form is proposed to react with superoxide through two concomitant pathways, giving the overall mechanism (reactions 11-14). The mechanism includes the formation of the inhibited complex, $Mn^{3+}SOD(H_2O)\text{-}O_2^{2-}$, simplified as $Mn^{3+}SOD\text{-}O_2^{2-}$. The formation of the inhibited complex occurs parallel to $Mn^{3+}SOD(OH^-)$ formation. This mechanism, which was first proposed by Bull, Niederhoffer, Yoshida, and Fee (1991) and adapted by Abreu and Cabelli (2010), can be described in the following reactions.

$$Mn^{3+}SOD(OH^-) + O_2^{\bullet-} (+H^+) \rightarrow Mn^{2+}SOD(H_2O) + O_2 \quad (k_1) \qquad (11)$$

$$Mn^{2+}SOD(H_2O) + O_2^{\bullet-} (+H^+) \rightarrow Mn^{3+}SOD(OH^-) + H_2O_2 \quad (k_2) \qquad (12)$$

$$Mn^{2+}SOD(H_2O) + O_2^{\bullet-} \rightarrow Mn^{3+}SOD(H_2O)\text{–}O_2^{2-} \quad (k_3) \qquad (13)$$

$$Mn^{3+}SOD(H_2O)\text{–}O_2^{2-} (+H^+) \rightarrow Mn^{3+}SOD(OH^-) + H_2O_2 \quad (k_4) \qquad (14)$$

Table 2.4. Comparison of rate constants in the kinetic mechanism of several MnSODs.

MnSOD	k_1 (/(nM^{-1} s^{-1}))	k_2 (/(nM^{-1} s^{-1}))	k_3 (/(nM^{-1} s^{-1}))	k_4 (/s^{-1})
E. coli[a]	1.1	0.9	0.2	60
Human[b]	1.5	1.1	1.1	120
D. radiodurans[c]	1.2	1.1	0.07	30

[a] *(Zheng, Domsic, Cabelli, McKenna, & Silverman, 2007)*.

[b] *(Perry et al., 2009)*.

[c] *(Abreu et al., 2008)*.

Single point mutations in human MnSOD tend to highly affect catalysis when the mutated residues are those necessary to conserve the hydrogen-bonded network in the inner or outer-sphere. Significant alterations in terms of redox potential, hydrogen-bond network disruption, or steric impediment for substrate binding are factors affecting the rate constants and catalytic activities. Substantial alteration of one or more factors above caused by a single substitution that could shut-down the catalytic activity is valuable to the study of the mechanism of MnSOD. Point mutations around the hydrogen-bond network strongly affect

the rate constant k_2 (reaction 12) and the inhibited-product dissociation rate constant k_4 (reaction 14). Other point mutations can affect different rate constants in the mechanism, but usually the gating remains the same ($k_2/k_3 \approx 1$) for human MnSOD. On the other hand, for wild-type *E. coli* and other prokaryotic MnSODs, such as that from *Deinoccocus radiodurans*, the ratios k_2/k_3 are much higher than that of human MnSOD, at ~5 and ~16, respectively. The value of k_2/k_3 determines the proportion of $O_2^{\bullet-}$ reacting through an outer-sphere (reaction 12) *versus* an inner-sphere pathway (reactions 13 and 14). Reaction 13 describes formation of the product-inhibited complex, whereas reaction 14 describes the rate of dissociation of the inhibited complex to form hydrogen peroxide.

The long journey to uncover the roles of particular residues in the mechanism of proton-coupled electron transfer of the *Ec*-MnSOD and human MnSOD is briefly summarised below. At the end of this section kinetic data for a range of mutants of human MnSOD and *Ec*-MnSOD are summarised in Tables 2.5 and 2.6, respectively.

2.6.1 Glutamine 146

Glutamine 146, an absolutely conserved outer-sphere residue in Mn-specific MnSODs, has been investigated structurally and spectroscopically by Edwards, Whittaker, Whittaker, Baker, and Jameson (2001a). In wild-type *Ec*-MnSOD, Gln146 participates in an extensive hydrogen-bonded network in the active site. Gln146 forms hydrogen bonds with the manganese-bound solvent and the phenolic hydroxyl of Tyr34. Mutations of the outer-sphere solvent-pocket residue, Gln146Leu and Gln146His, have dramatic effects on catalytic activity, retaining only 5-10% of the dismutase activity of the wild-type enzyme. However, X-ray crystallographic analyses of the site-directed mutants Gln146Leu and Gln146His reveal only subtle changes in protein structure (see Figure 2.9). The hydrogen-bonding network in the active site is disrupted by mutation of Glu146 and leads to a rearrangement of the Tyr34 and disorder of the Trp128 side chain (Edwards et al., 2001a).

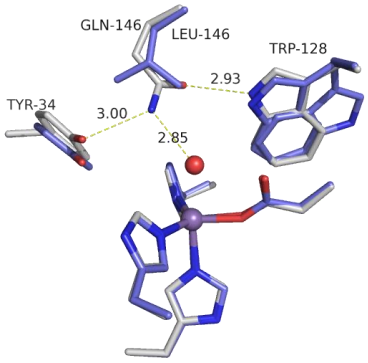

Figure 2.9. Superposition of Gln146Leu mutant of *Ec*-MnSOD onto wild-type *Ec*-MnSOD showing active-site differences.

Gln146Leu structure in purple (PDB entry: 1EN6) and the wild-type structure in grey (PDB entry: 1VEW). The hydrogen-bonding network is shown for wt *Ec*-MnSOD. This figure was drawn by PyMol.

In human MnSOD, the structure and function of Gln143 (Gln146 in *Ec*-MnSOD) have also been investigated by Hsieh et al. (1998) and Leveque et al. (2000). Hsieh et al. (1998) found that the mutation Gln143Asn made a significant change, where the side-chain amide nitrogen of Asn143 is 1.7 Å more distant from the manganese than in the wild-type enzyme (PDB: 1QNM). The Tyr34 side-chain hydroxyl in Gln143Asn shifts to be 0.6 Å more distant from the metal to accommodate an additional water molecule, which hydrogen bonds not only to Tyr34_OH and Asn143_OD1/ND2 but also to the water-derived Mn ligand. The mutation of the solvent-pocket residue Gln146Asn decreases the overall catalytic activity by 2-3 orders of magnitude compared with the wild-type human MnSOD, but interestingly it slightly increased thermal stability by 2 °C to 90.7 °C.

However, the mutation Gln143Ala to human MnSOD (PDB: 1EM1) made no significant change in the overall structure of the mutant enzyme (Leveque et al., 2000). There are, however, two new water molecules inserted into the hydrogen-bonded network at positions nearly identical with the OE1 and NE2 of the replaced Gln143 side chain. The mutation of the solvent-pocket residue Gln143Ala decreased k_{cat}/K_m by 250-fold and thermal stability was reduced by 16 °C. The mutant Gln143Ala showed a very low level of product inhibition and favoured Mn(II)SOD

in the resting state, whereas wild-type human MnSOD showed a high level of product inhibition and favoured an Mn(III) resting state. In addition, mutations to Gln143 alters metal specificity and active-site redox potential contributing to the decrease in catalytic activity for both mutants, Gln143Ala and Gln143Asn (Grove & Brunold, 2008; Leveque et al., 2000).

2.6.2 Tyrosine 34

Tyr34 is a strictly conserved gateway residue in the outer sphere of the manganese superoxide dismutases of bacteria, human and other organisms. Although Tyr34 of *Ec*-MnSOD and human MnSOD are structurally superimposable, structure-based mutational analysis of *Ec*-MnSOD and human MnSOD reveal that Tyr34 of *Ec*-MnSOD has different involvement and function to the Tyr34 of the human in performing SOD activities.

In *Ec*-MnSOD, conservative replacement of tyrosine by phenylalanine (Tyr34Phe, PDB: 1EN5) reduces by only 20% the superoxide dismutase activity relative to the wild-type *Ec*-MnSOD (M. M. Whittaker & Whittaker, 1997). Furthermore, the replacement of tyrosine by alanine (Tyr34Ala) interestingly retains essentially full superoxide dismutase activity of the wild-type *Ec*-MnSOD (Edwards et al., 2001a). Since the substitution of Tyr34Phe only gave small changes to the activity, Tyr34 is suggested not to be essential for superoxide dismutase activity. However, Tyr34 may function indirectly as a proton donor for turnover, coupled to a protonation cycle of the metal ligands which contribute to the catalytic rate enhancement of the *Ec*-MnSOD by as much as 20% over the observed steady-state rate. The water structure near the active site is largely conserved in the Tyr34Phe mutant, except that the water hydrogen-bonded to the hydroxyl group of Tyr34 in wild-type *Ec*-MnSOD is not observed in the Tyr34Phe mutant. However, as discussed later, mobile water molecules will not be observed in electron density maps, but such water molecules may be critical to the very rapid dismutation of superoxide.

In human MnSOD, similar replacement of tyrosine 34 by phenylalanine (Guan et al., 1998) led to two different crystal forms, orthorhombic (PDB: 1AP5, resolution 2.2 Å) and hexagonal (PDB: 1AP6, resolution 1.9 Å). However, both crystal forms show similar structures which are closely superimposable with that of wild-type human MnSOD. Moreover, the phenyl rings of

the Tyr34Phe mutant and Tyr34 of the wild-type enzyme have similar orientation, but in the absence of the hydroxyl in Tyr34Phe for both human and *Ec*-MnSOD, the hydrogen-bonded chain from Tyr34 and extending to the manganese-bound solvent ligand is broken (see Figure 2.10). Catalytic analysis result shows the k_{cat} for maximal catalysis of the Tyr34Phe is smaller by 10-fold than the wild-type, and the enzyme is more susceptible to product inhibition by peroxide than the wild-type. These effects may be caused by the absence of this hydroxyl in Tyr34Phe, which leads to less proton donation to product peroxyl and k_{cat} is decreased. Surprisingly, the Tyr34Phe mutant results in increased protein stability, with an increase in T_m as measured by differential scanning calorimetry, implying that the Tyr34 hydroxyl has no important role in stabilising active-site architecture.

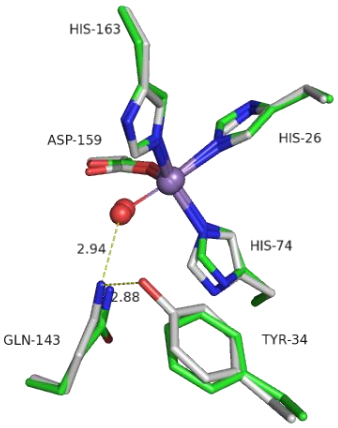

Figure 2.10. Diagram comparing the geometry of the active site in the wild-type and the Tyr34Phe mutant of human MnSOD.

The native (PDB: 1N0J) is shown in grey, and Tyr34Phe MnSOD (PDB: 1AP5) is in green. Diagram shows that Phe34 cannot form a hydrogen bond to NE2 of Gln143.

Further structure-based mutational analyses were performed to investigate the function of Tyr34 in human MnSOD through substitution of Tyr34 with five different amino acids: Tyr34Phe (PDB: 1AP5, 1AP6), Tyr34Ala (PDB: 1ZSP), Tyr34Asn (PDP: 2P4K), Tyr34His (PDB: 1ZTE), and Tyr34Val (PDB: 1ZUK) (Perry et al., 2009). All the mutants retained the protein structure of the active site and the tetrameric quaternary assembly, but caused significant decreases in the catalytic rate constant for the reduction of superoxide. The Tyr34Val mutant structure shows an altered hydrogen-bonding network (a water appears at the site of the

Tyr34 hydroxyl group of wild-type enzyme), which is associated with a rapid dissociation of the product-inhibited complex. Abreu, Rodriguez, and Cabelli (2005) reported that Tyr34 is important to maintain a hydroxide ligand bound to Mn^{3+} giving a thermodynamic barrier for proton transfer. The thermodynamic barrier is decreased only when superoxide substrate is bound. This facilitates proton transfer as part of electron transfer from $O_2^{\bullet-}$ to Mn^{3+} (proton-coupled electron transfer). Thus, mutations of Tyr34 raise this barrier to proton transfer to the bound hydroxide, which could affect the rate constant (k_1) value and lead to virtual shut-down of catalysis through reactions 13 and 14. However, given similar structural changes for the Tyr34Phe for the MnSOD from *E. coli* and human, the different effects on enzyme activity are difficult to explain.

2.6.3 Histidine 30 and tyrosine 174

The side chains of His30 and Tyr174 from adjacent subunits in dimeric *E. coli* manganese superoxide dismutase form a hydrogen bond across the dimer interface. In homotetrameric human MnSOD, the equivalent residues His30 and Tyr166 from adjacent subunits are also structurally linked by a hydrogen bond across the dimer interface. But in human MnSOD, this His30-Tyr166 participates in a hydrogen-bonded network that extends to the active site. Both residues His30 and Tyr174 (Tyr166 in human MnSOD) form part of the substrate access funnel in the active site.

The structure and function of residues His30 and Tyr174 in *E. coli* MnSOD activity have been extensively investigated. The replacement of His30 by either Ala or Asn reduces the SOD activity to 30% and 38% of wild-type MnSOD, respectively. The mutation of Tyr174Phe, which is quite remote from the MnSOD metal centre, retains 41% of the superoxide dismutase activity of the wild-type *E. coli* MnSOD. The structure of His30Ala MnSOD mutant (PDB: 1I08), which removes the Tyr174…His30 hydrogen-bond from the acceptor side, results in a substantial shift of the main-chain segment containing the Tyr174 residue with local protein local rearrangement. The structure of Tyr174Phe mutant (PDB: 1I0H) shows that the disruption of the same hydrogen bond from the donor side causes greater structural rearrangement. Reorientation of Phe174 gives a domino effect on adjacent residues and leads to a major rearrangement of the dimer interface and flipping of the His30 side chain (see

Figure 2.11). The structure suggests that the mutation at a remote position as in Tyr174Phe may affect the metal reactivity and alter the effective pK_a for hydroxide ion binding. The His30 imidazole NH group hydrogen bond is suggested to play a key role in substrate binding and analysis (Edwards et al., 2001a).

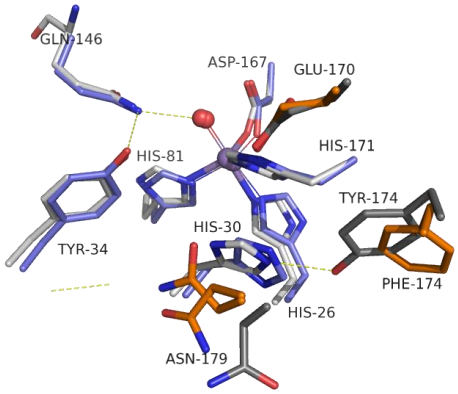

Figure 2.11. Structural comparison of wild-type *Ec*-MnSOD (PDB: 1VEW) and its Tyr174Phe mutant (PDB: 1I08).

Superposition of dimer wild-type *Ec*-MnSOD (grey) and its Tyr174Phe mutant (grey-blue and orange for residues from the other subunit of the canonical dimer).

In human MnSOD, structure-based mutations were performed to investigate the function of His30 through substitution of His30 with three different amino acids: His30Asp, His30Gln, and His30Val (A. S. Hearn et al., 2003). Among three mutants, k_{cat}/K_M of His30Val was decreased and product inhibition of His30Val was increased, both by two orders of magnitude compared with wild-type human MnSOD. Atom CG of the Val30 side chain occupies the approximate position of a water molecule in wild-type enzyme. The Val30 side-chain orientation has significantly interrupted catalysis by this overlap into the access channel which may blockade substrate-product access and exit and leads to the 100-fold decrease in the rate constant for dissociation of the product-inhibited complex compared with wild type.

A study to compare the effects of single and double mutations on superoxide dismutase activities of His30Asn, Tyr166Phe and His30Asn/Tyr166Phe (PDB: 1PM9) of human MnSOD

was carried out (A. S. Hearn et al., 2004). The results reveal that the site-specific mutants His30Asn and Tyr166Phe, and the corresponding double mutant showed a 10-fold decrease in steady-state constants for catalysis. However, the effect of the double mutant on thermal stability was not greater than that of either single mutant, and structurally the conformational changes of each mutant resulted in loss of hydrogen bonds across the dimer interface, which caused the decrease in catalysis.

2.6.4 Glutamic acid 170

In the homodimeric *Ec*-MnSOD, the absolutely conserved Glu170 (Glu162 in homotetrameric human MnSOD) spans the dimer interface and forms a hydrogen bond with manganese ligand His 171 (His 163 in human MnSOD) of an adjacent subunit. To study the function of Glu170, replacement by alanine has been investigated in both *E. coli* (E170A) and human (E162A) MnSOD.

There are significant differences noted in properties of *Ec*-MnSOD-Glu170Ala compared with an equivalent mutant from human MnSOD. The *E. coli* mutant loses catalytic activity completely and the dimer structure is destabilised in solution resulting in a mixture of dimer and monomer species. As isolated, iron has replaced manganese in the active site, which can then be replaced by manganese. Moreover, the iron-substituted Fe_2-*Ec*-MnSOD-Glu170Ala resembles authentic Fe-specific *Ec*-FeSOD in spectroscopy results, and wild-type (Mn_2) *Ec*-MnSOD and Mn_2-MnSOD-Glu170Ala are also spectroscopically similar. Reconstitution of Fe_2-MnSOD Glu170Ala with Mn(II) salts does not restore SOD activity. This is in contrast to the equivalent Glu162Ala mutation in human MnSOD, which is catalytically active although at only 5-25% of the wild-type human MnSOD activity. The Glu162Ala human MnSOD mutant (PDB: 3C3S) also retains its tetrameric form in solution and retains its specificity for manganese (Quint, Domsic, Cabelli, McKenna, & Silverman, 2008). The extensive tetrameric interface enforces retention of the canonical dimer structure, despite the loss of Glu162 in the Glu162Ala human MnSOD mutant.

These differences occur distinctly while the crystal structures of the human and *E. coli* MnSOD shows nearly superimposable residues for the ligands of the metal and outer-sphere side

chains of Glu146, Tyr34 and His30 (Figure 2.8). The different responses of the *E. coli* and human forms of MnSOD to replacements at residue 170 may be caused by a significantly different set of interactions, including van der Waals interactions that form part of the dimeric interface of human MnSOD between Phe66 and Gln119 though in a different orientation compared to that in *E. coli* MnSOD. This specific difference, although rather far from the manganese, is one of many interactions at the dimer interface that is likely to account for differences in properties of MnSOD from human and *E. coli*.

Table 2.5. Structure and activity of *Ec*-MnSOD featuring mutations of second-shell residues.

Enzyme	SOD activity (/(units/mg))	Relative activity	Structure	Reference
Ec-MnSOD	7300	100%	1VEW	(Edwards, Baker, et al., 1998)
Gln146His	600	8%	1EN4	(Edwards et al., 2001a)
Gln146Leu	340	5%	1EN6	(Edwards et al., 2001a)
Tyr34Phe	6000	82%	1EN5	(Edwards et al., 2001a; Whittaker & Whittaker, 1997)
Tyr34Ala	7300	100%	--	(Edwards et al., 2001a)
His30Ala	2200	30%	1I08	(Edwards, Whittaker, Whittaker, Baker, & Jameson, 2001b)
His30Asn	2800	38%	--	(Edwards et al., 2001b)
Tyr174Phe	3000	41%	1I0H, 1IX9, 1IXB, 1ZLZ	(Edwards et al., 2001b)
Glu170Ala	0	0	--	(Whittaker & Whittaker, 1998)

Table 2.6. Individual rate constants in the kinetic mechanism of human MnSOD and its mutants and the relative values compared to those of the wild-type enzyme.

Human MnSOD	Rate constant (/(nM^{-1} s^{-1}))			(/s^{-1})	Relative rate constant (in % of that of wt h-MnSOD)				Structure (PDB ref)	Reference
	k_1	k_2	k_3	k_4	k_1	k_2	k_3	k_4		
Wild-type	1.5	1.1	1.1	120	100	100	100	100	1N0J, 1LUV, 5VF9	(Borgstahl et al., 1992)
Y34A	0.25	< 0.02	0.38	330	17	< 1.8	35	280	1ZSP	(Perry et al., 2009)
Y34N	0.14	< 0.02	0.15	200	9	< 1.8	14	170	1ZTE	(Perry et al., 2009)
Y34H	0.07	< 0.02	0.04	61	5	< 1.8	4	51	1ZUQ	(Perry et al., 2009)
Y34V	0.15	< 0.02	0.15	1000	10	< 1.8	14	830	2P4K	(Perry et al., 2009)
Y34F	0.55	< 0.02	0.46	52	37	< 1.8	42	43	1AP5	(Guan et al., 1998)
H30N	0.21	0.40	0.68	480	14	36	62	400	2GDS	(Hearn et al., 2003)
H30Q	0.57	0.79	0.79	200	38	72	72	170	1LUW	(Hearn et al., 2003)
H30V	~0.005	~0.03	0.16	0.7	~0.3	~2.7	15	1	1N0N	(Hearn et al., 2003)
E162D	0.36	0.13	0.21	40	24	12	19	33	3C3T	(Quint et al., 2008)
E162A	0.06	0.05	0.09	30	4	5	8	25	3C3S	(Quint et al., 2008)
F66A	0.6	0.5	0.7	82	40	45	64	68	2QKA	(Zheng et al., 2007)
F66L	0.7	0.8	0.2	40	47	73	18	33	2QKC	(Zheng et al., 2007)
W123F	0.76	< 0.02	0.64	79	51	< 1.8	58	66	1SZX	(Greenleaf et al., 2004)
Y166F	0.2	0.2	0.2	270	13	18	18	230	1PL4	(Quint et al., 2008)
W161A	0.08	< 0.01	0.37	180	5	< 1	34	150	1JA8	(Hearn et al., 2001)
W161F	0.3	< 0.01	0.46	33	20	< 1	42	28	-	(Hearn et al., 2001)
W161V	na	na	0.27	265	na	na	25	220	-	(Hearn et al., 2001)
W161Y	na	na	0.20	130	na	na	18	110	-	(Hearn et al., 2001)
W161H	na	na	0.29	136	na	na	26	110	-	(Hearn et al., 2001)
H30F/Y166F	0.1	0.1	0.1	440	7	9	9	370	-	(Guan et al., 1998)
Y34F/W123F	0.55	< 0.22	0.46	52	37	< 20	42	43	-	(Greenleaf et al., 2004)
Y143N						k_{cat} <1%				(Hsieh et al., 1998)
Y143A						k_{cat}/K_M ~1/250				(Leveque et al., 2000)

2.7 Problems with the conventional view of the mechanism

MnSOD, as well as other SODs, protect cells from reactive oxygen species by catalysing the disproportionation of superoxide anion radicals. Considering that the substrate superoxide anion radical just has one single electron different than molecular oxygen product, this means that here the enzyme must have an extreme specificity and be finely tuned to perform its catalytic role, catalysing both the oxidation and reduction of the superoxide anion-radical. In addition, superoxide must be distinguished from other species that are roughly the same size in the cell (Crane et al., 1998). Studies have also been carried out to explain how this enzyme controls substrate specificity, substrate and product access, respectively, into and from the metal-ion active site.

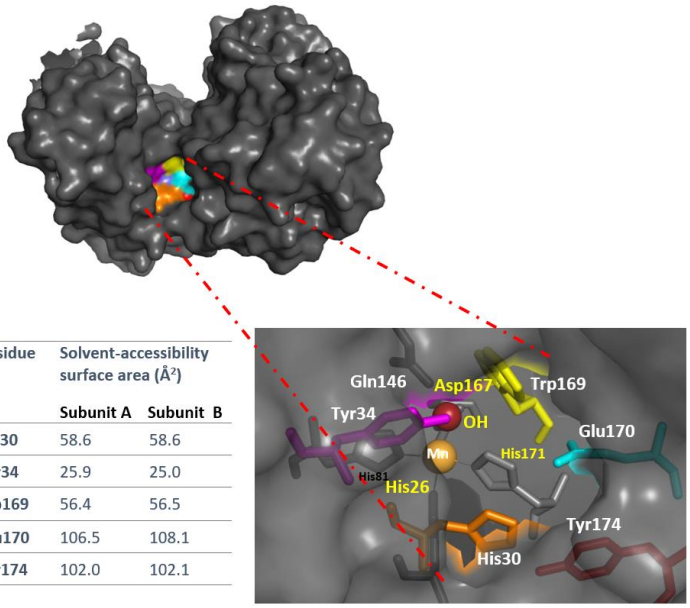

Residue	Solvent-accessibility surface area (Å²)	
	Subunit A	Subunit B
His30	58.6	58.6
Tyr34	25.9	25.0
Trp169	56.4	56.5
Glu170	106.5	108.1
Tyr174	102.0	102.1

Figure 2.12. The substrate gateway of the outer sphere of *Ec*-MnSOD.

The substrate gateway is constructed from Tyr34, His30 and Trp169 from one subunit, and two residues from the adjacent subunit of the canonical dimer: Glu170 and Tyr174 (top and middle). The substrate gateway provides access for small anions and solvent from the bulk solvent (outside surface of the protein) to enter the inner sphere through a solvent-filled funnel. The solvent-accessibility surface areas are calculated with PDBePISA online application (ebi.ac.uk). The picture was derived from PDB code 1VEW.

Substrate access to the active site occurs through a solvent-filled funnel that leads from the outside surface of the protein, which is exposed to the bulk solvent, towards the metal active site of each monomer, terminating at the metal-bound solvent molecule. The funnel is constructed from residues contributed by both subunits. The residues at the base of the funnel, Tyr34, His30 and Trp169 from one subunit and from the other Tyr174 and Glu170, are absolutely conserved among all Fe- and MnSODs and they partly shield the active site from the solvent, as shown in Figure 2.12. A small hole between the closely packed side chains provides access for small anions and solvent to enter the inner sphere. Thus, these essential residues have a key role as the substrate gateway (Edwards et al., 2001b).

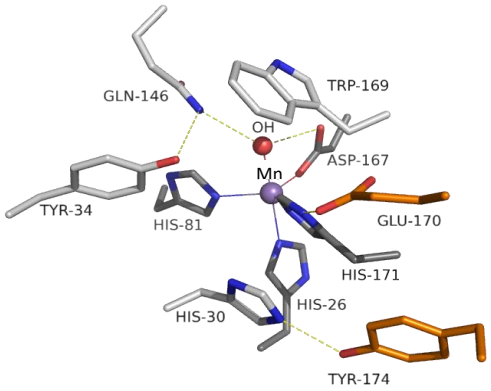

Figure 2.13. The inner (dark grey) and outer (light grey) spheres of the *Ec*-MnSOD.
The hydrogen-bonded network in yellow dashes links Tyr34, Gln146 and the hydroxo/water ligand. The side chains of protein ligand His171 and Glu170 from the adjacent subunit in dimer *Ec*-MnSOD form a hydrogen bond across the dimer interface, as well as the His30 and Tyr174. The residues from the adjacent subunit are shown in orange. The picture was derived from PDB code 1VEW using PyMol.

In the conventional view, a proton attaches to the coordinated hydroxide ligand on reduction to Mn(II) concomitant with oxidation of superoxide (see Figure 2.13). But the problem is that to transfer the proton from the solvent, the proton has to transfer from the gateway Tyr34, which is protic, to Gln146, which is hydrogen-bonded to Tyr34 and to the hydroxide ion ligand. However, Gln146 is non-protic and as noted in section 2.6.2, mutation of Tyr34 to Phe or Ala has negligible effect on activity, at least for *Ec*-MnSOD. Mutation of Gln146 to His causes

significant reduction to 10% in activity but mutation to Leu still leaves 5% residual activity (Edwards et al., 2001a).

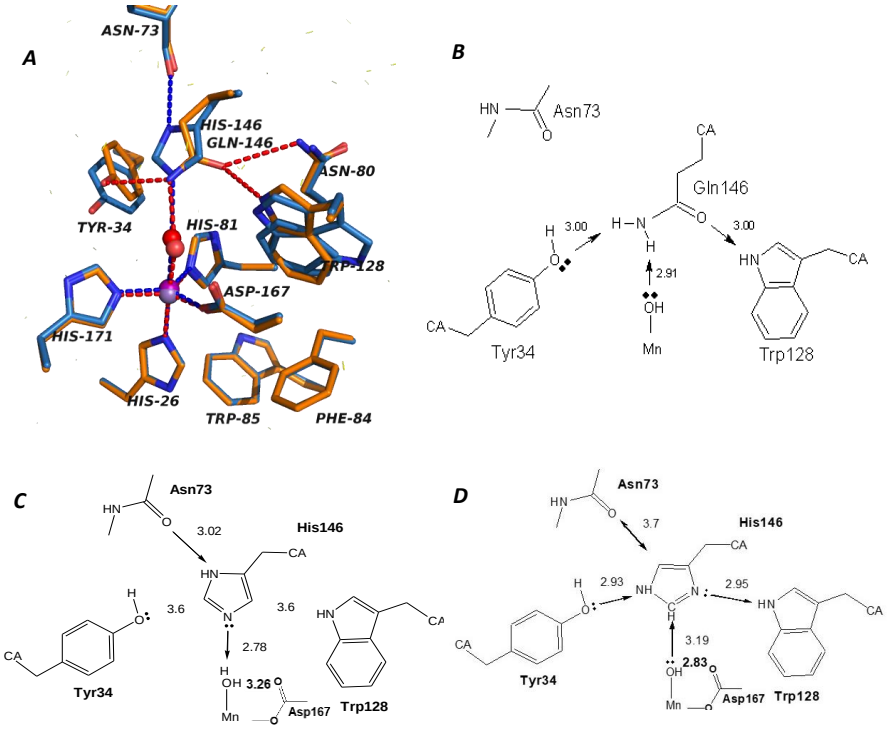

Figure 2.14. The hydrogen-bonding network of the generally accepted proton shuttle.

(A) Superposition of wild-type *Ec*-MnSOD onto its Gln146His mutant. (B) The hydrogen-bonding network for *Ec*-MnSOD. *Ec*-MnSOD-Gln146His (PDB: 1EN4) in blue and wild-type *Ec*-MnSOD in orange (PDB: 1VEW). (C) The hydrogen-bonding network for the Gln146His mutant of *Ec*-MnSOD. A new hydrogen bond is formed between Asn73_O and His146_ND1, but the Gln146His mutant has lost hydrogen bonding to the hydroxyl group of Tyr34 and to N-H of Trp128. Interestingly, the catalytic activity is not completely lost, leaving a question: how is the proton shuttled to the hydroxo ligand if it has to pass through Tyr34 and His146 (or Leu146). (D) The hydrogen-bonding network in FeSOD and cambialistic SODs with His equivalent to Gln146 of *Ec*-MnSOD (*Mycobacterium tuberculosis* (1IDS), *Propionobacterium shermanii* (1AR5, corrected), *Sulfolobus* (*Saccharolobus*) *solfataricus* (1WB8), *S. acidocaldarius* (1B06), *Pyrobaculum aerophilum* (1P7G, also MnSOD), *Thermobacterium* (*Methanothermobacter*) *thermoautotrophicum* (*thermoautotrophicus*) (1MA1).

Moreover, in SODs where in the wild-type or native form His replaces this Gln146, the His is unequivocally oriented to place the non-protic CE1-H moiety in a non-classical hydrogen-bonding contact with the coordinated hydroxide (see Figure 2.14). These SODs where histidine replaces Gln146 are typically FeSODs or are cambialistic (non-specific for Fe or Mn) SODs. As oriented neither Gln nor His is able to accept a proton from Tyr34 or to donate a proton to the metal-coordinated OH^-.

Finally, the site of putative proton addition to the coordinated hydroxide is blocked by proximity of Trp169, which participates in an n-π* interaction with the lone pair of electrons on the coordinated hydroxide (Figure 2.15). In all structures of active MnSODs, the distance of closest approach is 3.1-3.2 Å between the hydroxide and indole carbon atoms, a distance substantially shorter than van der Waals contacts of ~3.5 Å.

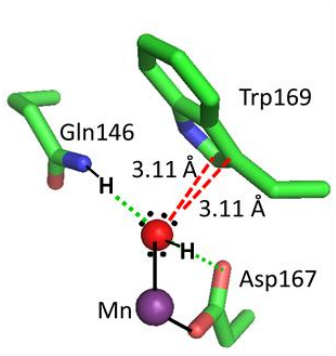

Figure 2.15. The n-π* interaction between the coordinated hydroxide and Trp169 in *Ec*-MnSOD.

In the 0.90 Å resolution structure of reduced *Ec*-Mn^{II}SOD-Y174F (PDB: 1IXB), only a single proton was observed attached to the water-derived ligand in both of the crystallographically independent subunits. This hydrogen atom was located between the hydroxide ligand and the carboxylate oxygen of metal ligand Asp167.

Gln146, therefore, appears unlikely to mediate transfer of a proton from bulk solvent to the coordinated hydroxide. In fact, entrance of superoxide and protons to and departure of hydrogen peroxide and dioxygen from the active site occur through a narrow hole at the base

of the substrate-access funnel, the substrate gateway. Thus, there appears to be a traffic problem with substrate and products each passing through the same small opening at rates in excess of 40,000 s^{-1}, which is close to the diffusion rate. The structure of MnSOD features many barriers to prevent the proton from getting near the metal ion and to enable diffusion-limited reaction rates.

The other empirical evidence against proton transfer onto the coordinated hydroxide comes from the ultra-high resolution (0.90 Å) structure of the highly active *Ec*-Mn^{II}SOD-Y174F mutant (PDB code 1IXB). Here, the electron density around the active site indicated that the solvent ligand is hydroxide rather than water in the reduced Mn(II) form of MnSOD, and that on reduction from Mn(III), the n-π* interaction of the coordinated hydroxide with Trp169 shortened by 0.10 Å for both crystallographically independent subunits (PDB 1IXB (Mn^{II}SOD) and 1IX9 (Mn^{III}SOD)). This means that the proton may be attached somewhere else in the enzyme rather than to the hydroxide ligand. These facts argue against the conventional view that upon reduction of Mn^{III} to Mn^{II} the coordinated hydroxide picks up a proton to become coordinated water. This model was reiterated in the review by Azadmanesh and Borgstahl (2018). Hence, the proton is suspected to have an alternative location near or in the active site.

Another fact that supports an alternative proton pathway is that the point mutation of Glu170, which is absolutely conserved and hydrogen bonds to metal ligand His171, completely deactivates the *Ec*-MnSOD enzyme (Whittaker & Whittaker, 1998). As shown in Figure 2.16, Glu170 of the opposite subunit almost symmetrically (see below) spans the dimer interface to form hydrogen bonds with His171 in the other subunit. This means that the Glu170 is not only absolutely conserved in the active site, but also it is figured to be important in the proton shuttle and/or in tuning the redox potential of the metal centre. There is no article to date that reports on altering the canonical dimeric MnSOD into discrete monomeric subunits and the effect this might have on the activity while retaining the Glu170.

2.8 Outer-sphere mechanism for proton delivery

If the Mn-coordinated hydroxide is not the site of protonation when Mn(III) is reduced by superoxide to Mn(II), then where is the proton that the nascent hydrogen peroxide picks up located? His30 sits guarding access to the metal centre. However, the His30Ala mutant still retains much of the activity of the wild-type enzyme (Table 2.5).

In the azide-bound structure of the active Y174F mutant of *Ec*-MnSOD (PDB: 1ZLZ), azide (N_3^-), which is a proxy for superoxide ($O_2^{\bullet-}$), binds in an ordered manner to Mn(III) at just one of the two subunits along with an added water molecule. Binding of N_3^-…H_2O completes a water relay to the absolutely conserved Glu170 (see Figure 2.16).

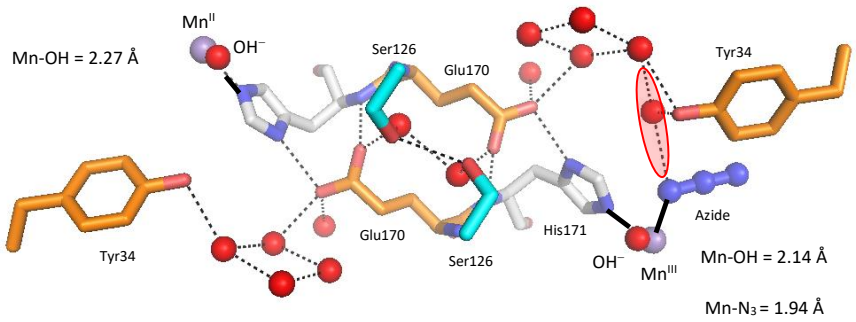

Figure 2.16. Water structure and interdimer cross-links connecting a pair of active sites in the azido complex of *Ec*-MnSOD-Y174F.

The absolutely conserved Glu170 (orange) is hydrogen-bonded to the Mn ligand His171 of the other subunit, forming a double bridge at the dimer interface. Also shown are the active-site residues for subunit A (Mn, dark purple; $^-$OH, red; His171, grey; and Ser126, cyan). Key metal-ligand bond distances are shown. Note the water molecule (pink-shaded ellipse) that accompanies the azide ligand. Note also the Mn-OH distances that support Mn(II) at the five-coordinate site and Mn(III) at the azide-bound site. The picture is derived from the PDB code 1ZLZ. Azide binds weakly to Mn(II).

A pre-analysis of the pK_a values of the wild-type *E. coli* MnSOD was calculated at pH 7.0 by PDB2PQR (program PropKa) (Olsson et.al., 2011) implemented at the APBS home (server.poissonboltzmann.org). The results show that Glu170 is the only residue of the outer-sphere which has a substantial difference in pK_a values between two subunits in a dimer

compared to other residues (see Table 2.7). The significance of this difference is reinforced by the difference being seen in both of the crystallographically independent dimers. Interestingly, the pK_a values of Glu170 residues sit close to pH 7: the Glu170 from one subunit is calculated to be partly protonated while the Glu170 from other subunit is calculated to be mostly deprotonated. For MnSOD operating at pH ~7, this Glu170 can function as a general acid/base.

Table 2.7. The pK_a values for outer sphere of wild-type *Ec*-MnSOD structure (PDB: 1VEW). Estimated pK_a values are calculated on line with pdb2pqr accessed from http://server.poissonboltzmann.org/. Dolinsky, Nielsen, McCammon, and Baker (2004).

Residue	pK_a values				Difference in pK_a values between two dimers
	Dimer 1		Dimer 2		
	Subunit A	Subunit B	Subunit C	Subunit D	
Tyr34	11.84	11.86	11.79	11.83	0.02 - 0.04
Gln146 (aprotic)					
His30	1.63	1.64	1.65	1.65	0.00 - 0.01
Tyr174	14.52	14.56	14.61	14.49	0.04 – 0.12
Glu170	7.14	6.52	7.13	6.47	**0.62 – 0.66**
His171	-6.05	-6.03	-6.00	-6.02	0.02

[a] Water molecules observed in subunits A and B are not observed in subunits C and D at the level of significance in 2F_o-F_c (1 sigma) and F_o-F_c (3 sigma) maps to be included in the model. The negative pK_a for His171 (protonated, imidazolium species) is a consequence of coordination to Mn.

Furthermore, to study the catalytic mechanism, the location of water molecule (HOH327) in the structure of wild-type MnSOD (PDB 1VEW) was examined. It shows that the presence of the solvent molecule, sitting between Glu170 of one subunit and Tyr34 of the other subunit, differ (see Figure 2.17) in one subunit compared to the other of the dimer. Moreover, these differences in the presence of solvent molecule were observed in a higher resolution structure of *E. coli* Mn(III)SOD as the Tyr174Phe mutant compared to Mn(II)SOD, both at 0.9 Å (PDB code 1IX9 and 1IXB, respectively).

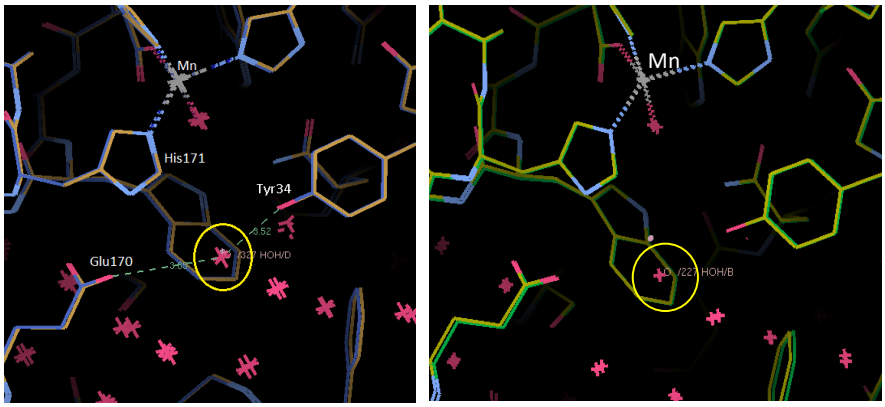

Figure 2.17. Comparison of outer-sphere residues and water molecules of the *Ec*-MnSOD wild-type dimer.

Subunit A superimposed to subunit B (right) and subunit C superimposed to subunit D (left). The structure shows the presence of water in subunits B and D, but absent in subunits A and C. Structures derived from PDB code 1VEW. Picture created by WinCoot.

2.9 Hypothesis on role of Glu170 in MnSODs

The hypothesis of this study is that proton accompanying reduction of the manganese centre is deposited on Glu170-OE2 and is then delivered to the nascent peroxo by a Grotthuss proton-hopping mechanism through the chain of water molecules established between the superoxide (azide proxy) and Glu170, as shown in Figure 2.16. The participation of Glu170 in an outer-sphere proton transfer avoids protons passing through the narrow hole at the base of the substrate-access funnel that can lead to a traffic problem, and thereby accommodates the very fast rate of the reaction. The Glu170 of the opposite subunit almost symmetrically spans the dimer interface. Therefore, a potentially key residue at the dimer interface, the strongly conserved serine 126, which hydrogen bonds to itself across the dimer interface, was mutated to aspartic acid and tryptophan with the intent to generate a monomeric species from a tight homodimer interface. The monomeric species produced by these mutations means the absence of the Glu170 side chain in the adjacent subunit. These structure-based mutational analyses were carried out to gain insight into the mechanism of the proton-coupled electron transfer (PCET) reaction in manganese superoxide dismutase. To date, there

have been no reports on producing monomeric MnSOD by disrupting the canonical dimeric MnSOD interface by a non-active site residue.

Serine 126 at the dimer interface was mutated to Asp, which is negatively charged if exposed to solvent at pH > 5, in an attempt to transform the dimeric protein into monomeric subunits by charge repulsion of the negative charge of two carboxylate side chains. On the other hand, mutation of serine 126 to tryptophan was intended to enforce monomeric MnSOD by steric bulk impediment of the bulky non-polar indole side chain.

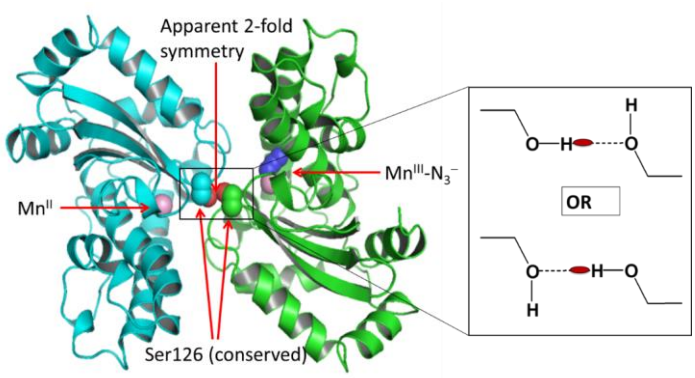

Figure 2.18. The subtly asymmetric dimer interface of *E. coli* MnSOD.

The dimeric quaternary structure is conserved in *E. coli* Mn and FeSOD. However, although *E. coli* MnSOD appears to have 2-fold symmetry (see Figure 2.18), there is a subtle asymmetry of *E. coli* MnSOD in the hydrogen bonding of Ser126 to itself (Figure 2.18). In addition, a highly conserved solvent molecule is more distant to the ND2 of the Asn145 of the subunit B than it is in subunit A when the structures are shown in pairs with Ser126 (see Figure 2.19). The α-amino of Ser126 is actually hydrogen-bonded to the α-carbonyl group of Asn145 of the same subunit at the dimer interface. The subtle asymmetry is also conserved in the *E. coli* azido MnSOD Y174F dimer (PDB: 1ZLZ) where the structure has azide bound with full occupancy at one of the subunits, whereas in other azido Mn- and FeSOD structures the azide is usually disordered in half occupancy at each site of the dimer (pdb codes: 1MNG; 5AG2).

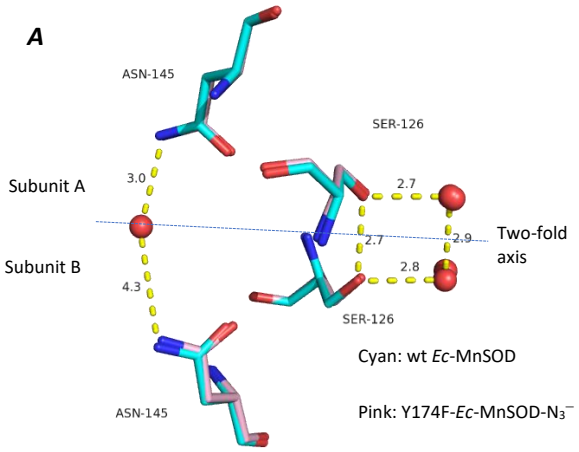

No	Distance (Å) h-MnSOD (orange)	*Ec*-FeSOD-N_3^- (dark blue)
1	2.8	2.6
2	2.6	2.6
3	2.8	2.9
4	3.1	3.0
5	2.7	2.7
6	2.8	2.8
7	2.8	2.7
8	2.7	2.7

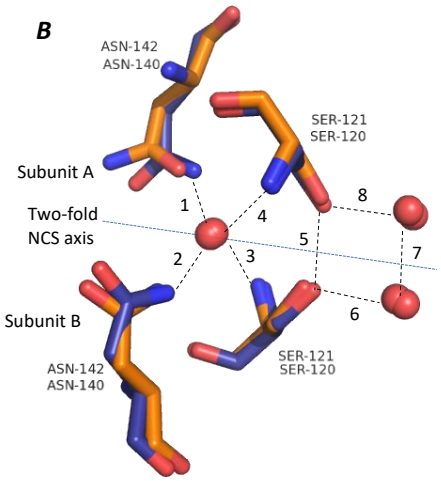

Figure 2.19. A comparison of the hydrogen bonding at the dimer interface for *Ec*-MnSOD, *Ec*-FeSOD and human MnSOD (PDB: 1ABM).

(A) *Ec*-MnSOD (cyan) superimposed on its Y174F mutant (pink). (B) Comparison of human MnSOD (PDB: 1ABM/1N0J, orange) and the azido derivative of *Ec*-FeSOD (PDB: 1ISC, dark blue). The thin blue line denotes the quasi-two-fold axis of the canonical dimer. In contrast to Asn145 for *Ec*-MnSOD, the equivalent residues for *Ec*-FeSOD and human MnSOD show negligible differences in hydrogen bonding, except possibly for the pair numbered 3 and 4 for human MnSOD. Ser120/121 and Asn140/142 (*Ec*-FeSOD/human MnSOD) are equivalent to Ser126 and Asn145 of *Ec*-MnSOD.

However, the asymmetry observed for the azido derivative of *Ec*-MnSOD-Y174F has not occurred for the azido derivative of *Ec*-FeSOD (PDB 1ISC) and for human MnSOD (PDB 1ABM/1N0J), where the hydrogen-bonding scheme between asparagine and serine of azido *Ec*-FeSOD and human MnSOD of the two subunits creates a highly symmetrical geometry. The azido group of *Ec*-FeSOD is disordered in half occupancy over the two subunits. A similarly symmetric interface is seen for *M. tuberculosis* FeSOD (PDB: 1IDS) and for the azido derivative of the FeSOD from *P. shermanii* (PDB: 1AVM) where there is aspartic acid instead of asparagine. *S. solfataricus* FeSOD (PDB: 1WB8) has threonine for serine and the corresponding asparagine hydrogen bonds directly across dimer interface to main chain. The distinct hydrogen-bonding scheme of the pair of Asn145 at the dimer interface of *Ec*-MnSOD raises a question: does this asymmetry propagate to the active site? The asymmetry in hydrogen bonding of the Asn145 amide side chain to a water molecule on the non-crystallographic two-fold axis maybe associated with discrete Mn(II) and Mn(III)-N_3^- sites for the azido complex of *Ec*-MnSOD-Y174F.

The structure of a human MnSOD-azide complex reveals that six-coordinate, azide-bound manganese occurs at only one pair of subunits of the tetrameric enzyme (PDB 5T30) (Azadmanesh, Trickel, & Borgstahl, 2017). Interestingly, pairs of subunits of the canonical dimer are related by a crystallographic two-fold axis, where one canonical dimer has azide in approximately half-occupancy, while the other canonical dimer of the tetramer has no azide coordinated.

2.10 Aims and research questions

SODs catalyse the disproportionation of the superoxide anion-radical ($O_2^{-\bullet}$) to hydrogen peroxide and dioxygen in a ping-pong, two-step, oxidation-reduction cycle that is diffusion-limited. As described in the section 2.7, there is still little known about where, when and how, or even if, proton transfer is intimately coupled with redox events at metal and superoxide centres. In the case of *Ec*-MnSOD, proton uptake has been shown to occur in the first step, where the metal ion is reduced and superoxide is oxidised. The site of proton localisation is generally assumed to the hydroxo ligand, but this has still not been unambiguously

determined and as discussed in Section 2.8 there is evidence to cast doubt that the hydroxo ligand receives a proton to become a metal-coordinated water molecule for the Mn(II) state. This research proposes to study the structure of interface mutants of *Ec*-MnSOD, specifically the Ser126Asp and Ser126Trp mutants to investigate the roles of dimerisation of the MnSOD in forming potential communication pathways between subunits of the dimer (Figure 2.17). This structural analysis may help to elucidate the mechanism of proton-coupled electron-transfer (PCET) reaction in manganese superoxide dismutase.

The specific research questions of this study are:

1. What are the structures of the MnSOD-S126D and MnSOD-S126W mutants? Are they dimeric or monomeric?
2. If the structures are monomeric, what will be the effects on the enzyme activity?
3. If the structures are monomeric, what is the effect of propionic acid or carboxylic acid addition, to complement loss of Glu170 interacting with metal ligand His171, on the activity and the structure of the mutant?
4. What level of cooperative behaviour exists between the subunits of the obligate dimer pair? Is there any potential communication pathways between subunits of the dimer? Does the bridge of Glu170 provide a proton shuttle?
5. What are the proposed potential proton-transfer pathways into the active site based on structural analysis? Can it explain why catalysis occurs near diffusion limits in MnSOD?
6. Where is the site of redox-coupled proton uptake located and whether or not there are multiple sites of proton uptake? Which residues are associated with pH-dependent behaviour?

Chapter 3 Methods

3.1 Media and reagents

3.1.1 Water source

For all experimental purposes and making up buffers, sterile deionised water was obtained from a Barnstead Nanopure™ system (ThermoScientific, Wilmington, DE, USA). Tap water was used for *E. coli* growth media prior to autoclaving sterilisation.

3.1.2 Media

Lysogeny Broth, LB medium) contains in one liter: 10 g tryptone, 5 g yeast extract, 10 g NaCl (Invitrogen).

Super Optimal Broth (SOB) contains in one liter: 2% w/v tryptone (20 g, Invitrogen), 0.5% w/v yeast extract (5 g, Invitrogen), 8.56 mM NaCl (0.5 g) or 10 mM NaCl (0.584 g), 2.5 mM KCl (0.186 g), $_{dd}$H2O to 1000 mL, 10 mM $MgCl_2$ (anhydrous: 0.952 g; hexahydrate: 2.033 g), 10 mM $MgSO_4$ (anhydrous: 1.204 g; heptahydrate: 2.465 g).

Super Optimal Broth with Catabolite repression (SOC) comprises (1 L): SOB with added 20 mM glucose (3.603 g L^{-1}).

3.1.3 Chemicals (Merck-Sigma-Aldrich, unless otherwise stated)

Acetic acid, acetonitrile, acrylamide, agarose (Hydragene), ammonium sulfate, ampicillin, bis-acrylamide, Bis-tris, Bis-tris propane, bromophenol blue, Coomassie brilliant blue R-250, DTT (1,4-dithiothreitol), EDTA disodium salt, EtBr (ethidium bromide), ethanol, formic acid, $CaCl_2.2H_2O$, D-glucose, glycerol, glycine, HCl (aqueous), kanamycin, KCl, KSCN, KH_2PO_4 (Unilab), methanol, $MgSO_4$, $MgCl_2$, $MnCl_2.4H_2O$, MOPS, NaCl, Na_2HPO_4 (Unilab), NaOH, PACT Premier™ (Molecular Dimensions), PEG 1500, PEG 3350, potassium acetate, RbCl, SDS (sodium dodecyl sulfate, Affymetrix), Tris, xanthine.

3.1.4 Biochemical products

Cytochrome c (Sigma-Aldrich), Dpn I (restriction enzyme) (Agilent Technologies), molecular size markers for DNA and protein (Invitrogen™), PfuTurbo™ DNA polymerase ll (Agilent Technologies), tryptone, xanthine oxidase (Sigma-Aldrich), yeast extract.

3.1.5 PBS (phosphate buffered saline)

The 10x PBS buffer (10 L) was prepared by dissolving 80 g NaCl, 2.0 g KCl, 14.4 g Na_2HPO_4, 2.4 g KH_2PO_4 in 800 mL deionised water. The pH was adjusted to 7.4 and the volume adjusted to 1.0 L with additional deionised water before autoclaving.

Transformation buffer 1

In addition, transformation buffer 1 (500 mL) was prepared by dissolving 6 g RbCl, 5 g $MnCl_2.4H_2O$, 0.75 g $CaCl_2.2H_2O$, 15 mL potassium acetate (1.5 M stock, pH 7.5) and 75 mL glycerol in sterile deionised water. The pH was adjusted to 5.8 with HCl.

Transformation buffer 2

Transformation buffer 2 (500 mL) was prepared by dissolving 6 g RbCl, 5.5 g $CaCl_2.2H_2O$, together with 10 mL MOPS (0.5 M stock, pH 6.8) and 75 mL glycerol in deionised H_2O. Both transformation buffers were sterilised by filtration through a 0.22 µm disposable filter then stored at 4 °C.

Running buffer for sodium dodecyl sulfate polyacrylamide gel electrophoresis (SDS-PAGE)

10x SDS-PAGE (1 L): 250 mM Tris, 1.92 M glycine, 1% SDS, pH 8.3. A 10x running buffer was prepared by dissolving 30.3 g Tris base, 144.1 g glycine, and 10 g SDS in 800 mL sterile deionised water, then adjusted to 1 L with additional sterile deionised water.

Sample buffer

125 mM Tris/HCl pH 6.8, 2.5% (w/v) SDS, 10 mM DTT, 50% (w/v) glycerol, 0.05% (w/v) bromophenol blue.

MOPS buffer

3-Morpholinopropane-1-sulfonic acid (MOPS) 0.5 M, pH 6.8. MOPS (104.63 g) was dissolved in 750 mL water, 10 N NaOH was used to adjust the pH 6.8 then adjusted to 1.0 L with additional sterile deionised water before being autoclaved.

TAE buffer

TAE buffer (50x) was prepared by dissolving 242.28 g Tris, 18.61 g EDTA disodium in 750 mL water. Then 57.1 mL mL glacial acetic acid was added and the final volume was adjusted to 1.0 L with additional deionised water.

SPG buffer

SPG buffer was prepared from succinic acid (1.48 g), $NaH_2PO_4.2H_2O$ (6.82 g), glycine (3.28 g), water to 80 mL; 10 M NaOH to desired pH, then made up to 100 mL.

3.2 Preparation of expression system

3.2.1 Strain, plasmid, and primers

The *SodA*- *E. coli* QC 781 strain was chosen as the host of the system to produce MnSOD mutants, while AB2463 strains produced wild-type MnSOD. The plasmid pDT1-5 contains an ampicillin antibiotic resistance plasmid and carries the sodA gene, which codes for MnSOD. This plasmid was first developed and was given by Danièle Touati (1983) from the Institut Jacques Monod, Centre National de la Rècherche Scientifique, Université Paris VII.

Table 3.1. Primers used in present study.

Primer	Sequence	Source
Mutation of MnSOD wt to S126D		
Forward	5′TCC CGC TTT GGT **GAC** GGC TGG GCA TGG3′	Salvador[s]
Reverse	5′CAC CAG CCA TGC CCA GCC **GTC** ACC AAA GCG GGA3′	Salvador[s]
Mutation of MnSOD wt to S126W[1]		
Forward	5′C CGC TTT GGT **TGG** GGC TGG GCA3′	IDT[s]
Reverse	5′TGC CCA GCC **CCA** ACC AAA GCG G3′	IDT[s]

Mutation of MnSOD wt to S126W[2]		
Forward	5'GCTTCCCGCTTTGGT**TGG**GGCTGGGCATGGC	IDT*
Reverse	5'CAGCCATGCCCAGCC**CCA**ACCAAAGCGGGAAGC	IDT*
Mutation of MnSOD wt to S122E[1] (Error: S126 was the intended target)		
Forward	5'GAAAAAGCGGCAGCT**GAA**CGTTTCGGTTCCGGCT	IDT*
Reverse	5'AGCCGGAACCGAAACG**TTC**AGCTGCCGCTTTTTC	IDT*
Mutation of MnSOD wt to S126E[2]		
Forward	5'GCTTCCCGCTTTGGT**GAA**GGCTGGGCATGGC	IDT*
Reverse	5'GCCATGCCCAGCC**TTC**ACCAAAGCGGGAAGC	IDT*
Mutation of MnSOD wt to E170Q[1]		
Forward	5'GGATGTGTGG**CAA**CATGCTTACTA	IDT*
Reverse	5'TAGTAAGCATG**TTG**CCACACATCC	IDT*
Mutation of MnSOD wt to E170Q[2]		
Forward	5'GGCCTGGATGTGTGG**CAA**CATGCTTACTACCTGAAATTCC	IDT*
Reverse	5'GGAATTTCAGGTAGTAAGCATG**TTG**CCACACATCCAGGCC	IDT*
Mutation of MnSOD wt to W169T		
Forward	5'GGCCTGGATGTG**ACG**GAACATGCTTACTAC	IDT*
Reverse	5'GTAGTAAGCATGTTC**CGT**CACATCCAGGCC	IDT*
Mutation of MnSOD wt to E170A		
Forward	5'CTGGATGTGTGG**GCA**CATGCTTACTACCT	IDT*
Reverse	5'AGGTAGTAAGCATG**TGC**CCACACATCCAG	IDT*

IDT: Primers were ordered from Integrated DNA Technologies™ (https://www.idtdna.com)

[S] Successfully produced mutants (S126D and S126W) by site-directed mutagenesis with correct sequence.

* Unsuccessful mutagenesis with various conditions: PCR amplification products show five fragment mutants (See Figure 3.1). E170Q1 and W169T sequencing results show only 80% accuracy of the wild-type. S126E2 sequencing result shows an extra mutation (A202V).

3.2.2 Determination of DNA concentration and purity

DNA plasmid concentration and purity were assessed using a Nano-drop ND-1000 spectrophotometer (Thermo Scientific, USA) for DNA sequencing purposes. Significant absorbance at 270 nm generally indicates phenol contamination. An OD_{260}:OD_{270} ratio of 1.2 indicates a clean DNA sample.

3.2.3 Site-directed mutagenesis

The QuikChange site-directed mutagenesis kit (Stratagene™) was used to make point mutations of single amino acids. The QuikChange site-directed mutagenesis method is performed using PfuTurbo™ DNA polymerase ll and a thermal temperature cycler.

3.2.4 Polymerase chain reaction

A sample reaction (first entry in Table 3.1) consists of: 1 µL 10x reaction buffer (Stratagene™ kit), 2 µL dsDNA template (5 ng/µL), 1 µL forward primer (25 ng/µL) (see Table 3.1), 1 µL reverse primer (25 ng/µL), 1 µL dNTP mix, and 4 µL sterile deionised water was added to a final reaction volume of 10 µL. Lastly 0.2 µL PfuTurbo^{TM} DNA Polymerase II (2.5 U/µL) was added. The temperatures used in the following cycles are for the case of the MnSOD-S126D mutant. Initial template denaturation of 1x2 mins was at 95 ^{o}C for the first segment. Then in the second segment, it was cycled for 16 times. For each cycle the temperature was set at 95 ^{o}C for 30 s, 53 ^{o}C for 60 s, and 68 ^{o}C for 11 min (total for ~3 hours) for denaturing, annealing, and extending. Lastly, the temperature was set at 65 ^{o}C for 7 min.

3.2.5 Agarose gel electrophoresis

Agarose gel electrophoresis (AGE) was used to separate and to assess the DNA fragments after PCR Amplification in a 0.9% agarose gel in 30 mL TAE 0.5x. DNA bands of PCR products and particular molecular size markers (Invitrogen^{TM} Nucleic Acid Marker) were seen using an ultraviolet (UV) transilluminator and pictures generated (Bio-Rad, Gel Doc, USA) were stained with ethidium bromide as a fluorescent tag. A representative electrophoresis gel is shown in Figure 3.1.

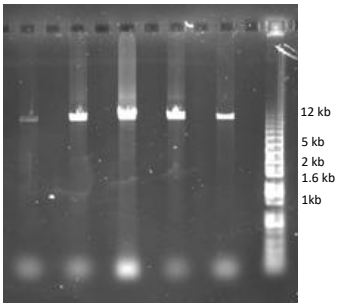

Figure 3.1 DNA fragments containing MnSOD gene mutants after PCR amplification.

Agarose gel showing DNA products after PCR Amplification (11.2 kb). Left to right, respectively, E170A, E170Q, S126E, S126W, W169T, and marker (Invitrogen^{TM}).

3.2.6 Transformation of XL-1 blue supercompetent cells

The reaction mixture from PCR (section 3.2.4) was cooled down in an icebath, then 0.2 µL restriction enzyme, DpnI (20 U/µL), was added, and incubated at 37 °C for an hour to digest methylated-parental DNA template. The nicked vector mutant, DpnI-treated DNA, from each sample reaction was transformed into XL-1 Blue supercompetent cells (Stratagene), prepared by heat-shock method at 42 °C. The transformed XL-1 Blue cells were then incubated in 0.5 mL SOC at 37 °C for an hour, then were plated on to LB plates supplemented with 100 µg/mL ampicillin and 15 µg/mL kanamycin for > 16 hours. A single colony from each mutant was picked and inoculated into 1xLB medium supplemented with 100 µg/mL ampicillin at 37 °C, 200 rpm for culture. On transformation, XL1-Blue supercompetent cells repair the nicks in the mutated plasmid.

3.2.7 DNA plasmid preparation

Cell pellets were prepared from an overnight 4 mL cell culture. Subsequently, the plasmids were immediately isolated from the pellet using High Pure Plasmid Isolation Kit (Roche™, Germany).

3.2.8 DNA sequencing

The MnSOD-S126D mutant was sequenced in both forward and reverse direction by the Massey Genome Service, Massey University, Palmerston North. The reaction in 0.2 mL tube contained ~400 ng/µL plasmid template, 3.2 pmol/µL forward or reverse primer. The product size of this reaction was ~0.7 kb.

3.2.9 Preparation of *SodA- E. coli* QC 781 supercompetent cells

A single colony of *SodA- E. coli* QC 781 host cell was picked and inoculated into 30 mL SOB broth in 250 mL flask to make competent cells at 37 °C with moderate agitation. The overnight culture (8 mL) was added to 200 mL SOB broth in a larger flask (2 L) and then cultivated at 37 °C with 200 rpm agitation until an OD_{600} of approximately 0.3 was achieved. The culture was split into four 50 mL sterile polypropylene centrifuge tubes, and then chilled on ice for 15 minutes. The cells were pelleted by centrifugation at 3000 x g for 15 minutes at 4 °C. The pellets were drained thoroughly. The pellets were resuspended by 16 mL transformation buffer-1 each then mildly vortexed. The pellets were resuspended by mild vortexing. The suspensions were incubated on ice for 15 minutes and the cells were pelleted as before. The

pellets were resuspended in 4 mL cold transformation buffer-2 for each. A 50 µL competent cell suspension was aliquoted in a sterile microcentrifuge tubes (1.7 mL), which were then flash- frozen in liquid nitrogen prior to -80 °C storage.

3.2.10 Transformation of pDT1-5 supercompetent cells

Microcentrifuge tubes containing competent cells were thawed on ice (approximately 20-30 min). Sterile polypropylene tubes were pre-chilled on ice and 300 µL of thawed cells were aliquoted to the prechilled tubes. A 3 µL aliquot of plasmid DNA (20 ng/µL) was added by gently stirring the cells while pipetting. The cells were incubated on ice for 40 minutes. The cells were heat shocked by incubating at 42 °C for 45 seconds. Next, 1 mL of SOC medium (no antibiotics) was added to each tube then the cells were incubated at 37 °C on a shaker with 200 rpm agitation for an hour to allow cell recovery and to generate the antibiotic resistance proteins encoded in the plasmid. The cells were plated out on LB agar media supplemented with 125 µg/mL ampicillin and incubated at 37 °C overnight.

3.2.11 Media, growth condition and antibiotic concentration

In order to produce manganese superoxide dismutase protein, *sodA- E. coli* QC781 cells containing pDT1-5 ampicillin-resistant sodA gene plasmid were grown in LB media with 125 µg/mL ampicillin and 150 µM $MnCl_2$ salts.

3.3 Protein expression

3.3.1 Small-scale protein expression of *Ec*-MnSOD and its S126D and S126W mutants

For a starter culture, a single colony was picked and inoculated into 5 mL 1xLB starter medium supplemented with 125 µg/mL ampicillin and grown overnight at 37 °C with 200 rpm agitation. A starter culture (25 µL) were inoculated into 5 mL (1:200) 1xLB starter medium supplemented with 125 µg/mL ampicillin, and 150 µM $MnCl_2$ salts. Selection pressure was maintained by additions of ampicillin hourly after OD600 reached 0.3, and a second addition of 1% glucose was made at midlog phase. Cultures were grown at 37 °C with 200 rpm agitation for overnight. The cells were harvested in an Eppendorf microtube by centrifugation at maximum speed (13,300 *g*) for 30 s in a benchtop centrifuge, resuspended in 500 µL of 1xPBS (phosphate buffered saline) and disrupted by sonication. The insoluble materials were pelleted by

centrifugation at maximum speed for a minute. The pellet was resuspended with 8 M urea in an equal volume as the supernatant. Both fractions were run side-by-side on a 15% SDS PAGE gel for monitoring of protein expression.

3.3.2 Large-scale expression of *Ec*-MnSOD-S126D and S126W

For a starter culture, a single colony was picked and inoculated into 200 mL 25 g/L LB starter medium supplemented with 100 µg/mL ampicillin and grown overnight at 37 °C with 200 rpm agitation. The starter culture was inoculated into 4 L of 1xLB (25 g/L) medium with 100 mg/L ampicillin, and 30 mg/L $MnCl_2$ salts. *Ec*-MnSOD wild-type culture was grown in 2xLB with 100 mg/L ampicillin, and 30 mg/L $MnCl_2$ salts. Cultures were grown in four flasks (5 L size) at 37 °C with vigorous agitation at a constant shaking speed (200 rpm) for overnight expression. The cells were harvested the next day by centrifugation at 6,000 rpm for 20 minutes using Fiberlite F9-4x1000y rotor at 4 °C. Large scale MnSOD-S126W expression used a fermentor. (See Table 3.2)

3.3.3 Large-scale expression of *Ec*-MnSOD wild-type

E. coli strain AB2463 (Touati, 1983), which contains an antibiotic resistance plasmid (pDT1-5) carrying the MnSOD gene, was grown at 37 °C in 2 L of 50 g/L LB medium (2xLB) in two flasks (5 L size) supplemented with 50 µL of 1 M $MnCl_2$ and 100 mg/L ampicillin. After the optical density of the culture medium at 600 nm reached ~ 0.3, an additional 50 µg/mL of ampicillin was added hourly (J. W. Whittaker & Whittaker, 1991). Cells were harvested after overnight growth.

3.4 Purification of wild-type *Ec*-MnSOD

The purification of wild-type *E*c-MnSOD was adapted from (J. W. Whittaker & Whittaker, 1991) with some modifications.

3.4.1 Selective precipitation by ammonium sulfate

The cell pellets were collected and resuspended in 40 mL lysis buffer (50 mM potassium phosphate buffer, pH 7.8) and lysed by two passages through a French Press (Aminco) at 5000 psi. Soluble protein was separated from the insoluble material by centrifugation at 17,000 *g* for 40 minutes in a Fiberlite F21S-8X50 rotor at 4 °C. The pellet was discarded and ammonium

sulfate was added to 50% of saturation with gentle stirring for one and a half hour on ice. Contaminating proteins that precipitated were removed by centrifugation at 17,000 *g* for 30 min in a Fiberlite F21S-8X50 rotor at 4 ºC. A second ammonium sulfate cut was carried out on the supernatant to 75% of saturation and stirred for two hours on ice. The pellet was resuspended in 24 mL of 20 mM potassium acetate, pH 5.5 and dialysed against 100 volumes of the same buffer overnight with a regular buffer replacement every 12 hours.

3.4.2 Cation exchange chromatography

Step 1.

Dialysate was transferred from the dialysis bag, then centrifuged at 17,000 *g* in a Fiberlite F21S-8X50 rotor at 4 ºC for 20 min to separate the insoluble fraction. The supernatant (25 mL) was loaded onto a cation exchange column packed with Sephadex CM-50 resin equilibrated with 20 mM potassium acetate, pH 5.5. The eluate was monitored at 280 nm. Proteins were eluted using a stepwise salt gradient (the same buffer but containing 1 M NaCl) until the final concentration entering the column was 200 mM potassium acetate, pH 5.5.

Step 2.

Fractions containing MnSOD WT (23 kDa) were pooled to separate other proteins at 32 kDa by the same column Sephadex CM-50 resin but modified with a shallow gradient instead of stepwise

3.4.3 Hydrophobic interaction chromatography

A hydrophobic interaction chromatography technique was used to separate MnSOD wild type from higher molecular weight proteins based on the differences in hydrophobicities of proteins. In 20 mM potassium acetate pH 5.5, 10 mL of protein sample from fraction A3 (0.1 mg/mL) was pre-salted with 2.5 M of NaCl and loaded onto a 50 mL tube containing washed phenyl-sepharose then inverted for two hours. The resin was washed by buffer (20 mM potassium acetate pH 5.5 containing 2.5 M NaCl then with 1 M NaCl). These eluates were pooled together, concentrated using micro Vivaspin 20 spin column with a MWCO of 10 kDa (Vivasciences), and washed two times by 0.2 M potassium phosphate pH 7.8 for SOD assay purposes. This pure MnSOD wild type was concentrated using micro Vivaspin 2 spin column until the concentration of protein reached 5 mg/mL.

3.5 Purification of *Ec*-MnSOD-S126D

3.5.1 Selective precipitation by ammonium sulfate

The cell pellets were collected and resuspended in 100 mL lysis buffer (50 mM potassium phosphate buffer, pH 7.8) and lysed by two passages through a French Press (Aminco) at 5000 psi. Soluble protein was separated from the insoluble material by centrifugation at 17,000 *g* for 40 minutes in a Fiberlite F21S-8X50 rotor at 4 ^{o}C. The pellet was discarded and ammonium sulfate was added to 60% of saturation with gentle stirring for an hour on ice (Green & Hughes, 1955). Contaminating proteins that precipitated were removed by centrifugation at 17,000 *g* for 30 min in a Fiberlite F21S-8X50 rotor at 4 ^{o}C. A second ammonium sulfate cut were carried out on the supernatant to 90% of saturation and stirred for two hours on ice. The pellet was resuspended in 16.5 mL of 10 mM potassium acetate, pH 5.5 and dialysed against 100 volumes of the same buffer for 2 days with a regular buffer replacement every 12 hours.

3.5.2 Cation exchange chromatography

A milky dialysate was transferred from the dialysis bag, then centrifuged at 17,000 *g* in a Fiberlite F21S-8X50 rotor at 4 ^{o}C for 20 min to separate the insoluble fraction. After keeping for one day, the protein solution was also getting milky, then centrifuged at 15,000 rpm in a Fiberlite F21S-8X50 rotor at 4 ^{o}C for 15 min. When the centrifuged solution was run in SDS-PAGE gel, some of the protein was insoluble. The supernatant (50 mL) was loaded onto a cation exchange column packed with Sephadex CM-50 resin equilibrated with 10 mM potassium acetate, pH 5.5. The eluate was monitored at 280 nm. Proteins were eluted using a stepwise salt gradient (the same buffer with contains 2 M NaCl) until the final concentration entering the column was 200 mM potassium acetate, pH 5.5.

3.6 Purification of *Ec*-MnSOD-S126W

3.6.1 Selective precipitation by ammonium sulfate

Cell pellets were collected and resuspended in 100 mL lysis buffer (50 mM potassium phosphate buffer, pH 7.8) and lysed by two passages through a French Press (Aminco) at 5000 psi. Soluble protein was separated from the insoluble material by centrifugation at 17,000 xg for 40 minutes in a Fiberlite F21S-8X50 rotor at 4 ^{o}C. The pellet was discarded and ammonium

sulfate was added to 60% of saturation with gentle stirring for an hour on ice (Green & Hughes, 1955). Contaminating proteins that precipitated were removed by centrifugation at 17,000 *g* for 30 min in a Fiberlite F21S-8X50 rotor at 4 °C. A second ammonium sulfate cut were carried out on the supernatant to 95% of saturation and stirred for two hours on ice. The pellet was resuspended in 16.5 mL of 10 mM potassium acetate, pH 5.5 and dialysed against 100 volumes of the same buffer for 2 days with a regular buffer replacement every 12 hours.

3.6.2 Cation exchange chromatography

A milky dialysate was transferred from the dialysis bag, then centrifuged at 17,000 *g* in a Fiberlite F21S-8X50 rotor at 4 °C for 20 min to separate the insoluble fraction. After dialysing for one day, the protein solution again became cloudy, and was removed from the dialysis bag and centrifuged at 15,000 rpm in a Fiberlite F21S-8X50 rotor at 4 °C for 15 min. SDS-PAGE gel showed that a portion of the protein was insoluble. The supernatant (50 mL) was loaded onto a cation exchange column packed with Sephadex CM-50 resin equilibrated with 10 mM potassium acetate, pH 5.5. The eluate was monitored at 280 nm. Proteins were eluted using a stepwise salt gradient (the same buffer which contains 2 M NaCl) until the final concentration entering the column was 200 mM potassium acetate, pH 5.5.

3.6.3 Sodium chloride precipitation

Peak fractions containing MnSOD-S126W were pooled in a beaker glass. Next, sodium chloride solution (up to 3.0 M concentration) was added with gentle stirring for an hour on ice. The pellet was resuspended in 10 mL of 10 mM Tris-Cl, pH 7.5 and dialysed against 100 volumes of the same buffer for 24 hours with a regular buffer replacement every 6 hours.

3.6.4 Anion exchange chromatography

An anion exchange technique was used to separate MnSOD-S126W from impurities based on their charges using positively charged diethyl-aminoethyl (DEAE) group. The protein sample (0.1 mg/mL) was loaded onto a 50 mL centrifuge tube containing washed DEAE then inverted for 30 minutes. The resin was washed gradually by buffer (5 mM Tris-Cl pH 7.5 containing 0.5 to 2 M NaCl). The eluate was collected, then desalted and concentrated using micro Vivaspin 20 with a MWCO of 10 kDa (Vivasciences). Table 3.2 summarises a comparison of protein expression and techniques of purification of MnSOD wild-type and S126D and S126W mutants.

Table 3.2. Comparison of protein expression and techniques of purification of *Ec*-MnSOD wild-type and its S126D and S126W mutants.

	Wild-type	**S126D**	**S126W**
1. Expression			
LB media	2X	1X	1X
Fermentor	Flask	Flask	Bioreactor
2. Purification			
Step 1 $(NH_4)_2SO_4$ precipitation	Yes	Yes	Yes
Step 2 Cation Exchange (Sephadex CM-50) stepwise salt gradient	Yes	Yes	Yes
Step 3	Shallow salt gradient, Sephadex CM-50 cation exchange	-	NaCl precipitation
Step 4	Hydrophobic interaction (phenyl sepharose HR5/5)	-	Anion exchange DEAE or Q-Sepharose (alternatively) with simple rotation in tubes

3.7 Protein analysis

3.7.1 Sodium dodecyl sulfate polyacrylamide gel electrophoresis (SDS-PAGE)

SDS-PAGE was performed according to Laemmli's method (Laemmli, 1970). Here, the proteins were separated in the presence of SDS and denaturing agents, then becoming fully denatured and dissociated. The rate at which SDS-bound protein migrates in a gel depends primarily on its size, enabling molecular weight estimation with refererence to protein markers.

Gels used for analysis of MnSOD mutants were prepared from an acrylamide solution as mini-gels with a 15% separating gel and a 5% stacking gel with a molar ratio of acrylamide:bisacrylamide of 29:1 (Bio-Rad Laboratories, USA). Protein samples were mixed with 2× sample buffer (125 mM Tris/HCl pH 6.8, 2.5% (w/v) SDS, 10 mM DTT, 50% (w/v) glycerol, 0.05% (w/v) bromophenol blue) and heated to 90 ^{o}C for 5 minutes before loading onto the gel. Gels were run at 200 Volts for 40 – 50 minutes. As reference for molecular

weights, the Precision Plus Protein™ (Bio-Rad Laboratories, USA) was used. The gel lane with standards is always labelled kDa in figures.

3.7.2 Protein detection and analysis

Protein band patterns were visualised and subjected to qualitative and quantitative analysis. Most proteins cannot be seen in a gel with the naked eye, but require using protein stains to aid visualisation. Here, the Coomassie staining solution and destaining solution was utilised to detect the proteins in polyacrylamide gels. Coomassie staining solution contains 2.5 g/L Coomassie Brilliant Blue R-250, 10% (v/v) acetic acid and 50% (v/v) methanol), while destaining solution contains (10% (v/v) acetic acid and 10% (v/v) methanol). The images were recorded with a GelDoc system (Bio-Rad Laboratories, USA), photocopier/scanner or a digital camera.

3.7.3 Molecular mass determination

A 2 µL sample was injected into an Agilent 1200 series analytical flow LC system running 0.1% (v/v) formic acid, 50% acetonitrile/water, at 0.1 mL/min on bypass mode (Agilent Technologies; Germany). The samples were analysed using an Agilent 6520 QTOF mass spectrometer (Agilent Technologies; Germany) using positive ion mode with a capillary voltage of 3500 V, a fragmentor voltage of 175 V, a skimmer voltage of 65 V, over a scan range of 350-3000, *m/z.* Data were stored in profile mode. Total ion chromatograms (TIC) obtained were examined and peaks within the range of 600-3000 *m/z* were deconvoluted using the pMod algorithm (Agilent MassHunter Workstation Qualitative Analysis software version B.03.01, Agilent Technologies; USA).

3.7.4 Protein quantitation

The protein concentration was determined based on the light absorption at a wavelength of 280 nm by aromatic residues tryptophan and tyrosine. The proteins' extinction coefficients were calculated with ProtParam on the ExPASy server (https://web.expasy.org/protparam/). The protein concentration, expressed per subunit, can be quantified using the the Beer-Lambert law, equation (15), after consideration of the molecular weight of the protein:

$$A = \varepsilon . b . c \quad .... \qquad (15)$$

A: Absorbance of the protein solution at 280 nm

ε: Wavelength-dependent molar absorptivity coefficient at 280 nm (L mol^{-1} cm^{-1})

b: Path length of the sample (cm)

c: Concentration (mol L^{-1})

3.8 Crystallisation

3.8.1 Protein preparation prior to crystallisation

For crystallisation purposes, *Ec*-MnSOD and mutants were obtained in sufficient amount with at least 95% purity to allow multiple trials and refinement of conditions needed to grow diffraction-quality protein crystals. To obtain this, the proteins were "cleaned" by size exclusion chromatography and filtered through a spin filter (500 µL Durapore 0.1 µm PVDF membrane filters, Merck Millipore, Germany) and spun at 21,000 *g* for 15 min at 4 °C.

3.8.2 Robot screening

High-throughput screening was performed with a Mosquito robot in 96-well Intelli plates (Greiner) for sitting-drop vapour diffusion crystallisation. With 100 nL of protein and 100 nL of mother liquor in a sitting drop, 16 µL of protein sample (containing ~15-20 mg/mL MnSOD and mutants) were required per each run. Here we used PACT Premier™ screen (Molecular Dimension) and JCSG-Plus™ screen (Molecular Dimension).

3.8.3 Optimisation

Optimisation screens were performed manually in 24-well VDX plates as sitting drops in micro-bridges or as hanging drops on siliconised glass cover slides and sealed with grease. Successful higher pH optimisations for *Ec*-MnSOD-S126D were obtained from PACT Premier™ screen subwell A5 (SPG Buffer pH 8.0 with 25% w/v PEG 1500) and subwell A6 (SPG Buffer pH 9.0 with 25% w/v PEG 1500) PACT PremierTM by extending pH range (8.4, 8.7, 9.0) and % (w/v) PEG 1500 range (19, 22, 25, and 28%), with and without 1.5% ethanol addition (See Table 3.3).

At lower pH, good crystals were also obtained from PACT Premier™ screen at subwell F4 containing 0.1 M Bis-tris propane pH 6.5, 0.2 M KSCN, and 20% PEG 3350. A second optimisation was performed by making variation of PEG 1500 and PEG 3350 from 26%, 28%, and 30% (w/v) in 0.1 M Bis-tris propane pH 6.5 and 6.8 with/without 1.5% ethanol addition (See Table 3.4).

For lower pH, further optimisation screens were performed by adding salts (KCl 0.1 M; $MnCl_2$ 0.01 M-0.02 M; KSCN 0.1-0.2 M), ethanol 1.5%, and various concentration of PEG 1500 (20% to 26%) in 0.1 M Bis-tris propane, pH 6.8 (See Table 3.5).

Table 3.3. Optimisation screen 1.

% PEG 1500	SPG buffer at pH:					
	8.4	8.7	9.0	8.4	8.7	9.0
19						
22						
25						
28						
				EtOH 1.5%		

Table 3.4. Optimisation screen 2.

0.1 M Bis-tris propane	PEG 1500			PEG 3350			0.2 M Salt
	26%	28%	30%	18%	20%	23%	
pH 6.5							KSCN
							KCl
pH 6.8							KSCN
							KCl

Table 3.5. Optimisation screen 3.

PEG 1500*	KCl 10 mM	KCl 10 mM EtOH 1.5 %	$MnCl_2$ 0.01M	$MnCl_2$ 0.02M	KSCN 0.2 M	KSCN 0.1 M EtOH 1.5 %
20 %						
23 %						
26 %						

*In buffer Bis-tris propane, pH 6.8.

Screens were transferred to 21 ^{o}C or 4 ^{o}C incubators and examined under a microscope directly after set-up, daily for one week and then once a week. The sitting drop screens showed better results in crystal formation for *Ec*-MnSOD-S126D and -S126W mutants at 21 ^{o}C.

3.8.4 Crystal mounting

Individual crystals of MnSOD-S126D and S126W were harvested in Cryo Loops (Hampton Research, USA) or Micro Loop (MiTeGen, USA) of suitable size and flash-frozen in liquid

nitrogen without cryoprotectant solution. For data collection on the home source, the loop holding the crystal was mounted on to the goniometer head in a stream of nitrogen gas at 120 K.

3.9 X-ray protein crystallography

3.9.1 Data collection

Data were collected in-house or at the Australian Synchrotron. In-house data collection was performed with an R-Axis IV++ image-plate area detector and MicroMax™-007 X-ray source with copper rotating anode (Rigaku, USA). X-rays were focused and monochromated with an AXCo PX70 capillary optic. Data collection at 100 K at the Australian Synchrotron was performed at beamlines MX1 and MX2. The assistance of beam-line staff and, for the *Ec*-MnSOD-S126W structure, of Associate Professor Andrew J Sutherland-Smith for help with data collection and processing is gratefully acknowledged.

3.9.2 Phasing, refinement, and molecular graphics software

The software package was CCP4 (Winn et al., 2011). Structures were solved by molecular replacement (MolRep) (Vagin & Teplyakov, 1997) using *E.coli* MnSOD wild-type structure, 1VEW, and refined using Refmac5 (Murshudov, Vagin, & Dodson, 1997). Model re-building and visual interpretation of electron density maps were performed using Coot version 0.7.1 (Emsley, Lohkamp, Scott, & Cowtan, 2010). Display and rendering images of protein structures were performed using PyMOL version 0.99 (DeLano, 2002) and Coot (Emsley et al., 2010).

3.10 Characterisation of MnSOD

3.10.1 SOD activity assay

The xanthine oxidase/cytochrome-*c*(Fe^{3+}) activity assay of McCord and Fridovich (1969) was performed to measure the SOD activity of MnSOD wild-type and its mutants. In this assay, xanthine oxidase (XOD) catalyses production of the superoxide radical by the reduction of xanthine in the presence of dioxygen. The superoxide radical then reduces oxidised cytochrome-*c*(Fe^{3+}). The rate of cytochrome-*c*(Fe^{3+}) reduction is followed spectrophotometrically at 550 nm. Superoxide dismutase inhibits the reduction of cytochrome *c* by competing for the superoxide radical:

$$\text{Xanthine} + O_2 + H_2O \xrightarrow{XOD} \text{Uric acid} + O_2^{\cdot-} + H^+ \quad (16)$$

$$\text{Cytochrome-}c(Fe^{3+}) + O_2^{\cdot-} \longrightarrow \text{Cytochrome-}c(Fe^{2+}) + O_2 \quad (17)$$

$$O_2^{\cdot-} + 2\,H^+ \xrightarrow{SOD} O_2 + H_2O_2 \quad (18)$$

In the SOD assay, one unit will inhibit the rate of reduction of cytochrome c by 50% in a coupled system, using xanthine and xanthine oxidase at pH 7.8 at 25 °C. Xanthine oxidase concentration should produce an initial (uninhibited) ΔA_{550} of 0.025 +/- 0.005 per minute. The ΔA_{550} for each inhibited test should fall within 40-60% of the uninhibited rate. Any value outside this range is considered invalid. Hence, the assay has a narrow concentration window, as for the MnSOD wild-type, it needs a very low concentration of SOD, whereas for the weakly active mutants the situation reversed. Assays were performed in triplicate in 1500 µL per reaction in 2 mL standard plastic cuvettes (using a Cary 300 UV-Vis spectrometer (Agilent Technologies, Mulgrave, Australia)).

Formatted: Not Highlight

To do the SOD assay, a blank, an uninhibited reaction, and tests were prepared by pipetting 1.4 mL of the cocktail and 0.05 mL of MnSOD or water (for a blank and uninhibited) with various dilutions to reach the allowed ΔA_{550} into a cuvettes (see Table 3.6). The stock cocktail comprised 50 mL of 0.0108 mM xanthine, 25 mL 0.216 mM KH_2PO_4 (pH 7.8 and 6.0 adjusted with 10 M NaOH or 10 M HCl, respectively), 1 mL 10.7 mM EDTA, 1 mL 1.10 mM cytochrome(Fe^{3+}) and made up to 100 mL with deionised water. The solutions were equilibrated to 25°C using a suitably thermostatted spectrophotometer and the absorbances were monitored at 550 nm until constant after adding xanthine oxidase (XOD) reagent (0.05 mL). The increases in absorbance at 550 nm were recorded to obtain the rates of each test, uninhibited, and the blank.

Table 3.6. Reaction mixtures of MnSOD assay

	Blank (/mL)	Uninhibited (/mL)	Test (/mL)
Cocktail	1.4	1.4	1.4
Purified water	0.1	0.05	-
MnSOD sample	-	-	0.05
Reagent XOD	-	0.05	0.05

The percent of inhibition and the units of activity per mL enzyme were calculated by the following equations:

$$\text{Percent Inhibition:} \quad \frac{(\Delta A_{550}/\text{min Uninhibited} - \Delta A_{550}/\text{min Inhibited})(100)}{(\Delta A_{550}/\text{min Uninhibited} - \Delta A_{550}/\text{min Blank})} \qquad (19)$$

$$\text{Units/mL Enzyme:} \quad \frac{(\text{Percent Inhibition})(DF)}{(50\%)(0.10)} \qquad (20)$$

where,

DF = Dilution Factor
50% = Inhibition of the rate of cytochrome c reduction per the unit definition
0.10 = Volume (in milliliters) of enzyme used in each test

Highly active wild-type *Ec*-MnSOD has an activity of ~7300 units/mg (J. W. Whittaker & Whittaker, 1991).

On the assumption that *Ec*-MnSOD-S126D was monomeric with loss of Glu170 from the active site, complementation experiments were run on *Ec*-MnSOD-S126D at pH 7.8 in the presence of 10-20 mM sodium propionate with wild-type *Ec*-MnSOD as control.

3.10.2 Analytical ultracentrifugation

Sedimentation velocity experiments were conducted using protein concentrations of 0.125 mg/mL, 0.25 mg/mL, and 0.5 mg/mL in 45 mM potassium phosphate, 100 mM NaCl, pH 6.0 and 7.8 at 20 °C. Data were collected in continuous mode at 290 nm at 50,000 rpm in a Beckman Coulter XL-I analytical ultracentrifuge housed in the School of Biological Sciences, University of Canterbury, Christchurch, New Zealand. Buffer density and viscosity and an estimate of the partial specific volume of MnSOD mutants were calculated using SEDNTERP. Data were fitted to a continuous sedimentation coefficient [*c*(*s*)] model and continuous mass [*c*(*M*)] model using SEDFIT (Schuck, 2000; Schuck, Perugini, Gonzales, Howlett, & Schubert, 2002). The assistance of Dr Sarah Kessans and Professor Renwick CJ Dobson in providing access, data collection and help with data interpretation is gratefully acknowledged.

3.10.3 Differential scanning calorimetry (nano-DSC)

DSC can be used to analyse the stability of a protein in dilute solution. The measurement involves determining changes in the partial molar heat capacity of the protein at constant pressure (ΔC_p). The experiments on stability of the *Ec*-MnSOD and its mutants were conducted at various protein concentrations of 0.25 mg/mL to 0.35 mg/mL in 10 mM Tris-Cl, pH 6.0 and 7.8. Data were collected at scan rates 1 °C/min in a TA Instruments™ Nano-DSC (differential scanning calorimeter). Data were background corrected and integrated using TA Instruments NanoAnalyze™ software version 3.3.0 (TA Instruments).

Testing reversibility of denaturing of Ec-*MnSOD-S126W*

A single scan of the *Ec*-MnSOD-S126W exhibited three well-separated endothermic events at T_m = 53 °C (labelled X), T_m = 63 °C (labelled Y), and T_m = 73 °C. To study the reversibility of these transitions, samples were heated to the temperature at end of each endothermic transition (T_m +~4-7 °C) and then cooled. This was repeated several times. Multiple scans were done on the same sample. A 300 μL of protein sample (0.2 mg/mL) was used for testing reversibility. However, only data from heating processes were collected. Multiple scans consist of:

1) Heating: with temperature range from 20 °C to 57.5 °C
2) Cooling, temperature range from 57.5 to 20 °C
3) Heating: with temperature range from 20 °C to 69 °C
4) Cooling, with temperature range from 69 to 20 °C
5) Heating: with temperature range from 20 °C to 80 °C
6) Cooling, temperature range from 80 to 20 °C
7) Heating: with temperature range from 20 °C to 100 °C

3.10.4 Circular dichroism (CD) spectroscopy

Circular dichroism (CD) spectra of *Ec*-MnSOD wild-type, *Ec*-MnSOD-S126D, and *Ec*-MnSOD-S126W were recorded on Chirascan™ CD spectrometer (Applied Photophysics, Surrey, United Kingdom) equipped with a TC125 temperature controller (Quantum North West). Near-UV (250–350 nm) spectra were recorded in a 10 mm Quartz Suprasil cell (#100-QX, Hellma, Essex,

United Kingdom), while far-UV (180-260 nm) spectra were recorded in a 0.1 mm cell at various temperatures (23 to 83°C). Sample concentrations were ~0.1 mg/mL and ~1 mg/mL for near-UV and far-UV measurements, respectively, each in 50 mM potassium phosphate buffer, pH 7.8. An average of 10 scans was recorded at 1 nm intervals at 0.25 s per point. The results were averaged and smoothed with a window factor of 3 nm and corrected for background signals from buffer.

Chapter 4 Characterisation of *Ec*-MnSOD-S126D

In this chapter, the role of Glu170 in the dismutation of superoxide by *Ec*-MnSOD was explored. Ser126, which hydrogen bonds to Ser126 from the adjacent subunit across the dimer interface was mutated to Asp, with the intention that at the pH of maximum activity, ~pH 7.8. Energetics calculations to estimate the charge repulsive energy were carried out using PISA to estimate the dimerisation stabilisation energy (Krissinel & Henrick, 2007). There would be charge repulsion of the negatively charged carboxylate side chain of the Asp126 residue that would lead to a monomeric species. The hypothesis was that activity might be recovered by complementation with, for example, propionic acid replacing the role of Glu170. In Chapter 5, the steric bulk of tryptophan, as the S126W mutant, was used to break apart the dimer. Both mutations led to unexpected results.

4.1 Expression and Purification

The expression of *Ec*-MnSOD-S126D in SodA- *E. coli* QC 781 cells resulted in a good level of expression of the protein in the soluble fraction. The control, soluble wild-type *Ec*-MnSOD protein, was also well expressed in *E. coli* strain AB2463. Unlike strain AB2465, SodA- *E. coli* QC781 does not carry the *E. coli* MnSOD gene. However, both strains AB2465 and SodA- *E. coli* QC781 are transformed by the plasmid of pDT1-5, which contains an ampicillin antibiotic resistance gene and carries the *sodA* gene, which codes for MnSOD.

Scaled-up protein expression involved several steps of purification (Figure 4.1). In the initial step, post-lysis centrifugation separated protein and non-protein parts of the cell lysate to produce crude extract in the supernatant. Ammonium sulfate precipitation at 60% of saturation to give more pure MnSOD-S126D protein in supernatant was followed by 90% of saturation in pellet. The stability of MnSOD-S126D at pH 7.8 provided an effective salt precipitation where many of the contaminating proteins are precipitated.

The next step was cation exchange chromatography (Figure 4.2). To ensure correct buffer pH was used for cation exchange, the pI value of MnSOD S126D was estimated using SEDNTERP

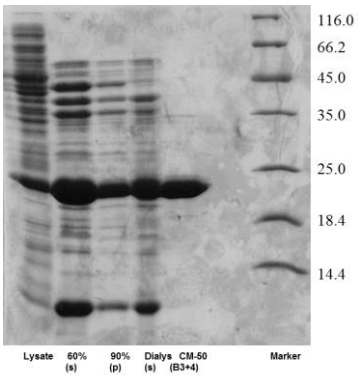

Figure 4.1. Coomassie-stained SDS-PAGE of *Ec*-MnSOD-S126D purification.

From left to right: lysate of crude extract, supernatant of ammonium sulfate precipitation at 60% of saturation, pellet of ammonium sulfate precipitation at 90 % of saturation, supernatant of dialysate after centrifugation, and pure enzyme (23 kDa) after cation exchange chromatography steps.

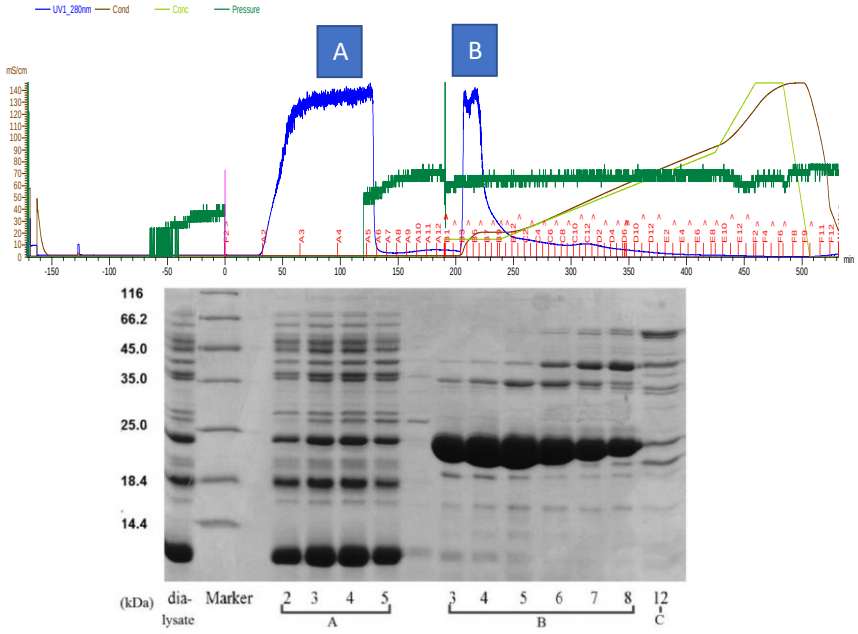

Figure 4.2. Cation exchange chromatography to purify *Ec*-MnSOD-S126D.

(Top) Cation exchange chromatogram (Sephadex-CM50) to purify *Ec*-MnSOD-S126D. (Bottom) Coomassie-stained SDS-PAGE of eluate fractions from cation exchange chromatography. *Ec*-MnSOD-S126D adsorbs to the matrix while other proteins pass through the column (A). Elution with a NaCl salt gradient leads to the enzyme being eluted quite early. *Ec*-MnSOD-S126D enzyme was distributed in fraction B.

(Laue, 1992; Lebowitz, Lewis, & Schuck, 2002), giving pI = 6.47. Here, potassium acetate pH 5.5 buffer was used in cation exchange chromatography (J. W. Whittaker & Whittaker, 1991). To prepare protein sample for cation exchange, the protein pellet obtained from ammonium sulfate fractionation was resuspended and dialysed against 100x volumes of 10 mM potassium acetate pH 5.5. At the end of the dialysis, centrifugation at 17,000 x*g* was carried out to separate insoluble material.

In cation exchange, the pH 5.5 potassium acetate buffer used as eluent is almost one magnitude below the pI (6.47). In low pH (pH lower than the pI), the side chains of glutamate and aspartate amino acids become protonated and thus the total net charge of protein becomes positive. The negative charge of the resin attracts the positively charged MnSOD more than the impurities do. By changing pH of the buffer and increasing the salt concentration, positively charged Na^+ ions will replace the protein desired (peak B) on the matrix (see Figure 4.2).

Table 4.1. Procedure used for purification of *Ec*-MnSOD mutants.

Steps	*Ec*-MnSOD wt	*Ec*-MnSOD-S126D	Buffer used
pI*	6.68	6.47	-
Lysis	√	√	50 mM potassium phosphate pH 7.8
Ammonium sulfate precipitation	√ 60 %/90 %	√ 50 %/75%	50 mM potassium phosphate pH 7.8
Cation exchange (Sephadex-CM50)	√ 10 mM potassium acetate pH 5.5/ against 1 mM NaCl	√ 10 mM potassium acetate pH 5.5/ against 1 mM NaCl	10 mM potassium acetate pH 5.5 against gradual 1 mM NaCl
Cation exchange (Sephadex-CM50)	√	-	20 mM potassium acetate pH 5.5/against 1 mM NaCl but shallow gradient
Hydrophobic interaction (phenyl superose)	√ 20 mM potassium acetate pH 5.5	-	Washed twice by same buffer with: 1) 2.5 M NaCl 2) 1 M NaCl

* pI: pH at calculated isoelectric point.

4.2 *Ec*-MnSOD-S126D activity

Given that a monomeric mutant of the *Ec*-MnSOD enzyme *Ec*-MnSOD-E170A lost its SOD activity (M. M. Whittaker & Whittaker, 1998a)), we were very interested in determining if the *Ec*-MnSOD-S126D mutant was catalytically inactive. The SOD assay was used to examine the superoxide dismutase activity of the mutant and the wild-type as control. The activity of *E. coli* MnSOD wild-type and MnSOD-S126D have all been characterised at pH 7.8, which is the optimum pH of the wild-type enzyme, and at pH 6.0.

Surprisingly, without knowing, at this stage, the oligomerisation state of the mutant, mutation of Ser126 to Asp significantly reduced the superoxide dismutase activity to 5.7 % and 4.2 % of that of the wild-type enzyme at pH 7.8 and 6.0, respectively (See Table 4.2).

Table 4.2. Activity assay of wild-type *Ec*-MnSOD and its S126D mutant

	Wt *Ec*-MnSOD (/(U/mg))	***Ec*-MnSOD-S126D % of Wt activity**
pH 6.0	8.4 (17) x 10^3	4.2 (4) %
pH 7.8	10.2 (9) x 10^3	5.7 (9) %
pH 7.8 (10-20 mM Na^+ propionate)[a]	12.2 (1.0) x 10^3	12.2 (5) %
Concentration range	1.3 – 2.2 nM	11 – 54 nM

[a] Complementation experiments were run at concentrations of 2.2 nM and 54 nM for wild-type *Ec*-MnSOD and its S126D mutant, respectively.

Based on SOD activity assay, mutation of Ser126 to Asp at the dimer interface site greatly reduced activity. These results raise questions. Is the loss of activity due to a change in quaternary structure of the mutants, that is loss of the dimer structure and consequent loss of dimer interface residue Glu170, discussed earlier as a key component of the protein shuttle? Alternatively, is the loss due to more subtle features arising from changes to the active site and addition of a negative charge somewhat close to the Mn active site?

Complementation experiments were run on the assumption that at pH 7.8 *Ec*-MnSOD-S126D was monomeric and that Glu170 was no longer part of the active site. Thus, if Glu170 is part of a proton shuttle and if propionate binds into the site vacated by Glu170, then an increase in activity of the S126D mutant should be observed. Wild-type *Ec*-MnSOD as the control showed a small 10% increase in activity in the presence of 10-20 mM sodium propionate, likely

an ionic strength effect. The S126D mutant showed a more than doubling of activity compared to its activity in the absence of sodium propionate. At the time of these experiments, the oligomeric status of *Ec*-MnSOD-S126D was not known. Further discussion is delayed to section 4.4 in the light of determining the oligomeric state of *Ec*-MnSOD-S126D.

4.3 X-ray structural characterisation of *Ec*-MnSOD-S126D at different pH

Diffraction-quality crystals of *Ec*-MnSOD-S126D were grown at different pH. At low pH, crystals were grown at pH 6.8 in 0.1 M Bis Tris propane, 23 % (w/v) PEG 1500, with 0.2 M KCl, and 1.5 % (v/v) ethanol. At higher pH, crystals were grown at pH 8.7 in 0.1 M SPG buffer (succinic acid, sodium dihydrogen phosphate, glycine), 28% (w/v) PEG1500 and 1.5%(v/v) ethanol. No cryoprotectant was added to freeze crystals. Lastly, crystals of *Ec*-MnSOD-S126D complexed with azide (*Ec*-azido-MnSOD-S126D), where azide is a competitive inhibitor of MnSOD and has long been studied as substrate mimic, were grown at pH 9.0 in 0.5 M SPG buffer, 19% (w/v) PEG 1500 and added sodium azide.

X-ray diffraction data from crystals of *Ec*-MnSOD-S126D at pH 6.8, *Ec*-MnSOD-S126D at pH 8.7, and *Ec*-azido-MnSOD-S126D crystals at pH 9.0, were measured at a resolution of 1.56 Å, 1.55 Å, and 1.53 Å, respectively (See Table 4.3). Interestingly, for the S126D mutant at pH 6.8, a triclinic crystal formed in space group *P*1 not previously observed. At pH 8.7, *Ec*-MnSOD-S126D crystallised in the primitive monoclinic space group $P12_11$ ($P2_1$). For *Ec*-azido-MnSOD-S126D, the commonly encountered orthorhombic space group $C222_1$ was observed. All the proteins crystallise with two homodimers in the asymmetric unit. Wild-type *Ec*-MnSOD and many of its mutants (Y34A, Q146L/H, H30A) also crystallise in $C222_1$ with two homodimers in the asymmetric unit. As discussed earlier, Glu170 from one subunit reaches across the dimer interface to hydrogen bond to metal-ligand His171 (Edwards, Baker, et al., 1998).

Table 4.3. Crystallographic data and refinement statistics for *Ec*-MnSOD-S126D.

	S126D at pH 6.8	**S126D at pH 8.7**	**S126D-azide at pH 9.1**
A. Data collection statistics			
Diffraction source	**AS-MX2**	**AS-MX2**	**AS-MX1**
Wavelength (/Å)	0.95370	0.95370	0.95370
Temperature (/K)	100	100	100
Detector	ADSC	ADSC	ADSC
Rotation range per-image (/°)	0.1	0.1	0.5
Exposure time per image (/s)	0.030	0.030	3?
Space group	*P*1	$P12_11$[a]	$C222_1$
# molecules in asymmetric unit	4	4	4
# molecules in unit cell	4	8	32
a (/Å)	46.70	97.89	98.93
b (/Å)	52.77	46.02	107.20
c (/Å)	86.30	103.71	179.98
α (/°)	94.3	90	90
β (/°)	91.7	118.16	90
γ (/°)	92.2	90	90
Volume (/Å^3)	211,800	411,900	1,908,700
Mosaicity (/°)	0.16	1.11	1.1
Resolution range (/Å)	46.64- 1.56 (1.57-1.56)	41.11-1.80 (1.84-1.80)	72.7-1.53 (1.56-1.53)
Total # of reflections	429,984	197,774	874,806
# unique reflections	111,802	70,985	141,282
Completeness (%)	95.5 (89.0)	93.4 (79.0)	98.5 (87.7)
Redundancy	3.8 (3.7)	2.8 (2.1)	6.2 (2.9)
I/s(*I*)	11.2 (4.1)	6.6 (1.7)	9.3 (0.9)
R_{mrg}	0.063 (0.246)	0.100 (0.424)	0.087 (0.728)
R_{pim}	0.038 (0.149)	0.068 (0.314)	0.037 (0.504)
$CC_{1.2}$	0.997 (0.936)	0.986 (0.737)	0.997 (0.727)
Wilson *B*-value (/Å^2)	7.97	17.3	19.0
B. Refinement Statistics			
Resolution range (/Å)	86.01-1.56 (1.60-1.56)	41.11-1.80 (1.85-1.80)	72.01-1.53 (1.57-1.53)
Completeness (%)	95.6 (92.6)	93.2 (79.2)	98.4 (88.1)
# reflections, working set	106,194 (7614)	67,424 (4225)	134,221 (8776)

# reflections, test set	5607 (390)	3558 (212)	7013 (466)
Final R_{work}	0.142 (0.153)	0.224 (0.2674)	0.178 (0.303)
Final R_{free}	0.168 (0.182)	0.248 (0.296)	0.206 (0.320)
# non-H protein atoms	6,699	6,621	6,664
# manganese ions	4	4	4
# azide ions	0	0	4 (x 0.25)
# waters	911	408	668
R.m.s. deviations			
Bonds (/Å)	0.010	0.009	0.009
Bond angles (/°)	1.79	1.57	1.69
Mean *B* factors (/Å^2) protein atoms	12	11	17
Ramachandran (COOT v0.9.8.7) Preferred/Allowed/Outlier (%)	95.97/3.76/0.27	96.78/2.96/0.26	95.28/4.33/0.39

[a] Data are twinned to give pseudo-orthorhombic cell in $B22_12$ (alternative setting of $C222_1$) with twin law pairing reflections (*h*,*k*,*l*) and (-*h*-*l*, -*k*,*l*) and twin fractions 0.906 and 0.094. Refinement in $B22_12$ could not be progressed beyond at R_{work} = 0.265 and R_{free} = 0.285; data merging statistics were also significantly worse than for merging in $P12_11$. The pseudo-orthorhombic cell, transformed to $C222_1$**,** has similar dimensions to that of wild-type *Ec*-MnSOD and *Ec*-MnSOD-S126D-azide.

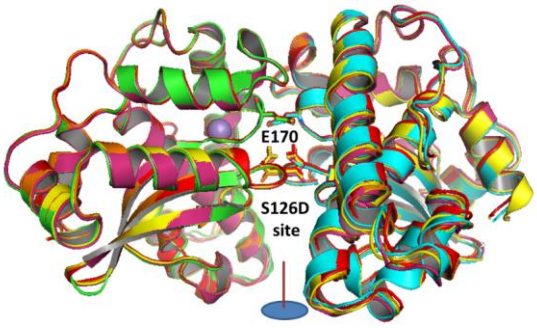

Figure 4.3. Superposition of *Ec*-MnSOD-S126D (pH 6.8) onto wild-type *Ec*-MnSOD (at pH 8.5; PDB: 1VEW).

Wild-type enzyme is coloured green (subunit A) and cyan (subunit B). The two dimers in the asymmetric unit of *Ec*-MnSOD-S126D are superimposed on to subunit A of wild-type *Ec*-MnSOD, where the bold letter denotes the subunit superimposed: **A**D (yellow), **D**A (orange), **B**C (red), **C**B (magenta). Superposition of subunits of the S126D mutant onto subunit A of wild-type enzyme have rmsd's of 0.31-0.39 Å; superpositions of dimers onto dimer have rmsd's of 0.41-0.47 Å.

All structures were dimeric with the canonical dimer interface maintained. Figure 4.3 shows the close superposition of *Ec*-MnSOD-S126D (pH 6.8) onto wild-type *Ec*-MnSOD (at pH 8.5). The pH 8.7 structure of *Ec*-MnSOD-S126D and the pH 9.1 structure of its azide derivative also show very similar close superpositions with wild-type *Ec*-MnSOD (and therefore with each other). The view is down the non-crystallographic two-fold axis. Figure 4.4 shows in space-filling representation the highly conserved interface between subunits of the dimer.

The Asp126 fits perfectly into the interface, such that the carboxylate side chain hydrogen bonds across the dimer interface to the pepide NH of Asp126, and *vice versa* for the other Asp126. This "handshaking" places the two Asp126 in close contact in the pH 6.8 and 8.1 structures. Therefore, there is a proton mediating this contact, $-C(=O)-O^{-}...H^{+}...O^{-}-C(=O)-$. Figure 4.5 illustrates this contact for the three structures at pH 6.8, pH 8.7 and, with partial binding of azide, pH 9.1. Whereas, the pH 6.8 and 8.7 structures share an approximately similar conformation of the Asp side chain, for the azide adduct, a distinctly different disordered arrangement is observed, such that close hydrogen bonding contacts do not occur. For all three S126D structures, an average pK_a of 9.5 is calculated by PropKa (Olsson et al., 2011) for the well-buried Asp126. The structural results are, therefore, congruent with calculated pK_a's

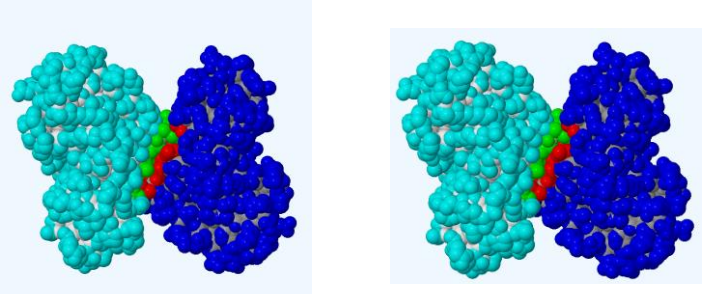

Figure 4.4. Dimer interface of *Ec*-MnSOD wild-type (left) and pH 6.8 structure of *Ec*-MnSOD-S126D (right).

The residues in contact are coloured green for the cyan-coloured subunit, and red for the blue-coloured. Only atoms accessible to water are coloured. The distinct interface area of the canonical dimer of wild-type *Ec*-MnSOD and MnSOD-S126D is exactly the same, 858 Å^2.

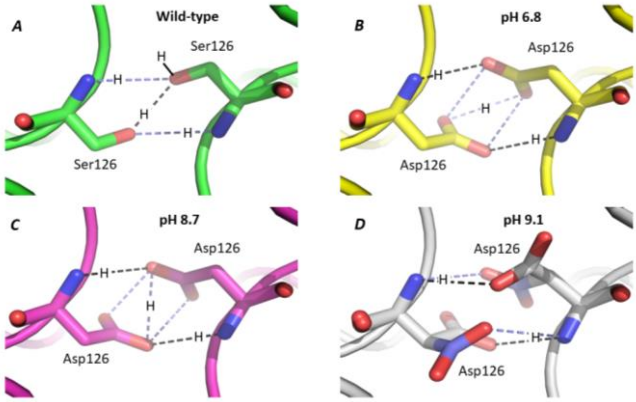

Figure 4.5. Hydrogen bonding of Asp126 across the dimer interface for *Ec*-MnSOD-S126D.

A, At pH 6.8 and pH 8.7 Asp126 shares approximately the same conformation. The carboxylate groups are poorly oriented for a canonical hydrogen bond C-O…H…O-C with C-O..H bond angles of ~120° and an O…H…O angle of ~120-180°. Thus, a single proton situated between the two carboxylate groups is inferred. However, at pH 9.1 in the partial azido structure, Asp126 adopts a pair of different conformations that still preserves hydrogen bonding to the peptide NH of Asp126 but not with itself. The Asp126 is disordered and the interface is, like that for wild-type enzyme with Ser126, intrinsically asymmetric. ***A***, Wild-type, Ser126. ***B***, Asp126 at pH 6.8. ***C***, Asp126 at pH 8.7. ***D***, Disordered Asp126 at pH 9.1 (azido adduct). Key hydrogen bonding contacts and the inferred positions of the protons mediating Ser126...Ser126 and Asp126...Asp126 contacts are shown, with hydrogen bonding to peptide NH of residue 126 in black dashes and hydrogen bonding of Ser126 or Asp126 with itself shown in slate-coloured dashes.

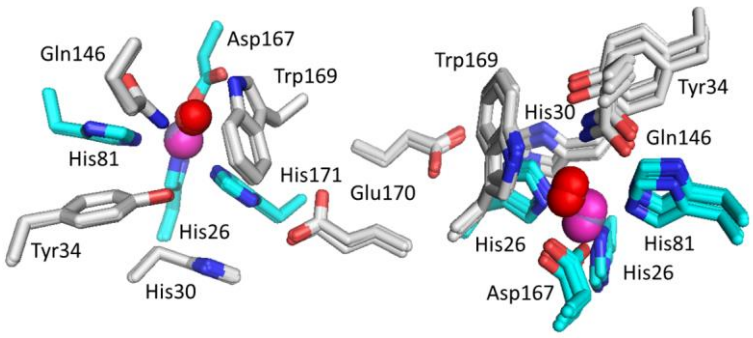

Figure 4.6. Superposition of one subunit of *Ec*-MnSOD-S126D onto wild-type *Ec*-MnSOD, highlighting the active site.

The stereochemistry of the active site is strongly conserved. There are small changes in the orientation of the other subunit across the dimer interface. Metal ligands are cyan-highlighted and second-shell residues that guard access to the active site are shown in grey. The Mn ion is shown as a magenta sphere and the coordinated hydroxide as a red sphere.

Figure 4.6 shows the active site of *Ec*-MnSOD-S126D superimposed onto that of wild-type *Ec*-MnSOD. Glu170 maintains the same position as in wild-type *Ec*-MnSOD. In addition, the water structure observed in wild-type *Ec*-MnSOD is strongly conserved in *Ec*-MnSOD-S126D (Figure 4.7).

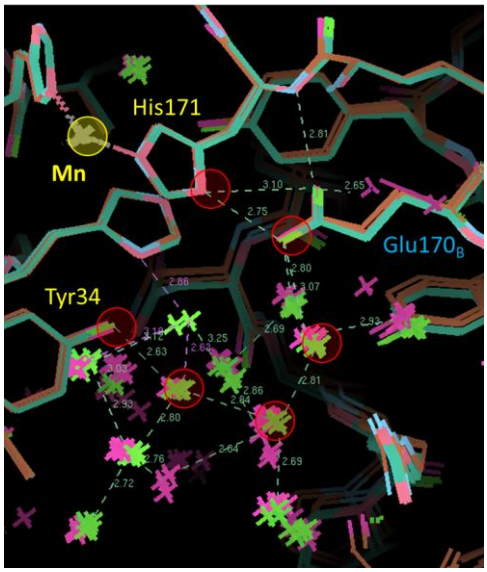

Figure 4.7. Conservation of water structure in the active site of *Ec*-MnSOD.

For wild-type *Ec*-MnSOD the four crystallographically independent subunits are superimposed and plotted (green crosses for water) and similarly for the four subunits of *Ec*-MnSOD-S126D (magenta crosses for water). The circled waters and residues connect a putative proton shuttle from Glu170 to the active site when $O_2^{-\bullet}$ (or azide mimic) coordinates.

Given the minimal structural changes to the active site and its water structure caused by the S126D mutation, why is activity so low? One possible answer is that under the conditions of activity measurements (nanomolar concentrations of enzyme) the *Ec*-MnSOD-S126D is no longer dimeric. Although the X-ray structures show the aspartate being accommodated at the dimer interface, has the aspartate destabilised this interface? In the next section, differential scanning calorimetry (DSC) and analytical ultracentrifugation experiments address this

question. Alternatively, does the negative charge on the aspartate perturb the electrostatic environment at the active site to prevent activity?

Assuming the protein remains dimeric at conditions of assay for enzyme activity, the Mn^{II}/Mn^{III} redox couple is carefully controlled by metal ligands and the second coordination shell. This is highlighted by the extreme metal specificity of *Ec*-MnSOD and *Ec*-FeSOD, which share identical ligands and near identical second-shell surroundings. Asp126 is in proximity to Trp169, which in turn interacts closely with the coordinated hydroxide ion, as shown in Figure 4.8.

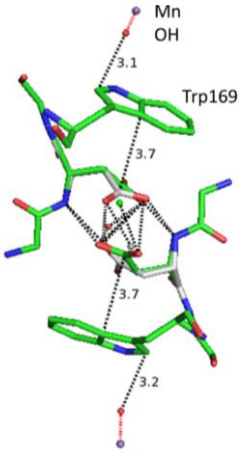

Figure 4.8. Charge communication from Asp126 to the Mn active site.

The Asp group sits 3.7 Å from Trp169 which makes a short 3.1 Å n-π* contact to the Mn-coordinated hydroxide.

4.4 Quaternary state characterisation of *Ec*-MnSOD-S126D in the solution state.

4.4.1 Sedimentation velocity analysis by analytical ultracentrifugation

What is the structure of the *Ec*-MnSOD-S126D mutant in solution? Is it dimeric or monomeric? To answer this question, analytical ultracentrifugation (AUC) has been utilised. AUC is very useful in the identification of the oligomeric state of proteins through sedimentation velocity experiments (Lebowitz et al., 2002). The information about sedimentation velocity (SV) analysis of the MnSOD and FeSOD is still limited, despite analytical ultracentrifugation being a well-established technique. The reemergence of analytical ultracentrifugation as a versatile tool to investigate protein interactions has occurred because of advances in AUC technology coupled with advancement of computational software for data analysis. To investigate the quaternary structure of *Ec*-MnSOD-S126D and to probe the stability of the quaternary structure in solution, a series of sedimentation velocity experiments were employed with

varying concentrations of the protein and pH. Sedimentation velocity experiments of *Ec*-MnSOD wild-type were also investigated as a reference.

4.4.2 *Ec*-MnSOD wild-type is a tightly associated dimer

Ec-MnSOD wild-type is known as a compact homodimer in a solution. Here, sedimentation velocity analysis of wild-type *Ec*-MnSOD was investigated in two pH states. In a pH 7.8 solution (10 mM Tris, 100 mM NaCl, pH 7.8), the result shows a narrow and symmetric *c*(*s*) distribution and continuous mass distribution, *c*(*M*). The sedimentation velocity data wild-type *Ec*-MnSOD gave a weight-average standardised sedimentation coefficient, $s_{20,w}$, of 3.4 $\pm$ 0.1 S(vedberg) and an average molar mass of 45.8 $\pm$ 0.5 kDa at concentrations of 2.8, 4.6, 8.3 μM in a pH 7.8 solution (Figure 4.9).

The continuous sedimentation coefficient and mass distributions show that wild-type *Ec*-MnSOD is a tightly associated dimer at all concentrations at pH 7.8. The average mass is determined to be ~45.8 kDa very close to that of the calculated dimeric mass of 46.14 kDa for wild-type *Ec*-MnSOD.

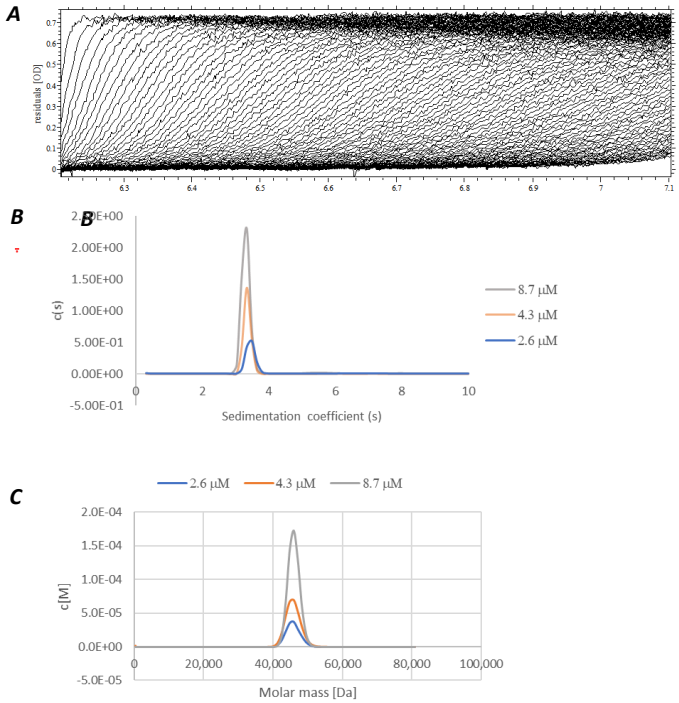

Figure 4.9. Quaternary structure of wild-type *Ec*-MnSOD at pH 7.8.

A, Sedimentation velocity data, showing absorbance *versus* distance from rotation axis *versus* time for *Ec*-MnSOD wild-type (only data from the 8.7 µM solution shown). ***B,*** Sedimentation coefficient *c*(*s*) distribution of *Ec*-MnSOD wild-type at pH 7.8. ***C,*** Continuous mass distribution *c*(*M*) obtained from the fitting of SV data of *Ec*-MnSOD at pH 7.8 (10 mM Tris, 100 mM NaCl). The apparent molar mass of the species represented by the peak has been found to be 45.8, 45.8, and 45.9 kDa, for 2.60 µM, 4.32 µM and 8.74 µM, respectively. For the 2.6 µM solution, *f*/*f*o=1.3, $s_{20,w}$ = 3.5 S and rmsd = $5.36.10^{-3}$. For the 4.3 µM solution, *f*/*f*o = 1.3, $s_{20,w}$ = 3.4 S and rmsd = $4.86.10^{-3}$. For the 8.7 µM solution, *f*/*f*o = 1.3, $s_{20,w}$ = 3.3 S and rmsd = $5.89.10^{-3}$.

Furthermore, the investigation of sedimentation velocity of wild-type *Ec*-MnSOD at pH 6.0 reveals a similar result to that at pH 7.8 (Figure 4.10). The sedimentation coefficients *c*(*s*) distribution shows a similar weight-average $s_{20,w}$ of 3.6 S and average molar mass of wild-type *Ec*-MnSOD of 46 kDa at concentrations of 1.7, 3.3 and 6.7 µM, suggesting that the dimer *Ec*-MnSOD wild-type at lower pH remains stable as a dimer.

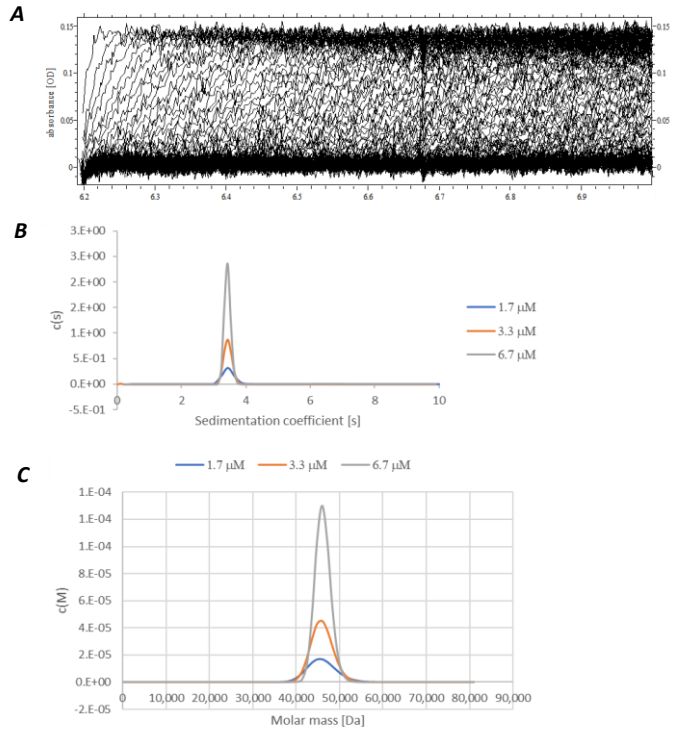

Figure 4.10. Quaternary structure of wild-type *Ec*-MnSOD at pH 6.0.

A, Sedimentation velocity data, showing absorbance *versus* distance from rotation axis *versus* time for wild-type *Ec*-MnSOD (only data from 1.7 µM solution shown). ***B,*** Sedimentation coefficients *c*(*s*) distribution of wild-type *Ec*-MnSOD at pH 6.0. For the 1.7 µM solution, *f*/*f*o = 1.3, $s_{20,w}$ = 3.6 S, and rmsd = $4.41.10^{-3}$. For the 3.3 µM solution, *f*/*f*o = 1.3, $s_{20,w}$ = 3.6 S, and rmsd = $4.52.10^{-3}$. For the 6.7 µM solution, *f*/*f*o = 1.3, $s_{20,w}$ = 3.4 S and rmsd = $5.05.10^{-3}$. ***C,*** Continuous mass distribution *c*(*M*) obtained from the fitting of SV data of *Ec*-MnSOD wild-type at pH 6.0 (10 mM Tris, 100 mM NaCl). The apparent molar mass of the species represented by the peak has been found to be 46.0, 45.9 and 45.9 kDa for 1.7 µM, 3.3 µM and 6.7 µM solutions, respectively.

4.4.3 *Ec*-MnSOD-S126D is partially monomeric

To investigate the quaternary structure of *E*c-MnSOD-S126D and to probe the stability of the dimer in solution, sedimentation velocity studies of the mutant were employed at similar pH and protein concentration ranges to those used for wild-type *Ec*-MnSOD experiments at pH 7.8 and pH 6.0.

At both pH 6.0 and 7.8, the continuous sedimentation coefficient and mass distributions of *Ec*-MnSOD-S126D substantially change with change in protein concentration at each pH, compared to those of *Ec*-MnSOD wild-type. At pH 7.8 over the concentration range from 1.8 to 7.0 μM, the sedimentation velocity analysis of *Ec*-MnSOD-S126D shows two peaks. Firstly, a tiny peak (3-7% relative to the main peak) of the is found at low sedimentation coefficient and is attributed to a monomer species, Secondly, the predominant species at higher molar mass and sedimentation coefficient represents dimeric *Ec*-MnSOD-S126D. Sedimentation velocity analysis of *Ec*-MnSOD-S126D at the different concentrations showed relatively narrow and symmetric *c*(*s*) and *M*(*s*) distributions. The weight-average standardised sedimentation coefficient and molar mass at each protein concentration are very close and repeatable, except that at highest concentration the monomer peak is barely visible and therefore gives imprecise values for the maxima in the *c*(*s*) and *c*(*M*) distributions.

Retrieved from the data of Figure 4.11, the average value of $s_{20,w}$ for *Ec*-MnSOD-S126D is 3.37 $\pm$ 0.04 S for the dimeric species and 1.3 $\pm$ 0.3 S for the monomeric species from three different concentrations. Moreover, the apparent molar mass of the species represented by the major peak has been found to be 46.5 ± 0.4 kDa for dimeric *Ec*-MnSOD-S126D and 17 ± 4 kDa for monomeric *Ec*-MnSOD-S126D, not significantly different to the expected values of 46.1 and 23.1 kDa. The relatively low precision of the molar mass of the monomeric species is due to its low relative abundance compared to the predominant dimer species (Figure 4.11).

The sedimentation velocity analysis results of *Ec*-MnSOD-S126D at lower pH 6.0 (50 mM potassium phosphate, 50 mM NaCl, pH 6.0) shows more prominently than at pH 7.8 the monomeric species, which is present as a relatively broad but symmetrical peak with a maximum in the *c*(*M*) distribution at 20.5 $\pm$ 2.1 kDa (Figure 4.12).

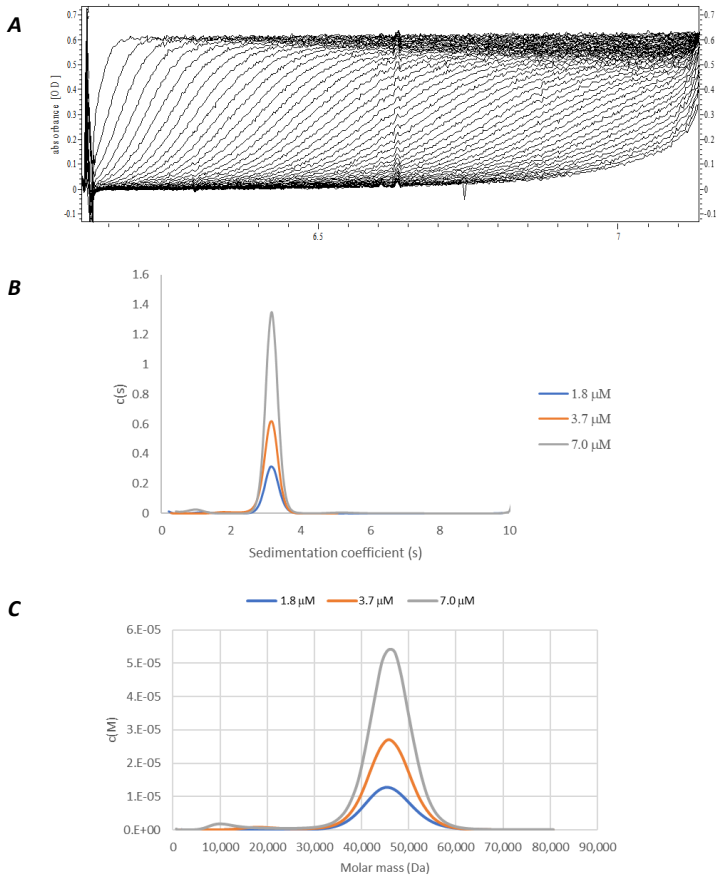

Figure 4.11. Quaternary structure of *Ec*-MnSOD-S126D at pH 7.8. ***A,*** Sedimentation velocity data, showing absorbance *versus* distance from rotation axis *versus* time for *Ec*-MnSOD-S126D (only data from 7 µM solution shown). ***B,*** Sedimentation coefficients *c*(*s*) distribution of *Ec*-MnSOD-S126D at pH 7.8. For the 1.8 µM solution, *f*/*f*o = 1.3, $s_{20,w}$ = 3.4 and 1.3 S and rmsd = $3.40.10^{-3}$. For the 3.7 µM solution, *f*/*f*o = 1.4, $s_{20,w}$ = 3.3 and 1.6 S and rmsd = $3.04.10^{-3}$. For the 7.0 µM solution, *f*/*f*o = 1.3, $s_{20,w}$ = 3.4 and 1.0 S and rmsd = $3.60.10^{-3}$. ***C,*** Continuous mass distribution *c*(*M*) obtained from the fitting of SV data of *Ec*-MnSOD-S126D at pH 7.8 (50 mM potassium phosphate, 100 mM NaCl, pH 7.8). The apparent molar mass of the dimeric species has been found to be 46.7, 46.9, and 45.9 kDa for 1.8 µM, 3.7 µM and 7.0 µM solutions, and for the monomeric species, the apparent molar mass is 21.8, 18.2, and 10.9 kDa, respectively.

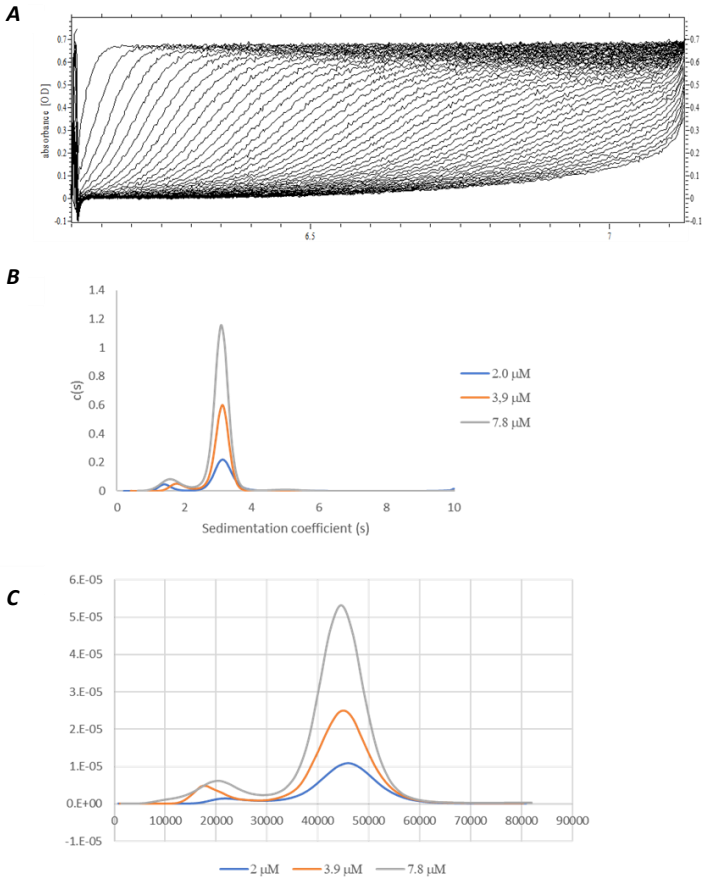

Figure 4.12. Quaternary structure of *Ec*-MnSOD-S126D at pH 6.0. ***A***, Sedimentation velocity data, showing absorbance *versus* distance from rotation axis *versus* time for *Ec*-MnSOD-S126D (only data from 7.8 mM solution shown). ***B***, Sedimentation coefficients *c*(*s*) distribution of *Ec*-MnSOD-S126D at pH 6.0. For the 2.0 mM solution, *f*/*f*o = 1.3, $s_{20,w}$ = 3.0 and 1.3 S, and rmsd = $3.40.10^{-3}$. For the 3.9 mM solution, *f*/*f*o = 1.4, $s_{20,w}$ = 3.1 S and 1.8 S, and rmsd = $3.90.10^{-3}$. For the 7.8 mM solution, *f*/*f*o = 1.3, $s_{20,w}$ = 3.1 and 1.6 S and rmsd = $4.70.10^{-3}$. ***C***, Continuous mass distribution *c*(*M*) obtained from the fitting of SV data of *Ec*-MnSOD-S126D at pH 6.0 (50 mM potassium phosphate, 100 mM NaCl, pH 6.0). The apparent molar mass of the dimeric species is 46.0, 45.5 and 44.6 kDa for 2.0 µM, 3.9 µM and 7.8 µM solutions, and for the monomeric species 23.3, 17.4 and 20.7 kDa, respectively.

The peak at higher sedimentation coefficient is quite narrow and symmetrical curve, giving a maximum in the *c*(*M*) distribution of 45.4 ± 0.5 kDa. The weight-average sedimentation coefficients of *Ec*-MnSOD-S126D at pH 6.0, 3.07 ± 0.04 S and 1.57 ± 0.18 S, are very similar to those of *Ec*-MnSOD-S126D at pH 7.8 for the dimer and monomer species, respectively (Figures 4.11 and 4.12).

The result reveals that the fraction of the monomeric species *Ec*-MnSOD-S126D mutant at lower pH is 9-12% relative to the main peak, which is higher than those at the higher pH for comparable concentrations (Table 4.4), suggesting that *Ec*-MnSOD-S126D dimer is less stable at the lower pH than at pH 7.8. The fractions of the protein mutant at lower pH are just above triple of those at the higher pH. Structurally, this result will be explained in the Discussion section with correlation to the pK_a of the point mutation.

Table 4.4. The calculation of monomer-dimer equilibrium of *Ec*-MnSOD-S126D at various pH and concentrations.

pH of S126D		Concentration (/μM)	*c*(monomer) (/Au)	*c*(dimer) (/Au)	*f*(monomer) (/Au)	K_D (/μM)
pH 7.8		1.8	0.012×2	0.160	0.13	0.035
		3.7	0.009×2	0.311	0.055	0.012
		7.0	0.018×2	0.593	0.057	0.024
pH 6.0		2.0	0.014×2	0.159	0.15	0.053
		3.9	0.035×2	0.315	0.18	0.16
		7.8	0.072×2	0.596	0.19	0.37

[a] Concentration *c* (in absorbance unit) obtained from the Sedfit software calculation. For the purpose of calculating *f* the multiplier of 2 corrects for the halved molar absorptivity of the monomer compared to the dimer.

Is the species appearing at a lower molar mass really a monomeric *Ec*-MnSOD-S126D species? The issue has arisen since the fraction value of the monomer in Table 4.4 does not increase as the concentration decreases. But it appears that the opposite is happening, resulting that the K_D is not constant but increases as the concentration increases. The monomer fraction remains stable at lower pH of all the experimental concentration range (Table 4.4). The K_D is derived from the monomer fraction for the monomer-dimer equilibrium as follows:

A_2 ==== A + A (21)

c

fc

---

c(1-*f*) *fc* *fc*

$K_D = [A]^2 / [A_2]$ (22) *c* = concentration of protein

$K_D = (fc)^2 / c(1-f)$ (23) *f* = fraction of the monomer

$K_D = \frac{f^2 c}{1-f}$ (20) (24) K_D = dissociation constant

Equilibrium constants can also be obtained from sedimentation equilibrium measurements, measured at various rotor speeds. The drift in values of K_D is attributed to errors in quantifying the amounts of monomer at low enzyme concentrations: an error in the absorbance for the monomer species of 20% at the lowest concentration changes K_D by almost 50%. Thus, for *Ec*-MnSOD-S126D at pH 7.8 and 6.0, the equilibrium constants that are considered trustworthy are those at the highest concentration, respectively 0.024 and 0.37 μM. The more than 10-fold increase in K_D at the lower pH is readily apparent qualitatively by comparing Figures 4.5B-D, which show the position of Asp126 in structures at pH 6.8, 8.7 and 9.1. This counterintuitive result that at high pH, where presumably charge repulsion of the aspartate carboxylate groups at the dimer interface would be maximised, is discussed below in the light of the structures obtained.

The above expression for K_D can be rearranged to solve for fraction of inactive monomer present under assay conditions.

$K_D = f^2 c/(1-f)$ (25)

where *f* is the fraction of monomer, calculated as

$f = c(\text{monomer})/(c(\text{monomer})+c(\text{dimer}))$ (26)

Rearranging, leads to:

$K_D (1-f) = cf^2$ (27)

$K_D - K_D f = cf^2$ (28)

$$cf^2 + K_D f - K_D = 0 \quad (29)$$

Solving the quadratic for the sensible root gives the fraction of monomer, *f*:

$$f = \frac{-K_D + \sqrt{(K_D{}^2 + 4.c.K_D)}}{2.c} \quad (30)$$

Substituting in the values for K_D (Table 4.4) and the concentrations for the activity assay (Table 4.2, leads to the following values summarised in Table 4.5 for (1-*f*), the fraction of dimer present at assay concentrations.

Table 4.5. Fraction of dimer (*f*) present at assay concentrations.

Enzyme	pH	K_D (/nM)	[MnSOD] (/nM)	*f*(dimer) assay	%activity (rel to wt)[a]	Absolute activity (/(U/mg))[a]
	7.8					
Wild-type		n.d.	1.3	~1.0	100	10200
		n.d.	2.2	~1.0		
S126D		24	11	0.25	5.7	581
			54	0.52		
	6.0					
Wild-type		n.d.	1.3	~1.0	100	8400
		n.d.	2.2	~1.0		
S126D		370	11	0.03	4.2	353
			54	0.11		

[a] Values taken from Table 4.2.

At pH 7.8, the protein is substantially dimeric at assay concentrations of *Ec*-MnSOD-S126D – this means that the 20-fold loss of activity is NOT due to the assaying on the monomer, but that Asp126 is perturbing the active site, as somewhere between 25 and 50% of the protein is dimeric. Put another way, if Asp126 (here structure suggests loss of proton) was neutral in its effects on MnSOD activity, 25-50% of wild-type activity would have been observed.

The complementation experiments (Table 4.2), where addition of sodium propionate was proposed to bind to complement the loss of Glu170 from the active site for *Ec*-MnSOD-S126D mutant, showed a more than doubling of activity compared to its activity in the absence of sodium propionate. At the time of those experiments, the oligomeric status of *Ec*-MnSOD-

S126D was not known. Subsequent analytical ultracentrifugation experiments (Tables 4.4, 4.5) showed that at pH 7.8 and at concentrations of 54 nM of enzyme, *Ec*-MnSOD-S126D was ~50% dimeric. Thus, the more than two-fold increase in activity in the presence of sodium propionate becomes an approximately four-fold increase when the concentration of monomer likely present is taken into consideration. Given the charge effects of Asp126 on the active site and activity discussed in the previous paragraph, restoration to full wild-type activity by complementation with sodium propionate was unlikely. Sodium propionate had only a minor (10%) effect on enzyme activity of wild-type *Ec*-MnSOD, as control. Therefore, the observation of significant increase in activity of the S126D mutant in the presence of sodium propionate enzyme suggests that propionate and Glu170 play a role in the uptake and delivery of protons in the enzymatic cycle of MnSOD.

At pH 6.0, on the other hand, the protein is substantially monomeric at *Ec*-MnSOD-S126D concentrations of assay, yet percent activity relative to wild type is about the same as at pH 7.8. Moreover, structures show that the Asp126 is only half protonated (see section 4.3 and Figure 4.5). So, there is less negative charge, and consequently less effect on activity of the dimer. The loss in activity here to 4.2% of wild-type at pH 6.0 is within a factor of about two corresponding to the fraction of dimer (3-11%) at assay concentrations.

The pH dependence of the thermodynamic stability of a protein changes due to differential electrostatic interactions between the two Asp126 from the two subunits at the dimer interface, which affects protein destabilisation differences (See Figure 4.5).

PISA calculations (Krissinel & Henrick, 2007) show that the solution-state stability of the dimer interface of wild-type *Ec*-MnSOD and its S126D mutant are very similar (~ −50 kJ mol^{-1}) (See Table 5.4). PISA does not account for differing states of protonation of Asp126 at different pH. This topic is discussed further in Chapter 5, when results for the *Ec*-MnSOD-S126W mutant are presented.

4.5 Thermal stability of *Ec*-MnSOD-S126D

The thermal stabilities of *Ec*-MnSOD-S126D and wild-type *Ec*-MnSOD as control at pH 7.8 were determined by differential scanning calorimetry (DSC). The disruption of the *Ec*-MnSOD dimer observed by analytical ultracentrifugation measurements causes not only a reduction in SOD

activity but also a decrease in stability of the folded *Ec*-MnSOD S126D relative to wild-type *Ec*-MnSOD.

After baseline subtraction, a single asymmetric endotherm is observed for both native *Ec*-MnSOD and the *Ec*-MnSOD-S126D mutant. The temperature of maximum heat capacity change, T_m, decreases, respectively, from 83° to 72 °C. These asymmetric endotherms are best fit by two partially overlapping Gaussian models (Figure 4.13), a larger broader one (labelled Y) and a smaller one (labelled Z). These two unfolding events occur at similar temperatures with only ~2 °C difference in temperature. The lower temperature transition, transition Y, has almost double the enthalpy change compared to that of the higher temperature transition, transition Z. Transition Y at 80-81 °C for wild-type *Ec*-MnSOD is attributed to the denaturation of the larger C-terminal domain, Gly87-Lys205, which involved the separation of N-terminal ligands to the manganese centre (His26 and His81) from the C-terminal ligands (Asp167 and His171), and spontaneous dissociation of the dimer. The second unfolding event (peak Z) is tentatively attributed to the N-terminal domain, which largely comprises a pair of helices.

The unfolding events of wild-type *Ec*-MnSOD give T_m ~81°C (labelled Y) and T_m ~83 °C (labelled Z), respectively. The S126D mutant has less thermal stability than the wild-type enzyme. The T_m for peaks Y and Z for S126D are decreased 10 °C relative to wild-type *Ec*-MnSOD (Figure 4.13). The magnitude of their endotherms for *Ec*-MnSOD-S126D are substantially smaller than those for wild-type enzyme. The T_m, enthalpy and A_w parameters for these species are summarised in Table 4.6.

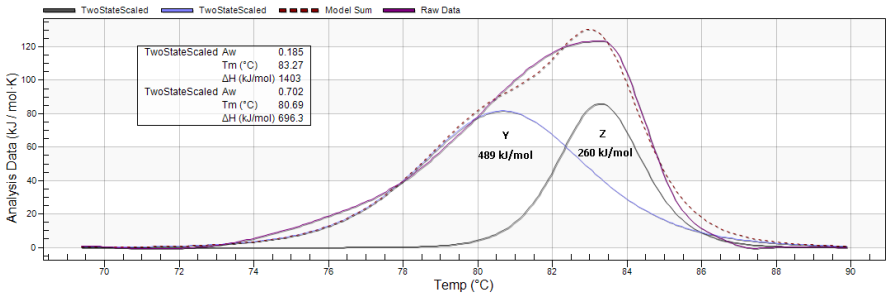

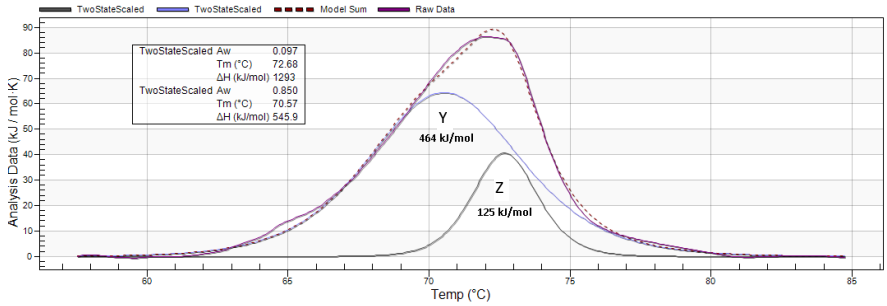

Figure 4.13. Differential scanning calorimetry (DSC) of *Ec*-MnSOD (upper) and *Ec*-MnSOD-S126D (lower) at pH 7.8.

The fits to a two-Gaussian model are shown. (A) A single scan of *Ec*-MnSOD at a concentration of 0.2 mg/mL produced an apparent single unfolding event with T_m = 83 °C. A two-Gaussian fit gives T_m ~81°C (Y) and ~83 °C (Z), respectively. (B) A single scan of *Ec*-MnSOD-S126D at a concentration of 0.125 mg/mL produced an apparent single unfolding event with T_m = 72 °C. A two-Gaussian fit gives T_m ~71°C (Y) and ~73 °C (Z), respectively.

Table 4.6. Single-scan DSC parameters for wild-type *Ec*-MnSOD and its S126D mutant.

	T_m(/°C)	A_w	$\Delta H_{van't\ Hoff}$ (/kJ mol^{-1})	ΔH_{cal} (/kJ mol^{-1})
Wild-type *Ec*-MnSOD	80.7	0.702	696	489
	83.3	0.185	1403	260
Ec-MnSOD-S126D	70.6	0.850	546	464
	72.7	0.097	1293	125

More information on the thermal stability of MnSOD S126D mutant can be obtained by monitoring the circular dichroism (CD) spectra in the far-UV and near-UV regions of the electromagnetic spectrum as a function of temperature. The far-uv region gives information on secondary structure; the near-uv region on tertiary structure. Circular CD spectroscopy was also used to confirm that the *Ec*-MnSOD mutants retained the same secondary and tertiary structure as the wild-type enzyme. The far-uv and near-uv CD spectra of wild-type *Ec*-MnSOD and its S126D and S126W mutants – the lattermost mutant is the focus of Chapter 5 -- are shown in Figure 4.14. At ambient temperature, the spectra of the S126D mutant are very similar to those of wild-type enzyme, establishing that this mutant does not have significantly perturbed secondary or tertiary structure.

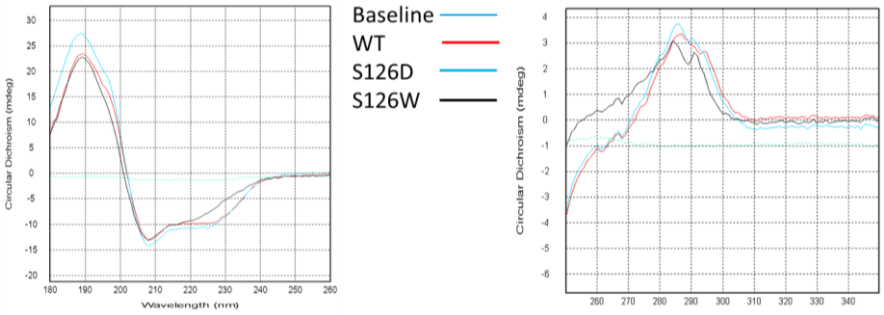

Figure 4.14. Circular dichroism spectra of wild-type *Ec*-MnSOD, *Ec*-MnSOD-S126D and *Ec*-MnSOD-S126W at 20 ºC and pH 7.8.

Left frame: far-UV spectra, 180-230 nm 2 mg/mL in 0.1 mm path-length cuvette. Right frame: near UV spectra, 250-360 nm, 2 mg/mL in 10 mm cuvette.

The CD spectra of *Ec*-MnSOD-S126D as a function of temperature are shown in Figure 4.15.

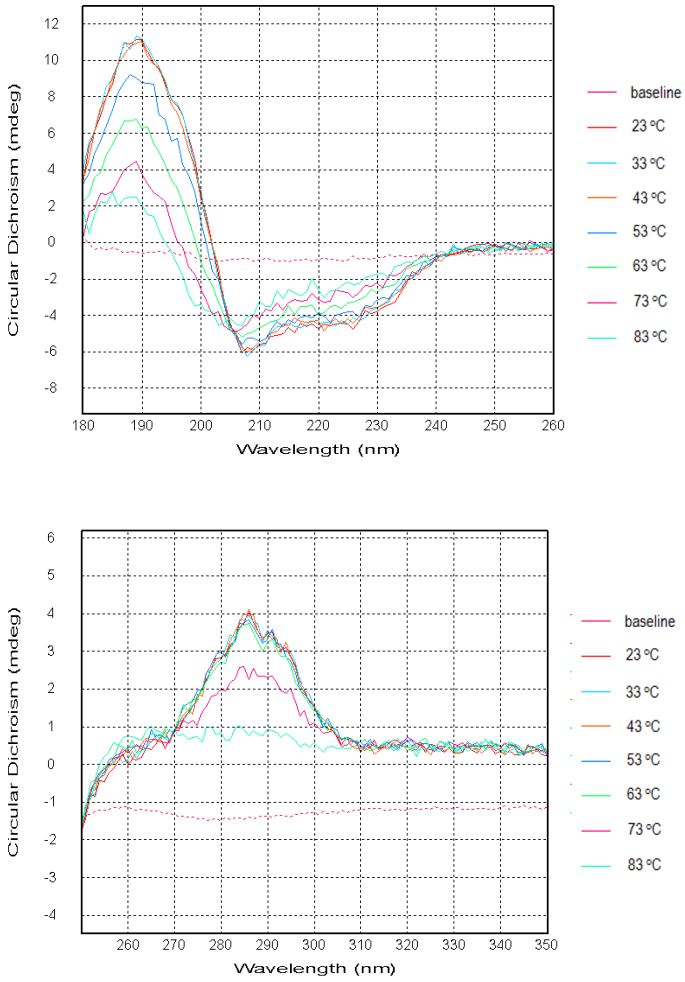

Figure 4.15. Circular dichroism spectra of *Ec*-MnSOD-S126D as a function of temperature.

Top: Far-UV CD spectra of *Ec*-MnSOD-S126D (180-260 nm) from 20 to 83 °C and 50 mM phosphate buffer at pH 7.8. Bottom: Near-UV CD spectra of *Ec*-MnSOD-S126D mutant (250-350 nm) from 23 to 83 °C and 50 mM phosphate buffer at pH 7.8.

MnSOD has an unusually large number of tryptophans in its sequence (6 out of 205 residues, concentrated in the C-terminal domain). These tryptophans contribute to signals in the near-UV region at ~285-295 nm and are sensitive monitors of tertiary structure, responding to changes in their chiral environment. The far-UV CD spectra show loss of secondary structure becomes pronounced at temperatures greater than ~53 ^{o}C. At 83 ^{o}C signal due to β-sheet at 220-230 nm is lost, but some signal consistent with α-helical structure is maintained. This is discussed further in Chapter 5. On the other hand, in the near-UV region signals attributable to tryptophans are completely gone at 83 ^{o}C and substantial loss of signal occurs at temperatures greater than ~70 ^{o}C. These results are consistent with the DSC results, where the lower temperature endotherm is associated with separation of the dimer and concomitantly denaturation of the much larger C-terminal domain, which contains five of the six tryptophan residues and where the higher temperature endotherm is associated with denaturation of the N-terminal domain which largely comparises a pair of long helices – the sole tryptophan sits under the unstructured, but well-ordered N-terminal tail.

4.6 Electrostatic surface analysis to gain insight into superoxide dismutation mechanism

Due to the anionic nature of the substrate, the solvent-accessible surface area near the active site was hypothesised to be basic, that is positively charged at pH ~7. To study this, the pK_a values and the electrostatic surfaces of *Ec*-MnSOD-S126D dimer were calculated at pH 7.0 by, respectively, PDB2PQR (program PropKa) (Olsson et al., 2011) and APBS (Jurrus et al., 2018), implemented at the APBS home (server.poissonboltzmann.org). PropKa deals only with proteins and their ionisable side chains. Thus, the resultant pqr file containing hydrogen-atom coordinates, as well as coordinates of CHNS atoms and partial charges on all protein atoms, does not include the manganese ions and either the hydroxide or both hydroxide and azide ligands. The hydrogen-bonding scheme and geometry were not optimised, as this optimisation leads to rotation of His groups that coordinate to the manganese centre in some cases. The force field (AMBER) and options chosen are indicated in the header of the pqr file. When PDB2PQR places the proton of Glu170_OE2 so that the proton clashes with the proton on His171_ND1 or places the proton of Tyr34_OH so that it with a proton on Gln146, or places the proton of Tyr174_OH so that it clashes with a proton on His30 (across the dimer interface), adjustments were done using COOT to ensure sensible hydrogen bonding. These corrections

made no difference to the resultant electrostatic surfaces calculated by APBS from the pqr file produced by PDB2PQR. Notwithstanding these deficiencies, the resulting electrostatic surfaces revealed differentiation in the substrate-binding pocket, as described in the next paragraphs.

Of immediate significance, the pK_a of interface residue Glu170 is anomalously high, lying in the range 6.2 to 8.8. Other ionisable and potentially ionisable residues in the vicinity of the active site have pK_a's that are little perturbed from standard values expected for a solvent-exposed residue. Moreover, in general for each dimer of *Ec*-MnSOD, one subunit has Glu170 with pK_a > 7.2, whereas the other subunit has Glu170 with pK_a < 6.8. Ionisable residues with pK_a ~7 often function as a general acid-base in enzymatic mechanisms taking place at pH ~7, providing protons in one step and accepting protons in another step of the mechanism.

The figures of electrostatic surfaces of *Ec*-MnSOD-S126D all look into the cavity by which substrates access and products leave the active site, which is located in the middle and just right of the centre of the figure (see Figures 4.16-4.19) The colours on the surface of the protein model corresponds to the electrostatic surface potential at a particular point on the protein surface. The grey, blue, or red colour give the electrostatic potential of neutral, positive or negative on the surface of the protein, respectively. The greater the intensity of blue and red shading, the greater the magnitude of the electrostatic potential. Functionally, the anionic substrate-binding metalloprotein will most likely have a pocket of positive charge. The positive charges help the enzyme to guide the substrate into the metal centre at the active site through an electrostatic guidance. But note, the electrostatic surfaces here are calculated with $Mn^{2+/3+}$/OH^-/azide stripped out, as neither PDB2PQR nor ABPS can handle metal ions or non-protein ions.

In general, the base of the substrate-binding pockets in the dimeric structures are shaded grey-pale red in one subunit and shaded blue in the other subunit. The pK_a calculation and electrostatic surfaces reveal two different states in *the Ec*-MnSOD-S126D dimer structure. Of the three *Ec*-MnSOD-S126D dimer structures, the electrostatic surfaces near the active site are consistent with an ordered Mn^{III}/Mn^{II} species, that is Mn^{III} in one subunit and Mn^{II} in the other subunit. The signatures were indicated by two possible states: first, the positive electrostatic potential in the substrate-binding pocket is associated with Mn as Mn^{II}, where the Glu170 (that extends across the dimer interface from the other subunit) is calculated to

be protonated (equation 21). Second, the less positive electrostatic potential in the substrate-binding pocket is associated with Mn as Mn^{III}, where the Glu170 (from the other subunit) is calculated to be deprotonated (Equation 22). Both states then result in an overall net zero charge in the active site of protein, once the metal ion and hydroxide ligand are added, as is generally observed for metalloproteins in their resting state(s).

$$[Mn^{2+}/OH^{-}/\text{Asp167-}COO^{-}/\textit{Glu170-COOH}]^{0} \quad \ldots (31)$$

$$[\textit{Mn}^{3+}\textit{/OH}^{-}\textit{/Asp167-COO}^{-}/\text{Glu170-}COO^{-}]^{0} \quad \ldots (32)$$

(*Italics* and normal font are used to highlight the different subunits involved.)

The resulting electrostatic surfaces indicate how anionic superoxide diffusion to the active site could be enhanced. The differentiation of electrostatic surface potential of the substrate binding pocket of the two subunits appears to be most influenced by a negatively-charged Glu170. Gaps of pK_a values between the two Glu170 in a dimer at a pH in the range of pH 7$\pm$1 provides a carboxylate group in protonated (pK_a > 7) and deprotonated state (pK_a < 7) when the pKa's were calculated at pH 7. As the Glu170 is the only residue of the outer sphere to the Mn centre which has a notable gap in pK_a value compared to that of the other subunit of the dimer, it provides further evidence against proton transfer onto the coordinated hydroxo ligand. Thus, the proton accompanying reduction of the manganese centre is deposited on Glu170_OE2. From here, the proton is then delivered to the nascent peroxo by a Grotthuss proton-hopping mechanism through the chain of water molecules established between Glu170_OE2 and the bound superoxide (as evidenced in the structure 1ZLZ where azide coordinated to Mn^{III} is a proxy for superoxide coordinated to an Mn^{III} site, Figure 2.16). This will be described more in section 4.7.

Interestingly, the distances of the coordinated hydroxide to Trp169 also differ depending on the oxidation/reduction state inferred for the two chains in a dimer (consistent with the 0.9 Å structures of *Ec*-MnSOD-Y174F) (See Table 4.7).

The negatively-charged Glu170 near the gate of the substrate-access funnel is partially neutralised by the nearby Mn^{III} and positively charged Arg181. Both Arg181 and Glu170, as well as Arg180, which guards entrance to the substrate-access funnel, come from the other subunit. In addition, Lys29 guards the substrate-access funnel. The anionic substrate is

attracted into the positively charged active-site pit through electrostatic guidance of this cluster of positively-charged residues.

4.6.1 Electrostatic surfaces of *Ec*-MnSOD-S126D at pH 8.7 and pH 6.8

For the *Ec*-MnSOD-S126D structure at pH 8.7 (synchrotron data), for chains A and C, the base of the substrate-access funnel is shaded grey, whereas for chains B and F it is shaded deep blue (Figure 4.16). For chain B and F, for calculations done at pH 7.0, Glu170 (from other subunit, or chain A/C) is calculated to be protonated (indicated by PropKa values, see Table 4.7). The positive electrostatic potential in the substrate-binding pocket is associated with Mn as Mn^{II}. Interestingly, consistent with the 0.9 Å *Ec*-MnSOD-Y174F structures, the distance of OH (coordinated to the Mn^{II}) to Trp169 for chain B and F is generally shorter than for chains A and C. A similar pattern of electrostatic potential is observed for the structure of *Ec*-MnSOD-S126D at pH 6.8 (Figure 4.16 and Table 4.7).

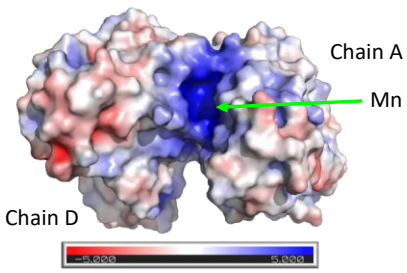

MnSOD-S126D at pH 6.8 chain A; pK_a = 8.81

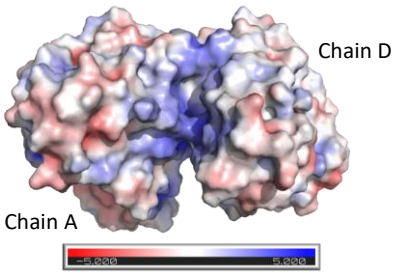

MnSOD-S126D at pH 6.8 chain D; pK_a = 6.63

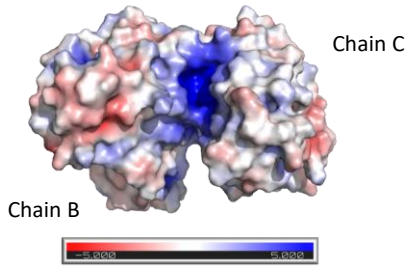

MnSOD-S126D at pH 6.8 chain C; pK_a = 8.78

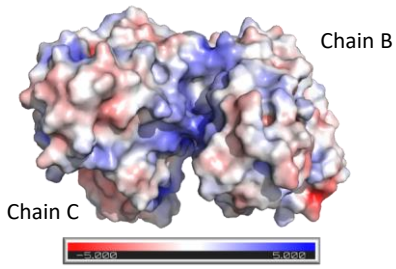

MnSOD-S126D at pH 6.8 chain B; pK_a = 6.57

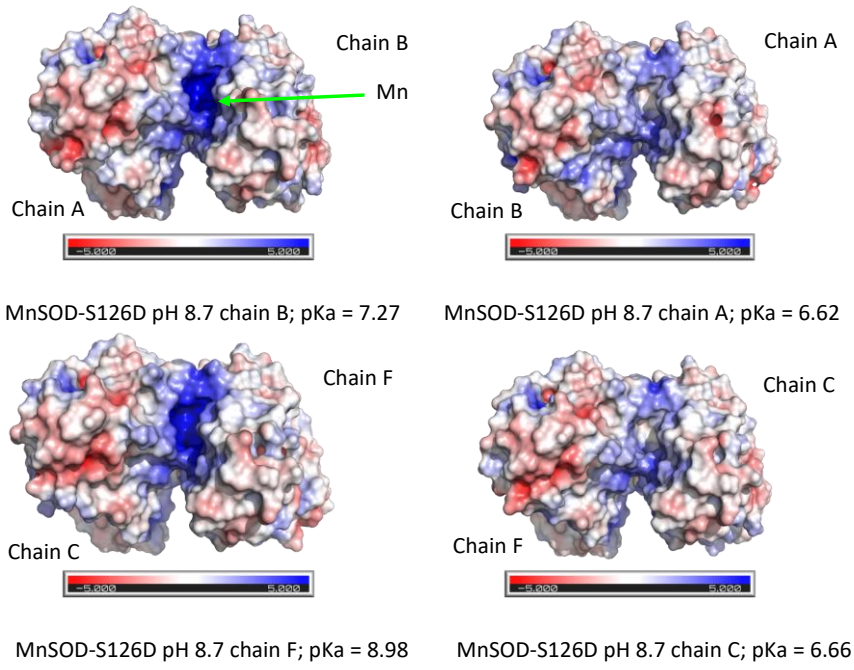

Figure 4.16. Electrostatic potential surfaces for *Ec*-MnSOD-S126D dimers.

Surfaces are calculated at pH = 7. The view labelled, for example, chain A is into the substrate access funnel and the active site formed from His26, His81, His171 and Asp167, all from chain A. The pK_a is for the Glu170 from the other subunit of the dimer.

4.6.2 Electrostatic surfaces for *Ec*-azido-MnSOD-S126D and *Ec*-azido-MnSOD-Y174F structures

For *Ec*-azido-MnSOD-S126D, the differentiation in pK_a for Glu170 is not so marked and this is attributed to the partial occupancy of the azido ligand in both subunits of the dimer (Figure 4.17). On the other hand, for the azido complex of *Ec*-MnSOD-Y174F (PDB: 1ZLZ), the azido ligand is found exclusively in full occupancy in only one subunit, while the other subunit (A) is azide-free and the Glu170 from the other subunit (B) is calculated to be protonated. Subunit A of *Ec*-azido-MnSOD-Y174F is clearly Mn(II) – it has a substantially elongated Mn-OH bond, similar in length to that observed in the 0.9-Å resolution structure of *Ec*-Mn(II)SOD-Y174F (PDB ID: 1ixb). As a consequence of the sixth ligand, azide, the Mn-OH bond length in subunit B is

slightly longer than that for the five-coordinate 0.9-Å resolution structure of *Ec*-Mn(III)MnSOD-Y174F (PDB ID: 1IX9), but still substantially shorter than that observed in chain A. Curiously, the electrostatic potential for both subunits is strongly positive near the active site, although at pH 7, Glu170 from subunit B projected into subunit A (the Mn(II) site) is mostly protonated and Glu170 from subunit B projected in subunit A (the Mn(III)-azido site) is partly deprotonated. However, the difference in pK_a is small and it appears that the negatively charged azido ligand has left a trace in subtle structural differences that have enhanced the positive electrostatic potential.

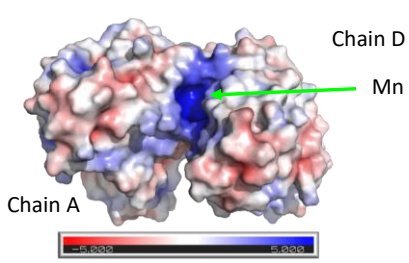

Ec-azido-MnSOD-S126D chain D; pK_a = 8.16

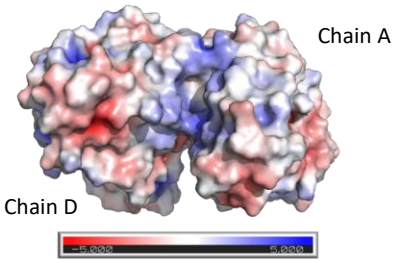

Ec-azido-MnSOD-S126D chain A; pK_a = 7.21

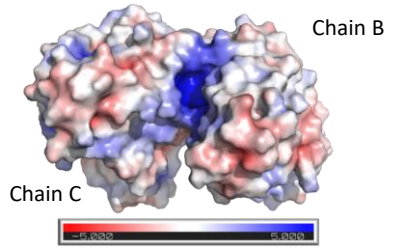

Ec-azido-MnSOD-S126D chain B; pK_a = 7.66

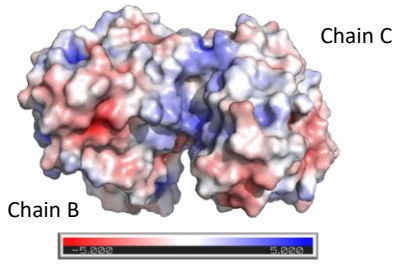

Ec-azido-MnSOD-S126D chain C; pK_a = 6.86

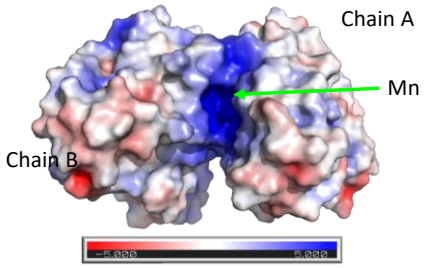

Ec-azido-MnSOD-Y174F chain A; pK_a = 8.12
(No azide present)

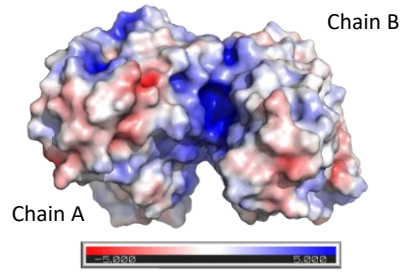

Ec-azido-MnSOD-Y174F chain B; pK_a = 6.27
(azide bound)

Figure 4.17. Electrostatic surfaces for *Ec*-azido-MnSOD-S126D and *Ec*-azido-MnSOD-Y174F structures.

Note: The electrostatic potentials for *Ec*-azido-MnSOD-S126D are compromised by partial occupancy of the azido ligand at the Mn centre. For the *Ec*-azido-MnSOD-Y174F structure one subunit has an azido ligand in full occupancy (and is unequivocally Mn^{III}), while the other subunit has an elongated Mn-OH bond, as expected for Mn^{II}.

4.6.3 Electrostatic surfaces of the 0.90-Å resolution structures of *Ec*-MnSOD-Y174F in its oxidised Mn(III) and reduced Mn(II) forms

Ec-MnSOD-Y174F is an active mutant that retains about half the activity of wild-type *Ec*-MnSOD. As such it is still turning over superoxide very quickly. The structure of this mutant in its reduced Mn(II) form has been determined to 0.90-Å resolution, giving unprecedented precision, and likely accuracy, to metal-ligand stereochemistry, including observation of the hydroxyl hydrogen positioned to hydrogen bond to the non-coordinated casrboxylate oxygen atom of Asp167. The structure of the mostly oxidised Mn(III) form has also been determined to 0.90-Å resolution. Some reduction of the Mn(III) centre is to be expected under X-rays, even from a second-generation synchrotron. The alternating pattern of electrostatic potential surfaces calculated for *Ec*-MnSOD-S126D and *Ec*-azido-MnSOD-Y174F is not observed here. The Mn(II) species shows a substantially more positive environment around the active site for both subunits compared to the Mn(III) species (Figure 4.18). For the oxidised Mn(III) species, at pH 7 the Glu170 projected into subunit A is partially deprotonated, whereas that projected into subunit B is partially protonated. However, the difference is small. A rather greater difference in pK_a for the the two Glu170 of the reduced Mn(II) species is calculated (Table 4.7). The intrinsic, although subtle, asymmetry in the hydrogen bonding Ser126_OG-H...*OG-Ser126* at the dimer interface, discussed earlier, possibly amplified by different crystal-packing effects on the subunits of the dimer, is tentatively advanced as the cause of the different calculated pK_a. This asymmetry may also be responsible for the fully ordered *Ec*-azido-MnSOD-Y174F structure, whereas all other Mn- and FeSOD azido structures feature 50-50 disorder of the azido in the subunits of the dimer.

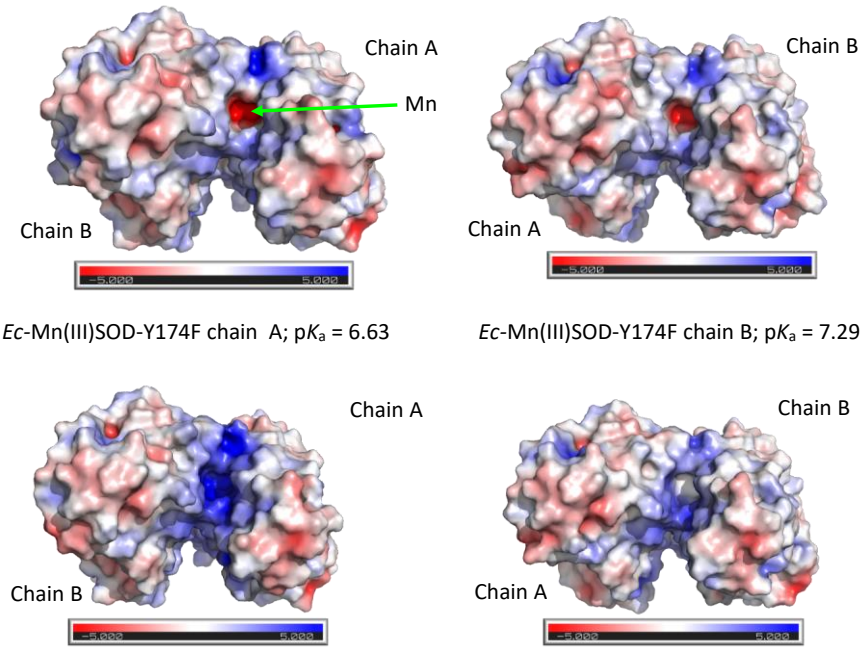

Ec-Mn(III)SOD-Y174F chain A; pK_a = 6.63

Ec-Mn(III)SOD-Y174F chain B; pK_a = 7.29

Ec-Mn(II)SOD-Y174F chain A; pK_a = 8.13

Ec-Mn(II)SOD-Y174F chain B; pK_a = 6.31

Figure 4.18. Electrostatic surfaces of the 0.90-Å resolution structures of *Ec*-MnSOD-Y174F in its oxidised Mn(III) and reduced Mn(II) forms.

4.6.4 Electrostatic surfaces of *Ec*-FeSOD and cambialistic *Propionibacterium shermanii* FeSOD

Does the pattern of one subunit of the canonical dimer having the metal ion in its oxidised state and the other subunit having it in its reduced state also occur for the closely isostructural FeSOD? The FeSOD from *E. coli* is as specific for iron as the *Ec*-MnSOD is for Mn. On the other hand, the FeSOD from *P. shermanii, Psh*-FeSOD, is a cambialistic SOD being active with either metal, but much less so than the metal-specific Mn- and FeSOD from *E. coli*. The PropKa-calculated pK_a values for the Glu170-equivalent residues are entered in Table 4.7. Of note is that the p*I* calculated for these two FeSODs (4.88 for *Ec*-FeSOD and 4.79 for *Psh*-FeSOD) are two log-units less than that calculated for *Ec*-MnSOD of 6.80 (varies slightly from wild-type to one or other mutant). The calculated pK_a of the *Ec*-MnSOD Glu170-equivalent residues are

noticeably reduced compared to the *Ec*-MnSOD values (Table 4.7). The electrostatic potentials calculated at pH 7 show a strongly negative potential near the active site of *Psh*-FeSOD (Figure 4.19). However, this charge may be neutralised when the enzyme is working in its preferred acidic environment. The calculated pK_a and derived electrostatic potentials for these two FeSOD are suggestive of a role for Glu170 in shuttling a proton onto the nascent peroxo moiety, but they are not as persuasive as the results of these calculations for *Ec*-MnSOD.

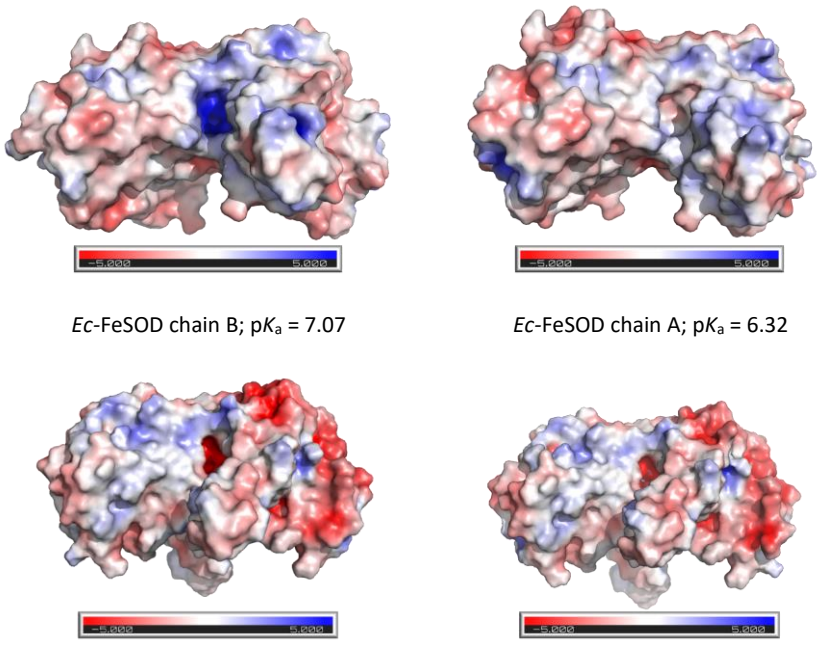

Ec-FeSOD chain B; pK_a = 7.07

Ec-FeSOD chain A; pK_a = 6.32

Psh-FeSOD chain A; pK_a = 6.61

Psh-FeSOD chain B; pK_a = 5.79

Figure 4.19. Electrostatic surfaces of the iron specific FeSOD from *E. coli* and the cambialistic FeSOD from *P. shermanii*.

Table 4.7. Calculated pK_a values for Glu170 (and its equivalents) and M-OH distances and hydroxide distances to the absolutely conserved Trp169 (and its equivalents) for MSOD structures (M = Fe, Mn) with resolution better than 1.8 Å.

	pK_a Glu170 (other subunit) [*d*(M-OH), *d*(Mn-OH…Trp169) /Å][a]			
Molecule \ Chain	**A [B]**	**B [A]**	**C [D(F)]**	**D(F) [C]**
S126D pH 8.7 (1.8 Å resoln, $P2_1$)	7.27 [2.38, 3.02]	6.62 [2.16, 3.21]	8.98 [2.23, 3.07]	6.66 [2.10, 3.16]
S126D pH 6.8 (1.56 Å resoln, *P*1)	6.63 [2.19, 3.14]	8.78 [2.22, 3.09]	6.57 [2.21, 3.14]	8.81 [2.26, 3.07]
Azide-S126D pH 9.1 (1.50 Å resoln, $C222_1$, 1ZLZ)[b]	2.56 [2.22, 3.11]	6.88 [2.21, 3.08]	7.66 [2.15, 3.07]	1.96 [2.18, 3.10]
Y174F pH 8.5 (Mn^{III}, 0.90 Å resoln, $P2_1$, 1IX9)[d]	7.29 [2.16, 3.16]	6.63[c] [2.12, 3.20]		
Y174F pH 8.5 (Mn^{II}, 0.90 Å resoln, $P2_1$, 1IXB)	6.31 [2.26, 3.09]	8.13 [2.27, 3.09]		
Azide-Y174F pH 8.5 (azide bound to chain B, 1.55 Å resoln, $P2_1$, 1ZLZ)[e]	8.12 [2.14, 3.11]	6.27 [2.27, 3.14]		
Ec-FeSOD (1.80 Å resoln, $P2_12_12_1$, 1ISA)[f]	7.07 [2.06, 3.21]	6.32 [2.03, 3.32]		
Psh-FeSOD (1.60 Å resoln, $C222_1$, 1AR5)[g]	5.79 [2.14, 3.18]	6.61 [2.10, 3.20]		

[a] Glu170(A) is associated with subunit B; Glu170(C) is associated with subunit D (or F).

[b] Note: the azide is disordered over the four subunits in ~25% occupancy in each.

[c] PDB2PQR has assigned a proton to His30.

[d] Some evidence of partial reduction of Mn in subunit B.

[e] The azide, uniquely in Fe/MnSOD structures, is present in only 1 site in full occupancy. This structure represents a transition state species, where the Glu170 on subunit A is protonated and poised to deliver a proton to the nascent peroxo (azido-proxy) species in subunit B.

[f] *Ec*-MnSOD-Glu170 = *Ec*-FeSOD-Glu159; *Ec*-MnSOD-Trp169 = *Ec*-FeSOD-Trp158

[g] *Ec*-MnSOD-Glu170 = *Psh*-FeSOD-Glu164; *Ec*-MnSOD-Trp169 = *Psh*-FeSOD-Trp163

4.7 Proposed mechanism for superoxide dismutation

In the following mechanism, two key solvent molecules are shown as they are found in the structure of *Ec*-MnSOD-S126D. Here, the role that the Grotthuss proton-hopping mechanism may play in the proton-coupled electron-transfer of the MnSOD is discussed. We have chosen arbitrarily to have superoxide approach the Mn centre in its oxidised Mn(III) state.

4.7.1 First catalysis step of the superoxide dismutase: $O_2^{-\bullet} + H^+ + Mn^{3+} \rightarrow O_2 + Mn^{2+}\ldots H^+$

In the initial step, there is a net +1 charge at the manganese centre, consisting of $[Mn^{3+}/OH^-/Asp167\text{-}COO^-]^{+1}$, and the Glu170 from the other subunit has a −1 charge as it is unprotonated and is hydrogen bonded to protein ligand His171. So, overall, the entire active site is neutral. This actual MnSOD active site with a positive charge is attractive for the anionic substrate superoxide. Subsequently, the superoxide comes in to the active site to give six coordination with the manganese metal ion (Figure 4.20) .

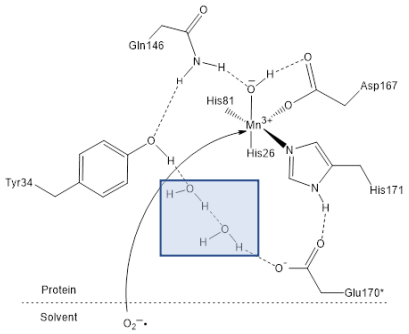

Figure 4.20. The first step of catalysis of superoxide dismutation: approach of superoxide to the Mn(III) centre.

Note that Glu170 from the other subunit of the dimer is deprotonated and a pair of water molecules bridge between Tyr34 and Glu170.

On coordination to the Mn(III) centre, the superoxide transfers one electron to the Mn^{3+} to form Mn^{2+}. There is now a net zero charge at the manganese centre of $[Mn^{2+}/OH^-/Asp167\text{-}COO^-]^0$, while including the deprotonated Glu170 gives the entire active site a decrease in charge from zero to −1. To maintain an overall net neutral charge, a proton is transferred onto the Glu170-OE2, which has been made more basic due to the electron transferred from the

superoxide onto the Mn^{3+}. The electron-rich Mn^{2+} communicates to Glu170-OE1 through hydrogen bonding to metal-ligand His171 (Figure 4.21).

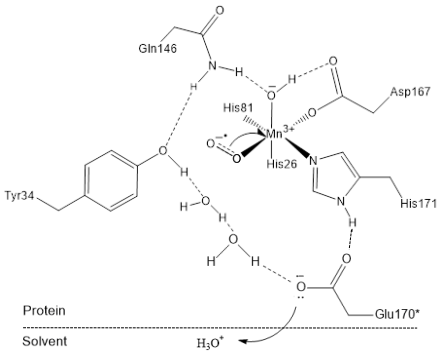

Figure 4.21. Transfer of proton from solvent to Glu170-OE1.

Note: At pH of maximum activity, the superoxide ion is partially protonated, and this proton may be transferred onto Glu170-OE1 as superoxide approaches the metal centre.

Electron transfer from coordinated superoxo species to Mn^{3+} ion produces an oxygen molecule, which then diffuses from the active site. The overall entire net charge remains neutral, and a vacant site is left for another superoxide to approach. The rearranged hydrogen bonding network and departure of molecular oxygen are illustrated in Figure 4.22.

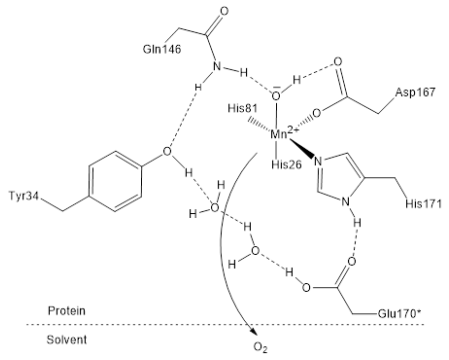

Figure 4.22. Departure of molecular oxygen from the active site and the rearranged hydrogen-bonding network between Glu170 and Tyr34.

4.7.2 Second half-reaction: $O_2^{-\bullet} + H^+ + Mn^{2+}...H^+ \rightarrow H_2O_2 + Mn^{3+}$

In the next step, the active site is neutral as $[Mn^{2+}/OH^-/Asp167\text{-}COO^-]^0$. Moreover, the carboxylate side chain of Glu170 is protonated, so that overall the active site remains neutral. However, the active site with Mn^{2+} is now less positive than with Mn^{3+}.

The studies of electrostatic potential surfaces of *Ec*-MnSOD-S126D at pH 6.8 and 8.7, described in the previous section 4.6, reveal that protonation of Glu170 from the other subunit leads to the positive electrostatic potential in the accessible surface area near the active site. Thus, the active site is still attractive for and leads the superoxide to enter.

Comparing two states of Mn^{2+} and Mn^{3+}, overall, the active site never becomes repulsive with a negatively charged region for receiving a negatively charged superoxide ion. Figure 4.23 shows superoxide entering and approaching the Mn^{2+} site.

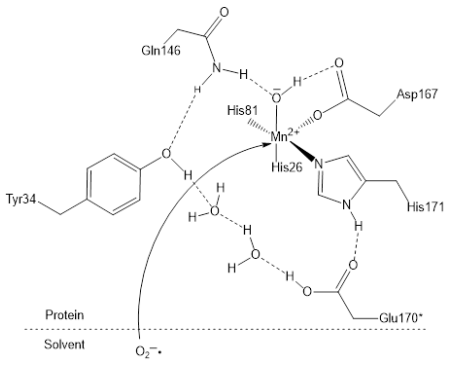

Figure 4.23. Superoxide approaches the vacant site at the Mn^{2+} centre.

After entry of the superoxide ion, there is now a net −1 charge at the manganese centre. This state is very unstable, and an electron is transferred from Mn^{2+} to the superoxide, potentially as an outer-sphere transfer, and concomitantly a proton is transferred (Figure 4.24). The nascent peroxo species is hydrogen bonded to a water molecule that is connected via other water molecules to the protonated Glu170 from the other subunit.

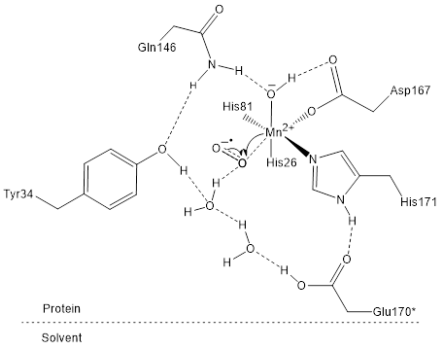

Figure 4.24. Electron transfer from Mn^{2+} onto superoxide, forming a peroxo species.

Concomitantly, a proton is transferred by a Grotthuss proton-hopping mechanism from Glu170-OE1 onto the nascent peroxo species (Figure 4.25). This is the state modelled by the Mn(III)-azido species.

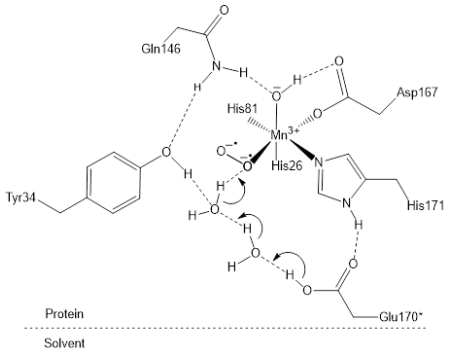

Figure 4.25. Proton transfer onto nascent peroxo species by Grotthuss proton hopping.

The catalytic cycle is now almost complete. Once protonated, the hydroperoxo species is a poor ligand to the Mn^{3+} centre and it leaves the active site picking up another proton from solvent to form the other product hydrogen peroxide, H_2O_2 (Figure 4.26).

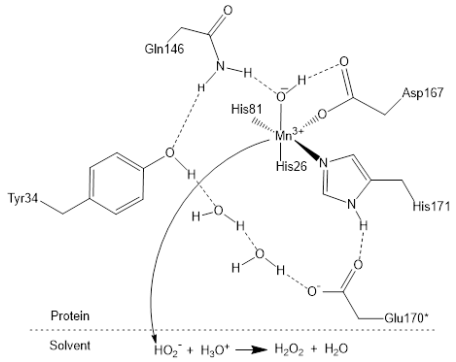

Figure 4.26. Departure of the hydroperoxo species and acquisition of a proton from solvent to form hydrogen peroxide. The active site is ready to accept and oxidise another superoxide anion-radical.

4.8 The substrate-inhibited species

The hypothesis that Glu170 is the site of protonation, and not the coordinated hydroxide ion, for *Ec*-MnSOD appears confounded by the results of the E162A mutant of human MnSOD, which retains about 25% of the activity of wild-type enzyme (Quint et al., 2008) whereas the

equivalent E170A mutation for *Ec*-MnSOD abolishes activity (Whittaker & Whittaker, 1998). For the E162A mutant of human MnSOD, there is a mostly buried ion assigned by Quint, Domsic, Cabelli, McKenna, and Silverman (2008) as a sulfate but more likely is a phosphate ion that is located at the site of the Glu162 carboxylate group and hydrogen bonding in a manner very similar to that of Glu162. Given substantial burial, this group is likely a phosphate ion that is bound during protein expression and is carried through protein purification. Thus, this ion is performing the role of Glu162; that it is complementing the missing carboxylate group as the general acid/base.

In the Introduction reactions 13 and 14 described the appearance and disappearance of a substrate-inhibited species, where the peroxo anion remains trapped and bound to the Mn^{3+} site. Whereas the formation of this species is a major side reaction for human MnSOD, it is a minor side reaction for *Ec*-MnSOD and is almost negligible for the MnSOD from *Deinococcus radiodurans* (Table 2. 4). The assumption made by these and other authors (Abreu et al., 2008) is that the hydroxide ion becomes protonated on reduction of the Mn centre in normal turnover. The formation of the substrate-inhibited species (reaction 13) is then due to slow delivery of protons from the coordinated water and solvent to what is assumed to be an outer-sphere reaction of Mn^{2+}-OH_2 with superoxide. The key hypothesis of this thesis is that in normal turnover Glu170 (and its equivalent Glu162 in human MnSOD) is the location of the proton bound in the Mn reduction step, and the water-derived species coordinated to the Mn remains as hydroxide. Therefore, the substrate-inhibited species forms when a proton is transferred onto the coordinated hydroxide; the decreased negative charge promotes binding of the nascent peroxo species as peroxide.

Reactions 11-14 now become:

$Mn^{3+}SOD(OH^-)..Glu\text{-}COO^- + O_2^{\bullet-} (+H^+) \rightarrow Mn^{2+}SOD(HO^-)\ldots Glu\text{-}COOH + O_2$ (k_1) (11')

$Mn^{2+}SOD(HO^-)\ldots Glu\text{-}COOH + O_2^{\bullet-} (+H^+) \rightarrow Mn^{3+}SOD(OH^-)\ldots Glu\text{-}COO^- + H_2O_2$ (k_2) (12')

$Mn^{2+}SOD(HO^-)\ldots Glu\text{-}COOH + O_2^{\bullet-} (+H^+) \rightarrow O_2^{2-}\text{–}Mn^{3+}SOD(H_2O)\ldots Glu\text{-}COOH$ (k_3) (13')

$O_2^{2-}\text{–}Mn^{3+}SOD(H_2O)\ldots Glu\text{-}COOH \rightarrow Mn^{3+}SOD(OH^-)\ldots Glu\text{-}COO^- + H_2O_2$ (k_4) (14')

4.9 Conclusions

1. Except at the position of mutation, *Ec*-MnSOD-S126D dimer shows very little difference to the wild-type dimer, yet enzymatic activity is greatly reduced.

2. Analytical ultracentrifugation (AUC) measurements giving K_D indicate that at pH 7.8 *Ec*-MnSOD-S126D is substantially dimeric at assay concentrations of enzyme, indicating that the reduced enzyme activity is correlated with negatively charged Asp126 perturbing electrostatics, but not structure, at the Mn site.

3. Analytical ultracentrifugation (AUC) measurements giving K_D indicate, on the other hand, that at pH 6.0 the protein is substantially monomeric at assay concentrations of enzyme, and activity is proportionately reduced from that observed for wild-type enzyme, indicating that less negatively charged half-protonated Asp126 perturbs the active site less than fully deprotonated Asp126 at pH 7.8.

4. Coupled with the analysis in Chapter 2 that the coordinated hydroxide is an an environment that is unfavourable sterically and electrostatically for protonation of that hydroxide when Mn is in the +2 oxidation state. Complementation experiments where the propionate anion that replaces the Glu170 in monomeric *Ec*-MnSOD-S126D increased activity by at least a factor of two, coupled with structural, thermodynamic and activity data suggest that Glu170 is the site of proton uptake and delivery in the MnSOD enzymatic cycle.

5. Tentatively I suggest that subtle structural differences in subunits of the intrinsically asymmetric canonical dimer collectively manifest themselves in differences in the pK_a of Glu170, such that at pH ~7.0 one subunit (say A) has a negatively charged Glu170 from the other subunit (B) projected into it and the other subunit (B) has a protonated Glu from the one subunit (A) projected into it. The former situation is proposed to correspond to Mn(III) and the latter to Mn(II), as this maintains charge neutrality in the active site.

Chapter 5 Characterisation of *Ec*-MnSOD-S126W

In Chapter 4, the strongly conserved serine 126, which hydrogen bonds to serine 126 from the adjacent subunit across the dimer interface, was mutated to aspartic acid in an attempt to transform the dimeric protein into monomeric subunits by charge repulsion of the negative charge of two carboxylate side chains. The expected monomeric species produced by these mutation would mean the absence of the Glu170 side chain in the adjacent subunit. However, structural and AUC results show that the strategy of charge repulsion produced partial monomer with predominantly dimer species, where the carboxylate side chain of Asp126 hydrogen bonds across the dimer interface to the peptide NH of Asp126 and at pH 6.8 to itself via a shared proton. Nonetheless, the S126D mutation led to significantly reduced superoxide dismutase activity.

Here, in Chapter 5, an alternative strategy is reported to generate a monomeric species from a tight homodimer interface. Serine 126 was mutated to tryptophan. The mutation of serine 126 to tryptophan was intended to enforce monomeric MnSOD by steric bulk impediment by the bulky non-polar indole side chain. The experimental results of the *Ec*-MnSOD-S126W will be presented including characterisation of its quaternary state. These structure-based mutational analyses are intended to gain insight into the mechanism of the proton-coupled electron transfer reaction in manganese superoxide dismutase which was discussed in part in Chapters 2 and 4 and will be further discussed in the next chapter.

5.1 Expression and purification of *Ec*-MnSOD-S126W

The plasmid pDT1-5, which contains an ampicillin antibiotic resistance plasmid and carries the *sodA* gene that codes for *Ec*-MnSOD. was successfully modified using site-directed mutagenesis to encode expression of *Ec*-MnSOD-S126W, following the method described in the previous chapter. *Sod A- E. coli* QC781, which does not carry *E. coli* MnSOD gene, was transformed by the plasmid. The expression of *Ec*-MnSOD-S126W in *SodA- E. coli* QC781 cells resulted in a good level of expression of the protein in the soluble fraction. The soluble *Ec*-MnSOD-wild-type protein was produced in *E. coli* strain AB2463 to be used as a control in assays.

In a small-scale protein expression of *Ec*-MnSOD-S126W, the 23-kDa protein of *Ec*-MnSOD-S126W was expressed in high yield in the soluble fraction (Fig. 5.1).

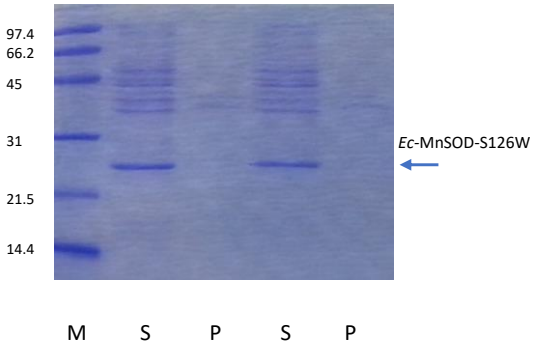

Figure 5.1. Coomassie-stained SDS-PAGE of *Ec*-MnSOD-S126W purification.

From left to right: Molecular weight markers (in kDa axis), supernatant (S) and pellet (P) in a 5 mL media with 25 mL tube, and supernatant (S) and pellet (P) in a 50 mL media with 250 mL flask (see Chapter 3 for details of method).

Optimisation of the purification of the scaled-up protein expression involved several steps that are slightly different to *Ec*-MnSOD wild type and its S126D mutant (see Table 5.1). In the initial step, post-lysis centrifugation similarly separated soluble protein and non-protein parts of the cell lysate to produce a crude extract in supernatant. Ammonium sulfate precipitation at 60% of saturation gave purer *Ec*-MnSOD-S126W protein in the supernatant. This was followed by 95% of saturation, which precipitated *Ec*-MnSOPD-S126W into pellet. This saturation was 5% higher than that used for wild-type *Ec*-MnSOD. The stability of *Ec*-MnSOD-S126W at pH 7.8 provided an effective salt precipitation where many of the contaminating proteins were separated from the target protein.

Purification continued with cation exchange chromatography. Here, potassium acetate pH 5.5 was used in cation exchange chromatography (J. W. Whittaker & Whittaker, 1991). The pI value of *Ec*-MnSOD-S126W was estimated using SEDNTERP (Laue, 1992; Lebowitz et al., 2002), which gave pI = 6.68. The *Ec*-MnSOD-S126W protein has net positive surface charge below this pI value. Therefore, to separate *Ec*-MnSOD-S126W from impurities a negatively charged Sephadex CM-50 ion exchange resin was used.

To prepare the protein sample for cation exchange, the protein pellet obtained from ammonium sulfate fractionation was resuspended and dialysed against 100x volumes of 10

mM potassium acetate pH 5.5. At the end of the dialysis, centrifugation at 17,000 xg was carried out to separate insoluble material.

In cation exchange, the pH 5.5 potassium acetate buffer, which was used as the eluent, is almost 1.2 magnitude below the pI (6.68). In low pH (pH lower than the pI), side chains of carboxylate amino acids, Asp and Glu, draw protons from water, and thus the total net charge of protein becomes more positive. The negatively charged resin attracts MnSOD to the resin more than the impurities. By changing the electrolyte charge of the buffer and increasing the salt concentration, the positively charged Na^+ ion will displace the protein from the resin matrix. Overall, cation exchange effectively separated the impurities which lack interaction with the Sephadex resin in the column.

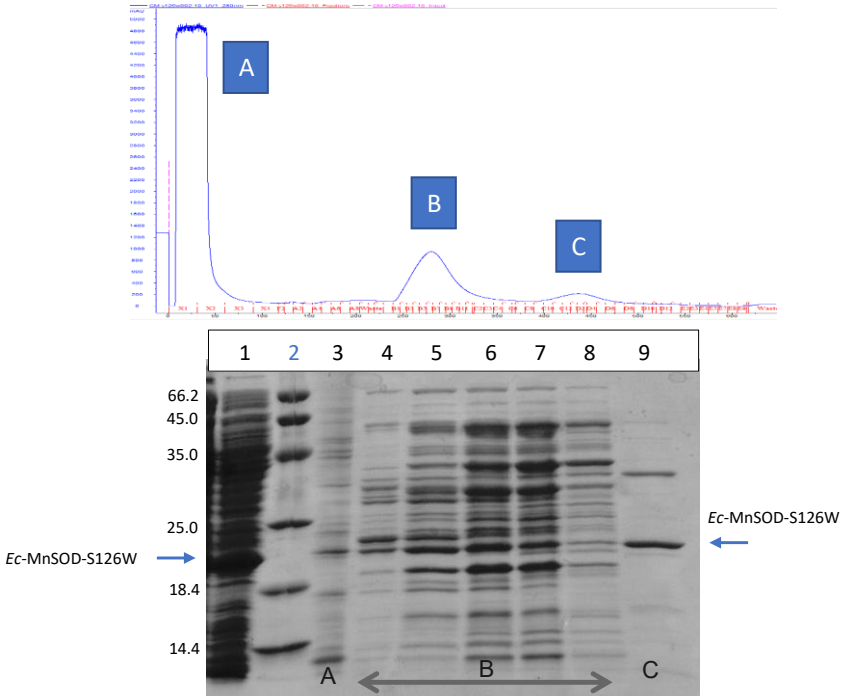

Figure 5.2. Purification of *Ec*-MnSOD-S126W by cation exchange chromatography.

(Top) Cation exchange chromatogram (Sephadex-CM50) to purify *Ec*-MnSOD-S126W. (Bottom) Coomassie-stained SDS-PAGE of *Ec*-MnSOD-S126W of pre-chromatography solution and eluate fractions from cation exchange chromatography. Lane 1: The pellet produced on precipitation with

95% ammonium sulfate of the solution retained after precipitation with 60% ammonium sulfate (overloaded). Lane 2: Molecular weight ladder (blue). Lane 3: Flow-through of weakly adsorbed species. Lanes 4-8: Peak B of cation-exchange chromatogram (top). *Ec*-MnSOD-S126W adsorbs to the matrix (B and C) while other proteins pass through the column (A). Elution with a NaCl salt gradient (see Chapter 4) leads the enzyme eluted quite early in fraction B, but still impure. Lane 9: A purer *Ec*-MnSOD- S126W partition with low molecular impurities eluted later which was distributed in fractions C (top) in small amount.

Table 5.1. Procedure used for purification of *Ec*-MnSOD and its mutants.

Steps	**Wt *Ec*-MnSOD**	***Ec*-MnSOD-S126D**	***Ec*-MnSOD-S126W**	**Buffer used**
pI*	6.68	6.47	6.68	-
Lysis	√	√	√	50 mM potassium phosphate pH 7.8
Ammonium sulfate precipitation	√ 60 %/90 %	√ 50 %/75%	√ 60 %/95%	50 mM potassium phosphate pH 7.8
Cation exchange (Sephadex-CM50)	√ 20 mM potassium acetate pH 5.5/ against 1 M NaCl	√ 10 mM potassium acetate pH 5.5/ against 1 M NaCl	√ 10 mM potassium acetate pH 5.5/ against 1 M NaCl	10 mM potassium acetate pH 5.5 against gradual 1 M NaCl
Cation exchange (Sephadex-CM50)	√	-	-	20 mM potassium acetate pH 5.5/against 1 M NaCl but shallow gradient
Sodium chloride precipitation	-	-	√ Sodium chloride added gradually up to 3 M on ice and stirred	Resuspend in 10 mL of 10 mM Tris-Cl, pH 7.5 and dialysed
Hydrophobic interaction (phenyl superose)	√ 20 mM potassium acetate pH 5.5	-	-	Washed twice by same buffer with: 3) 2.5 M NaCl 4) 1 M NaCl
Anion exchange chromatography	-	-	Washed gradually by 5 mM Tris-Cl pH 7.5 containing 0.5 to 2 M NaCl	Using DEAE resin in tube, inverted for 30 mins

To separate the impurities of *Ec*-MnSOD-S126W, sodium chloride precipitation is effectively used which added gradually up to 3 M on ice and stirred. However, there are impurities at

higher (above 31 kDa) and lower (below 21.5 kDa) molecular weight. (See Figure 5.3, lane 2). Hydrophobic interaction did not effectively separate *Ec*-MnSOD-S126W from the impurities. So, anion exchange chromatography was chosen, as it has different charge properties at higher pH. In a mini-preparation experiment, we compared two different resins: Q-anion exchange and DEAE-anion exchange. The resin was placed in a tube with the protein sample, inverted for 30 mins at low temperature (4 ^{o}C). Then the contents were washed gradually by 5 mM Tris-Cl pH 7.5 containing 0.5 to 2 M NaCl. The results show that Q-anion exchange resin is less effective than DEAE-anion exchange resin to bind the impurities, as shown in Figure 5.3. For the final step of purification of *Ec*-MnSOD-S126W, DEAE-anion exchange was applied in larger scale purification.

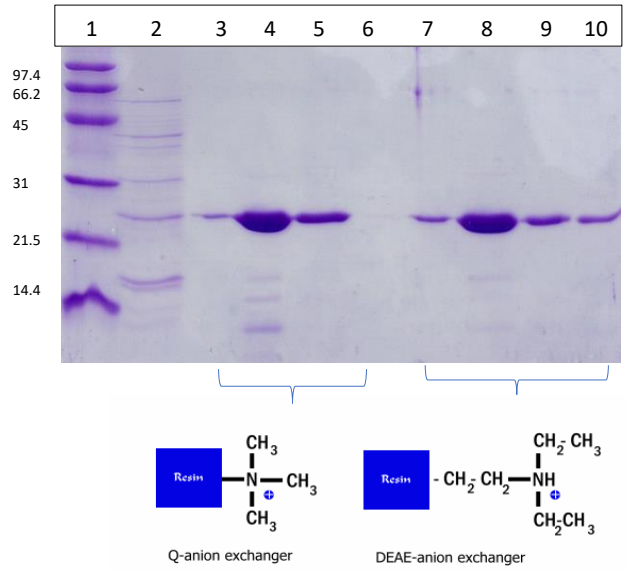

Figure 5.3. Anion exchange to purify *Ec*-MnSOD-S126W.

In a miniprep in a simply rotated tubes, Q-anion exchange (lanes 3 to 6) was less effective than DEAE-anion exchange (lanes 7-10) to bind the low molecular impurities in the final step. Lane 1: Molecular weight markers (in kDa axis), lane 2: weakly adsorbed species.

5.2 *Ec*-MnSOD-S126W activity

Given that monomeric mutants of the Ec-MnSOD enzyme, Ec-MnSOD-E170A and -E170Q lose their SOD activity (M. M. Whittaker & Whittaker, 1998a)), we were very interested in determining if the Ec-MnSOD-S126W mutant was also catalytically inactive. The SOD assay was used to examine the superoxide dismutase activity of the mutant with the wild-type as control. The activity of Ec-MnSOD wild-type and Ec-MnSOD-S126W have all been characterised at pH 7.8, which is the optimum pH of the wild-type, and also at pH 6.0.

Surprisingly, without knowing at this stage, the oligomerisation state of the mutant, mutation of Ser126 to Trp significantly reduces the superoxide dismutase activity to 0.1% of that of the wild-type enzyme at both pH 7.8 and 6.0 (see Table 5.2).

Table 5.2. Activity assay of wild-type *Ec*-MnSOD and its S126W mutant.

	***Ec*-MnSOD-wt (/(U/mg))**	***Ec*-MnSOD-S126W % of wt activity**
pH 6.0	8.4 (17) x 10^3	0.1 %
pH 7.8	10.2 (9) x 10^3	0.1 %
MnSOD concent. range	1.3 – 2.2 nM	50 - 1000 nM

Based on SOD activity assay, mutation of Ser126 to Trp at dimer interface site has destroyed activity. These results raise a question: is the loss of activity due to change in quaternary structure of the mutants? Alternatively, is the loss due to more subtle features arising from mutation of dimer interface residue Ser126? In contrast to the S126D mutant, complementation experiments with propionic acid for the S126W mutant did not lead to any increase in activity.

5.3 X-ray structural characterisation of *Ec*-MnSOD-S126W

Crystals of *Ec*-MnSOD-S126W were grown at pH 7.5. Crystals were also grown at lower pH (pH 6.8 in 0.1 M Bis-tris propane, 23 % (w/v) PEG 1500, 0.2 M KCl and 1.5 % (v/v) ethanol). No cryoprotectant was added to freeze the crystals.

X-ray diffraction data from *Ec*-MnSOD-S126W crystals grown at pH 7.5 were measured at a resolution of 2.85 Å in the hexagonal space group $P6_322$, with unit cell dimensions of $a = b =$ 115.36 Å, and c = 124.47 Å. Data collection and refinement statistics are summarised in Table 5.3. The protein crystallises with the canonical dimer interface approximately retained but with the C-terminal helices, residues 182-205, folded out, domain-swapping to form a dodecamer (Figure 5.5). On the other hand, the canonical oligomerisation of *Ec*-MnSOD, as in wild-type and the S126D mutant, is a dimer. X-ray diffraction data at the Australian Synchrotron were collected by Associate Professor Andrew Sutherland-Smith.

Table 5.3. Crystallographic data and refinement statistics.

	***Ec*-MnSOD-S126W at pH 7.5**
A. Data collection statistics	
Code of sample	J5
Diffraction source	**AS-MX1**
Wavelength (/Å)	0.95370
Temperature (/K)	100
Detector	ADSC
Rotation range per-image (/°)	1
Exposure time per image (/s)	10
Space group	$P6_322$
No. of molecules in asymmetric unit	2
No. of molecules in cell	24
a (/Å)	115.36
b (/Å)	115.36
c (/Å)	124.47
α (/°)	90
β (°)	90
γ (/°)	120
Volume (/Å^3**)**	1,434,500
Mosaicity (/°)	0.12

Resolution range (/Å)	46.36-2.85 (3.01-2.85)
Total # reflections	251,997 (35,581)
# unique reflections	11,930 (1684)
Completeness (%)	99.9 (99.7)
Redundancy	21.1 (21.1)
I/s(I)	13.1 (4.4)
R_{mrg}	0.198 (0.652)
R_{pim}	0.061 (0.202)
$CC_{1.2}$	0.997 (0.942)
Wilson B-value (/Å^2)	26.9
B. Refinement Statistics	
Resolution range (Å)	99.9-2.85 (2.93-2.85)
Completeness (%)	99.89 (99.53)
No. of reflections, working set	11,310 (808)
No. of reflection, test set	598 (39)
Final R_{work}	0.169 (0.272)
Final R_{free}	0.221 (0.307)
No. of protein non-H atoms	3,260
Manganese ions	2
Water	13
R.m.s. deviations	
Bonds (Å)	0.005
Angles (^{o})	1.48
Mean B factors (Å^2)	
Protein atoms	34
Ramachandran (COOT v0.9.8.7) Preferred/Allowed/Outlier (%)	94.83/3.94/1.23

The high conservation of structure of all but residues 181-205 is shown in Figure 5.4. The rmsd for superposition of 161 residues (residues 177-205 and helix and loop 109-125 omitted) from individual subunits of wild-type *Ec*-MnSOD and its S126W mutant is 0.32 Å. Although the Cα atoms of the mutation site at residue 126 share a common position, Trp126 cannot fit into the space occupied by Ser126. Residue 126, along with its side chain is reoriented dragging not only the loop connecting helix 109-122 to beta strand 127-134 into a new conformation (Figure 5.5) but altering helix 109-122. In the S126W mutant, this helix winds another half turn with the last two turns in a tighter 3_{10} conformation (helix now 109-125). As a result, Phe124

of the S126W mutant occupies the space of Arg181 for wild-type *Ec*-MnSOD, the first residue of the C-terminal tail (residues 181-205). This prevents the C-terminal tail of the S126W mutant from poking into the hole provided by loop 86-96, which links the N-terminal domain (residues 1-87) to the C-terminal domain (residues 88-205).

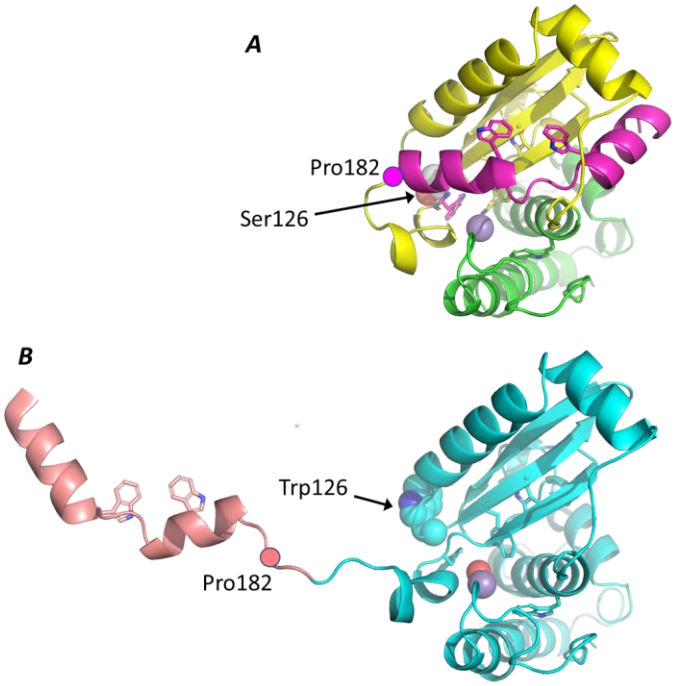

Figure 5.4 Structure of one subunit of wild-type *Ec*-MnSOD (*A*) and *Ec*-MnSOD-S126W highlighting key domains.

A, Wild-type *Ec*-MnSOD. The N-terminal domain (residues 1-87) is shown in green, the C-terminal domain (residues 88-180) in yellow and the C-terminal tail (residues 181-205) in magenta. ***B***, *Ec*-MnSOD-S126W. The C-terminal tail (residues 181-205) is shown in puce, the remainder in cyan. Trp residues are shown, carbon atoms coloured according to domain. Ser126 and Trp126 are shown as spheres.

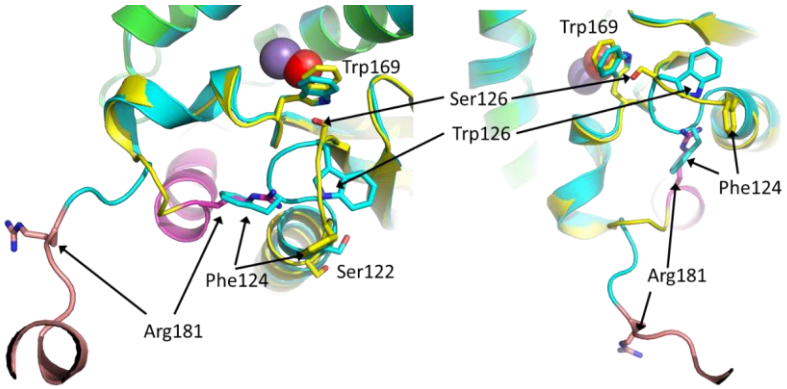

Figure 5.5. Two views of the superposition of the dimer interface region of wild-type *Ec*-MnSOD and its S126W mutant.

Ser/Trp126 in the loop 122-126 adopts a completely different conformation, such that in the S126W mutant Phe124 is placed in the space occupied by Arg181 of wild-type enzyme, causing the C-terminal tail (residues 181-205) to be flipped out. Colouring as in Figure 5.4.

In Figure 5.6, the superposition of subunit A of the dimer of *Ec*-MnSOD-S126W onto subunit A of wild-type *Ec*-MnSOD shows the movement of chain B of *Ec*-MnSOD-S126W away from the canonical dimer interface. The C_β atoms of Lys113 are shown as spheres, highlighting movement. In chain A, Lys113 is part of the helix that is substantially distorted by the S126W mutation and there is a separation of C_β of 0.9 Å in chains A and in chains B the shift leads to a separation of C_β of 2.6 Å. Focussing on the interface, for chains A, the Ser126 C_α are separated by 0.5 Å; for chains B this separation is substantially increased to 3.7 Å. The rearrangement of the canonical dimer interface appears to be mostly a shift with negligible rotation.

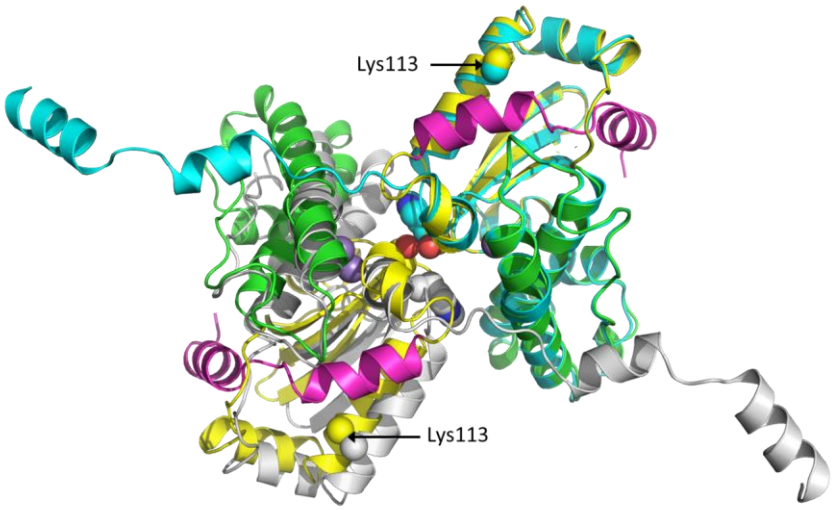

Figure 5.6. Superposition of *Ec*-MnSOD-S126W onto wild-type *Ec*-MnSOD.

Subunits A are superimposed (rmsd 0.37 Å for 165 residues). The dimer of *Ec*-MnSOD-S126W superimposes poorly onto the dimer of wild-type *Ec*-MnSOD with rmsd of 1.70 Å. Wild-type *Ec*-MnSOD is shown with N-terminal (residues 1-87) in green, C-terminal (residues 88-180) in yellow and the C-terminal tail (residues 181-205) in magenta. *Ec*-MnSOD-S126W is shown in cyan for subunit A and grey for subunit B. The Ser126 and Trp126 residues are shown as spheres. To highlight shift of chain B relative to chain A the C_β of Lys113 are shown as spheres.

As shown in Figure 5.7, there is substantial change in the active site of the enzyme upon the S126W mutation. In addition to movement of Trp169, Gln146 of *Ec*-MnSOD-S126W moves so that the amide's carbonyl oxygen hydrogen bonds to the coordinated water-derived ligand. This is in contrast to wild-type enzyme where the amide NH_2 group hydrogen-bonds to the coordinated hydroxide, as discussed in the Introduction (Chapter 2) and discussed further below. Remarkably, Glu170 still reaches across the dimer interface to hydrogen bond to His171. The water-derived ligand in the S126W mutant is almost certainly water and not hydroxide, as one proton is needed to hydrogen bond to Asp167 and another is needed to hydrogen bond to the amide carbonyl oxygen atom (see also Figures 2.8, 2.9 and 2.14).

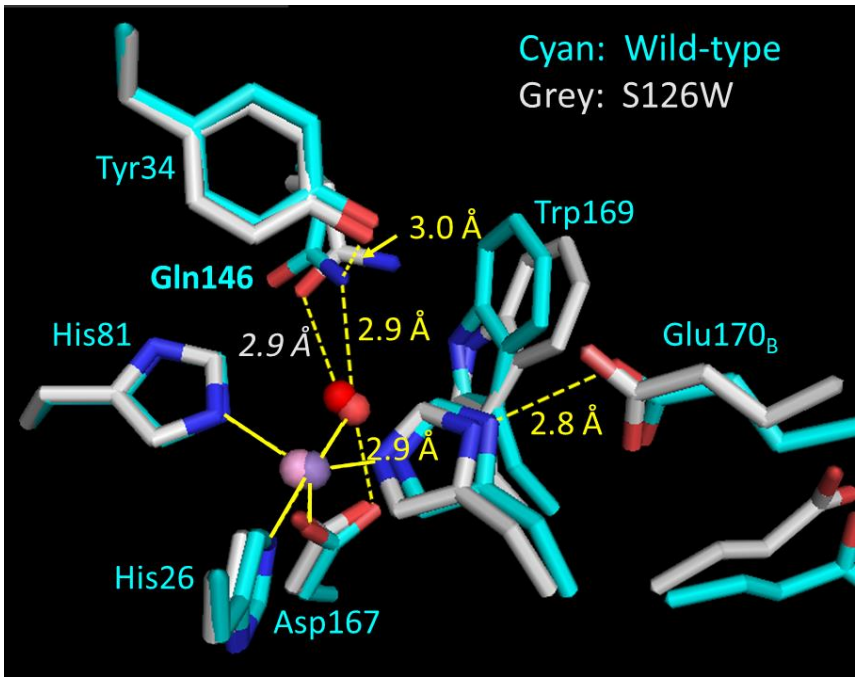

Figure 5.7. Superposition of active site of *Ec*-MnSOD-S126W (grey) onto that of wild-type *Ec*-MnSOD (cyan).

Although the active site superimposes closely, second-shell residues Gln146, Trp169 and, especially, Glu170 from the other subunit of the dimer are substantially displaced.

Application of crystallographic two-fold symmetry shows that the flipped-out C-terminal tail (residues 181-205) of one subunit pokes into the hole created by the flipped-out domain of another subunit, as shown in Figure 5.8. There is remarkably close superposition of the C-terminal tail, residues 181-205, of the domain-swapped *Ec*-MnSOD-S126W with that of wild-type *Ec*-MnSOD.

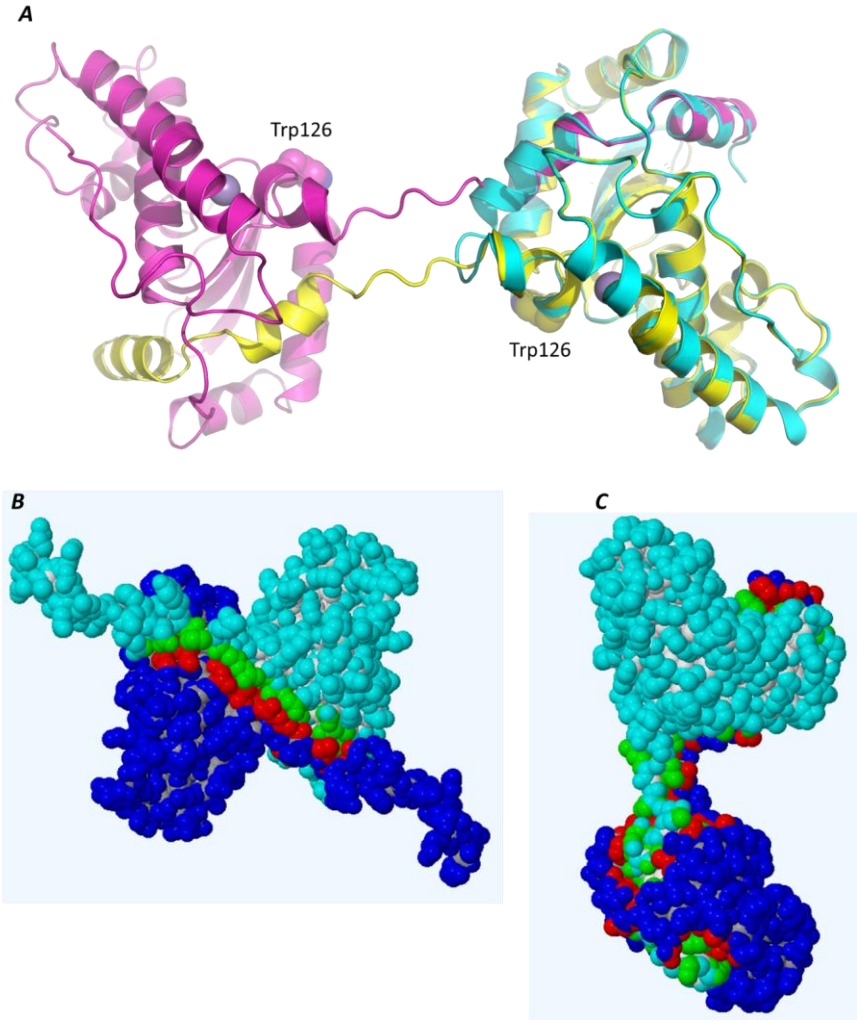

Figure 5.8. Domain swapping of the C-terminal tails (residues 181-205) of *Ec*-MnSOD-S126W.

A, Ec-MnSOD-S126W is shown in magenta and yellow. The two molecules are related by a crystallographic two-fold axis. Wild-type *Ec*-MnSOD (cyan) is superimposed on one subunit of the S126W mutant. ***B***, Space-filling representation of the canonical dimer interface for *Ec*-MnSOD-S126W. ***C***, Space-filling representation of the interface for the domain-swapped dimer of *Ec*-MnSOD-S126W. Solvent-exposed residues not in contact are shown in blue and cyan spheres. Respectively, for cyan and blue subunits, green and red spheres show residues in contact across the interfaces.

Interfacial contact areas and Gibbs free energy change to bury that surface from solvent are provided in Table 5.4 for wild-type *Ec*-MnSOD and its S126W and S126D mutants. In wild-type *Ec*-MnSOD about 9% of the surface is buried, with an associated strongly favourable Gibbs free energy change. The Complexation Significance Score (CSS) calculated by PISA gives a value of 1.000 for this interface, indicating high probability of formation in aqueous solution. No other solvent-stable interfaces are indicated. For the S126D mutant, the canonical interface area is identical (see also Chapter 4). The total protein surface area is somewhat less than that of wild-type and this is attributed to greater caution in interpreting electron density maps of highly flexible side chains for the S126D mutant compared to wild-type enzyme, as well as a somewhat lower temperature of data collection. Space group and crystal packing do not seem to be a factor here: wild-type *Ec*-MnSOD and S126D-azide (pH 9.1) are in space group $C222_1$, S126D (pH 6.8) is in space group $P1$, S126D (pH 8.7) is pseudo-$C222_1$ in space group $P12_11$ (twinned) and S126W is in space group $P6_322$.

For *Ec*-MnSOD-S126W, the surface area of an individual molecule is greatly increased over that of the wild-type and S126D mutant, due to the flipping out of the C-terminal tail (residues 181-205). In addition, the canonical dimer interface, while more extensive, an artefact of the flipped out C-terminal tail, has markedly decreased stability due to movement of one subunit away from the other (Figure 5.6 and Table 5.4). The domain-swapped interface is extensive in the area buried and very favourable in terms of Gibbs free energy changes, in large part because of the interaction of the pair of extended stands between the subunits (Figure 5.8 and Table 5.4). The C-terminal tail of *Ec*-MnSOD-S126W fits into the adjacent subunit the same as in wild-type enzyme (Figure 5.8A).

Table 5.4. Contact areas (/Å^2) and free-energy [/kJ mol^{-1}] of interfaces for wild-type *Ec*-MnSOD and its S126D and S126W mutants.[a]

Surface area (/Å^2) [ΔG (/kJ mol^{-1})]	Canonical dimer	Domain-swapped	Other
Wild-type (1vew, $C222_1$, pH 8.5) (9697 Å^2)[b]	858 [–50][c]	---	348-188 [–15 - –2]
S126D (pH 6.8, $P1$) (9441 Å^2)[b]	858 [–51][c]	---	483-119 [–8 - –1]
S126D (pH 8.7, $P12_11$) (9393 Å^2)[b]	861 [–51][c]	---	494-118 [–9 - –2]
S126D-Azide (pH 9.1, $C222_1$) (9493 Å^2)[b]	859 [–56][c]	---	363-132 [–14 - –]
S126W (12,227 Å^2)[b]	1143 [–25][c]	3005 [–182][c]	265-123 [–11 - –4]

[a] Calculated using PISA (Krissinel & Henrick, 2007). [b] Average of four. [c] Average of two.

Application of space group symmetry operations around the crystallographic 3-fold axis on the quasi-canonical dimer interface species (the asymmetric unit) and the domain-swapped dimer creates a remarkable dodecameric arrangement of subunits (Figure 5.9A, B). Only weak interactions occur between these dodecameric assemblies, where the domain-swapped C-terminal tail (residues 181-205) contacts itself. The interaction area is small with only weakly favourable Gibbs free energy (Figure 5.9C and Table 5.4).

Given the extensive and thermodynamically very stable domain-swapped interface, is this dimer species, or a higher-order oligomer, seen in solution? In the next section, analytical ultracentrifugation (AUC), circular dichroism (CD) spectroscopy and differential scanning calorimetry are used to try and answer this question.

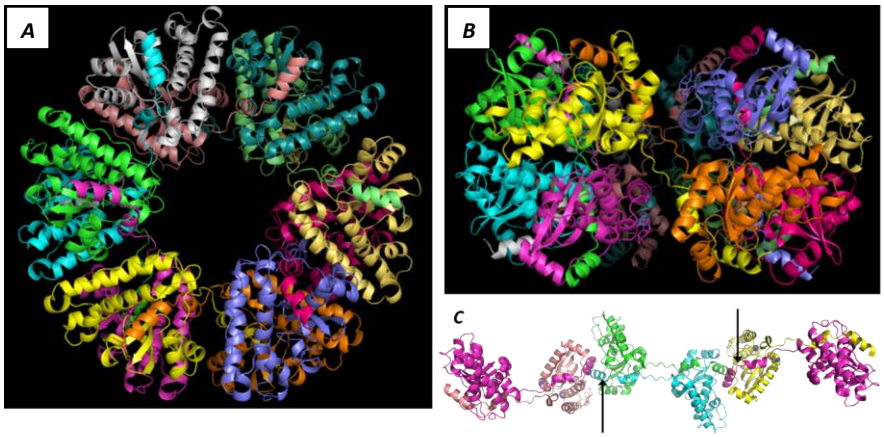

Figure 5.9. The dodecameric assembly of *Ec*-MnSOD-S126W.

The C-terminal tail of one subunit pokes into the space vacated by the C-terminal tail of another subunit. Along with the quasi-dimer interface, this leads *via* crystallographic symmetry to the dodecameric species. The most stable interface is that created by the domain swapping of the C-terminal tail. ***A***, Dodecameric assembly of *Ec*-MnSOD-S126W viewed down the crystallographic three-fold axis. ***B***, Side-on view of dodecamer. ***C***, Daisy-chain of domain-swapped molecules, looking down a crystallographic two-fold axis. There is a weak interface between the C-terminal helices (residues 194-203) arrowed. Trp126 at the quasi-canonical dimer interface are highlighted as spheres.

5.4 Characterisation of the quaternary state of *Ec*-MnSOD-S126W in the solution state

5.4.1 Sedimentation velocity analysis by analytical ultracentrifugation

In this study, the structure of the *Ec*-MnSOD-S126W mutant in the solution state was observed by utilising analytical ultracentrifugation (AUC) through sedimentation velocity experiments (Lebowitz et al., 2002). In sedimentation velocity, the movement of solutes in high centrifugal fields is interpreted using hydrodynamic theory to define the size, shape and interactions of macromolecules. Here, we can observe the size of *Ec*-MnSOD-S126W protein in the solution state in kDa; then we can interpret the oligomeric state of the mutant and provide some evidence on the effect of pH and concentration to the interactions between monomers to form oligomers. The shape is also interpreted based on the frictional value.

To investigate the quaternary structure of *Ec*-MnSOD-S126W and to probe the stability of the quaternary structure in solution, a series of sedimentation velocity experiments were employed with varying concentrations of the protein and pH. Sedimentation velocity experiments of *Ec*-MnSOD wild-type and *Ec*-MnSOD-S126D have been reported in Chapter 4 as a reference.

5.4.2 *Ec*-MnSOD-S126W is predominantly monomeric in solution

To investigate the quaternary structure of *Ec*-MnSOD-S126W and to probe its stability in a solution, sedimentation velocity studies of the mutant were employed at similar pH and protein concentrations to those used for the *Ec*-MnSOD wild-type experiments at pH 7.8 and pH 6.0.

The results show that at both pH 6.0 and 7.8, the continuous sedimentation coefficient and mass distributions of *Ec*-MnSOD-S126D significantly change with change in protein concentration at each pH, compared to those of *Ec*-MnSOD wild-type. At pH 7.8 with concentrations of 0.6 and 1.3 mg/mL, the sedimentation velocity analysis of *Ec*-MnSOD-S126W shows one peak in the *c*(*s*) distribution at sedimentation coefficient value 2.17 S, which in the c(M) distribution gives a molar mass of 23.9 ± 0.4 kDa, attributed to a monomeric *Ec*-MnSOD-S126W mutant. However, at higher concentration of 2.6 mg/mL, the sedimentation velocity analysis of *Ec*-MnSOD-S126W shows two peaks, first the predominant species at lower molar mass and sedimentation coefficient attributed to a monomeric species of the mutant, and secondly a minor peak found at higher sedimentation coefficient of 3.0 S and molar mass of 42.9 kDa attributed to dimeric *Ec*-MnSOD-S126W. Sedimentation velocity analysis of *Ec*-MnSOD-S126D at 0.6 and 1.3 mg/mL showed a relatively broad and slightly asymmetrical curve, tending to widen at higher S values. The weight-average standardised sedimentation coefficient and molar mass at each protein concentration are very close and repeatable indicating dimer species for wild-type *Ec*-MnSOD and *Ec*-MnSOD-S126D.

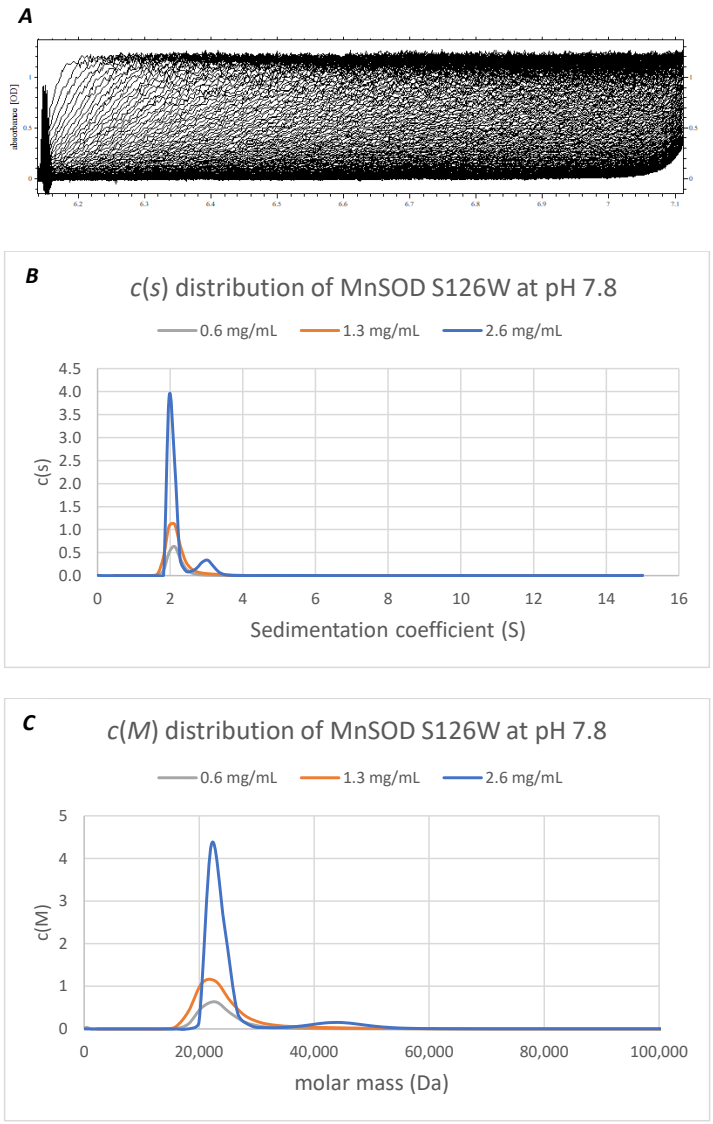

Figure 5.10. Analytical ultracentrifugation of *Ec*-MnSOD-S126W at pH 7.8, revealing quaternary structure.

A, Sedimentation velocity data, showing absorbance *versus* distance from rotation axis *versus* time for *Ec*-MnSOD-S126W (only data from 2.6 mg/mL solution shown). ***B***, Sedimentation coefficient *c*(*s*) distribution of *Ec*-MnSOD-S126W at pH 7.8. For the 0.6 mg/mL solution, *f*/*f*o = 1.3, $s_{20,w}$ = 2.3 S and

rmsd = 8.61.10^{-3}. For the 1.3 mg/mL solution, f/f_o = 1.3, $s_{20,w}$ = 2.3 S and rmsd = 7.95.10^{-3}. For the 2.6 mg/mL solution, f/f_o = 1.4, $s_{20,w}$ = 2.1 S and rmsd = 1.42.10^{-2}. ***C***, Continuous mass distribution *c*(*M*) obtained from the fitting of SV data of *Ec*-MnSOD-S126W at pH 7.8 (50 mM potassium phosphate, 100 mM NaCl, pH 7.8). The apparent molar mass of the monomeric species has been found to be 23.5 kDa, 23.7 kDa, and 24.4 kDa for 0.6 mg/mL, 1.3 mg/mL, and 2.6 mg/mL solutions, respectively, and for the dimeric species, the apparent molar mass is 42.9 kDa (only at 2.6 mg/mL).

Retrieved from the data of Fig. 5.10, the average value of $s_{w,20}$ for *Ec*-MnSOD-S126W is 2.13 $\pm$ 0.04 S for the monomeric species from three different concentrations, and 3.03 S for the dimeric species (only at 2.6 mg/mL). Moreover, the apparent molar mass of the species represented by the major peak has been found to be 22.3 ± 0.2 kDa for monomeric *Ec*-MnSOD-S126W, a value insignificantly different to the expected values of 23.1 kDa, and the minor peak has been found to 44.8 ± 0.6 kDa for dimeric *Ec*-MnSOD-S126W, slightly different to the expected value of 46.1 kDa. The relatively low precision of the molar mass of the dimeric species is due to its low relative abundance compared to the predominant monomer species.

The sedimentation velocity analysis results of *Ec*-MnSOD-S126W at lower pH 6.0 (50 mM potassium phosphate, 50 mM NaCl, pH 6.0) shows more prominently with a single narrow and relatively symmetrical curve in all concentrations. The maximum in the *c*(*M*) distribution at 22.5 $\pm$ 0.6 kDa is attributed to the monomeric species of the *Ec*-MnSOD-S126W mutant (Figure 5.11).

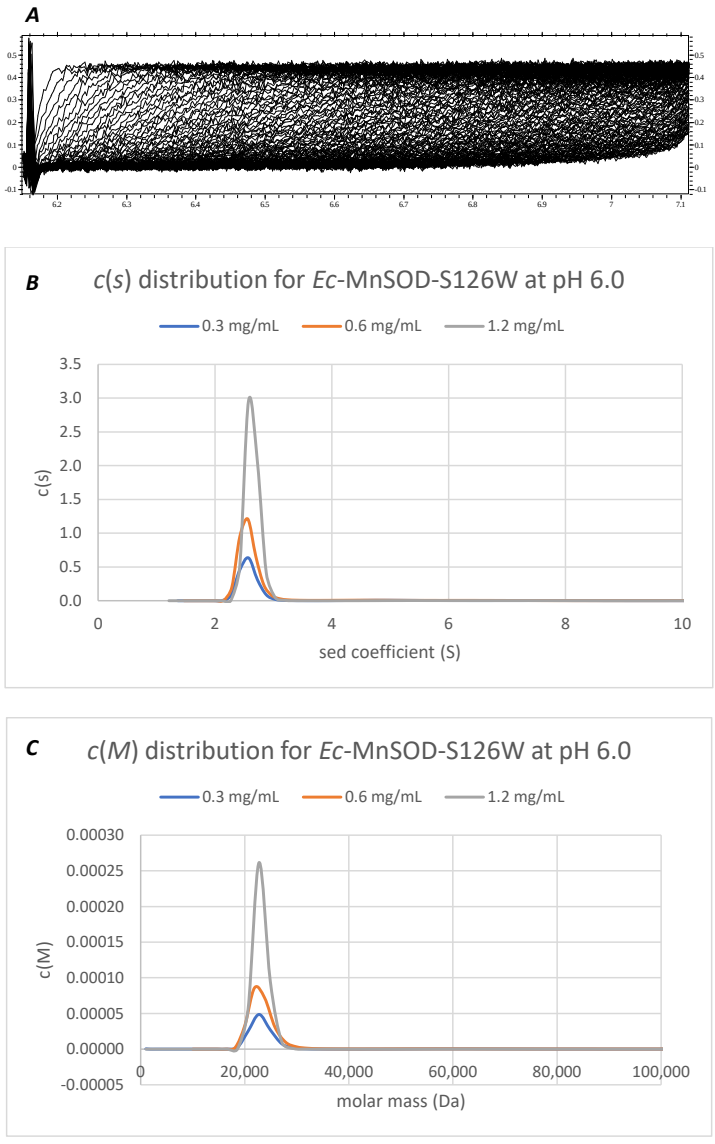

Figure 5.11. Analytical ultracentrifugation of *Ec*-MnSOD-S126W at pH 6.0, revealing quaternary structure.

A, Sedimentation velocity data, showing absorbance *versus* distance from rotation axis *versus* time for *Ec*-MnSOD-S126W (only data from 0.6 mg/mL solution shown). ***B***, Sedimentation coefficients *c*(*s*) distribution of *Ec*-MnSOD-S126W at pH 6.0. For the 0.3 mg/mL solution, *f*/*f*o = 1.1, $s_{20,w}$ = 2.6 S, and

rmsd = 8.76x10^{-3}. For the 0.6 mg/mL solution, *f*/*f*o = 1.1, $s_{20,w}$ = 2.6 S, and rmsd = 9.84x10^{-3}. For the 1.2 mg/mL solution, *f*/*f*o = 1.05, $s_{20,w}$ = 2.7 S and rmsd = 4.30x10^{-3}. ***C***, Continuous mass distribution *c*(*M*) obtained from the fitting of SV data of *Ec*-MnSOD-S126W at pH 6.0 (50 mM potassium phosphate, 100 mM NaCl, pH 6.0). The apparent molar masses of the monomeric species are 23.2, 23.1 and 23.1 kDa for 0.3, 0.6, and 1.2 mg/mL solutions, respectively.

Unlike MnSOD wild-type, there is no visible peak found at higher sedimentation coefficient attributed to dimer species at all concentrations. The weight-average sedimentation coefficients of *Ec*-MnSOD-S126W at pH 6.0, 2.59 $\pm$ 0.02 S, and the weight-average molar mass of *Ec*-MnSOD-S126W at pH 6.0, 23.9 $\pm$ 0.4 kDa, both attributed to monomer species of *Ec*-MnSOD- S126W.

5.4.3 Higher-order oligomerisation states of *Ec*-MnSOD-S126W are found in solution

Further analysis of SV-AUC data at higher sedimentation coefficients shows that there are observable higer-order oligomers, but with *c*(*s*) values more than three orders of magnitude smaller than those for monomeric species. There are several reproducible peaks other than monomer and dimer, which indicate the presence of higher oligomerisation states of *Ec*-MnSOD-S126W mutant in solution at both pH 7.8 and 6.0. In the continuous *c*(*s*) distribution model, the calculated M_w of each peak can be displayed. The results show that the molecular weights collected from all continuous c(s) distributions at all pH and concentrations are: 120 ± 10 kDa, 200 ± 10 kDa, and finally 261 ± 20 kDa. These peaks are barely visible and therefore give imprecise values for the maxima in the *c*(*s*) distributions and M_w values. If the highest molecular weight is attributed to the dodecamer, does the dodecameric *Ec*-MnSOD-S126W species really exist? How could this structure of dodecameric *Ec*-MnSOD-S126W could be formed when the wild-type *Ec*-MnSOD exists as a dimer? The answer to this question will be discussed in Chapter 6: Discussion.

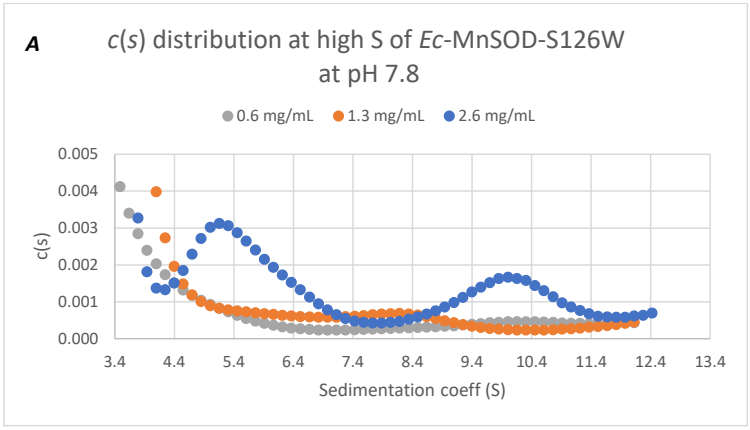

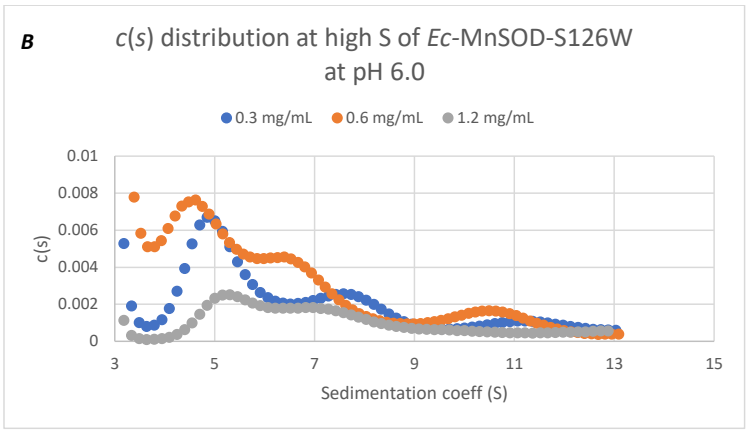

Figure 5.12. Large size quaternary structures of *Ec*-MnSOD-S126W at various pHs and concentrations.

A, Sedimentation coefficient *c*(*s*) distribution of *Ec*-MnSOD-S126W at pH 7.8. ***B***, Sedimentation coefficient *c*(*s*) distribution of *Ec*-MnSOD-S126W at pH 6.0. Reproducible sedimentation coefficients at 5, 7 and at 10 S, as the highest oligomeric state.

5.4.4 Thermal stability of *Ec*-MnSOD-S126W by differential scanning calorimetry

The thermal stability of *Ec*-MnSOD-S126W was determined by differential scanning calorimetry (DSC). The thermal stability of wild-type *Ec*-MnSOD described in Chapter 4 is also used for comparison to *Ec*-MnSOD-S126W at same pH 7.8. The disruption of the dimer interface of *Ec*-MnSOD-S126W mutant giving predominantly monomeric species observed by analytical ultracentrifugation measurements has shown that the steric bulk of Trp has successfully destabilised the dimeric quaternary structure, as well as deactivating the function of SOD enzyme.

After baseline subtraction, a three-peaked asymmetric endotherm is observed for the *Ec*-MnSOD-S126W mutant. Compared to *Ec*-MnSOD-wild-type, the temperature of maximum heat capacity of *Ec*-MnSOD-S126W mutant (T_m), changes, decreases from 83° to 73 °C. These endotherms can be fitted by three symmetrical two-state curves with minor overlapping at each boundary to the adjacent peak (Figure 5.13): at lowest temperature, a broad small endotherm (labeled X), a large one (labeled Y), and at highest temperature a small one (labeled Z). These three events occur at different temperatures with ~10 °C gaps one to another: respectively, 53 °C, 63 °C, and 73 °C.

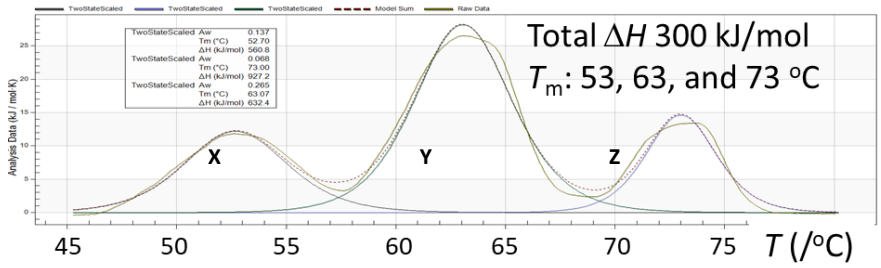

Figure 5.13. Differential scanning calorimetry thermogram of *Ec*-MnSOD-126W dimer interface mutant results in three two-state fits at 53 °C, 63 °C, and 73 °C.

The observed data are shown as the brown solid line, the calculated fits as solid grey, green and blue lines for transitions X, Y and Z, respectively, and the sum of the calculated fits as the dotted line.

As the temperature transitions obviously indicate three independent events, it is interesting to know what is going on in each event by analysing and interpreting multi-scan differential

scanning calorimetry results of *Ec*-MnSOD-S126W. The experiments on stability of the *Ec*-MnSOD-S126W mutants were conducted at various protein concentrations of 0.2 mg/mL (you have given only one concentration here) in 10 mM Tris-Cl, pH 7.8, conditions similar to studies on enzyme activity. Data were collected at scan rates 1 °C/min in a TA Instruments™ Nano-DSC (differential scanning calorimeter). With reference to the single-scan result described above, the experiments of multi-scan Nano-DSC were set into 7 phases, summarised in Table 5.5.

Table 5.5. Multi-scan nano DSC were set into 7 phases.

Phase 1	Phase 2	Phase 3	Phase 4	Phase 5	Phase 6	Phase 7
Heated to 57 ^{o}C	Cooled	Heated to 70 ^{o}C	Cooled	Heated to 80 ^{o}C	Cooled	Heated to 100 ^{o}C

There are four different heating steps from 57 to 100 ^{o}C and three cooling steps back to 20^{o}C. In phase 1, when the protein sample was heated to 57 ^{o}C, a single symmetric endotherm is observed. The temperature of maximum heat capacity is reproducible (52 ^{o}C), similar to transition X from the previous experiment, for which T_m is ~53 ^{o}C (See Figure 5.14A). The sample was then cooled (phase 2). In phase 3, where the protein sample was then heated to 70 ^{o}C, two symmetrical endothermic curves are observed: the first is similar to the transition X of phase 1 but with some loss of intensity in transition X, the second is absolutely similar to transition Y, for which T_m is ~63 ^{o}C. Transition X is reversible, since heating to 57 ^{o}C for the second time, it does not lead to the *Ec*-MnSOD-S126W mutant becoming unfolded (See Figure 5.14B). After cooling the protein sample (phase 4), it is reheated to 80 ^{o}C. Two symmetrical endotherm curves are observed. The transition X curve, as expected, appears although with loss of intensity, that is now lower than that of phase 3 and phase 1. Surprisingly, transition Y does not appear on the third heating (phase 5), indicating that transition Y is irreversible (Figure 5.14C). The second endotherm curve is absolutely similar to the transition Z in the single-scan experiment, for which T_m is ~73 ^{o}C. After cooling the protein sample (phase 6), it is reheated to 100 ^{o}C. There is no peak found, which means that the third heating in phase 5 leads to unfolding, where the overall protein is denatured after exceeding 80 ^{o}C (Fig. 5.14D). Table 5.6 summarises transition temperatures and enthalpy changes. The fitting algorithm

produces two enthalpy changes, the van't Hoff and the calorimetric. Both are somewhat artefactual as a result of the $\underline{A}_w$ parameters, which for simple fits of a single isotherm and known concentration should have a value of one but which clearly deviate from this value. However, on the assumptions that (1) there is no loss of protein to denaturation for transition X and Y and (2) transition X in phase 3 and 5 is associated with the same process as in phase 1 and the single scan, the A_w parameters of the single scan can be used to scale the calorimetric enthalpy changes for phases 3 and 5, as in the footnote to Table 5.5. This leads to calorimetric enthalpy changes for transitions X, Y and Z in phases 1 (only X), 3 (X and Y) and 5 (X and Z) that are similar to those derived for the single-scan endotherms.

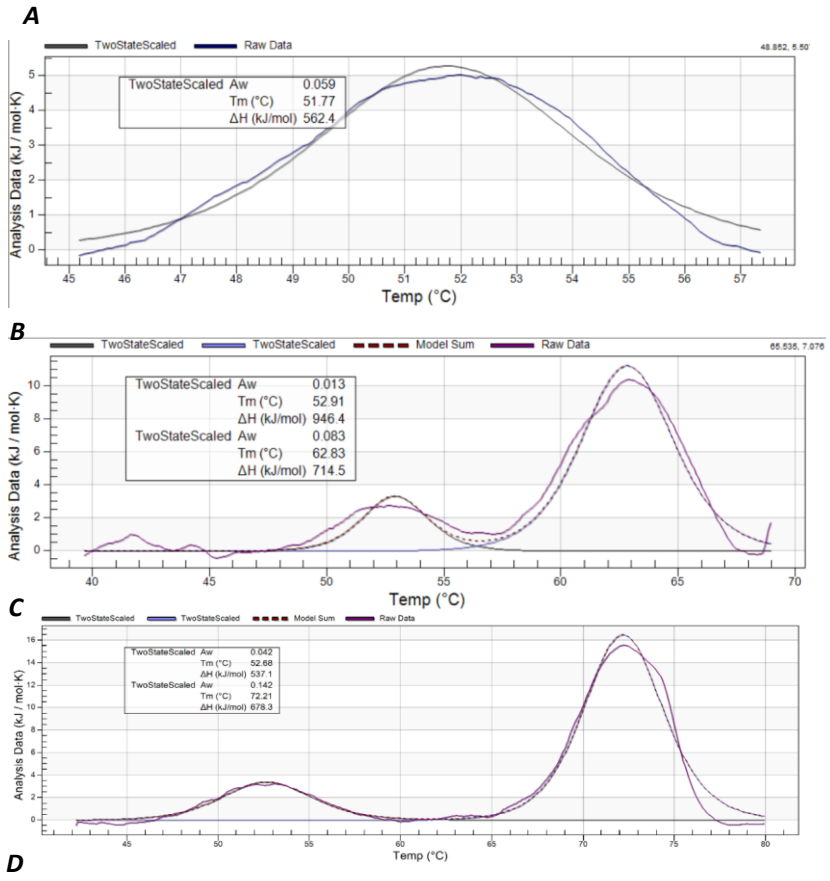

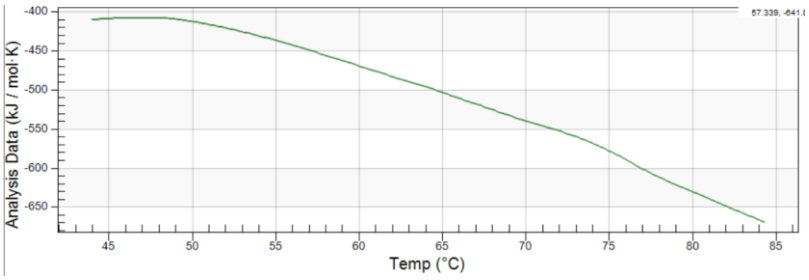

Figure 5.14. Multi-scan differential scanning calorimetry thermograms of MnSOD S126W dimer interface mutant.

These are performed at various stages of heatings to analyse the reversibility of each transition events, including the final unfolding step up to 100 °C. ***A***, Phase 1 scan where sample is heated from 20 °C to 57.4 °C. ***B***, Phase 3 scan where sample from phase 1 has been cooled to 20 °C and then heated to 70 °C. ***C***, Phase 5 scan where sample from phase 3 has been cooled to 20 °C and then heated to 80 °C. ***D***, Phase 7 where sample from phase 5 has been cooled to 20 °C and then heated to 100 °C.

Table 5.6. Single- and multi-scan DSC parameters for *Ec*-MnSOD-S126W.

Phase	Transition	T_m(/°C)	A_w	$\Delta H_{van't\ Hoff}$ (/kJ mol^{-1})	ΔH_{cal} (/kJ mol^{-1})	ΔH_{cal} scaled[a] (/kJ mol^{-1})
Single-scan	X	53	0.137	561	77	77
	Y	63	0.265	632	167	167
	Z	73	0.068	927	63	63
Multi-scan						
1	X	52	0.059	562	33	76
3	X	53	0.013	946	12	109
3	Y	63	0.083	715	59	188
5	X	53	0.042	537	23	75
5	Z	72	0.142	678	96	46
7	---	---	---	---	---	

[a] The scaled values are calculated as ΔH_{cal}(scaled) = ΔH_{cal}. *A_w(single scan)/A_w(phase *n*).

The AUC measurements indicate that the bulk of *Ec*-MnSOD-S126W is monomeric, and, therefore, interpretation of DSC data is made assuming monomeric protein. In the first

heating, one interpretation of the data is that transition X at 53 °C for *Ec*-MnSOD S126W is attributed to the reversible flipping out and unfolding of the C-terminus domain of the monomer *Ec*-MnSOD S126W residues 181 to 205. This transition also occurs for the second and third heating (phases 3 and 5). The second unfolding event (peak Y), which also occurred in the second heating (phase 3) is attributed to the irreversible denaturation of residues 1-87 (N-terminal domain of *Ec*-MnSOD), which involved the separation of N-terminal metal-binding ligands, His26 and His81, from the C-terminal ligands, Asp167 and His171. The third unfolding event (peak Z) comes up in the third heating is attributed to the denaturation of the rest of the C-terminal domain, residues 88-180. The reason for assigning irreversible denaturation of the N-terminal before denaturation of residues 88-180 of the C-terminal domain is that the initial endotherm is reversible. This would be incompatible with the next event being irreversible denaturation (transition Y) of the bulk of the C-terminal domain, but reversible refolding of residues 181-205 on cooling.

An alternative and preferred explanation is that reversible transition X is associated with separation of the N-terminal domain from the C-terminal domain. Trp126 is immediately adjacent to Trp169, which forms part of the interface between the N- and C-terminal domains, as well as being part of the canonical dimer interface. Trp126 also influences the conformation of the dimer-interface loop 122-126, which then leads to steric clashes with the C-terminal tail (residues 181-185) that results in it flipping out to avoid these contacts (Figure 5.8) . Transition Y is associated with unfolding of the C-terminal domain (see below for support for this conjecture from circular dichroism. Transition Z, which has a noticeably smaller enthalpy change than transition Y, is then associated with unfolding of the smaller N-terminal domain. Figure 5.15 shows schematically the three transitions.

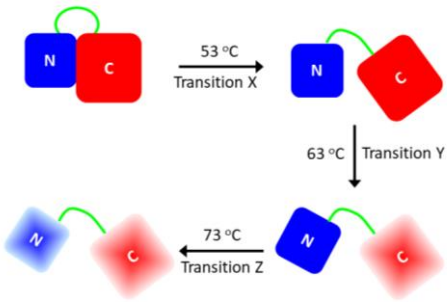

Figure 5.15. Schematic of the thermal denaturation of *Ec*-MnSOD-S126W.

Bold shaded shapes indicate folded protein; gradient-shaded shapes denote unfolded protein. N and C denote the N-terminal and C-terminal domains.

5.4.5 Circular dichroism analysis of secondary and tertiary structural changes of *Ec*-MnSOD-S126W

To get more insight into the distinctive thermal stability of *Ec*-MnSOD-S126W, compared to wild-type *Ec*-MnSOD and its S126D mutant, circular dichroism (CD) measurements in the far-UV and near-UV were made over the temperature range 20 to 100 ^{o}C to characterise thermal stability. Circular dichroism (CD) spectroscopy can also be used to confirm whether, or not, *Ec*-MnSOD-S126W mutant retained the same secondary and tertiary structure in solution as the wild-type enzyme, noting that CD does not give insight into quaternary structure.

Before analysing thermal stability, CD spectra at room temperature (20 ^{o}C) were examined for differences in secondary and tertiary structure for *Ec*-MnSOD-S126D and *Ec*-MnSOD-S126W compared to wild-type *Ec*-MnSOD. The far-uv CD spectra of wild-type *Ec*-MnSOD and its S126D and S126W mutants are shown in Figure 5.16 A. The spectrum of the S126W mutant shows significant differences in the range 218 to 240 nm compared to the very similar spectra of wild-type enzyme and its S126D mutant, establishing that the S126W mutant has significantly perturbed secondary structure, as a result of a mutation intended to disrupt quaternary structure.

To check whether, or not, the mutations had affected tertiary structure, CD spectra in the near-uv region (280-360 nm) were also measured. *Ec*-MnSOD is particularly rich in tryptophan residues (there are six Trp, distributed with five in the C-terminal domain, residues 88-205, and one in the N-terminal domain, residues 1-87). Thus, the region 285-295 nm, where Trp residues in chiral environments typically give CD signals, is likely to be very sensitive to any perturbations in tertiary structure. Wild-type *Ec*-MnSOD and its S126W mutant show significant differences in this region with the valley and peaks in the region 285-295 nm shifted to shorter wavelength as a result of the S126W mutation (Figure 5.16B). For monomeric *Ec*-MnSOD, dimer-interface residues Trp169 and mutated Trp126 now lie on the surface and may not contribute significantly to the CD signal in the near-UV region due to conformational flexibility.

Wavelength (nm)

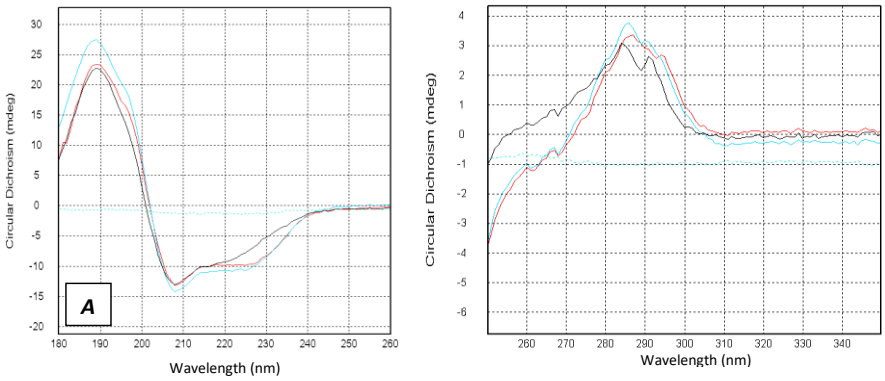

Figure 5.16. Comparison of circular dichroism spectra of wild-type *Ec*-MnSOD and its S126D,

Far-UV (***A***) and near-UV (***B***) circular dichroism spectra of *Ec*-MnSOD-S126W compared to wild-type and the S126D mutant at 20 °C and 50 mM phosphate buffer at pH 7.8. Baseline (green); wild-type (red); S126D (blue); S126W (black).

Trp189 and 194 become more exposed on unfolding of the C-terminal tail, residues 181-205. On loss of the N-terminal domain, Trp169 becomes even more exposed. Trp128 and Trp130 in the C-terminal domain 87-180 remain substantially buried. There is only one Trp in the N-terminal domain, Trp85, which is well buried inside this domain, when folded.

Modelling of the far-UV spectra indicates that the changes are consistent with partial loss of helical structure for the S126W mutant compared to wild-type and the S126D (Figure 5.17 and Table 5.7). This loss of helicity and increase in beta-sheet content in the ***solution state*** are tentatively associated with the two helices of the C-terminal tail (residues 181-205) that in ***crystalline*** *Ec*-MnSOD-S126W are folded and inserted (domain-swapped) into a neighbouring molecule, and so on to form the observed dodecamer, but in the solution state are unfolded.

Table 5.7. Modelling of circular dichroism spectra by BeStSel[a].

	%helix X-ray	%helix BeStSel	%beta X-ray	%beta BeStSel	%coil/turn X-ray	%coil/turn BeStSel	NRSMD (Scale)
Wild-type	45	46	11[b]	10	44	43	0.022 (0.25)
S126D	45	48	11	11	44	41	0.018 (0.22)
S126W	45 (36)[c]	36	11 (21)[c]	23	44	41	0.030 (0.27)

[a] Helix (wild-type): 20-44, 65-86, 96-107, 109-122, 181-190, 194-203; total = 93/205 residues. Beta strand: 127-134, 137-144, 161-167; total = 23/205 residues. Coil/strand is 89/205. As determined in the X-ray structures of wild-type *Ec*-MnSOD and its S126D and S126W mutants. As calculated from PDB: 1VEW by DSSP in PyMol. These numbers are 1-2 residues. The errors in the BeStSel percentages are approximately ±1-2%, determined by testing the sensitivity of the scale factor scale factor (or equivalently the concentration, which is known to a relative precision of at best 10%).

[b] No parallel beta strands were calculated, consistent with X-ray structures.

[c] If residues 181-190 and 194-203 form an antiparallel beta sheet, then the number of residues in alpha helices decreases to 73 and the number in beta strands increases to 43.

The agreement between calculated and observed far-UV CD spectra is visually very good, with the normalised root-mean-square deviation (NRMSD) less than 0.03.

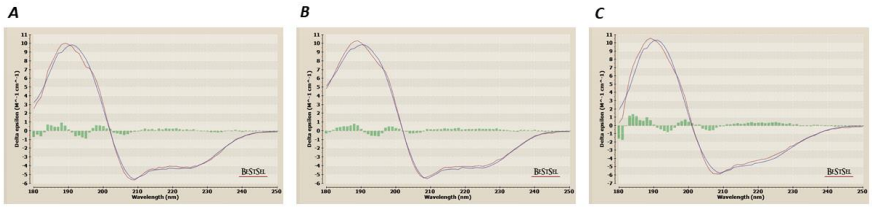

Figure 5.17. BeStSel modelling of far-UV spectra of wild-type *Ec*-MnSOD and its S126D and S126W mutants.

A, wild-type *Ec*-MnSOD. ***B***, *Ec*-MnSOD-S126D. ***C***, *Ec*-MnSOD-S126W. Conditions as described in caption to Figure 5.10. Red line traces the experimental data; the blue line is the calculated spectrum. Table 5.7 summarises the fitting parameters. BeStSel: https://bestsel.elte.hu/index.php

Turning attention now to thermal stability, CD spectra were measured over the temperature range 20 to 100 °C for *Ec*-MnSOD-S126W. Figure 5.18A (far-UV) CD spectra shows that some secondary structure is still present at 73 °C, but the near-UV CD spectra shown in Figure 5.18B reveals that aromatic signals from residues Trp (285-295 nm) and Tyr and Phe (250-280 nm) are lost at 53 °C, most signal is lost at 63 °C, and all signal is lost at 73 °C. The N-terminal domain has 5 Phe and Tyr, whereas the C-terminal domain has 10 of these residues. The near uv-CD data are consistent with the DSC results, where reversible transition X is due to separation of the domain interface, transition Y is due unfolding of the aromatic-residue-rich C-terminal domain and transition Z is due unfolding of the relatively aromatic-residue-poor N-terminal domain.

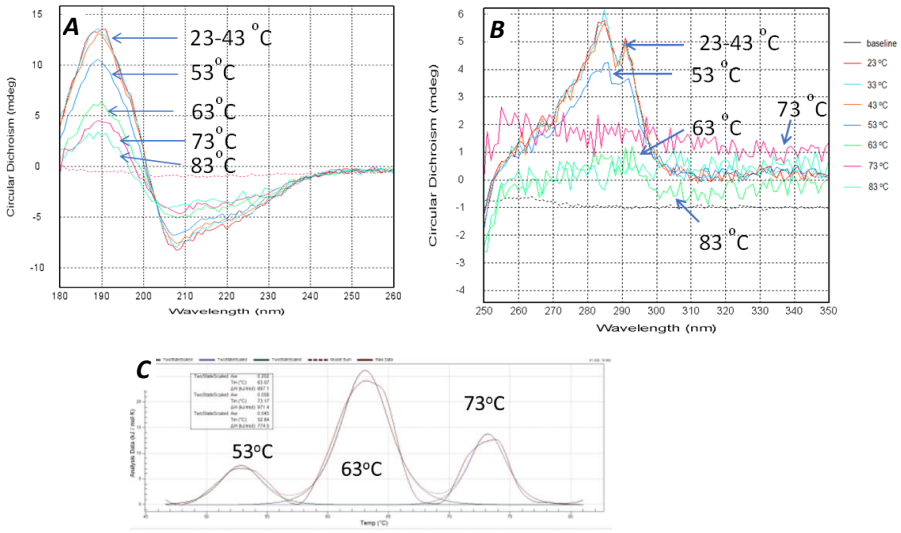

Figure 5.18. Circular dichroism spectra of *Ec*-MnSOD-S126W as a function of temperature.

A, Far-uv and ***B***, near-UV circular dichroism spectra of *Ec*-MnSOD-S126W at 23 to 83 °C. Measurement performed with nominal protein concentration of 0.2 mg/mL (8.7 µM per subunit) in 50 mM phosphate buffer at pH 7.8 in a 1 mM cell. For reference, the DSC thermogram is shown in frame ***C***.

Taken together, the X-ray structure of *Ec*-MnSOD-S126W, along with DSC, AUC and CD data, indicate that the C-terminal tail is flipped out in the solution state and the protein is mostly monomeric. In addition, the loss of helical structure and gain in beta-sheet content in solution for the S126W mutant, compared to wild-type enzyme and its S126D mutant, indicate that the C-terminal tail (residues 181-205) does not adopt in solution to any significant extent the pair of α-helices that are observed in the dodecameric species seen in the crystalline state.

5.5 Kinetic and thermodynamic aspects of *Ec*-MnSOD-S126W domain swapping

Figure 5.8B and 5.8C showed, respectively, the residues in contact in the canonical dimer and the domain-swapped dimer of *Ec*-MnSOD-S126W; Figure 4.4 showed residues in contact for the canonical dimers of wildtype *Ec*-MnSOD and its S126D mutant; and Table 5.4 summarised the areas in contact and their interfacial free-energies, as calculated by PISA (pdbe.org/pisa). For *Ec*-MnSOD-S126W the canonical dimer interface, although greater than that of wild-type enzyme due to contacts from the repositioned loop 179-183 of the C-terminal domain, is nonetheless substantially weaker by a factor of ~2, due to partial separation and reorientation (Figure 5.6). This weaker interaction is consistent with AUC observations of predominantly monomeric species in solution for *Ec*-MnSOD-S126W.

On the other hand, as documented in Table 5.4, the domain-swapped interface of *Ec*-MnSOD-S126W is very large (~25% of the surface area is buried) with a correspondingly very large free-energy of association (-187 kJ mol^{-1}). So, why is this dimer, or the dodecameric association, not seen in solution? The circular dichroism data indicated a substantial loss of helical content for *Ec*-MnSOD-S126W compared to wild-type enzyme and its S126D mutant. This loss was attributed to loss of helical structure of the largely hydrophobic C-terminal domain of monomeric species in solution. A rough estimate of the entropic contribution to the free energy of folding into a well-ordered helical domain can be calculated as

$$-T\Delta S = -n\,RT \ln W \qquad (33)$$

where n is the number of residues, R = 8.314 J mol^{-1} K^{-1}, T = 298 K, and W is the number of configurations of each amino acid. W can be calculated as the product of the number of allowed conformations of backbone φ and ψ angles (roughly 2.5 for α, β and inverse α), the number of allowed conformations for side-chain χ_1 and χ_2 (3 each) for a total of 27. This leads

then to $-T\Delta S \approx -200$ kJ mol^{-1}. The enthalpic contribution to the free energy of folding from hydrogen-bonding in the α-helices is compensated by the loss of hydrogen bonding to water and background ions. Very roughly then, this entropic contribution can be equated to the free energy of folding and to the free energy of activation. With respect to thermal energy, $RT \approx$ 2.5 kJ mol^{-1}, association into a domain-swapped form will be very slow, that is of the time scale of crystallisation (many weeks here).

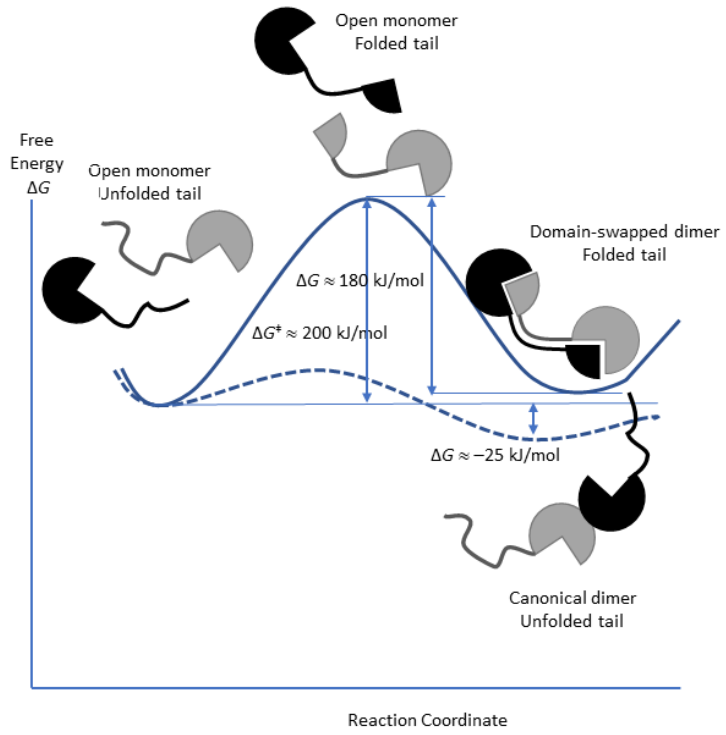

Figure 5.19. Interplay of kinetic and thermodynamic factors in oligomerisation of *Ec*-MnSOD-S126W.

The free energy of activation is roughly estimated as ~200 kJ mol^{-1}. The free energy of association of the domain swapped dimer is estimated by PISA to be ~187 kJ mol^{-1} from the state where the C-terminal domain of a monomer is folded in solution.

5.6 Concluding remarks

The S126W mutation at the dimer interface and also near to the interdomain interface produced the desired monomeric protein in solution. However, the bulky Trp126 group also caused changes to the conformation of the loop preceding the C-terminal pair of helices, residues 181-205, which in wild-type protein tucks back into the structure to create a topological knot. In the crystal structure of *Ec*-MnSOD-S126W, the canonical dimer interface is substantially weakened and rearranged. The steric bulk of Trp126 clashes with Trp169 and shifts the loop leading into the C-terminal tail, so that this tail flips out and domain-swaps with an adjacent molecule to create a dodecameric species in the crystalline state, traces of which are observed by AUC. Relative to wild-type enzyme, the S126W mutant showed an unusual three-stage unfolding of the protein, as observed by DSC. In addition, CD spectroscopy indicated that the S126W mutant had substantially different secondary structure and tertiary structure compared to wild-type enzyme. The X-ray structure and the solution-state DSC and CD data together point to the steric bulk of the Trp126 perturbing the loop that leads into the C-terminal tail. Moreover, the data suggest that in solution this tail is unable to tuck into its parent molecule, and likely has adopted a two-stranded beta sheet conformation.

The monomeric nature of *Ec*-MnSOD-S126W and consequent loss of Glu170 in the active site of the enzyme, along with a perturbed active site where Gln146 has moved, leads to this mutant being enzymatically dead. The data here point to Glu170 being a key part of the active site. As with the S126D mutant, Glu170 cannot be ruled out as the site of protonation.

Chapter 6 Conclusions and Perspectives

As given in section 2.9, I proposed to study the structure of interface mutants of *E. coli* MnSOD, specifically the Ser126Asp and Ser126Trp mutants, to investigate the roles of Glu170. This Glu170 is absolutely conserved across all MnSODs and FeSODs, which all share a common dimer structure. The Glu170 from one subunit forms part of the active site of the other subunit of the canonical dimer and is hypothesised to be part of a proton shuttle that delivers a proton by a Grotthuis proton-hopping mechanism through water molecules to the superoxide as it is reduced to peroxide by electron transfer from the Mn(II) centre. To achieve the goal, Ser126 which hydrogen bonds to itself across the dimer interface, was mutated with the intent to generate a monomeric species, which would lead to loss of SOD activity, if the Glu170 was the key factor. In addition, there had been no reports to date on generating monomeric MnSOD by mutating a non-active site residue to disrupt the canonical dimeric MnSOD interface.

To achieve the main goal, there were some specific questions outlined in section 2.9 and repeated below guiding this research:

Research Questions

1. What are the structures of the MnSOD-S126D and MnSOD-S126W mutants? Are they dimeric or monomeric?
2. If the structures are monomeric, what will be the effects on the enzyme activity?
3. If the structures are monomeric, what is the effect of propionic acid or carboxylic acid addition, to complement loss of Glu170 interacting with metal ligand His171, into the activity and the structure of the mutant?
4. What level of cooperative behaviour exists between the subunits of the obligate dimer pair? Are there any potential communication pathways between subunits of the dimer? Does the bridge of Glu170 provide a proton shuttle?
5. What are the proposed potential proton-transfer pathways into the active site based on structural analysis? Can it explain why catalysis occurs near diffusion limits in MnSOD?
6. Where is the site of redox-coupled proton uptake located and whether or not there are multiple sites of proton uptake? Which residues are associated with pH-dependent behaviour?

The sections below are aligned approximately with these research questions, except that the unexpected structures of the mutants did not allow questions 5 and 6 to be addressed directly.

However, there is no evidence collected that gives a negative answer to the role of Glu170 as the residue involved in proton uptake and delivery. Glu170 hydrogen bonds to His171 of the adjacent subunit for the S126D and S126W mutants very similarly to that observed for wild-type *Ec*-MnSOD but at conditions of assay for the S126W mutant, the molecule is monomeric and inactive with the crystal structure revealing substantially different positioning of Gln146 in the active site. For the S126D mutant, at conditions of assay at pH >7, the structure is increasingly dimeric. The low activity is therefore assigned to the negative charge of the aspartate affecting the redox potential of the Mn centre so that a cycle of superoxide dismutation stalls with the enzyme unable to oxidise superoxide. At pH < 7, the S126D mutant is primarily monomeric and residual activity is approximately zero. In these cases, no conclusions can be made concerning potential proton pathways or the site of proton uptake and delivery.

Conversely if the S126D mutant is monomeric, then Glu170 appears essential for activity, as it is no longer present in the active site. The complementation experiments failed due either to the charge effect of the negatively charged Asp126 that might kill activity as a dimer or to failure of propionic acid to complement the loss of Glu170 in the active site.

6.1 Structure of *Ec*-MnSOD-S126D and *Ec*-MnSOD-S126W

Charge repulsion *versus* steric bulk is based on mutants *Ec*-MnSOD-S126D and *Ec*-MnSOD-S126W, respectively, and results are compared to wild-type *Ec*-MnSOD. The analytical ultracentrifugation results show that *Ec*-MnSOD-S126D is mostly dimeric, especially at higher pH (Table 4.5), whereas for *Ec*-MnSOD-S126W the tryptophan enforces a mostly monomeric species in the solution state.

At ambient temperature, the circular dichroism (CD) spectra of the *Ec*-MnSOD-S126D mutant are very similar to those of wild-type enzyme in the far-UV, which reports on secondary structure, and in the near-UV, which reports on tertiary structure, establishing that this mutant does not have significantly perturbed secondary or tertiary structure. Conversely, CD spectroscopy indicates that the *Ec*-MnSOD-S126W mutant has substantially different secondary structure and tertiary structure compared to wild-type enzyme. In addition, modelling of the far-UV CD spectra indicates that the changes in ellipticity observed for *Ec*-

MnSOD-S126W are consistent with partial loss of helical structure and increase in beta-sheet content compared to wild-type and the S126D mutant. As discussed below, these changes are associated with tertiary structure change.

Based on differential scanning calorimetry measurements, *Ec*-MnSOD-S126D and *Ec*-MnSOD -S126W mutants are less stable than the wild-type. These mutants denature more easily, with ~10 ^{o}C reduction in "melting" temperature relative to the wild-type enzyme but the S126W mutant has a very different melting profile. For *Ec*-MnSOD-S126D, likewise MnSOD wild-type, the thermogram can be modelled with two partially overlapping Gaussian curves. However, the *Ec*-MnSOD-S126W endotherms require three symmetrical two-state curves with minor overlapping. The differences in the Gaussian models for the S126W mutant indicate a different protein structure for the S126W mutant relative to wild-type *Ec*-MnSOD and its S126D mutant in the aqueous solution state.

Based on the analysis of the protein crystal structures of *Ec*-MnSOD-S126D at pH 6.8, 8.7, and 9.1 (with azide adduct), there is consistently minimal structural changes to the active site and its water structure caused by the S126D mutation. The interface between subunits of the dimer is highly conserved, and the orientation of the other subunit across the dimer interface changes only slightly and still retains the canonical dimer of all Mn- and FeSODs.

The S126W mutation produced the desired monomeric protein in solution, and consistent with this, in the crystal structure of *Ec*-MnSOD-S126W, the canonical dimer interface is substantially weakened and rearranged. The bulky Trp126 group causes changes to the conformation of the loop bearing Trp126 that affect the loop preceding the C-terminal pair of helices, residues 181-205. This tail no longer folds into the molecule, but instead is directed away from the protein and inserts (domain-swapped) into a neighbouring molecule to create observed dodecameric species in the crystalline state, traces of which are observed by AUC. The solution-state DSC and CD data together support the X-ray structure and point to the steric bulk of the Trp126 perturbing the loop that leads into the C-terminal tail.

6.2 Effect of mutations on enzyme activity

The stereochemistry of the active site, the dimer interface and Glu170, and the water structure observed for *Ec*-MnSOD-S126D are strongly conserved compared to wild-type *Ec*-MnSOD. So why does the mutation lead to the loss of catalytic activity?

In detail, the protein crystal structures show that the Asp126 carboxylate group sits approximately 3.7 Å from Trp169, which makes a short 3.1 Å n-π^* contact to the Mn-coordinated hydroxide. This is emphasised by the extreme metal specificity of *Ec*-MnSOD and *Ec*-FeSOD, as the Mn(II)/Mn(III) redox couple is carefully controlled by metal ligands and by the second and third coordination shells. First, assuming the protein remains dimeric at conditions of assay for enzyme activity (see Table 4.5 for calculations of percent dimer in solution at assay concentration of enzyme) evidence, the electrostatic effect of the aspartate is the unexpected factor to cause loss of superoxide dismutase activity of *Ec*-MnSOD-S126D.

The second assumption that may cause deactivation by the S126D mutant is that the protein is monomeric at conditions of assay. Based on analytical ultracentrifugation, *Ec*-MnSOD-S126D is less stable as a dimer than the wild-type. Considering that the protein concentration used in the activity test experiment is very dilute (11-54 nM), there is no concentration dependence of activity observed, which gives a limited concentration window. Analytical ultracentrifugation has helped to observe quaternary structure, but this also may not pertain at the usually much lower concentrations of enzymatic assay. So, the loss of catalytic activity of *Ec*-MnSOD-S126D mutant may possibly be due to loss of dimer. The activity of the S126D mutant at low pH (6.0) is less than that at high pH (7.8), which is relevant to the analytical ultracentrifugation results that show more partially monomeric enzyme at low pH.

There is substantial change in the active site of the enzyme upon the S126W mutation. Due to movement of Trp169, Gln146 of *Ec*-MnSOD-S126W moves so that its amide carbonyl group is in hydrogen-bonding contact with water-derived ligand in the S126W mutant and not the amide NH_2 group as in wild-type enzyme. Thus, this water-derived ligand is almost certainly water and not hydroxide. This is contrary to evidence that the coordinated hydroxide remains as hydroxide for both Mn(II) and Mn(III) states, as revealed in the ultra-high resolution (0.90 Å) structures of the highly active *Ec*-MnSOD-Y174F mutant in its Mn(II) and Mn(III) states. Hence, no activity is expected for the *Ec*-MnSOD-S126W mutant.

6.3 Complementation experiments

Based on the SOD assay, a more than two-fold increase in activity of *Ec*-MnSOD-S126D was observed on addition of 10-20 mM propionic acid. At the pH of measurement, pH 7.8, analytical ultracentrifugation measurements suggest that at assay concentrations 25-50% of this mutant is dimeric. Only a small 10% increase in activity of wild-type enzyme was observed in parallel control experiments. Thus, there appears to be a significant recovery of activity on adding propionate to replace the missing Glu170 in the active site of monomeric protein. Propionic acid might be a poor choice of carboxylate-bearing molecule where a better choice might have been a carboxylate at one end of a short alkyl chain and a polar uncharged at the other end to interact better with water. Therefore, the complementation experiments suggests that Glu170 is the site of proton uptake and delivery. This is consistent with the critical analysis made in Chapter 2 that the generally accepted site of proton uptake and delivery, the Mn-coordinated hydroxide, is incorrect.

Knowing that the S126W mutant is monomeric at assay conditions, that the active-site structure has significantly changed, and that the enzyme is inactive, the complementation experiment was not run. Moreover, there was not have enough sample to do additional SOD assays. Preparing *Ec*-MnSOD-S126W protein was much more challenging relative to wild-type *Ec*-MnSOD and its S126D mutant. Therefore, it is almost certain that the addition of propionate acid would not complement loss of Glu170 interacting with metal ligand His171, as there is substantial change in the active site of the enzyme upon the S126W mutation.

6.4 pH-dependent behaviour

The AUC measurements signal a pH-dependent behaviour of *Ec*-MnSOD-S126D since it gives a higher proportion of monomeric protein at pH 6.0 compared to pH 7.8 in the solution state. From the X-ray protein structure analysis of *Ec*-MnSOD-S126D at different pH, can structural differences be seen at the molecular level in the crystalline state, and can residues be identified that are associated with pH-dependent behaviour? Obviously, there is direct dependence of the enzyme on pH as well as on temperature to the structure and function, and more specifically to the particular level of the alteration on the interaction between the amino acids that compose the protein chains.

By superimposing the structure of *Ec*-MnSOD-S126D at various pH, it is observed that at pH 6.8 and pH 8.7, compared to pH of optimum activity for wild type enzyme of 7.8, Asp126 shares approximately the same conformation, where like the wild-type enzyme with Ser126, it hydrogen bonds to itself, but Asp126 also hydrogen bonds to the peptide NH across the dimer interface (Figure 4.5). However, at the highest pH of pH 9.1, in the partial azido structure, Asp126 adopts a pair of different conformations (Figure 4.5). *Ec*-MnSOD-S126D still preserves hydrogen bonding to the peptide NH of Asp126 but the disorder leads to the interface being intrinsically asymmetric, like the wild-type enzyme with Ser126. Moreover, the carboxylate oxygens are sufficiently distant to each other to infer that there is no longer shared proton between the two Asp126. This is consistent with the PropKa3.1 (Olsson et al., 2011) prediction of an average pK_a for Asp126 in dimeric *Ec*-MnSOD-S126D of 9.64 (pH6.8), 9.99 (pH 8.7) and 9.61 (pH 9.1, azide structure).

6.5 Cooperative behaviour

The results of an analysis of electrostatic surfaces of *Ec*-MnSOD and the S126D and S126W mutants, with $Mn^{2+/3+}$/OH^-/azide stripped out, shows that the dimeric *Ec*-MnSOD-S126D dimer has positive substrate-binding pockets, with one of its subunits consistently less positive than the other subunit. The pK_a calculation and electrostatic surfaces reveal two different states in the *Ec*-MnSOD-S126D dimer structure: that is Mn^{III} in one subunit and Mn^{II} in the other subunit, which is consistent across the three *Ec*-MnSOD-S126D dimer structures, and also for wild-type *Ec*-MnSOD-S126D.

The signatures are indicated by criss-cross of the Mn and Glu170 alternative charges. First, the positive electrostatic potential in the substrate-binding pocket is associated with Mn as Mn^{II}, where the Glu170 (from the other subunit) is calculated to be protonated. Second, the less positive electrostatic potential in the substrate-binding pocket is associated with Mn as Mn^{III}, where the Glu170 (from the other subunit) is calculated to be deprotonated. Both states then result in an overall net zero charge in the active site of protein, as shown below:

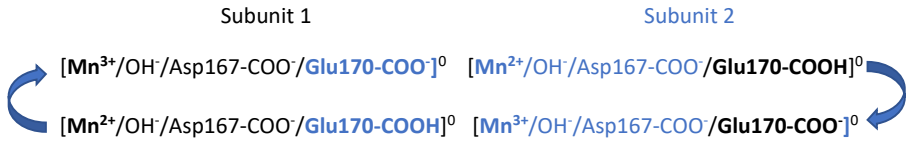

Does the bridge of Glu170 provide a proton shuttle? The calculated pK_a of Glu170 (pH 7.0 ±1.5) and derived electrostatic potentials of *Ec*-MnSOD-S126D are suggestive of a role for Glu170 in shuttling a proton onto the nascent peroxo moiety. This cooperative behaviour also occurs between the subunits of the obligate dimer pair for active *Ec*-azido-MnSOD-Y174F mutant, where in one subunit azide is bound to Mn^{3+} while in the other subunit no azide is bound and distances to of the water-derived ligand are indicative of Mn^{2+}. Here the hydrogen bonding of a water molecule to azide, a proxy for superoxide, completes a water relay to the absolutely conserved Glu170. The electrostatic surface results are also in line with a study that substitution of Glu170 with Ala lead to an inactive MnSOD (M. M. Whittaker & Whittaker, 1998b). However, in the absence of an X-ray structure, the lack of activity may be due to a variety of factors: (i) the protein is no longer dimeric (which suggests that Glu170 in intrinsically required as a proton shuttle and activity could be restored by complementation – the foundation of my work on the *Ec*-MnSOD mutants; (ii) the protein is dimeric, again implicating Glu170 in a proton shuttle; (iii) the loss of the hydrogen bond between Glu170 and His171 changes the redox potential at the Mn centre so that the enzyme cannot complete a catalytic cycle; (iv) the loss of Glu170 changes structure at the active site causing the enzyme to be inactive.

6.6 Proton transfer pathway

The proposed mechanism of the proton transfer pathway is related with the two different states of the dimer in section 6.5. Overall, there are two proton uptake steps in the catalytic cycle. First, there is a net +1 charge at the manganese centre consisting of $[Mn^{3+}/OH^{-}/Asp167\text{-}COO^{-}]^{+1}$, and an unprotonated Glu170-COO^{-} that is hydrogen bonded to protein ligand His171 (see Figure 4.21). This highly positive substrate-binding pocket with Mn(III) attracted anion superoxide substrate to diffuse to give six coordination. To maintain an overall net neutral charge, a proton is transferred to Glu170 producing Glu170-COOH. Finally, the electron is

transferred from superoxo to Mn(III) to form Mn(II) and producing an oxygen molecule that then diffuses from the active site. The overall entire net charge remains neutral.

Second, the first step leaves active-site neutral as $[Mn^{2+}/OH^{-}/Asp167\text{-}COO^{-}]^{0}$ and protonated Glu170-COOH. However, as described in Section 6.5, the substrate-binding pocket is still basic but less positive and still attractive for and leads the superoxide to enter. Thus, the second half reaction begins with the entry of the superoxide ion. Now there is a net of -1 which is very unstable and leads to the Mn(II) transferring the electron to the superoxide, via an outer-sphere mechanism, to forms peroxo which is hydrogen bonded to a water molecule connected to the protonated Glu170-COOH from the other subunit. Here, a second proton is transferred concomitantly by a Grotthuss proton-hopping mechanism from Glu170-COOH onto the nascent peroxo species to form a hydroperoxo ligand to the Mn(III). This ligand leaves the active site and picks up another proton from solvent to produce hydrogen peroxide.

Proton delivery to the nascent peroxo by a Grotthuss proton-hopping mechanism as previously described enables the superoxide dismutase reaction to operate close to diffusion rate, unlike the conventional view which has many barriers where the proton has to pass through the gateway Tyr34 and Gln146 prior to protonate the hydroxo ligand to form a water ligand. So, the participation of Glu170 in an outer-sphere proton transfer avoids protons passing through the narrow hole at the base of the substrate-access funnel that can lead to a traffic problem, and thereby accommodates the very fast rate of the reaction.

6.7 Redox-coupled proton uptake site

For *Ec*-MnSOD-S126W, Glu170 hydrogen bonds to His171 of the adjacent subunit very similarly to that observed for wild-type *Ec*-MnSOD and its S126D mutant, but at conditions of assay the molecule is likely monomeric and inactive with the crystal structure revealing substantially different positioning of Gln146 in the active site. For the S126D mutant, if at conditions of assay the structure is dimeric, then the low activity is assigned to the negative charge of the aspartate affecting the redox potential of the Mn centre so that a cycle of superoxide dismutation stalls with the enzyme unable to oxidise superoxide. In these cases, no conclusions can be made concerning potential proton pathways or the site of proton uptake and delivery.

Conversely if the S126D mutant is monomeric, then Glu170 appears essential for activity, as it is no longer present in the active site. The complementation experiments succeeded only in part for propionate anion to complement the loss of Glu170 in the active site of monomeric *Ec*-MnSOD-S126D, due to the charge effect of the negatively charged Asp126 that reduced activity of the dimer.

6.8 Final remarks

The question of '*What is the role of Glu170 from adjacent subunit in proton-coupled electron transfer of* Ec-*MnSOD?*' has driven this study and this has not been answered for more than two decades since Whittaker (1998b) found that Glu170Ala led to inactive enzyme.

This study is the first report where mutation of *Ec*-MnSOD successfully produces partially and fully monomeric species (*Ec*-Mn-SOD-S126D and *Ec*-MnSOD-S126W, respectively) in aqueous solution state with their X-ray crystal structures solved. The single substitution is targeted at a non-active residue at the dimer interface with the intention to enforce monomeric MnSOD at dimer interface.

But the best laid plans went awry for both mutants. First, while the Ser126Asp mutation was intended to break the dimer apart by charge repulsion, this mutation is, in fact, accommodated with only relative small changes in secondary, tertiary and quaternary structures and the mutated enzyme retains its active site. Interestingly, the catalytic activity of the S126D mutant is almost but not completely abolished, with 4.2 % of that of the wild-type enzyme. This leaves two possibilities for the enzyme's loss of activity. First, the electrostatic effect of the Asp126 to Trp169 as the guardian to MnSOD's redox potential and metal selectivity. Secondly, the S126D deactivation may be due to loss of dimeric structure at the conditions of assay, meaning loss of Glu170 from other subunit and its predicted role in proton transfer. Fortunately, according to the pK_a and the surface charge analysis, the structures of *Ec*-MnSOD-S126D give insight about the proton-transfer pathway. The results indicated that the Glu170 has a key role as part of the proton shuttle that delivers a proton by a Grotthuss proton-hopping mechanism, which furthermore supports the mechanism of proton-coupled electron transfer in this study.

The second plan, steric bulk tryptophan for the *Ec*-MnSOD-S126W mutant changes significantly the secondary, tertiary, and quaternary structures, along with the active site, and these lead to complete deactivation. Although the dimer is observed in the crystalline state, conformation changes at the C-terminal tails are accommodated by domain swapping with the other molecules to form a dodecamer in ther crystalline state. However, the mutation of Ser126 to Trp illustrates the *Law of Unintended Consequences*,(Norton, n.d.) where a single mutation has successfully produced a new quaternary structures. I believe that this is a rare illustration where a single mutation has "evolved" complexity. Evolving complexity does not require multiple mutations. Here one mutation to a conserved dimer interface led to altered tertiary structure and a completely different quaternary association, although coupled with a complete loss of activity in for *Ec*-MnSOD-S126W.

Structural changes of monomeric *Ec*-MnSOD-S126W at various temperatures showed interesting behaviour data when investigated by DSC and circular dichroism measurements. These results enabled us to explain what is going on with *Ec*-MnSOD-S126W in aqueous solution due to environmental changes.

6.9 Potential future work

Taking into account all that has been obtained from this research, future work should be able to produce a monomeric *Ec*-MnSOD mutant that preserves the stereochemistry of the active site without side effects or disruption caused by amino acid substitution. Possibly the larger-sized Glu in place of Asp at position 126 would give both steric bulk and charge repulsion to enhance monomer formation, as well as placing the negative charge of the Glu carboxylate group further from Trp169.

Secondly, in regards to the question 3 (*If the structures are monomeric, what is the effect of propionic acid or carboxylic acid addition, to complement loss of Glu170 interacting with metal ligand His171, into the activity and the structure of the mutant?*), and the mutant gained with desired characteristic in previous paragraph, the study on the effect of propionic acid or carboxylic acid addition to complement loss of Glu170 is still relevant and essential to do. It is hoped that the future work can have X-ray protein structures that capture the interaction of the added propionic acid or other carboxylic acid with the His171 metal ligand.

References

Abreu, I. A., & Cabelli, D. E. (2010). Superoxide dismutases—a review of the metal-associated mechanistic variations. *Biochimica et Biophysica Acta (BBA) - Proteins and Proteomics, 1804*(2), 263-274. https://doi.org/10.1016/j.bbapap.2009.11.005

Abreu, I. A., Hearn, A., An, H., Nick, H. S., Silverman, D. N., & Cabelli, D. E. (2008). The kinetic mechanism of manganese-containing superoxide dismutase from Deinococcus radiodurans: a specialized enzyme for the elimination of high superoxide concentrations. *Biochemistry, 47*(8), 2350-2356.

Abreu, I. A., Rodriguez, J. A., & Cabelli, D. E. (2005). Theoretical studies of manganese and iron superoxide dismutases: superoxide binding and superoxide oxidation. *The Journal of Physical Chemistry B, 109*(51), 24502-24509.

Ansenberger-Fricano, K., Ganini, D., Mao, M., Chatterjee, S., Dallas, S., Mason, R. P., . . . Bonini, M. G. (2013). The peroxidase activity of mitochondrial superoxide dismutase. *Free Radical Biology and Medicine, 54*, 116-124.

Asensio, A. C., Marino, D., James, E. K., Ariz, I., Arrese-Igor, C., Aparicio-Tejo, P. M., . . . Moran, J. F. (2011). Expression and localization of a Rhizobium-derived cambialistic superoxide dismutase in pea (Pisum sativum) nodules subjected to oxidative stress. *Molecular plant-microbe interactions, 24*(10), 1247-1257.

Azadmanesh, J., & Borgstahl, G. E. J. A. (2018). A review of the catalytic mechanism of human manganese superoxide dismutase. *Antioxidants, 7*(2), 25.

Azadmanesh, J., Trickel, S. R., & Borgstahl, G. E. (2017). Substrate-analog binding and electrostatic surfaces of human manganese superoxide dismutase. *Journal of structural biology, 199*(1), 68-75.

Bedard, K., Lardy, B., & Krause, K.-H. (2007). NOX family NADPH oxidases: not just in mammals. *Biochimie, 89*(9), 1107-1112.

Borgstahl, G. E., Parge, H. E., Hickey, M. J., Beyer Jr, W. F., Hallewell, R. A., & Tainer, J. A. (1992). The structure of human mitochondrial manganese superoxide dismutase reveals a novel tetrameric interface of two 4-helix bundles. *Cell, 71*(1), 107-118.

Bull, C., & Fee, J. A. (1985). Steady-state kinetic studies of superoxide dismutases: properties of the iron containing protein from Escherichia coli. *Journal of the American Chemical Society, 107*(11), 3295-3304.

Bull, C., Niederhoffer, E. C., Yoshida, T., & Fee, J. A. (1991). Kinetic studies of superoxide dismutases: properties of the manganese-containing protein from Thermus thermophilus. *Journal of the American Chemical Society, 113*(11), 4069-4076.

Carlioz, A., & Touati, D. (1986). Isolation of superoxide dismutase mutants in Escherichia coli: is superoxide dismutase necessary for aerobic life? *The EMBO journal, 5*(3), 623-630.

Crane, B. R., Arvai, A. S., Ghosh, D. K., Wu, C., Getzoff, E. D., Stuehr, D. J., & Tainer, J. A. (1998). Structure of nitric oxide synthase oxygenase dimer with pterin and substrate. *Science, 279*(5359), 2121-2126.

DeLano, W. L. (2002). Pymol: An open-source molecular graphics tool. *CCP4 Newsletter on Protein Crystallography, 40*(1), 82-92.

Dolinsky, T. J., Nielsen, J. E., McCammon, J. A., & Baker, N. A. (2004). PDB2PQR: An automated pipeline for the setup of Poisson–Boltzmann electrostatics calculations. *Nucleic acids research, 32*(suppl_2), W665-W667.

Edwards, R. A., Baker, H. M., Whittaker, M. M., Whittaker, J. W., Jameson, G. B., & Baker, E. N. (1998). Crystal structure of *Escherichia coli* manganese superoxide dismutase at 2.1-Å resolution. *Journal of Biological Inorganic Chemistry, 3*(2), 161-171. 10.1007/s007750050217

Edwards, R. A., Whittaker, M. M., Whittaker, J. W., Baker, E. N., & Jameson, G. B. (2001). Outer sphere mutations perturb metal reactivity in manganese superoxide dismutase. *Biochemistry, 40*(1), 15-27. 10.1021/bi0018943

Edwards, R. A., Whittaker, M. M., Whittaker, J. W., Baker, E. N., & Jameson, G. B. (2001). Removing a hydrogen bond in the dimer interface of *Escherichia coli* manganese superoxide dismutase alters structure and reactivity. *Biochemistry, 40*(15), 4622-4632.

Edwards, R. A., Whittaker, M. M., Whittaker, J. W., Jameson, G. B., & Baker, E. N. (1998). Distinct metal environment in Fe-substituted manganese superoxide dismutase provides a structural basis of metal specificity. *Journal of the American Chemical Society, 120*(37), 9684-9685.

Ekoue, D. N., He, C., Diamond, A. M., & Bonini, M. G. (2017). Manganese superoxide dismutase and glutathione peroxidase-1 contribute to the rise and fall of mitochondrial reactive oxygen species which drive oncogenesis. *Biochimica et Biophysica Acta (BBA)-Bioenergetics, 1858*(8), 628-632.

Emsley, P., Lohkamp, B., Scott, W. G., & Cowtan, K. (2010). Features and development of Coot. *Acta Crystallographica Section D: Biological Crystallography, 66*(4), 486-501.

Fridovich, I. (1997). Superoxide Anion Radical ($O_2^{\cdot-}$), Superoxide Dismutases, and Related Matters. *Journal of Biological Chemistry, 272*(30), 18515-18517.

Glorieux, C., & Calderon, P. B. (2017). Catalase, a remarkable enzyme: targeting the oldest antioxidant enzyme to find a new cancer treatment approach. *Biological Chemistry, 398*(10), 1095-1108.

Green, A. A., & Hughes, W. L. (1955). [10] Protein fractionation on the basis of solubility in aqueous solutions of salts and organic solvents. *Methods in Enzymology, 1*, 67-90.

Greenleaf, W. B., Perry, J. J. P., Hearn, A. S., Cabelli, D. E., Lepock, J. R., Stroupe, M. E., . . . Silverman, D. N. (2004). Role of hydrogen bonding in the active site of human manganese superoxide dismutase. *Biochemistry, 43*(22), 7038-7045.

Grove, L. E., & Brunold, T. C. (2008). Second-sphere tuning of the metal ion reduction potentials in iron and manganese superoxide dismutases. *Comments on Inorganic Chemistry, 29*(5-6), 134-168.

Guan, Y., Hickey, M. J., Borgstahl, G. E., Hallewell, R. A., Lepock, J. R., O'Connor, D., . . . Tainer, J. A. (1998). Crystal structure of Y34F mutant human mitochondrial manganese superoxide dismutase and the functional role of tyrosine 34. *Biochemistry, 37*(14), 4722-4730.

Hearn, A. S., Fan, L., Lepock, J. R., Luba, J. P., Greenleaf, W. B., Cabelli, D. E., . . . Silverman, D. N. (2004). Amino acid substitution at the dimeric interface of human manganese superoxide dismutase. *J Biol Chem, 279*(7), 5861-5866. 10.1074/jbc.M311310200

Hearn, A. S., Stroupe, M. E., Cabelli, D. E., Lepock, J. R., Tainer, J. A., Nick, H. S., & Silverman, D. N. (2001). Kinetic analysis of product inhibition in human manganese superoxide dismutase. *Biochemistry, 40*(40), 12051-12058.

Hearn, A. S., Stroupe, M. E., Cabelli, D. E., Ramilo, C. A., Luba, J. P., Tainer, J. A., . . . Silverman, D. N. (2003). Catalytic and structural effects of amino acid substitution at histidine 30 in human manganese superoxide dismutase: insertion of valine C gamma into the substrate access channel. *Biochemistry, 42*(10), 2781-2789. 10.1021/bi0266481

Hsieh, Y., Guan, Y., Tu, C., Bratt, P. J., Angerhofer, A., Lepock, J. R., . . . Silverman, D. N. (1998). Probing the active site of human manganese superoxide dismutase: the role of glutamine 143. *Biochemistry, 37*(14), 4731-4739. 10.1021/bi972395d

Imlay, J. A. (2002). How oxygen damages microbes: Oxygen tolerance and obligate anaerobiosis. In *Advances in Microbial Physiology* (Vol. 46, pp. 111-153): Academic Press. https://doi.org/10.1016/S0065-2911(02)46003-1

Janik, I., & Tripathi, G. (2013). The nature of the superoxide radical anion in water. *The Journal of Chemical Physics, 139*(1), 014302.

Krissinel, E., & Henrick, K. (2007). Inference of macromolecular assemblies from crystalline state. *Journal of Molecular Biology, 372*(3), 774-797.

Laemmli, U. (1970). SDS-page Laemmli method. *Nature, 227*, 680-685.

Lancaster, V. L., LoBrutto, R., Selvaraj, F. M., & Blankenship, R. E. (2004). A cambialistic superoxide dismutase in the thermophilic photosynthetic bacterium Chloroflexus aurantiacus. *Journal of Bacteriology, 186*(11), 3408-3414.

Laue, T. M. (1992). Computer-aided interpretation of analytical sedimentation data for proteins. *Analytical ultracentrifugation in biochemistry and polymer science*, 90-125.

Lebowitz, J., Lewis, M. S., & Schuck, P. (2002). Modern analytical ultracentrifugation in protein science: a tutorial review. *Protein Science, 11*(9), 2067-2079.

Leveque, V. J., Stroupe, M. E., Lepock, J. R., Cabelli, D. E., Tainer, J. A., Nick, H. S., & Silverman, D. N. (2000). Multiple replacements of glutamine 143 in human manganese superoxide dismutase: effects on structure, stability, and catalysis. *Biochemistry, 39*(24), 7131-7137.

McCord, J. M. (1976). Iron-and manganese-containing superoxide dismutases: structure, distribution, and evolutionary relationships. In *Iron and Copper Proteins* (pp. 540-550): Springer.

McCord, J. M., & Fridovich, I. (1969). Superoxide dismutase an enzymic function for erythrocuprein (hemocuprein). *Journal of Biological Chemistry, 244*(22), 6049-6055.

McCord, J. M., & Fridovich, I. (1988). Superoxide dismutase: the first twenty years (1968-1988). *Free Radical Biology & Medicine, 5*(5-6), 363.

Miller, A.-F., Padmakumar, K., Sorkin, D. L., Karapetian, A., & Vance, C. K. (2003). Proton-coupled electron transfer in Fe-superoxide dismutase and Mn-superoxide dismutase. *Journal of Inorganic Biochemistry, 93*(1), 71-83.

Muller, F. L., Lustgarten, M. S., Jang, Y., Richardson, A., & Van Remmen, H. (2007). Trends in oxidative aging theories. *Free Radical Biology and Medicine, 43*(4), 477-503.

Murshudov, G. N., Vagin, A. A., & Dodson, E. J. (1997). Refinement of macromolecular structures by the maximum-likelihood method. *Acta Crystallographica Section D: Biological Crystallography, 53*(3), 240-255.

Narayana, P., Suryanarayana, D., & Kevan, L. (1982). Electron spin-echo studies of the solvation structure of superoxide ion (O2-) in water. *Journal of the American Chemical Society, 104*(13), 3552-3555.

Norton, R. (n.d.). *Unintended consequences.* Retrieved January 11, 2023, from https://www.econlib.org/library/Enc/UnintendedConsequences.html

Oberley, L. W. (2005). Mechanism of the tumor suppressive effect of MnSOD overexpression. *Biomedicine & Pharmacotherapy, 59*(4), 143-148.

Parker, M., Blake, C., Barra, D., Bossa, F., Schinina, M., Bannister, W., & Bannister, J. (1987). Structural identity between the iron-and manganese-containing superoxide dismutases. *Protein Engineering, 1*(5), 393-397.

Perry, J. J., Hearn, A. S., Cabelli, D. E., Nick, H. S., Tainer, J. A., & Silverman, D. N. (2009). Contribution of human manganese superoxide dismutase tyrosine 34 to structure and catalysis. *Biochemistry, 48*(15), 3417-3424. 10.1021/bi8023288

Quint, P. S., Domsic, J. F., Cabelli, D. E., McKenna, R., & Silverman, D. N. (2008). Role of a glutamate bridge spanning the dimeric interface of human manganese superoxide dismutase. *Biochemistry, 47*(16), 4621-4628.

Roth, J. P., Yoder, J. C., Won, T.-J., & Mayer, J. M. (2001). Application of the Marcus cross relation to hydrogen atom transfer reactions. *Science, 294*(5551), 2524-2526.

Schuck, P. (2000). Size-distribution analysis of macromolecules by sedimentation velocity ultracentrifugation and lamm equation modeling. *Biophysical Journal, 78*(3), 1606-1619.

Schuck, P., Perugini, M. A., Gonzales, N. R., Howlett, G. J., & Schubert, D. (2002). Size-distribution analysis of proteins by analytical ultracentrifugation: strategies and application to model systems. *Biophysical Journal, 82*(2), 1096-1111.

Sedlak, E., & Musatov, A. (2017). Inner mechanism of protection of mitochondrial electron-transfer proteins against oxidative damage. Focus on hydrogen peroxide decomposition. *Biochimie, 142*, 152-157.

Shigenaga, M. K., Hagen, T. M., & Ames, B. N. (1994). Oxidative damage and mitochondrial decay in aging. *Proceedings of the National Academy of Sciences, 91*(23), 10771-10778.

Smith, M. W., & Doolittle, R. F. (1992). A comparison of evolutionary rates of the two major kinds of superoxide dismutase. *Journal of Molecular Evolution, 34*(2), 175-184.

Stadtman, E. R., & Berlett, B. S. (1998). Reactive oxygen-mediated protein oxidation in aging and disease. *Drug Metabolism Reviews, 30*(2), 225-243.

Tabares, L. C., Bittel, C., Carrillo, N., Bortolotti, A., & Cortez, N. (2003). The single superoxide dismutase of Rhodobacter capsulatus is a cambialistic, manganese-containing enzyme. *Journal of Bacteriology, 185*(10), 3223-3227.

Thomas, D. C. (2018). How the phagocyte NADPH oxidase regulates innate immunity. *Free Radical Biology and Medicine, 125*, 44-52.

Touati, D. (1983). Cloning and mapping of the manganese superoxide dismutase gene (sodA) of Escherichia coli K-12. *Journal of Bacteriology, 155*(3), 1078-1087.

Vagin, A., & Teplyakov, A. (1997). MOLREP: an automated program for molecular replacement. *Journal of Applied Crystallography, 30*(6), 1022-1025.

Visner, G. A., Dougall, W., Wilson, J., Burr, I., & Nick, H. (1990). Regulation of manganese superoxide dismutase by lipopolysaccharide, interleukin-1, and tumor necrosis factor. Role in the acute inflammatory response. *Journal of Biological Chemistry, 265*(5), 2856-2864.

Whittaker, J. W., & Whittaker, M. M. (1991). Active site spectral studies on manganese superoxide dismutase. *Journal of the American Chemical Society, 113*(15), 5528-5540.

Whittaker, M. M., & Whittaker, J. W. (1997). Mutagenesis of a proton linkage pathway in Escherichia coli manganese superoxide dismutase. *Biochemistry, 36*(29), 8923-8931. 10.1021/bi9704212

Whittaker, M. M., & Whittaker, J. W. (1998). A glutamate bridge is essential for dimer stability and metal selectivity in manganese superoxide dismutase. *Journal of Biological Chemistry, 273*(35), 22188-22193. 10.1074/jbc.273.35.22188

Winn, M. D., Ballard, C. C., Cowtan, K. D., Dodson, E. J., Emsley, P., Evans, P. R., . . . McCoy, A. (2011). Overview of the CCP4 suite and current developments. *Acta Crystallographica Section D: Biological Crystallography, 67*(4), 235-242.

Yost, F. J., & Fridovich, I. (1976). Superoxide and hydrogen peroxide in oxygen damage. *Archives of Biochemistry and Biophysics, 175*(2), 514-519.

Zhao, Y., Xue, Y., Oberley, T. D., Kiningham, K. K., Lin, S.-M., Yen, H.-C., . . . Clair, D. S. (2001). Overexpression of manganese superoxide dismutase suppresses tumor formation by modulation of activator protein-1 signaling in a multistage skin carcinogenesis model. *Cancer Research, 61*(16), 6082-6088.

Zheng, J., Domsic, J. F., Cabelli, D., McKenna, R., & Silverman, D. N. (2007). Structural and kinetic study of differences between human and Escherichia coli manganese superoxide dismutases. *Biochemistry, 46*(51), 14830-14837.

Zhong, W., Oberley, L. W., Oberley, T. D., & St Clair, D. K. (1997). Suppression of the malignant phenotype of human glioma cells by overexpression of manganese superoxide dismutase. *Oncogene, 14*(4), 481.

Appendix A - MUHEC Approval

13/86 **Analysis of inquiry in students' conversations in the biochemistry laboratory**
Jatnika Hermawan (HEC: Southern B Application 13/86)
Department: Institute of Fundamental Sciences
Supervisor: Dr Zoe Jordens; Prof Geoffrey Jameson; Dr Gillian Norris

The Massey University Human Ethics Committee (MUHEC): Southern B considered the above application at their meeting held on Thursday 14 November 2013.

The application was provisionally approved, subject to the fulfilment of the conditions below to the satisfaction of Dr Nathan Matthews (Chair).

Please note that the Committee is always willing to enter into dialogue with applicants over the points made. There may be information that has not been made available to the Committee, or aspects of the research may not have been fully understood.

SECTION B
Q21/LETTER OF REQUEST

- Appendix 9 – it is noted that the request to conduct the research should be in the form of a formal letter, rather than an information sheet. Please reframe and provide a draft request letter.
  A draft letter is now provided as appendix 10.
- Please provide a copy of the permission letters, when received.
  The permission letters will be forwarded when received.

Q22

- Please provide further information regarding recruitment, e.g. who will make the approach to the staff and how will that be undertaken?
  The week before the lab class starts, brief details about the project will be sent to all students via the learning management system (Stream). At the start of the laboratory session in week 1, Jatnika Hermawan and Zoe Jordens will introduce the project to the students: what, when, who, why and how the project will be undertaken. To avoid potential feelings of coercion, the project will be explained in the lab without the staff involved in teaching in attendance.

  Jatnika will make the approach to the staff by personal email giving an outline of the project and providing an information sheet inviting them to participate. This will be followed up with a personal meeting to provide more information, answer any questions and to complete the consenting process for those willing to participate.

Q24

- The committee would not usually agree to the use of class time for research and would recommend that a minimal introduction within class time is undertaken (5 minute's maximum) with follow-up outside of class time for those that are interested. Please comment and adjust the application and public documentation accordingly.
  The total time for student participants is anticipated to be approximately 10 min class time and 50 min outside class time, comprising: (1) brief verbal introduction at start of the (computer/artificial) lab in week 1 (5 minutes of approx. 1.5 hour computer lab) with follow-up outside of class time after lab in week 1 has finished for those that are interested(20 min) (2) collection of signed consent forms at the start of lab in week 2 (5 minutes maximum), (3) Questionnaire (30 min outside class time after week 4). The

time at the beginning of the lab sessions will not interfere with the students' lab work as these sessions are timetabled for six hours but the experimental work is usually completed within five hours.

For staff participants, the questionnaire should require approximately 30 min to complete (at the end of the course).

Q31/INFORMATION SHEETS

- Make clear in the information sheets that transcripts will not be given back.

  This is now stated on the information sheet for students (appendix 2)

SECTION E

Q50

- Note: The response should be "Yes" – participants will not be anonymous and everyone in class will know who is participating.

  A revised application form is attached on which this has been changed. A comment has also been added: Participants will not be anonymous as everyone in class will know who is participating by the presence of voice recorders on the benches of participants. Q25 has also been amended to 'No' on the revised application form to agree with this (attached).

Q55

- The researcher must ensure that the data and consent forms are stored separately.

  We appreciate the need for this and have amended question 55 on the revised application form (attached).

SECTION I

- Should there be issues in regard to ethnicity that the researcher wishes to discuss, the committee would suggest Dr Nik Roskruge, Kaiarahi Māori, College of Sciences as an appropriate contact for cultural consultation.

  Thank you for this contact, who we will contact if necessary.

SECTION K

Q74/INFORMATION SHEET

- Participants have the right to receive a summary of the findings (rather than having to request one); therefore, please outline the mechanism for providing the summary and make clear in the information sheet.

Student participants will be asked on their consent form whether they want to receive the summary of findings and, if they do, to provide a non-Massey email address (or mailing address) solely for this purpose (described on amended student information and consent sheets - appendix 2 and 4 –attached).

For the research community scholarly articles will be published in peer-reviewed higher education journals. For practitioners, conference presentations, guidelines, and articles in content specific education journals will be developed and delivered. Participants can elect to receive a copy of these presentations.

STUDENT INFORMATION SHEET

- Please proof-read the information sheet thoroughly in order to eliminate grammatical, typographical and other errors. For example, currently the information sheet jumps between first and third person tense. The information sheet should be invitational in tone and directed toward the participants, e.g. the final bullet point on page 1 could read "A summary of findings will be provided to you".

This has been amended (appendix 2 attached).

- Refer to Qs 31 and 74 above – include relevant details.
  These details are included on the amended information and consent sheets (attached).
- The committee noted that if there is no way of deleting a participant's contributions to the group conversations, then it must be clear that whilst participants can withdraw, their contributions up to the point of withdrawal will remain. Please comment.
  We thank the committee for highlighting this potential issue and have now added the following statement under 'your rights': 'As there is no way of deleting your contributions to the recorded group conversations, you can withdraw at any time but your contributions up to the point of withdrawal will remain.'
- Ensure the inclusion of the correct committee approval statement on the information sheets as follows: *"This project has been reviewed and approved by the Massey University Human Ethics Committee: Southern B, Application 13/86. If you have any concerns about the conduct of the research, please contact Dr Nathan Matthews, Chair, Massey University Human Ethics Committee: Southern B, telephone 06 350 5799 x 80877, email humanethicsouthb@massey.ac.nz."*
  This statement has now been added.
- Please provide a copy of the amended information sheet.
  The amended student information sheet is attached as appendix 2.

STAFF INFORMATION SHEET

- What will happen if a member of staff does not want to be involved (in this instance, students would not be able to participate either)? Please comment.
  If a member of staff does not want to be involved, this would remove only one source of the data, the end of course staff questionnaire. The focus of the study is on students' conversations and, ideally, this would include any conversations that the group has with a staff member. In the event that a staff member does not wish to participate and be recorded in these conversations (and the students had agreed to participate) we would request that the member of staff turned off the voice recorder while they were present and turned it on again at the end of their conversation with the students. This will enable recording of the students groups' conversations without recording the contribution of the staff member. In this way the students would still be able to participate.

- The committee noted that if there is no way of deleting a participant's contributions to the group conversations, then it must be clear that whilst participants can withdraw, their contributions up to the point of withdrawal will remain. Please comment. Note: In addition, if a staff member withdraws part way through, if contributions to the point of withdrawal are not able to be included, students' contributions would also be null and void. Refer to Qs 31 and 74 above – include relevant details.
  We thank the committee for highlighting this potential issue and have now added the following statement under 'your rights': 'As there is no way of deleting your contributions to the recorded group conversations, you can withdraw at any time but your contributions up to the point of withdrawal will remain.'

- Ensure the inclusion of the correct committee approval statement on the information sheets as follows: *"This project has been reviewed and approved by the Massey University Human Ethics Committee: Southern B, Application 13/86. If you have any concerns about the conduct of the research, please contact Dr Nathan Matthews,*

Chair, Massey University Human Ethics Committee: Southern B, telephone 06 350 5799 x 80877, email humanethicsouthb@massey.ac.nz."
This statement has now been added.

- Please provide a copy of the amended information sheet.
  The amended staff information sheet is attached as appendix 3.

PERMISSION LETTER

- The committee noted that the request to conduct research should not be in the form of an information sheet but in the form of a formal letter of request. Please provide a copy of the letter of request to the Pro Vice-Chancellor.
  A draft letter is now provided as appendix 10.
- Note: Participant's rights should not be included in the letter.
  These have been removed.

Please supply to the Secretary, one (1) copy of this email with the reply inserted under each point, plus any amended documents which should clearly identify changes made, e.g. using track changes, italics or bold font. Please ensure that your Supervisor has checked your response before you submit your reply. Do not begin your research until you receive your final letter of approval.

Yours sincerely
Dr Nathan Matthews, Chair
Massey University Human Ethics Committee: Southern B

Patsy Broad
PA/Research Ethics Administrator
Research Ethics Office
Courtyard Complex, Room 1.25
Turitea Campus
Massey University/Te Kunenga ki Purehuroa
Private Bag 11222
Palmerston North 4442
NEW ZEALAND

Extension: 81082
Phone (DDI): 06 350 5573
Email: p.l.broad@massey.ac.nz
Fax 06 350 5622

Appendix B – Questionnaires and the Responses

MASSEY UNIVERSITY
TE KUNENGA KI PŪREHUROA
UNIVERSITY OF NEW ZEALAND

Analysis of Inquiry in Students' Conversations in the Biochemistry Laboratory

QUESTIONNAIRE FOR STAFF - 1

Introduction

Please share your views on your teaching/experience in the lab and the students' learning during the three weeks of Experiment Two in paper 122.322 by answering the following questions as honestly as possible. Your thoughtful and complete responses to the following questions will be most appreciated. Responses that include specific examples and illustrations will provide the most useful data. Please do not put your name on this questionnaire. Please do not identify students by name, but only by group. Please put your completed form in Jatnika's mailbox on level 4 Science Tower B by the end of March. Thank you for your participation.

---

1. What do you think is the most challenging part of Experiment Two and why?

The most challenging part was the correct determination of protein concentration. This should have been easy – but for some reason all found it difficult – the interpretation of their results need much guidance from (hidden name) and myself. They all still have problems with dilutions and fail to analyse the reasons for errors. Also organization of time seemed to be lacking in most groups – figuring out what had to be done first – in what order.

2. In relation to the most challenging part of Experiment Two, do you think the students enjoyed and developed an understanding of this part? Please explain why (or why not).

No, but they learned something I hoped – I hope they looked back from their SDS PAGE and realized where they had gone wrong – I think they realized just how difficult it is to get accurate results.

3. Please indicate how you helped students to answer their questions and the relative frequency. Please mark a tick (√) in the appropriate box.

METHOD OF FINDING ANSWER	RARELY	SOME TIMES	OFTEN	ALWAYS
Explanation (told students the answer)		√		
Guiding students towards the answer (perhaps by asking a question)		√		
Encouraging students to find out the answer from their results			√	
Other. Please describe:				

4. Please indicate how often you think the students used the following activities to answer their questions in the lab:

METHOD OF FINDING THE ANSWER	RARELY	SOME TIMES	OFTEN	ALWAYS
Searching the internet (if available)		√		
Consulting their lecture notes in the lab	√			
Looking up in a text book	√			
Asking the lecturer or technician in charge of the lab				√
Discussion with classmates in their group				√
Discussion with classmates in other groups			√	

5. In addition to practical skills and theory directly associated with this protein purification experiment,what other benefits would you expect your students to gain from Experiment Two?

- *How to solve problems – what to do when things go wrong – how to "rescue" a mistake. To know how to conduct a "real" protein purification difficulties, pitfalls –*
- *How to use sophisticated equipment (most took charge on day 2-).*
- *Interpretaion of result*

6. To what extent do you think that the goals of Inquiry-Based Learning were practised by the students in this laboratory?

As much as possible they had to work out things for themselves
-Assays
-[Protein] dilutions
-how to run the assay
-how to interpret data
-different between total protein [protein]
They may seem simple – but complex for them

7. If you have any other comments relating to the laboratory please include them here.

Sometimes you have to give the students the answers in the interests of time- the first 2 days were very long – especially 2nd (the last group left after 7 pm-start at 9 – only ½ hour break-
But staff stayed at request of student who wanted to get it right.

QUESTIONNAIRE FOR STAFF – 2

1. What do you think is the most challenging part of Experiment Two and why?

The most challenging part is on Day Two when the students need to use the AKTA systems t run their purification columns. This could be considered the most challenging practical component. Possibly the most challenging theoretical aspect is the concentration and desalting step which requires calculations that many students find difficult.

2. In relation to the most challenging part of Experiment Two, do you think the students enjoyed and developed an understanding of this part? Please explain why (or why not).

Yes I think so particularly using the AKTA instruments. The students did develop their understanding of the concentration concept and calculation as evidenced by reasonable looking SDS-PAGE gels at the end f the experiment.

3. Please indicate how you helped students to answer their questions and the relative frequency. Please mark a tick (√) in the appropriate box.

METHOD OF FINDING ANSWER	RARELY	SOME TIMES	OFTEN	ALWAYS
Explanation (told students the answer)		√		
Guiding students towards the answer (perhaps by asking a question)				√
Encouraging students to find out the answer from their results				√
Other. Please describe:				

4. Please indicate how often you think the students used the following activities to answer their questions in the lab:

METHOD OF FINDING THE ANSWER	RARELY	SOME TIMES	OFTEN	ALWAYS
Searching the internet (if available)	√			
Consulting their lecture notes in the lab	√			
Looking up in a text book	√			
Asking the lecturer or technician in charge of the lab			√	
Discussion with classmates in their group				√
Discussion with classmates in other groups				√

5. In addition to practical skills and theory directly associated with this protein purification experiment,what other benefits would you expect your students to gain from Experiment Two?

- *Skills from working in groups i.e. task management*
- *Time management skills owing to the experiment taking all day, i.e. when to schedule breaks etc*
- *Scientific writing skills*

6. To what extent do you think that the goals of Inquiry-Based Learning were practised by the students in this laboratory?

To a reasonable extent. The practical class is lengthy and complex (3x6 hour sessions) and the lab manual contains the minimum information so students do need to develop their own plans (to a limited degree) for the practical.

7. If you have any other comments relating to the laboratory please include them here.

QUESTIONNAIRE FOR STAFF - 3

1. What do you think is the most challenging part of Experiment Two and why?

Is for the students to learn how to work as an individual as part of a larger group effort. As an individual they need to be competent with the experimental techniques, accurate with recording of methods used and results obtained, and have confidence in their lab partners abilities. They need to also have the confidence to question and if necessary correct the actions/results of their partners while explaining why it is needed. In first and second year experiments, the groups are too large and there is not enough work for everyone, so some students can get through these ears without gaining the confidence and competency needed for this experiment.

2. In relation to the most challenging part of Experiment Two, do you think the students enjoyed and developed an understanding of this part? Please explain why (or why not).

Yes they did. There is great satisfaction to be had by providing correct information/reliable results/assistance to your peers. It provides them with the realisation that their effort is needed and appreciated, it also helps overcome some students' shyness.

3. Please indicate how you helped students to answer their questions and the relative frequency. Please mark a tick (√) in the appropriate box.

METHOD OF FINDING ANSWER	RARELY	SOME TIMES	OFTEN	ALWAYS
Explanation (told students the answer)	√			
Guiding students towards the answer (perhaps by asking a question)			√	
Encouraging students to find out the answer from their results			√	
Other. Please describe: ***Students are slow to recognize-***		√		

4. Please indicate how often you think the students used the following activities to answer their questions in the lab:

METHOD OF FINDING THE ANSWER	RARELY	SOME TIMES	OFTEN	ALWAYS
Searching the internet (if available)	√			
Consulting their lecture notes in the lab	√			
Looking up in a text book	√			
Asking the lecturer or technician in charge of the lab			√	
Discussion with classmates in their group				√
Discussion with classmates in other groups		√		

5. In addition to practical skills and theory directly associated with this protein purification experiment,what other benefits would you expect your students to gain from Experiment Two?

-

6. To what extent do you think that the goals of Inquiry-Based Learning were practised by the students in this laboratory?

I do not know why the goals of inquiry – based learning are exactly. The experiment is very structured with no allowance for variations of procedure. The main variable is that no one knows the exact answers. This causes the student some concern when we as supervisors/demonstrators to tell them that their results are correct. There is not a lot of time for exploration of alternate methods.

7. If you have any other comments relating to the laboratory please include them here.

The microphones had only a small effect on the social environment that occurs during this experiment. The days are long and students get tired so we attempt to create a "fun" atmosphere which often includes music and laughter.

MASSEY UNIVERSITY

COLLEGE OF SCIENCES

TE WĀHANGA PŪTAIAO

Analysis of Inquiry in Students' Conversations in the Biochemistry Laboratory

QUESTIONNAIRE, Students - 1

Introduction

Please share your views of your experiences during the three weeks of doing Experiment Two in paper 122.322 by answering the following questions as honestly as possible. Your thoughtful and complete responses to the following questions will be most appreciated. Responses that include specific examples and illustrations will provide the most useful data. Please put your group's number at the top of this page but do NOT include your name. An electronic version in Word will be available on Stream for downloading if you wish. Please hand in the completed form at Monday's lecture (24th March) or leave in Jatnika Hermawan's mail box on level 4 Science Tower B by the end of next week. Thank you.

---

1. What part of Experiment Two did you enjoy the most? Please explain why.
Day 2 during chromatography, because the preparation was easy (no mixing reagents all day) and our results were good.

2. What do you think is the most challenging part of Experiment Two and why?
Obtaining accurate protein concentrations because there are many to obtain using the Bradford test. Small errors can make a big difference and after doing it all day you get pretty careless.

3. During the three laboratory sessions, did you find yourself wanting to find out more? Please explain.
Only with the chromatograms. Learning about them is one thing, but transferring that knowledge to a device in front of you is different. Therefore I asked the demonstrators what was happening at each step and I quickly understood it all.

4. When you had a question relating to Experiment Two, how did you find the answer? Please indicate which method(s) you used, and how frequently, below.

METHOD OF FINDING THE ANSWER	RARELY	SOME TIMES	OFTEN	ALWAYS
Searching the internet				
Consulting your lecture notes		√		

Looking up in a text book				
Asking the lecturer or technician in charge of the lab			√	
Discussing with classmates in your group			√	
Discussing with classmates in other groups			√	

5. If the staff helped you to answer your questions please indicate how they did this below with a tick (√) in the appropriate box.

METHOD OF FINDING THE ANSWER	RARELY	SOME TIMES	OFTEN	ALWAYS
Explanation (told the answer)			√	
Guiding you towards the answer (perhaps by asking you a question)		√		
Encouraging you to find out the answer from your results		√		
Other. Please describe:				

6. Did your questions help your learning? Please explain.
Yes, I learnt how to automatic chromatograms work / relate to theory learnt.

7. What benefits do you think you have gained from your experiences in experiment two?
The ability to work consistently in a lab all day.

8. Describe how Experiment Two might be improved to help you to understand protein purification and encourage you to learn more about this topic.
It was pretty good as is.

9. If you have any other comments relating to the laboratory please include them here.

10. Did the presence of the microphone at your bench change your conversations and behaviour in any way? Please describe briefly the nature and extent of these changes.

Yeah, we would occasionally reference it and the would be transcriber, and sometimes talk directly to it, but otherwise it did not change the content of our conversation.

Questionnaire, Students - 2

1. What part of Experiment Two did you enjoy the most? Please explain why.
The second day. because we knew how to do the assays and collecting fractions was also easy to understand.

2. What do you think is the most challenging part of Experiment Two and why?

The first day. Because we didn't know exactly what we were doing and was a little confused on the procedure.

3. During the three laboratory sessions, did you find yourself wanting to find out more? Please explain.

I wanted to find out if we had done things correctly because we wouldn't know till the last day.

4. When you had a question relating to Experiment Two, how did you find the answer? Please indicate which method(s) you used, and how frequently, below.

METHOD OF FINDING THE ANSWER	RARELY	SOME TIMES	OFTEN	ALWAYS
Searching the internet		√		
Consulting your lecture notes			√	
Looking up in a text book	√			
Asking the lecturer or technician in charge of the lab				√
Discussing with classmates in your group			√	
Discussing with classmates in other groups			√	

5. If the staff helped you to answer your questions please indicate how they did this below with a tick (√) in the appropriate box.

METHOD OF FINDING THE ANSWER	RARELY	SOME TIMES	OFTEN	ALWAYS
Explanation (told the answer)	√			
Guiding you towards the answer (perhaps by asking you a question)			√	
Encouraging you to find out the answer from your results		√		
Other. Please describe:				

6. Did your questions help your learning? Please explain.

Yes, by having questions it helped me understand better when they were answered instead of looking it up myself.

7. What benefits do you think you have gained from your experiences in experiment two?

I have learnt important skills and knowledge of how to purify a protein.

8. Describe how Experiment Two might be improved to help you to understand protein purification and encourage you to learn more about this topic.

Having questions in the lab book to provoke learning more about protein purification.

9. If you have any other comments relating to the laboratory please include them here.

–

10. Did the presence of the microphone at your bench change your conversations and behaviour in any way? Please describe briefly the nature and extent of these changes.

Yes, we constantly talked about how long it would take to transcribe all our conversations. But when we were doing practical task it did not affect us.

Questionnaire, Students - 3

1. What part of Experiment Two did you enjoy the most? Please explain why.

   - ***Use of new equipments such as the IEX chromatogram***
   - ***Working on actually experiment to purify protein***

2. What do you think is the most challenging part of Experiment Two and why?

   - ***Day three and all of the concentrators***
   - ***Lack of understanding in how they worked and calculation that were necessary.***

3. During the three laboratory sessions, did you find yourself wanting to find out more? Please explain.

   - ***Not really***
   - ***Live was provided in lab and lectures which was useful***

4. When you had a question relating to Experiment Two, how did you find the answer? Please indicate which method(s) you used, and how frequently, below.

METHOD OF FINDING THE ANSWER	RARELY	SOME TIMES	OFTEN	ALWAYS
Searching the internet	√			
Consulting your lecture notes		√		
Looking up in a text book	√			
Asking the lecturer or technician in charge of the lab			√	
Discussing with classmates in your group				√
Discussing with classmates in other groups			√	

5. If the staff helped you to answer your questions please indicate how they did this below with a tick (√) in the appropriate box.

METHOD OF FINDING THE ANSWER	RARELY	SOME TIMES	OFTEN	ALWAYS
Explanation (told the answer)		√		
Guiding you towards the answer (perhaps by asking you a question)		√		
Encouraging you to find out the answer from your results			√	
Other. Please describe:				

6. Did your questions help your learning? Please explain.

Obviously I ask questions because I didn't know the answer which help learning.

7. What benefits do you think you have gained from your experiences in experiment two?

Practical knowledge and techniques on purifying proteins.

8. Describe how Experiment Two might be improved to help you to understand protein purification and encourage you to learn more about this topic.

-

9. If you have any other comments relating to the laboratory please include them here.

-

10. Did the presence of the microphone at your bench change your conversations and behaviour in any way? Please describe briefly the nature and extent of these changes.

I forgot about them after a minutes

Questionnaire, Students - 4

1. What part of Experiment Two did you enjoy the most? Please explain why.

I enjoyed the labs not being so detailed that we were just following a recipe, it was nice to have accomplished something ourselves, and felt like we did a lot of it on our own knowledge. I also liked working in a group and having people to discuss the experiment with, but yet still have a lot of work to do ourselves.

2. What do you think is the most challenging part of Experiment Two and why?

The most challenging part of experiment 2 was having to use so much new equipment that we hadn't seen before. We got a bit of explanation on how to use them but not a lot and our group all found it challenging and time consuming understanding how to use the equipment. Also the lab book was very undetailed, so I found it really hard to prepare for labs and get myself organized.

3. During the three laboratory sessions, did you find yourself wanting to find out more? Please explain.

Because we were in the lab for such a long time (i.e. 5 hours 1 week) I wasn't interested in going home and finding out more. I found what we were doing interesting, but did not have the time to find out more.

4. When you had a question relating to Experiment Two, how did you find the answer? Please indicate which method(s) you used, and how frequently, below.

METHOD OF FINDING THE ANSWER	RARELY	SOME TIMES	OFTEN	ALWAYS
Searching the internet	√			
Consulting your lecture notes		√		
Looking up in a text book	√			
Asking the lecturer or technician in charge of the lab				√
Discussing with classmates in your group				√
Discussing with classmates in other groups				√

5. If the staff helped you to answer your questions please indicate how they did this below with a tick (√) in the appropriate box.

METHOD OF FINDING THE ANSWER	RARELY	SOME TIMES	OFTEN	ALWAYS
Explanation (told the answer)	√			
Guiding you towards the answer (perhaps by asking you a question)			√	

Encouraging you to find out the answer from your results			√	
Other. Please describe:				

6. Did your questions help your learning? Please explain.

Sometimes I was confused a lot of the time about what the equipment was actually doing for us because of the lack of practice with it. When I asked questions about the equipment they generally helped my learning of how to use them.

7. What benefits do you think you have gained from your experiences in experiment two?

I know how to assay! It was a great lab for teaching us how to work with little help, so therefore a lot of trial and error. I find after doing this lab my other labs for other papers seem extremely easy and are more just like following a recipe. This lab got me more confident with a lot of equipment and I feel like I gained a lot of skills.

8. Describe how Experiment Two might be improved to help you to understand protein purification and encourage you to learn more about this topic.

The lab book needs to be more detailed. I also think at the beginning of the lab it would be great to have some demonstrations on the new equipment used in that lab. Maybe a little bit more guidance in the first of the 3 labs to help with our understanding.

9. If you have any other comments relating to the laboratory please include them here.

The labs were too long. It was hard to concentrate for such long period of time. I feel that it would be better to make the lab run over 4 weeks rather than 3 and spread the work at a bit. I just found that after a certain length of time it was too hard to concentrate and mistakes were made. Also I tended to get much grumpier with my group.

10. Did the presence of the microphone at your bench change your conversations and behaviour in any way? Please describe briefly the nature and extent of these changes.

At the beginning it felt a bit weird but after 5 minutes I forgot it was there and it did not change anything. I would have charged what I said on the basis of it being there.

Questionnaire, Students - 5

1. What part of Experiment Two did you enjoy the most? Please explain why.

Going from the original crude material (chicken) to our pure protein on days 1 and 2. Found it interesting that we could go from a bunch of proteins to selectively finding our one of interest.

2. What do you think is the most challenging part of Experiment Two and why?

Getting my head around some of the calculations as some of them required more thinking, such as going from a low concentration and trying to concentrate it more.

3. During the three laboratory sessions, did you find yourself wanting to find out more? Please explain.

I was content with the amount of info we were given. If there was anything extra I wanted to know, I would ask the lab demonstrators/technicians for more info. If we were constantly bombared with new information, it might have become over whelming.

4. When you had a question relating to Experiment Two, how did you find the answer? Please indicate which method(s) you used, and how frequently, below.

METHOD OF FINDING THE ANSWER	RARELY	SOMETIMES	OFTEN	ALWAYS
Searching the internet	√			
Consulting your lecture notes		√		
Looking up in a text book		√		
Asking the lecturer or technician in charge of the lab				√
Discussing with classmates in your group				√
Discussing with classmates in other groups		√		

5. If the staff helped you to answer your questions please indicate how they did this below with a tick (√) in the appropriate box.

METHOD OF FINDING THE ANSWER	RARELY	SOME TIMES	OFTEN	ALWAYS
Explanation (told the answer)			√	
Guiding you towards the answer (perhaps by asking you a question)		√		
Encouraging you to find out the answer from your results		√		
Other. Please describe:	√			

6. Did your questions help your learning? Please explain.

They helped me understand what was going on in the experiment, or if something went wrong. E.g. on the first day, a major step went wrong and had to be fixed. When I got confused, Gxxx was able to guide me in the right direction.

7. What benefits do you think you have gained from your experiences in experiment two?

A bit more team management i.e. making sure I know what each person in the team is up to so I know what I should be doing.

8. Describe how Experiment Two might be improved to help you to understand protein purification and encourage you to learn more about this topic.

Being able to watch each step. E.g. one person would be doing the chromatography whilst I was doing assays, so did not get time to watch the whole chromatography process from the start. This is more of a self management problem from my end though.

9. If you have any other comments relating to the laboratory please include them here.

-

10. Did the presence of the microphone at your bench change your conversations and behaviour in any way? Please describe briefly the nature and extent of these changes.

No, didn't puer realise it was there most of the time.

Questionnaire, Students - 6

1. What part of Experiment Two did you enjoy the most? Please explain why.

Getting good at measuring activity by doing it so many times.

2. What do you think is the most challenging part of Experiment Two and why?

Length (left at 7). Got really tired. The column machines were confusing. I didn't understand what the tubes were doing and why, along with the chromatography procedure (when each buffer went in and why).

3. During the three laboratory sessions, did you find yourself wanting to find out more? Please explain.

Yes. The chromatography machines- they were cool but very complicated because you couldn't see what was happening once the solution went into the box.

4. When you had a question relating to Experiment Two, how did you find the answer? Please indicate which method(s) you used, and how frequently, below.

METHOD OF FINDING THE ANSWER	RARELY	SOME TIMES	OFTEN	ALWAYS
Searching the internet		√		
Consulting your lecture notes	√			
Looking up in a text book			√	
Asking the lecturer or technician in charge of the lab				√
Discussing with classmates in your group				√
Discussing with classmates in other groups		√		

5. If the staff helped you to answer your questions please indicate how they did this below with a tick (√) in the appropriate box.

METHOD OF FINDING THE ANSWER	RARELY	SOME TIMES	OFTEN	ALWAYS
Explanation (told the answer)				√
Guiding you towards the answer (perhaps by asking you a question)	√			
Encouraging you to find out the answer from your results		√		
Other. Please describe:				

6. Did your questions help your learning? Please explain.

Yes. Found at what I was doing and making sure I was on the right track so I didn't waste time.

7. What benefits do you think you have gained from your experiences in experiment two?

Note-taking (of data); dilutions; how to measure activity/what the units mean.

8. Describe how Experiment Two might be improved to help you to understand protein purification and encourage you to learn more about this topic.

Explain how the chromatography machines work as a class and properly with diagrams and when/why each solution goes in.

9. If you have any other comments relating to the laboratory please include them here.

-

10. Did the presence of the microphone at your bench change your conversations and behaviour in any way? Please describe briefly the nature and extent of these changes.

No. If I looked at it I'd remember we were being recorded, but then immediately forgot about it.

Questionnaire, Students - 7

1. What part of Experiment Two did you enjoy the most? Please explain why.

The length of the Lab sessions, and exposure to the entire process of protein purification. The length of the Lab sessions removed a lot of the pressure that was previously felt in past 3 hour lab session. This loss of time pressure (not total loss), reduction of time pressure in the lab session opened doors previously closed. 1) The labs felt less over whelming, 2)because of (1) the lab staff, students, and work became more personal and that allowed for New Zealationship to blossom and overall one was capable of becoming connected to ones work and others. I personally enjoyed expose to the whole picture, knowing things is flowed. Knowing how we know what we know removes this flow! This knowledge does become powerful.

2. What do you think is the most challenging part of Experiment Two and why?

Team work and trust during experiment two there is need for real trust for the first time in Labs. We work in pairs and sometimes 3's through out our under graduate degrees, but the lab length and amount of work requires true delegation and for the first time, to leave on aspect of/part of the experiment per day to someone else completely. Only one person and purify something at one time, and we don't need 6 standards 3x duplicates? I don't like depending on others like that, because I am prove to over preparation in case of the unexpected, and like all undergraduate 3rd year students, I hold my self in higher extreme then I should- a little arrogance makes it fun though.

3. During the three laboratory sessions, did you find yourself wanting to find out more? Please explain.

Not really, that's why I liked it. Seeing the whole process mad it, the experiment, easier to understand, and to grasp. This, backed up with lectures that overlapped the Labs so well, provided the theory and background needed to make sense of the rest.

4. When you had a question relating to Experiment Two, how did you find the answer? Please indicate which method(s) you used, and how frequently, below.

METHOD OF FINDING THE ANSWER	RARELY	SOME TIMES	OFTEN	ALWAYS
Searching the internet	√			
Consulting your lecture notes		√		
Looking up in a text book		√		
Asking the lecturer or technician in charge of the lab			√	
Discussing with classmates in your group	√			
Discussing with classmates in other groups	√			

5. If the staff helped you to answer your questions please indicate how they did this below with a tick (√) in the appropriate box.

METHOD OF FINDING THE ANSWER	RARELY	SOME TIMES	OFTEN	ALWAYS
Explanation (told the answer)	√			√
Guiding you towards the answer (perhaps by asking you a question)		√		
Encouraging you to find out the answer from your results				√
Other. Please describe: ***The sarcastic lure*** 😜 ***Making light of mistakes, causing a closer look. Making trial and error with a little sport!***		√		

6. Did your questions help your learning? Please explain.

Yes, because each question represents a block which needs to be over come before one can progress. My questions help my progression to understanding the problem that I was facing at the time.

7. What benefits do you think you have gained from your experiences in experiment two?

This is hard to answer, because the effect of Lab 2 over the 3 day expose you to so much. I have definite in all aspects of my life in small ways. Especially in Lab confidence which can be seen by my approach to other courses lab sessions whichFYI seem rather light weight and easy now.

8. Describe how Experiment Two might be improved to help you to understand protein purification and encourage you to learn more about this topic.

No recommendations here, nothing is totally perfect, especially above 0^{o} Kelvin but this course is damn close imo

9. If you have any other comments relating to the laboratory please include them here.

The only impediment I found to hinder my learning was other groups. The interference and distraction did cause a loss of focus for my group.

10. Did the presence of the microphone at your bench change your conversations and behaviour in any way? Please describe briefly the nature and extent of these changes.

Not at all, 99.999% of the time I totally forget that it was there.

Questionnaire, Students - 8

1. What part of Experiment Two did you enjoy the most? Please explain why.

Learning to use new machines like IEX, and working in a group with good hardworking people.

2. What do you think is the most challenging part of Experiment Two and why?

Getting everything done in the day-so much to do! Was also tricky getting my head around some of the stuff.

3. During the three laboratory sessions, did you find yourself wanting to find out more? Please explain.

Occasionally, such as why are we doing some things, but –hidden staff name-- was happy to explain and so was –hidden staff name--.

4. When you had a question relating to Experiment Two, how did you find the answer? Please indicate which method(s) you used, and how frequently, below.

METHOD OF FINDING THE ANSWER	RAREL Y	SOME TIMES	OFTEN	ALWA YS
Searching the internet			√	
Consulting your lecture notes		√		
Looking up in a text book	√			
Asking the lecturer or technician in charge of the lab				√
Discussing with classmates in your group				√
Discussing with classmates in other groups			√	

5. If the staff helped you to answer your questions please indicate how they did this below with a tick (√) in the appropriate box.

METHOD OF FINDING THE ANSWER	RARELY	SOME TIMES	OFTEN	ALWAYS
Explanation (told the answer)		√		
Guiding you towards the answer (perhaps by asking you a question)		√		
Encouraging you to find out the answer from your results		√		
Other. Please describe: ***The sarcastic lure*** 😊				

Making light of mistakes, causing a closer look. Making trial and error with a little sport!				

6. Did your questions help your learning? Please explain.

Yes - helped me figure out what I was doing at some stages / why

7. What benefits do you think you have gained from your experiences in experiment two?

Better time management and lab skills – learning to do calculations at home before hand/be prepared. Learn about different techniques, and had practical application of what had done in lectures – clarified/helped understand things better.

8. Describe how Experiment Two might be improved to help you to understand protein purification and encourage you to learn more about this topic.

Maybe spread things over an extra day so not so rushed

9. If you have any other comments relating to the laboratory please include them here.

-

10. Did the presence of the microphone at your bench change your conversations and behaviour in any way? Please describe briefly the nature and extent of these changes.

Not at all! After just a few minutes we forgot it was there, remembering occasionally after catching a glimpse of it but forgetting again just as quickly.

Appendix C – Biochemistry Lab Report on Bovine β-Lactoglobulin

The Effect of Single Mutations of Recombinant Bovine β-Lactoglobulin into Protein Expression and Folding in *Escherichia coli*

1. Introduction

BLG, the origins, the roles and types

Bovine β-lactoglobulin (BLG) is the predominant whey protein in the milk of many mammals, but not including humans, rodents, and lagomorphs. It is the major protein in the whey of cow's milk with a concentration of ~0.3 mg/mL in concentration, compared to α-lactalbumin (~0.1 mg/mL), serum albumin (~0.04 mg/mL), and immunoglobulin (~0.08 mg/mL) (Bell & McKenzie, 1964). The actual physiological function of BLG is still unknown, but as a member lipocalin superfamily, it is most likely to be involved in transportation of small hydrophobic ligands, which can bind in the hydrophobic cavity. Some molecules that have been suggested to be transported are retinol or fatty acids (Wu, Pérez, Puyol, & Sawyer, 1999). Simply, BLG might have a major role as a convenient nutritional protein left over in milk with some other function in the mother (Sawyer & Kontopidis, 2000).

Generally speaking, there are three genetic variants of BLG which occur commonly in cow's milk, A, B and C. Variants A and B differ at two sites, Asp64 in A is changed to Gly in B, and Val118 in A is changed to Ala in B. Variants B and C differ at one site, Gln59 in B is changed to His in C. This is reflected in the slight difference in their isoelectric points (pI) measured at room temperature in 0.1 M KCl. These are 5.26, 5.34, and 5.33, for A, B, and C, respectively. Physically, variant C is the most thermally stable at ~pH 7, whereas variant B is the most susceptible to thermal denaturation (Manderson, Hardman, & Creamer, 1995). Consequently, these differences affect the industrial processing of milk with respect to coagulation during heat treatment.

Structural biology and relevant recent studies of bovine BLG

BLG is made up from 162 amino acid residues (MW 18.4 kDa). There are five cysteine residues which form two disulfide bonds (Cys66-Cys160 and Cys106-Cys119) leaving a free thiol (Cys121) (Figure A.1-A). The secondary and tertiary structures of BLG are largely preserved from below pH ~2 to higher than pH 8 (McKenzie & Sawyer, 1967). As shown in Figure A.1-B, the secondary structure of the protein is dominated by β-sheet that is arranged in a very rigid eight-stranded (A-H) up and down β-barrel. The β-barrel forms calyx, a large cavity lined with hydrophobic residues, which are accessible to the bulk solvent at pH ≥ 7.3.

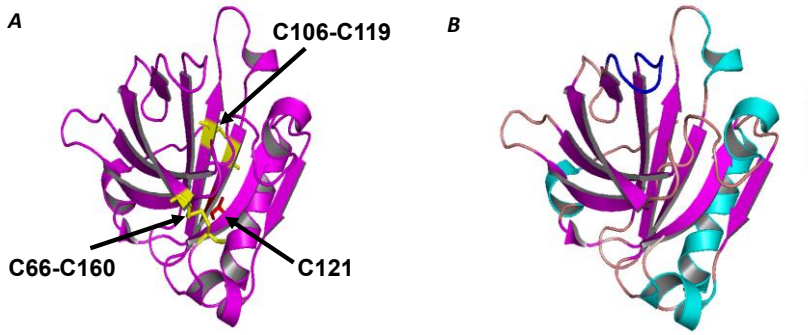

Figure C.1. The structure of bovine β-lactoglobulin.

(**A**) BLG with two disulfide bonds and one free thiol. (**B**) Beta strands are shown in magenta, α-helices are shown in cyan, and random coils are shown in pink. A dark blue coil represents the E-F loop, which undergoes a pH-dependent conformational change (the Tanford transition). The structure was derived from PDB ID 2AKQ.

A remarkable feature of BLG tertiary structure is the dramatic pH-dependent conformational change in the E-F loop between residues 85 and 90 called the *Tanford transition* (Qin et al., 1998). It occurs within micro to milliseconds when the pH rises above 7.0 (Sakurai & Goto, 2006) and is associated with deprotonation and exposure to solvent of the carboxylate group of the Glu89 side chain (Tanford, Bunville, & Nozaki, 1959) providing a structural basis for a variety of pH-dependent chemical, physical and spectroscopic phenomena. This Glu89 is conserved across all BLG.

In terms of quaternary structure (Figure A.2), this globular protein is a dimer at physiological pH, but becomes monomeric at low pH and very low ionic strength (pH < 3.0 and I < 10 mM) (McKenzie & Sawyer, 1967). As shown in Figure A.2-B, salt bridges between the AB-loop and hydrogen bonds between the I-strands of each monomer play important roles in dimer formation (Sakurai & Goto, 2002). It has been suggested that the dimer interface is preserved and the hydrophobic pocket is maintained over a wide range of pH and ionic strength (Adams, Anderson, Norris, Creamer, & Jameson, 2006). Figure 2.2-A shows that a short intermolecular β-sheet is formed between the I strands of each monomer, strengthened by four intermolecular hydrogen bonds between main-chain atoms. It also shows the salt bridge between Asp33 and Arg40 that links the two AB loops of each monomer (Sakurai & Goto, 2002).

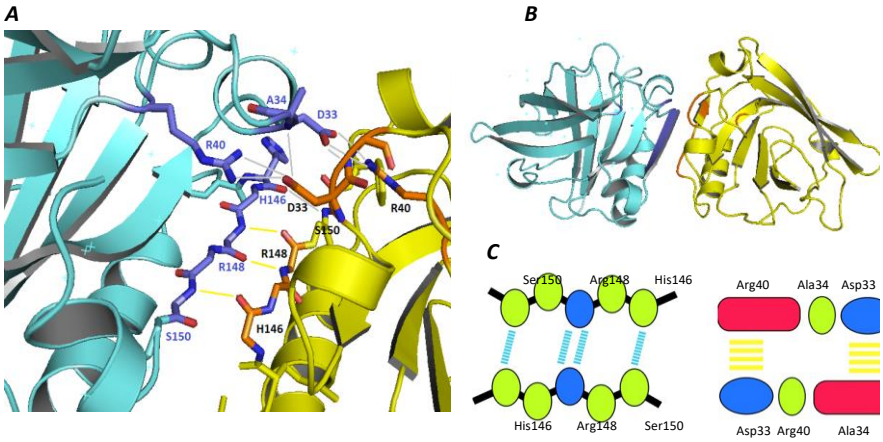

Figure C.2. The dimer interface of BLG.

(A) I-strands and A-B loops in detail. (**B**) The dimeric quaternary structure of BLG. The structures were derived from PDB ID 2AKQ. **(C)** Schematic representation of the dimer interface shows four hydrogen bonds between I-strands (left), and salt bridges at the A-B loops (right) (Sakurai & Goto, 2006).

Production of recombinant BLG in prokaryotic system

There have been many efforts to produce recombinant bovine β-lactoglobulin in several organisms, such as in bacteria, yeast, mammalian cells and baculovirus. The production of soluble and correctly folded protein in high yields has proved difficult (Batt, Rabson, Wong, &

Kinsella, 1990; Chatel, Adel-Patient, Créminon, & Wal, 1999; Cho, Batt, & Sawyer, 1994). Large quantities of insoluble recombinant protein were produced as inclusion bodies in *Escherichia coli* (*E. coli*), but refolding was a daunting prospect, and obtaining the "native" fold is never guaranteed. The difficulty in producing recombinant protein in heterologous systems arises because of the lack of cell machinery responsible for folding, post-translational modification and secretion of the proteins involved.

Initially, attempts to produce recombinant BLG in a yeast expression system were preferred because of the high yield and ability to isotopically label the recombinant protein for NMR studies. However, the BLG produced often had extracellular polysaccharides associated with it, compromising its purity. Studies to produce eukaryotic proteins, including BLG, in prokaryotic systems have since been successful. For example, Ariyaratne et al. (2002) successfully produced a recombinant BLG A in *E. coli* by constructing a synthetic gene and providing a thioredoxin chimera using the pTrxFus expression vector. The BLG A-thioredoxin fusion protein was then cleaved using enterokinase to produce soluble folded BLG A in a final yield of 15 mg/L of culture. Unfortunately, this system proved to be unreliable for the production of recombinant BLG B.

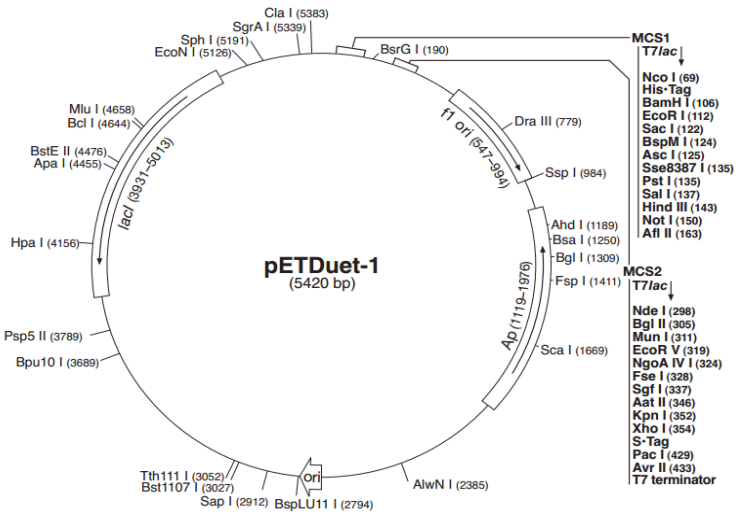

Figure C.3. The map of pETDuet-1 vector.

The commercial vector has two multiple cloning sites (MCS), each preceded by a T7 promoter/lac operator and a ribosomal binding site. In the BLG expression system, MCS1 was occupied by the DsbC, while MCS2 was occupied by the BLG gene.

A cost-effective reliable expression system and a simple reproducible purification protocol for recombinant BLG has since been developed by the same research group. Here, recombinant BLG A or B is expressed in a soluble and correctly folded form by co-expressing BLG with the disulfide bond isomerase DsbC from the dual expression vector, pETDuet-1 (Figure A.3) in the *E. coli* Origami cells (Ponniah et al., 2010). *E. coli* Origami, a Novagen commercial strain is a trxB/gor double mutant and is conducive to the formation of disulfide bonds. It has disrupted thioredoxin and glutathione reductase genes which alters the reducing environment in the cell supporting formation of disulfide bonds. The presence of DsbC, a thiol disulfide bond isomerase and chaperone, was employed to reshuffle disulfide bonds during *in vivo* folding.

Structural studies of BLG

BLG is widely studied as a model for protein folding and because of its importance to the milk industry. One driver was to solve the problem of heat-induced aggregation and gelation that occurred in whey processing (De Jong, 1997). There are over 100 crystal structures of bovine BLG and two NMR structures deposited in the Protein data Bank (PDB) ; there are also many structures of BLG from other animals. Furthermore, it has proved to be a good model protein to study the relationship between folding and biological function. BLG has been extensively used as a model to study the protein folding pathway due to its small size and isolatable refolding intermediates. It has also been used as a model for conformational change because of the ability to change its structure from mainly β to mainly α structure in different solvents (Hamada, Segawa, & Goto, 1996).

BLG, as previously described is a predominantly β-sheet protein, but has a markedly high helical propensity. During its refolding reaction, an intermediate with non-native α-helical structure accumulates because the local interactions between neighbouring amino acid residues favour the α-helical structure. Subsequently, the α-helix to β-sheet transition of BLG occurs. This transition follows a non-hierarchical mechanism and hydrophobic interactions

play important roles in stabilizing the native state of BLG (Chamani, 2006). Therefore, BLG became an intriguing model to analyse the conformation and stability of the intermediate of protein folding. On this basis, it may act as a model to elucidate the α-to-β-transition mechanism that is central to several biologically important processes, which precipitate a number of conformational diseases, such as Creutzfeldt-Jakob disease (CJD) (Kovacs & Budka, 2008) and Alzheimer's disease (Wood, Maleeff, Hart, & Wetzel, 1996).

Scope of Research

This study on BLG was primarily intended to improve my technical skills in biochemistry prior to undertaking my main project on MnSOD (Chapters 2 to 6). This part of my study has provided an invaluable opportunity for me to increase my knowledge and skills in recombinant protein technology, protein purification and protein structure analysis by circular dichroism technique.

Purposes

The purposes of this study are:

1. To investigate the effects of single mutations of BLG A: Trp61Gln, Trp19Gln, Trp19His, Leu22Pro, and Lys83Pro on the production of recombinant protein.
2. To investigate the effect of these mutations on the function of BLG A; its ability to bind *cis*-parinaric acid using spectroscopic methods.

The conformational change of all mutants was monitored by circular dichroism (CD) spectroscopy, both in the far-UV to monitor changes in secondary structure, and in the near-UV to monitor changes in the tertiary structure. From a kinetic standpoint, cis-trans proline isomerisation is a very slow process. The progress of protein folding can be impeded by trapping a proline residue crucial for folding in a non-native isomer.

As shown in Figure A.4, four positions are targeted in BLG A in this study to yield five different mutants of BLG A: Trp61Gln, Trp19Gln, Trp19His, Leu22Pro and Lys83Pro. To produce all of

BLG mutants, we utilized a pETDuet-1-DsbC-BLG A system in *E. coli* Origami (Ponniah et al., 2010). Here, we also use the BLG A wild-type as the control.

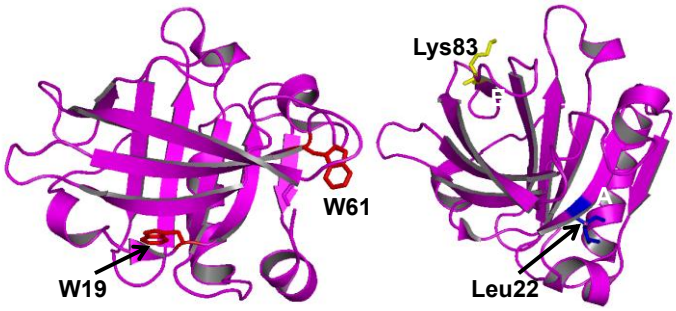

Figure C.4. Single mutations at four different positions are targeted to obtain five different mutants of the BLG A protein.

Left: Trp19Gln, Trp19His and Trp61Gln. Right: Leu22Pro and Lys83Pro.

Research Questions

The focus of the study will be on the following questions:

1. Are the recombinant BLG A mutants expressed in the pETDuet-1 system soluble?
2. What are the effects on the structure substituting the hydrophobic residues Trp19 and Trp61 by the residues Gln and His?
3. What are the effects of substituting Lys83 on the EF loop and Leu22 on strand A with Pro which is an amino acid that plays an important role in folding due to its propensity to disrupt secondary structure elements (α helices and β strands)?
4. Do these mutations of BLG A conserve its functional capability?

Hypothesis

Substitution of specific amino acids in wild-type BLG A sequence affects the folding process of the mutant protein, specifically the α-β transition, producing a protein that is soluble, but potentially with a different secondary structure.

2. Results

A sufficient amount of pure protein for each BLG A mutant is required for CD spectrometry to analyse protein folding. In order to produce recombinant protein and mutants, a dual expression vector pETDuet-1 was utilised, which expresses recombinant BLG A concomitantly with the disulfide bond isomerase (DsbC) in *E. coli* Origami cells (Ponniah et al., 2010), as previously described in section 2.1.3.

Expression of wild-type BLG A

Prior to the study of the BLG mutants, recombinant wild-type BLG A was produced to provide a control for CD spectroscopy analysis and also to learn how the expression system works. Transformation of *E. coli* Origami cells with the plasmid pETDuet-1 containing both the DsbC and BLG A genes resulted in an ampicillin-resistant cell as indicated by the growth of single colonies in LB-agar supplemented with 100 μg/mL ampicillin. Transformed cells were then cultured in one litre of LB broth (in a 5 L flask) supplemented with 100 μg/mL ampicillin with shaking at 200 rpm at 37 ^{o}C. The expression was induced by the addition of isopropyl-β-D-thiogalactopyranoside (IPTG) to a final concentration of 0.5 mM once it reached an OD_{600} of 0.4-0.6. The temperature was reduced to 25 ^{o}C and cells cultured overnight. The cells were harvested and lysed, and the protein was purified in three steps: anion exchange chromatography, low pH precipitation, and size exclusion chromatography.

The soluble fraction of BLG A was firstly purified by anion exchange chromatography (HR 30/10, GE Healthcare). Proteins were eluted using a stepwise NaCl gradient in 20 mM Bis-Tris, pH 6.5 (Figure A.5-A). As shown in Figure A.5-B (lane 1), two protein species of approximately 18.4 kDa and 23 kDa corresponding to BLG and DsbC, respectively, were found overexpressed mostly in the soluble fraction rather than the insoluble fraction (Figure A.5-B, lane 2). Fractions A10 and A11 (lanes 8 and 9) contained reasonable amounts of BLG at fractions with 0.2 M NaCl. But only fraction A11 was used due to fewer impurities for the subsequent low pH precipitation step. The overexpressed chaperone DsbC was found mostly in lane 6.

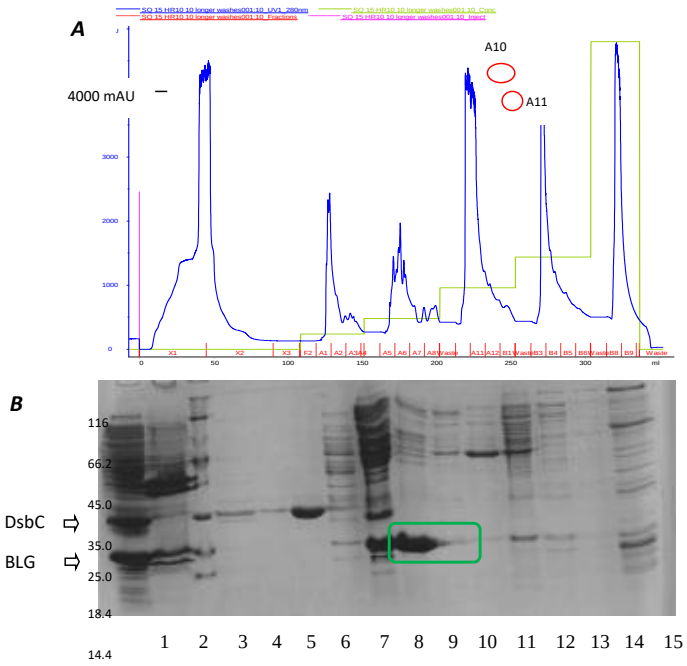

Figure C.5. Purification profile of recombinant BLG A co-expressed with DsbC in *E. coli* Origami.

(**A**) Anion exchange chromatogram of BLG A purification. BLG A was eluted of 0.2 M NaCl at fraction A11. (**B**) Coomassie-stained SDS gel of eluted fractions from anion exchange chromatography. Lane 1, soluble crude lysate; lane 2, insoluble lysate; lane 3, molecular weight marker; lanes 4 to 15, all fractions of eluate; lane 8, A10 eluate fraction; lane 9, A11 eluate fraction.

At low pH (2.6), almost all contaminating *E. coli* proteins precipitated at 7% (w/v) NaCl (Figure not shown), while BLG precipitated at 30% (w/v) NaCl. Thus, the 30% NaCl pellet containing BLG A was resuspended in 50 mM sodium phosphate buffer at pH 7.4 before dialysis against the same buffer. A small amount of insoluble protein was found in the dialysate, which was BLG that presumably had not attained the correct conformation at low pH. The sample was centrifuged at 30,000 *xg* for 20 minutes to remove insoluble protein. The soluble fraction was then loaded onto the size exclusion column (Superdex 75 10/300 GL, GE Healthcare) to remove the small amount of high molecular weight impurities (Figure A.6-A,B, lane 1). Peak

fractions (Figure A.6-A) containing pure monomeric BLG (Figure A.6-B, lanes 2 to 9) were pooled and concentrated by ultrafiltration. The concentrated BLG A is shown in Figure A.6-C.

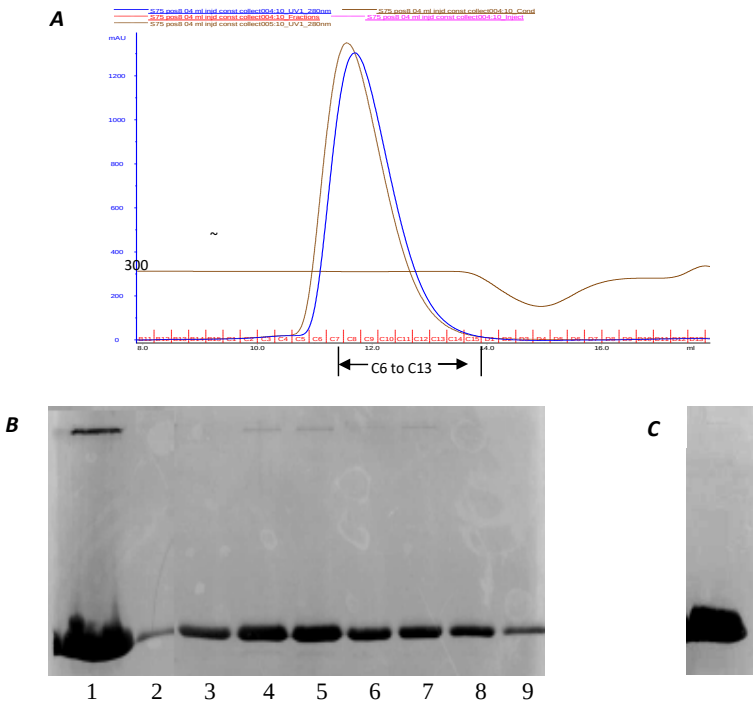

Figure C.6. Purification profile of BLG A expressed in *E. coli*.

(**A**) Size exclusion chromatogram of BLG A purification. (**B**) Coomassie-stained SDS gel of eluted fractions from size exclusion chromatography (SEC). Lane 1, dialysate, from 30% NaCl pellet; lanes 2 to 9, fractions of eluate. (**C**) concentrated BLG A cut off with a 10 kDa MWCO.

CD Spectroscopy Analysis of BLG A

To investigate the possibility of conformational change in the BLG A mutants, the samples were subjected to both far- and near-UV CD analysis. The far-UV spectrum is used to compare important characteristics of the secondary structure of both wild-type and mutant BLGs while the near-UV region allows comparison about the tertiary structure of the samples. As shown

in Figure A.7-A, the spectrum shows a typical of far-UV spectra of BLG A with a positive band at 196 nm and minimum band at 215 nm. The near-UV region which was observed at the 250-350 nm region, shows a sharp minimum at 293 nm and a strong shoulder at 286 nm (Figure A.7-B) and is characteristic of correctly folded protein of BLG A. These bands are attributed to Trp19 and Trp61residues (Kelly & Price, 1997).

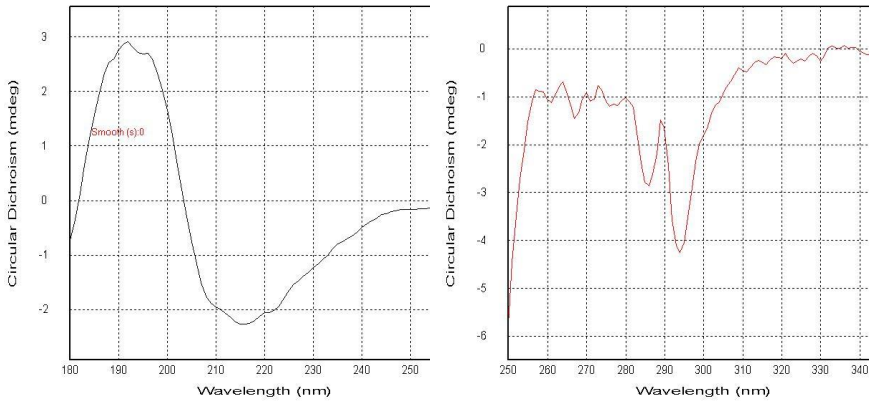

A ***B***

Figure C.7. Far-UV (**A**) and Near-UV (**B**) CD spectra of recombinant BLG A.

Each spectrum represents an average of 10 accumulated scans at 1 nm intervals, 0.25 s per point with baseline subtracted. Samples were measured at 25 °C using a BLG concentration of 1 mg/mL.

Mutation of BLG mutants: Trp19Gln, Trp19His, Trp61Gln, Lys83Pro and Leu22Pro

In order to prepare the vectors used to produce the protein mutants, five plasmids containing the following mutations in the BLG gene, Trp19Gln, Trp19His, Trp61Gln, Lys83Pro, and Leu22Pro, were prepared using the appropriate primers with PCR. The forward and reverse mutagenic primers used to amplify the DNA fragment coding for BLG A are listed in Table A.1. Lastly, the amplified mutated plasmids were transformed into XL1-Blue super-competent cells to repair the nicked mutated plasmids.

Table C.1. The forward and reverse mutagenic primers used to amplify the DNA fragment coding for the BLG A.

BLG A mutant		sequences
Trp19Gln	Forward primers	5'-GTG GCG GGT ACG CAG TAT AGC CTG GCC AT -3'
Trp19His		5'-AG AAA GTG GCG GGT ACG CAT TAT AGC CTG GCC ATG G -3'
Trp61Gln		5'- ATT CTG CTG CAG AAA CAG GAA AAC GAT GAA TGT -3'
Leu22Pro		5'- GGT ACG TGG TAT AGC CCG GCC ATG GCT GC-3'
Lys83Pro		5'-C AAG ATT CCG GCT GTG TTT CCG ATC GAT GCG CTG AAC GAG -3'
Trp19Gln	Reverse primers	5'-AT GGC CAG GCT ATA CTG CGT ACC CGC CAC -3'
Trp19His		5'- C CAT GGC CAG GCT ATA ATG CGT ACC CGC CAC TTT CT-3'
Trp61Gln		5'- ACA TTC ATC GTT TTC CTG TTT CTG CAG CAG AAT-3'
Leu22Pro		5'- GC AGC CAT GGC CGG GCA ACC ACG TAC C-3'
Lys83Pro		5'- CTC GTT CAG CGC ATC GAT CGG AAA CAC AGC CGG AAT CTT G -3'

The plasmids coding BLG A mutants were isolated and purified prior to DNA sequencing analysis. As shown in Table A.2, the point mutation targets were successfully substituted. Each plasmid containing a BLG A mutant was then transformed into the *E. coli* Origami (DE3) supercompetent cells.

Table C.2 Analysis result of protein alignment of BLG A mutants against BLG A wildtype.

The DNA sequencing was translated into amino acids and then compared to the wild-type sequence. The point mutation is shown by the red shaded the letter.

MUTANTS	ALIGNMENTS
W19Q	WT -----MLIVTQTMKGLDIQKVAGTWYSLAMAASDISLLDAQSAPLRVYVEELKPTPEGDL W19Q.F EGDIHMLIVTQTMKGLDIQKVAGTQYSLAMAASDISLLDAQSAPLRVYVEELKPTPEGDL ********** ********** ********** WT EILLQKWENDECAQKKIIAEKTKIPAVFKIDALNENKVLVLDTDYKKYLLFCMENSAEPE W19Q.F EILLQKWENDECAQKKIIAEKTKIPAVFKIDALNENKVLVLDTDYKKYLLFCMENSAEPE ********** WT QSLVCQCLVRTPEVDDEALEKFDKALKALPMHIRLSFNPTQLEEQCHI W19Q.F QSLVCQCLVRTPEVDDEALEKFDKALKALPMHIRLSFNPTQLEEQCHI **********
W61Q	WT -----MLIVTQTMKGLDIQKVAGTWYSLAMAASDISLLDAQSAPLRVYVEELKPTPEGDL W61Q.F EGDIHMLIVTQTMKGLDIQKVAGTWYSLAMAASDISLLDAQSAPLRVYVEELKPTPEGDL ********** ********** ********** WT EILLQKWENDECAQKKIIAEKTKIPAVFKIDALNENKVLVLDTDYKKYLLFCMENSAEPE W61Q.F EILLQKQENDECAQKKIIAEKTKIPAVFKIDALNENKVLVLDTDYKKYLLFCMENSAEPE ****** ********** ********** WT QSLVCQCLVRTPEVDDEALEKFDKALKALPMHIRLSFNPTQLEEQCHI W61Q.F QSLVCQCLVRTPEVDDEALEKFDKALKALPMHIRLSFNPTQLEEQCHI **********
L22P	WT -----MLIVTQTMKGLDIQKVAGTWYSLAMAASDISLLDAQSAPLRVYVEELKPTPEGDL L22P.F EGDIHMLIVTQTMKGLDIQKVAGTWYSPAMAASDISLLDAQSAPLRVYVEELKPTPEGDL

MUTANTS	ALIGNMENTS
	********** **********
	WT EILLQKWENDECAQKKIIAEKTKIPAVFKIDALNENKVLVLDTDYKKYLLFCMENSAEPE L22P.F EILLQKWENDECAQKKIIAEKTKIPAVFKIDALNENKVLVLDTDYKKYLLFCMENSAEPE **********
	WT QSLVCQCLVRTPEVDDEALEKFDKALKALPMHIRLSFNPTQLEEQCHI L22P.F QSLVCQCLVRTPEVDDEALEKFDKALKALPMHIRLSFNPTQLEEQCHI **********
W19H	WT ----------LIVTQTMKGLDIQKVAGTWYSLAMAASDISLLDAQS W19H.1 XXXYRGLADNNSPSYISVEGDIHMLIVTQTMKGLDIQKVAGTHYSLAMAASDISLLDAQS ********** **********
	WT APLRVYVEELKPTPEGDLEILLQKWENDECAQKKIIAEKTKIPAVFKIDALNENKVLVLD W19H.1 APLRVYVEELKPTPEGDLEILLQKWENDECAQKKIIAEKTKIPAVFKIDALNENKVLVLD **********
	WT TDYKKYLLFCMENSAEPEQSLVCQCLVRTPEVDDEALEKFDKALKALPMHIRLSFNPTQL W19H.1 TDYKKYLLFCMENSAEPEQSLVCQCLVRTPEVDDEALEKFDKALKALPMHIRLSFNPTQL **********
	WT EEQCHI W19H.1 EEQCHI ******
K83P	WT ------LIVTQTMKGLDIQKVAGTWYSLAMAASDISLLDAQSAPLRVYVEELKPTPEGDL K83P.F EGDIHMLIVTQTMKGLDIQKVAGTWYSLAMAASDISLLDAQSAPLRVYVEELKPTPEGDL **********
	WT EILLQKWENDECAQKKIIAEKTKIPAVFKIDALNENKVLVLDTDYKKYLLFCMENSAEPE K83P.F EILLQKQENDECAQKKIIAEKTKIPAVFPIDALNENKVLVLDTDYKKYLLFCMENSAEPE ********** **********
	WT QSLVCQCLVRTPEVDDEALEKFDKALKALPMHIRLSFNPTQLEEQCHI K83P.F QSLVCQCLVRTPEVDDEALEKFDKALKALPMHIRLSFNPTQLEEQCHI **********

As shown in Figure A.8, only four of five mutants were successfully transformed, as shown by the presence of ampicillin-resistant colonies in LB-Agar. The lack of colonies for the Leu22Pro mutant could be because this mutation produces unfolded protein which may cause stress to the cell and inhibit its growth.

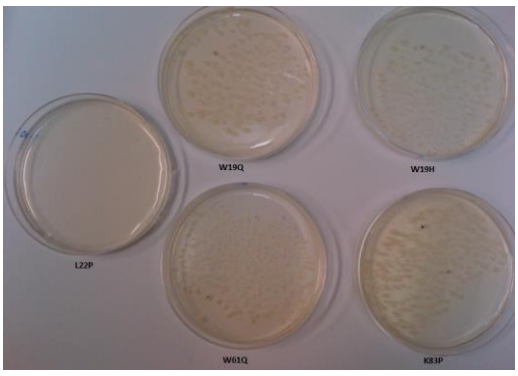

Figure C.8. The agar plates of single colonies from the five BLG A mutants.

Efforts to obtain soluble protein of BLG A mutants

A single colony of each mutant was picked and inoculated for small scale expression in 5 mL LB broth as for the BLG A wild-type expression, and grown with shaking at 37°C. When the culture reached an OD600 of ~0.4-0.6, the expression of the target protein was induced by adding IPTG to a final concentration of 0.5 mM and the cultures incubated at 25 °C overnight. The expression of each mutant in *E. coli* Origami was analyzed by separating the soluble and insoluble cell extracts on SDS-PAGE as shown in Figure A.9.

As shown in Figure A.9, two protein species of approximately 18.4 kDa and 23 kDa, corresponding to BLG wild-type and DsbC, respectively, were found to be overexpressed mostly in the soluble fraction. However, the solubility of all mutant BLG was significantly decreased. Overall, for each mutant more than 90% of the BLG protein was found in insoluble form. This means that the conditions which were used to produce wild-type protein cannot be adopted successfully for the mutants. Thus, a series of experiments were carried out in which some variables of the cell culture conditions were modified in order to enhance the solubility of protein mutants.

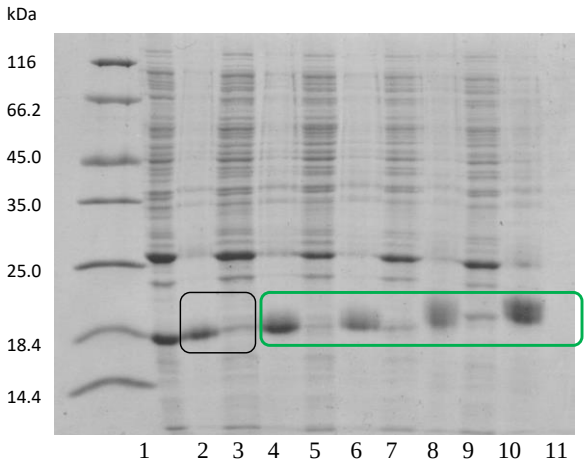

Figure C.9. Coomassie-stained SDS gel of recombinant BLG A in *E. coli* Origami (DE3) at 25°C.

Lane 1, molecular weight marker; lanes 2 and 3, soluble and insoluble cell extracts for BLG A wild-type; lanes 4 and 5, soluble and insoluble cell extracts for BLG A W19Q; lanes 6 and 7, soluble and insoluble

cell extract for BLG A W19H; lanes 8 and 9, soluble and insoluble cell extract for BLG A K83P; lanes 10 and 11, soluble and insoluble cell extract for BLG A W61Q.

This showed that the amino acid substitutions significantly affected protein solubility. This may be due to the protein being unable to fold into its native structure, perhaps being trapped in an alpha-helical intermediate. Consequently, the process of α-to-β-transition could be interrupted affecting protein folding leading to the formation of inclusion bodies which were insoluble. The conformational changes during the folding process may also lead to some disorder in disulfide bond formation. Theoretically, if the reshuffling process rate of DsbC exceeds the rate of inclusion body formation, protein folding can be stabilised. Thus, in order to optimise the chaperone's ability to perform its function, efforts were made to reduce rate of synthesis of the target protein that could potentially assist to improve protein solubility. Controlling the induction temperature and the growth medium (the inducer titration and auto-induction) is a common approach to improving folding (Schultz, Martinez, & De Marco, 2006).

Reducing the temperature of induction from 37 to 15-20 ^{o}C can change the solubility level of an overproduced protein (Sun et al., 2005). This slows both transcription and translation rates, and reduces the strength of hydrophobic interactions. To test the effect of temperature during induction, protein expression of BLG mutants was carried out at 16 ^{o}C and 37 ^{o}C. Unfortunately, as shown in Figure A.10-A, reducing the temperature of induction to 16 ^{o}C was ineffective both for the mutants and for wild-type BLG. DsbC was also expressed in smaller amounts in the soluble fractions for all mutants. On the other hand, wild-type and almost all the BLG mutants were undetectable in both soluble and insoluble fractions. An exception was the expression of the K83P mutant (Figure A.10-A, lane 10). Approximately 90% of BLG K83P mutant was found in the soluble fraction, which was contrary to the expression of the other protein mutants.

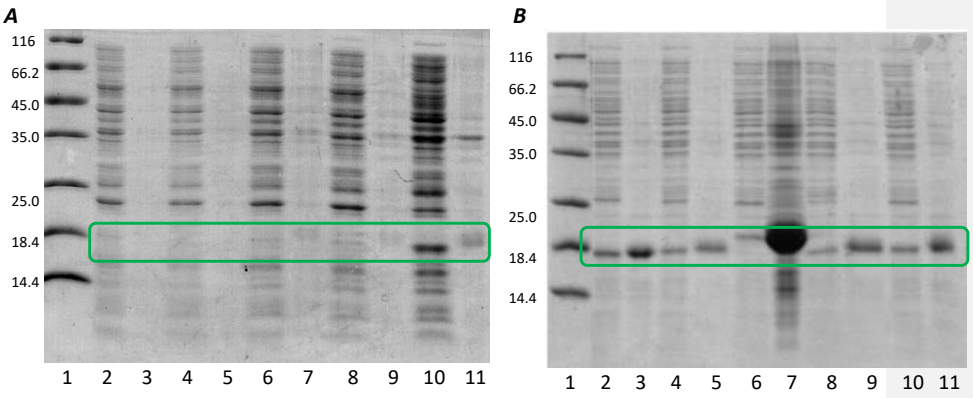

Figure C.10. Coomassie-stained SDS gel of recombinant BLG A in *E. coli* Origami (DE3) at lower and higher temperature.

(**A**) At 16 °C culture: Lane 1, molecular weight marker; lanes 2 and 3, soluble and insoluble cell extracts for wild-type; lanes 4 and 5, soluble and insoluble cell extracts for BLG A W19Q; lanes 6 and 7, soluble and insoluble cell extract for BLG A W19H; lanes 8 and 9, soluble and insoluble cell extract for BLG A W61Q; lanes 10 and 11, soluble and insoluble cell extract for BLG A K83P. (**B**) At 37 °C: Lane 1, molecular weight marker; lanes 2 and 3, soluble and insoluble BLG A wild-type; lanes 4 and 5, soluble and insoluble cell extracts for BLG A W19Q; lanes 6 and 7, soluble and insoluble cell extract for BLG A W61Q; lanes 8 and 9, soluble and insoluble cell extract for BLG A W9H; lanes 10 and 11, soluble and insoluble cell extract for BLG A K83P.

Increased temperature at induction, as shown in Figure A.10-B, yielded different results for protein solubility. As a comparison, the amount of co-expressed protein DsbC in the 37 °C culture from all mutants and control is less than the amount of DsbC from the 16 °C culture. In contrast, the percentage of soluble BLG mutants from the 37 °C culture is more than that from cultures which were expressed at 16 °C. Interestingly, the wild-type BLG A is more insoluble in the 37 °C culture than in the 25 °C culture.

Because the expression system of pETDuet-1 is preceded by a T7 promoter, decreasing the concentration of IPTG as an inducing agent could potentially improve the protein folding. Similarly, in the case of the BLG A W19Q mutant, varying the dose of IPTG affected the BLG A W19Q solubility. As shown in Figure A.11-A, at concentrations of IPTG below 30 µM, the

solubility of the BLG W19Q potentially increased. However, in the case of the BLG W19Q, the protein solubility fluctuated with the different induction times for 37 ºC cultures as shown in Figure A.11-B.

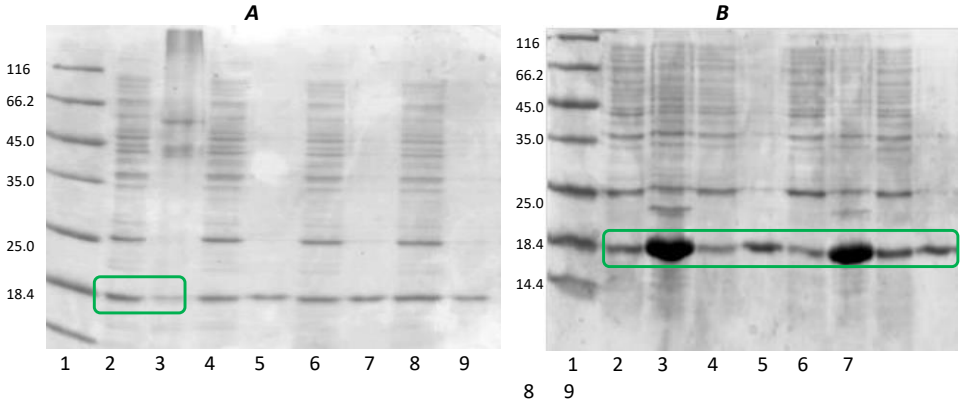

Figure C.11. Coomassie-stained SDS gel of recombinant BLG A W19Q in *E. coli* Origami (DE3): The influence of induction factors.

(**A**) Expression profile at various IPTG concentration: lane 1, molecular weight marker; lanes 2 and 3, soluble and insoluble fraction at 20 µM IPTG; lanes 4 and 5, soluble and insoluble fraction at 30 µM IPTG; lanes 6 and 7, soluble and insoluble fraction at 40 µM IPTG; lanes 8 and 9, soluble and insoluble fraction at 50 µM IPTG; (**B**) Expression profile at different times of induction: lane 1, molecular weight marker; lanes 2 and 3, soluble and insoluble fraction after 2 hours; lanes 4 and 5, soluble and insoluble fraction after 3 hours; lanes 6 and 7, soluble and insoluble fraction after 4 hours; lanes 8 and 9, soluble and insoluble fraction after 6 hours.

Auto-induction is a method of inducing production of recombinant protein that requires no inducer and can result in a higher culture density and concentration of target protein compared to IPTG induction. Autoinduction minimizes sporadic expression and unintended induction of expression, and allows cells to accept and to express highly toxic proteins (Studier, 2005). As shown in Figure A.12-A, no bands were found for DsbC and BLG after four hours of culture. The BLG A W19Q mutant and DsbC are then found in a small amount after eight hours. In contrast, BLG A mutants were overexpressed in the insoluble fraction after overnight culture, except soluble DsbC. Similarly, the insoluble BLG A mutants were also produced in

smaller amounts. Significantly, BLG A wild-type was overproduced in auto-induction system at 30 °C with a predominantly soluble fraction (~60%).

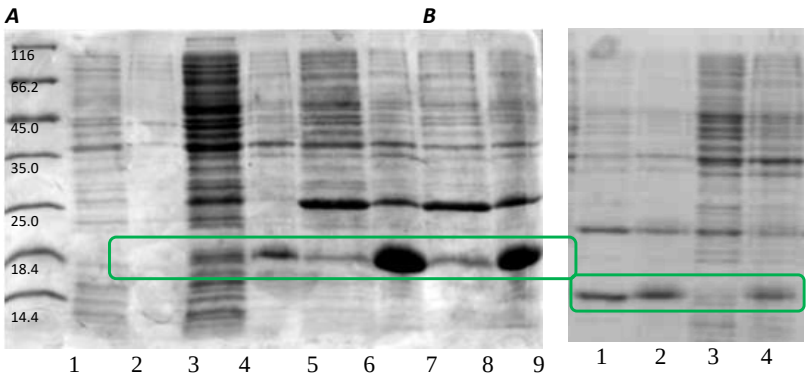

Figure C.12. Coomassie-stained SDS gel of recombinant BLG A W19Q mutant in an auto-induction system.

(**A**) Expression of BLG W19H in auto-induction system at 30 °C in various times. Lane 1, molecular weight marker; lanes 2 and 3, soluble and insoluble cell extracts after 4 hours; lanes 4 and 5, soluble and insoluble cell extracts after 8 hours; lanes 6 and 7, soluble and insoluble cell extracts after 16 hours; lanes 8 and 9, soluble and insoluble cell extracts after 22 hours. (**B**) Control. Lanes 1 and 2, the expression of BLG A wildtype at 30 °C in auto-induction system in soluble and insoluble fractions; lanes 3 and 4, the expression of BLG A W19Q mutant at 25 °C in soluble and insoluble fractions.

3. Potential Future Work

Wild-type BLG has been over-expressed successfully through *E. coli* Origami transformation with the plasmid pETDuet-1 containing both the DsbC and BLG A genes. Wild-type BLG has successfully been purified through three steps: anion exchange chromatography, low pH precipitation, and size exclusion chromatography. The CD spectra analysis at far- and near-UV wavelengths shows correctly folded protein of BLG A with a typical of far-UV spectra of BLG A. Wild-type BLG was successfully over-expressed through either induction with IPTG or autoinduction protocols.

On the other hand, among five mutants, four of the five mutants were successfully transformed as shown by the presence of ampicillin-resistant colonies in LB-Agar: BLG W19Q, BLG W19H, BLG W61Q, BLG L22P, and BLG K83P. The lack of colonies for the BLG L22P mutant could be because this mutation produces unfolded protein which may cause stress to the cell and inhibit its growth.

In 5 mL LB broth preparation, the four mutants have successfully over-expressed DsbC and the BLG mutants at 25 ^{o}C incubation. However, for each mutant more than 90% of the BLG protein was found in insoluble form. The conditions that were used to produce wild-type protein cannot be adopted successfully for the mutants.

Several variables of the cell culture conditions were modified in order to enhance the solubility of the mutant proteins, including controlling the induction temperatures to 16 ^{o}C and 37 ^{o}C, and the growth medium (the inducer titration and auto-induction). However, BLG mutants were undetectable in both soluble and insoluble fractions, except a small amount of the BLG A K83P mutant was expressed at at 16 ^{o}C. With controlling induction time with IPTG, in the case of the BLG A W19Q mutant, varying the dose of IPTG affected the BLG A W19Q solubility. The solubility of the BLG W19Q potentially increased. However, in the case of the BLG W19Q, the protein solubility fluctuated with the different induction times for 37 ^{o}C cultures. With auto-induction, the BLG A W19Q mutant and DsbC were found in small amounts after eight hours. In contrast, BLG A mutants were over-expressed in the insoluble fraction after overnight culture, except for soluble DsbC.

Based on the results achieved and the problems faced, there are some possible and potential future approaches to try. As the BLG A K83P mutant seems more stable than others, especially in low temperature culture (at 16 ^{o}C), a study of the conformational properties of this mutant for future work should be triggered.

Stabilisation of the non-natively folded possibly alpha-helical intermediate could be hypothesised by considering that Lys83 residue, which is located in the edge of E strand, links the first beta sheet (strands A-D) with the second beta sheet (strands E-H). A single beta-strand interaction at the pivot point between Lys83 and Glu74 could play a role in this case.

A further study of BLG is the interaction between the BLG and the ligand. The capability of BLG in binding the cis-parinaric acid in the calyx is reflected in the changes of the CD spectrum.

4. Experimental Detail

Preparation of expression system

In order to obtain the mutant BLG, the pETDuet-1 ampicillin resistant plasmid containing the *DsbC* and BLG A genes was used as a template for standard site-directed mutagenesis procedures. The template has been previously constructed by Ponniah et al (2010) in the same research group.

Site-directed mutagenesis

A sample reaction consists of: 1 μL 10x reaction buffer, 0.2 μL dNTP mix (10 mM each), 25 ng of each primer (see Table 3.2), 10 ng DNA template, 0.1 μL Pfu Ultra DNA Polymerase (5 U/μL), and lastly ddH2O was added to a final volume of 10 μL. Initial template denaturation 1x30sec was at 95 ^{o}C for the first segment. Then in the second segment, it was cycled for 16 times. Each cycle the temperature was set at 95 ^{o}C for 30 sec, 60 ^{o}C for 60 sec, and 68 ^{o}C (total for ~3 hours) for denaturing, annealing, and extending. The reaction was cooled down in icebath, then 0.2 μL restriction enzyme, Dpn I (20 U/μL), was added, and incubated at 37 ^{o}C for an hour to digest methylated-parental DNA template. The nicked vector mutant, DpnI-treated DNA, from each sample reaction was transformed into XL-1 Blue supercompetent cells (Stratagene) by heat-shock method at 42 ^{o}C. The transformed XL-1 Blue cells were then incubated in 0.5 mL SOC at 37 ^{o}C for an hour, then were plated on to LB plates supplemented with 100 μg/mL ampicillin and 15 μg/mL kanamycin for > 16 hours. A single colony from each mutant was picked and inoculated into 1xLB medium supplemented with 100 μg/mL ampicillin at 37 ^{o}C, 200 rpm for overnight culture.

Sequencing DNA

For sequencing purposes, cell pellets were prepared from ~4 mL cell culture. Subsequently, the plasmids were isolated from the pellet using High Pure Plasmid Isolation Kit (Roche®,

Germany). The mutants were sequenced in both forward and reverse direction by Massey Genome Service, Massey University, Palmerston North. The forward and reverse mutagenic primers (IDT®, USA) are listed in Table 2.1. The reaction consisted of 400 ng of plasmid and 3.2 mol of UP2 primer for forward direction, or T7 Terminator for reverse direction in a total of 15 µL. The product size of this reaction was 0.8 kb.

Transforming the cells

Prior to transforming the plasmid mutants, *E. coli* Origami (DE3) (Novagen) cells were prepared in advance. Either the pETDuet-DsbC-BLG A wild-type or mutants was transformed into the *E. coli* Origami super-competent cells by heat-shock method. After an hour incubation in 0.5 mL SOC at 37^{o}C, the cells of each mutant were plated on LB plates supplemented with 100 µg/mL ampicillin and 15 µg/mL kanamycin. The plates were incubated at 37 ^{o}C for more than 16 hours.

Expression

Small scale expression of BLG A wild type

For a starter culture, a single colony from either BLG A wild-type or BLG A mutant plate was picked and inoculated into 5 mL 1xLB starter medium supplemented with 100 µg/mL ampicillin and 15 µg/mL kanamycin. The culture was incubated at 37 ^{o}C and shaken at 200 rpm overnight. Then 25 µL of starter culture was inoculated into 5 mL (1:200) 1xLB medium supplemented with 100 µg/mL ampicillin. When the culture reached an OD_{600} of 0.4-0.6, expression of the target protein was induced by adding IPTG to a final concentration of 0.5 mM and the cultures were incubated at 25 ^{o}C overnight. Refer to Section 1.6 of this Appendix, the soluble and the insoluble protein fractions were analysed by SDS-PAGE to see the extent of induction.

Large scale expression of BLG A

For a starter culture, a single colony was picked and inoculated into 10 mL 1xLB starter medium supplemented with 100 µg/mL ampicillin and 15 µg/mL kanamycin and grown

overnight at 37 °C with 200 rpm agitation. The 5 mL starter culture was inoculated into 1 L (1:200) of 1xLB medium in a 5 L flask with 100 μg/mL ampicillin. When the culture reached an OD_{600} of 0.4-0.6, IPTG was added to a final concentration of 0.5 mM and incubation continued at 25 °C with a constant shaking speed (200 rpm) for overnight expression. The cells were harvested the next day by centrifugation at 6,000 rpm for 20 minutes using a Fiberlite F9-4X1000Y rotor at 4 °C.

Purification of BLG A

The cell pellets were collected and resuspended in 20 mL lysis buffer (20 mM Bis-Tris, pH 6.5) and lysed by two passages through a French Press (Aminco) at 4000 psi. Soluble protein was separated from the insoluble material by centrifugation at 17,000 x*g* for 40 minutes in a Fiberlite F21S-8X50 rotor at 4°C.

The pellet was discarded and the clarified cell lysate was then filtered through 0.8 syring filter before being loaded onto an anion exchange column (HR 30/10, GE Healthcare) packed with Source Q resin with a bed volume of approximately 24 mL. Proteins were eluted using a stepwise NaCl gradient in 20 mM Bis-Tris, pH 6.5. Fractions were analysed by SDS-PAGE (15% acrylamide) and those fractions containing purified BLG were pooled. The concentration of the protein sample was then adjusted to 1-2 mg/mL before being subjected to NaCl fractionation at low pH (~2.6). Then, NaCl was added to a final concentration of 7% (w/v) with gentle stirring for an hour in room temperature. Contaminating proteins precipitated under these conditions were removed by centrifugation at 30,000 x*g* for 30 min in a Fiberlite F21S-8X50 rotor at 4 °C. A second NaCl cut were carried out by increasing to a final concentration of 30% NaCl (w/v) to precipitate the BLG A. The pellet was resuspended in a minimum volume of sodium phosphate buffer pH 7.4 and subjected to dialysis overnight against the same buffer at 4 °C. Dialysate was centrifuged at 30,000 *xg* for 30 min in a Fiberlite F21S-8X50 rotor at 4 °C to remove insoluble material. The supernatant was concentrated by ultrafiltration (Vivaspin 20, 10 kDa MWCO, Vivascience) and subjected to size exclusion chromatography (Superdex 75 10/300 GL, GE Healthcare) in 50 mM sodium phosphate, pH 2.6. Peak fractions containing pure monomeric BLG were pooled, concentrated, and washed by 10 mM phosphate buffer, pH 7.5 using ultrafiltration (Vivaspin 20, 10 kDa MWCO, Vivascience) and filtered through 0.22 μm syringe filter prior to CD spectroscopy analysis.

Circular Dichroism Spectroscopy

A solution of recombinant BLG A was analysed by circular dichroism (CD) spectroscopy (Applied Photophysics, Surrey, UK) equipped with a TC125 temperature controller (Quantum North West). Data near-UV (250-350 nm) spectra were recorded in a 10 mm Quartz Suprasil cell at 25^{o}C. An average of 10 scans was recorded at 1 nm intervals at 0.25 s per point. The spectra were averaged and smoothed with a factor of 2 and corrected for background signal from buffer (also smoothed).

Modification of cell culture to enhance the mutants BLG solubility

There were several variations in the culture conditions tried to produce soluble mutant BLG. These treatments were intended to over-produce recombinant BLG mutants in a soluble state. All mutant cultures were cultivated in small-scale expressions. The condition was varied in four variables: temperature of induction (16 ^{o}C and 37 ^{o}C), the concentration of IPTG (20, 30, 40, and 50 μM), length of induction (2, 3, 4 and 6 hours), and the use of autoinduction-media. One variable was changed at a given time to assess the effect on expression. Thus, for method of protein expression due to BLG mutants similarly refer to the Section 1.4.1 of this chapter, excluding the auto-induction, because in autoinduction the IPTG titration is not required. Thus, auto-induction does not require any culture density monitoring due to inducer titration.

To initiate the autoinduction, a medium was prepared which contains 1% peptone, 0.5% yeast extract, 25 mM Na_2HPO_4, 25 mM KH_2PO_4, 50 mM NH_4Cl, 5 mM Na_2SO_4, 2 mM $MgSO_4$, 0.5% glycerol, 0.05 % α-D-glucose, 0.2 % α-lactose, and also trace elements: 50 mM $FeCl_3$, 20 mM $CaCl_2$, 10 mM $MnCl_2$, 10 mM $ZnSO_4$, 2 mM $NiCl_2$, 2 mM Na_2MoO_4, and 2 mM H_3BO_3. The media for auto-induction as well as for LB media were sterilized by autoclaving prior to use for cell culture cell. 100 μM/mL ampicillin was also applied in all the cell cultures to maintain selection pressures.

For a starter culture, cells containing pETDuet-1-DsbC-BLG A mutants were picked from glycerol cell stock in the -80 ^{o}C freezer instead of single colony on agar plates, and inoculated into 5 mL auto-induction media starter medium supplemented with 100 μg/mL ampicillin and

15 μg/mL kanamycin. The culture was incubated at 37 °C and shaken at 200 rpm overnight. Then, 25 μL of starter culture was inoculated into 5 mL (1:200) auto-induction medium supplemented with 100 μg/mL ampicillin and incubated at 30 °C overnight. The soluble and the insoluble protein fractions were analysed by SDS-PAGE.

Monitoring the protein expression by SDS-PAGE

SDS PAGE was carried out in order to monitor the protein expression, for either the small-scale or the large-scale expression and to assess protein purity at each purification step. In terms of small-scale expression, the expression of the BLG A wild-type or mutants in the *E. coli* Origami (DE3) strain was analysed by separating the soluble and insoluble cell extracts on SDS-PAGE. Thus, a routine analysis was prepared by harvesting the cells in Eppendorf microtube scale. Initially, the cells were centrifuged at maximum speed (13,300 x*g*) for 30 s in a benchtop centrifuge, then resuspended in 500 μL of 1xPBS (phosphate buffered saline) and disrupted by sonication on ice, using an ultrasonic liquid processor sonicator (Misonix type S-4000), setting at 20% for 15 seconds. The insoluble materials were pelleted by centrifugation at maximum speed for a minute. The pellet was then resuspended with 8 M urea in an equal volume as the supernatant. Both soluble and insoluble fractions were run side-by-side on a 15% SDS PAGE gel for monitoring protein expression.

Two protein species of approximately 18.4 kDa and 23 kDa, corresponding to BLG and DsbC, respectively can be detected. Thus, protein markers with 116 kDa to 14.4 kDa in molecular weight were applied in this stage. The SDS-PAGE was performed on a 15% acrylamide gel for a separation range of 10.50 kDa under a constant voltage of 200 V in 45 minutes (Laemmli, 1970).

References

Adams, J. J., Anderson, B. F., Norris, G. E., Creamer, L. K., & Jameson, G. B. (2006). Structure of bovine β-lactoglobulin (variant A) at very low ionic strength. *Journal of Structural Biology, 154*(3), 246-254.

Ariyaratne, K., Brown, R., Dasgupta, A., de Jonge, J., Jameson, G. B., Loo, T. S., . . . Norris, G. E. (2002). Expression of bovine β-lactoglobulin as a fusion protein in *Escherichia coli*: a tool for investigating how structure affects function. *International Dairy Journal, 12*(4), 311-318.

Batt, C. A., Rabson, L. D., Wong, D., & Kinsella, J. E. (1990). Expression of recombinant bovine beta-lactoglobulin in Escherichia coli. *Agricultural and Biological Chemistry, 54*(4), 949.

Bell, K., & McKenzie, H. (1964). β-Lactoglobulins.

Chamani, J. (2006). Comparison of the conformational stability of the non-native *α*-helical intermediate of thiol-modified *β*-lactoglobulin upon interaction with sodium *n*-alkyl sulfates at two different pH. *Journal of Colloid and Interface Science, 299*(2), 636-646.

Chatel, J.-M., Adel-Patient, K., Créminon, C., & Wal, J.-M. (1999). Expression of a Lipocalin in Prokaryote and Eukaryote Cells: Quantification and Structural Characterization of Recombinant Bovine β-Lactoglobulin. *Protein Expression and Purification, 16*(1), 70-75.

Cho, Y., Batt, C. A., & Sawyer, L. (1994). Probing the retinol-binding site of bovine beta-lactoglobulin. *Journal of Biological Chemistry, 269*(15), 11102-11107.

De Jong, P. (1997). Impact and control of fouling in milk processing. *Trends in Food Science & Technology, 8*(12), 401-405.

Hamada, D., Segawa, S.-i., & Goto, Y. (1996). Non-native α-helical intermediate in the refolding of β-lactoglobulin, a predominantly β-sheet protein. *Nature Structural & Molecular Biology, 3*(10), 868-873.

Kelly, S. M., & Price, N. C. (1997). The application of circular dichroism to studies of protein folding and unfolding. *Biochimica et Biophysica Acta-Protein Structure and Molecular Enzymology, 1338*(2), 161-185.

Kovacs, G. G., & Budka, H. (2008). Prion diseases: from protein to cell pathology. *The American Journal of Pathology, 172*(3), 555-565.

Laemmli, U. K. (1970). Cleavage of structural proteins during the assembly of the head of bacteriophage T4. *Nature, 227*(5259), 680-685.

Manderson, G., Hardman, M., & Creamer, L. (1995). Thermal denaturation of β-lactoglobulin A, B, and C. *Journal of Dairy Science, 78*, 132.

McKenzie, H., & Sawyer, W. (1967). Effect of pH on beta-lactoglobulins. *Nature, 214*, 1101-1104.

Ponniah, K., Loo, T. S., Edwards, P. J., Pascal, S. M., Jameson, G. B., & Norris, G. E. (2010). The production of soluble and correctly folded recombinant bovine β-lactoglobulin variants A and B in *Escherichia coli* for NMR studies. *Protein Expression and Purification, 70*(2), 283-289.

Qin, B. Y., Bewley, M. C., Creamer, L. K., Baker, H. M., Baker, E. N., & Jameson, G. B. (1998). Structural basis of the Tanford transition of bovine β-lactoglobulin. *Biochemistry, 37*(40), 14014-14023.

Sakurai, K., & Goto, Y. (2002). Manipulating monomer-dimer equilibrium of bovine β-lactoglobulin by amino acid substitution. *Journal of Biological Chemistry, 277*(28), 25735-25740.

Sakurai, K., & Goto, Y. (2006). Dynamics and mechanism of the Tanford transition of bovine β-lactoglobulin studied using heteronuclear NMR spectroscopy. *Journal of Molecular Biology, 356*(2), 483-496.

Sawyer, L., & Kontopidis, G. (2000). The core lipocalin, bovine β-lactoglobulin. *Biochimica et Biophysica Acta (BBA)-Protein Structure and Molecular Enzymology, 1482*(1), 136-148.

Schultz, T., Martinez, L., & De Marco, A. (2006). The evaluation of the factors that cause aggregation during recombinant expression in E. coli is simplified by the employment of an aggregation-sensitive reporter. *Microbial Cell Factories, 5*(1), 28.

Studier, F. W. (2005). Protein production by auto-induction in high-density shaking cultures. *Protein Expression and Purification, 41*(1), 207-234.

Sun, Q.-M., Cao, L., Fang, L., Chen, C., Dai, J., Chen, L.-L., & Hua, Z.-C. (2005). Expression, purification of human vasostatin120–180 in *Escherichia coli,* and its anti-angiogenic characterization. *Protein Expression and Purification, 39*(2), 288-295.

Tanford, C., Bunville, L. G., & Nozaki, Y. (1959). The reversible transformation of β-lactoglobulin at pH 7.5. *Journal of the American Chemical Society, 81*(15), 4032-4036.

Wood, S. J., Maleeff, B., Hart, T., & Wetzel, R. (1996). Physical, morphological and functional differences between pH 5.8 and 7.4 aggregates of the Alzheimer's amyloid peptide A β. *Journal of Molecular Biology, 256*(5), 870-877.

Wu, S.-Y., Pérez, M. D., Puyol, P., & Sawyer, L. (1999). β-Lactoglobulin binds palmitate within its central cavity. *Journal of Biological Chemistry, 274*(1), 170-174.